



**HAL**  
open science

# Regulation and function of the LHL4 protein, a new actor of photoprotection in the green microalga *Chlamydomonas reinhardtii*

Marie Dannay

► **To cite this version:**

Marie Dannay. Regulation and function of the LHL4 protein, a new actor of photoprotection in the green microalga *Chlamydomonas reinhardtii*. *Vegetal Biology*. Université Grenoble Alpes [2020-..], 2023. English. NNT : 2023GRALV032 . tel-04368501

**HAL Id: tel-04368501**

**<https://theses.hal.science/tel-04368501>**

Submitted on 1 Jan 2024

**HAL** is a multi-disciplinary open access archive for the deposit and dissemination of scientific research documents, whether they are published or not. The documents may come from teaching and research institutions in France or abroad, or from public or private research centers.

L'archive ouverte pluridisciplinaire **HAL**, est destinée au dépôt et à la diffusion de documents scientifiques de niveau recherche, publiés ou non, émanant des établissements d'enseignement et de recherche français ou étrangers, des laboratoires publics ou privés.

THÈSE

Pour obtenir le grade de

**DOCTEUR DE L'UNIVERSITÉ GRENOBLE ALPES**

École doctorale : CSV-Chimie et Sciences du Vivant

Spécialité : Biologie Végétale

Unité de recherche : LPCV – Laboratoire de Physiologie Cellulaire et Végétale

**Regulation and function of the LHL4 protein, a new actor of photoprotection in the green microalga *Chlamydomonas reinhardtii*.**

**Régulation et fonction de la protéine LHL4, un nouvel acteur de la photoprotection chez la microalgue verte *Chlamydomonas reinhardtii*.**

Présentée par :

**Marie DANNAY**

Direction de thèse :

<b>Dr. Giovanni FINAZZI</b> CNRS Alpes, France	Directeur de thèse
<b>Pr. Roman ULM</b> Université de Genève, Suisse	Co-Directeur de thèse
<b>Dr. Guillaume ALLORENT</b> CNRS Alpes, France	Co-Directeur de thèse
<b>Dr. Emilie DEMARSY</b> Université de Genève, Suisse	Co-Encadrante de thèse

Thèse soutenue publiquement le **28 avril 2023**, devant le jury composé de :

<b>Pr. Christel CARLES</b> Université Grenoble Alpes, France	Présidente
<b>Pr. John CHRISTIE</b> Université de Glasgow, Ecosse	Rapporteur
<b>Dr. Xenie JOHNSON</b> CEA Cadarache, France	Rapporteuse
<b>Dr. M. Águila RUIZ-SOLA</b> Université de Séville, Espagne	Examinatrice
<b>Pr. Roman ULM</b> Université de Genève, Suisse	Co-directeur de thèse

Invités :

<b>Dr. Guillaume ALLORENT</b> CNRS Alpes, France	Co-Directeur de thèse
<b>Dr. Emilie DEMARSY</b> Université de Genève, Suisse	Co-Encadrante de thèse
<b>Dr. Stéphane RAVANEL</b> INRAE Lyon-Grenoble-Auvergne-Rhône-Alpes, France	





*“Once an idea is out and about, it can’t be called back, silenced or erased. You can’t contain it, any more than you could put the head of a dandelion back together after the wind has scattered its seeds.”*

*P.W. Catanese*

## **ACKNOWLEDGEMENTS/REMERCIEMENTS**

This thesis was probably the most rewarding years of my life, in many ways. Doing a PhD is a story of perseverance. I have learned and grown from this, and I am happy to be able to make a small contribution to Science with this work.

First of all, I would like to express my gratitude to my two thesis reviewers, Pr John Christie and Dr. Xenie Johnson, for taking the time to review this manuscript. I would also thank all the other jury members: Pr Christel Carles, Dr M. Águila Ruiz-Sola, and Dr Stéphane Ravanel for agreeing to evaluate my thesis work. I would also like to thank the members of my thesis committee, who accompanied me during these three years: Pr Michel Goldschmidt-Clermont and Pr Christian Fankhauser, for their feedback and advice on my work.

I would then like to thank most warmly my four supervisors: Dr Giovanni Finazzi, Pr Roman Ulm, Dr Emilie Demarsy, and Dr Guillaume Allorent. I will always be grateful to the four of you for choosing me for this project, and I consider myself privileged to have worked alongside scientists of such stature.

Giovanni, merci d'avoir toujours pris le temps de venir discuter, de suivre le projet, d'avoir toujours apporté des idées de manip, et proposé des solutions, merci d'avoir toujours été à l'écoute. J'ai découvert au cours de cette thèse quelqu'un de profondément humain, ainsi qu'un grand scientifique, et je pense que toute l'équipe est extrêmement chanceuse de t'avoir.

Roman, thank you for always being kind and patient with me (we have come a long way with molecular biology!), and thank you for always welcoming me warmly during my stays in Geneva. I think it has been a great opportunity and an enrichment to be able to work with you, and it has always been a real pleasure to see you always coming up with new ideas to help us advance and pursue the project.

Emilie, merci pour l'addiction aux ramens ? Blague à part, un grand merci à toi aussi pour ta patience et ta gentillesse. Merci d'avoir toujours été pédagogue. Merci de t'être toujours rendue disponible pour m'aider, que ce soit de loin via toutes les petites réunions qu'on a pu faire pour comprendre ce qui clochait avec mes qPCRs, mais aussi pour avoir toujours

pris du temps pour m'aider dans mes expériences ou partager un moment en-dehors du labo lors de mes venues à Genève.

Et Guillaume... Ach ! Tous les remerciements du monde n'y suffiraient pas ! Je vais essayer de faire court. Quand j'ai accepté de travailler sur ce projet de thèse, je n'y connaissais pas grand-chose en algues, et quasiment rien en photosynthèse. Si je l'ai fait, c'était pour une raison principale qui était que je savais pertinemment que ça se passerait très bien avec toi. Et pas une fois je n'ai regretté ce choix au cours des dernières années. Alors oui, on en ressort peut-être un peu plus zinzins qu'au début, mais je garderai plein de bons souvenirs de ma thèse, et repenserai toujours avec joie aux chamailleries (je maintiens que tu vas t'ennuyer maintenant), aux chansons, aux jeux de mots douteux, aux memes, et aux mauvaises imitations d'accents. Bon, et dans tout ça, on a quand même trouvé le temps de faire un peu de bonne science (ou en tous cas d'essayer), avec des manip parfois un peu tirées par les cheveux, parfois un peu à des heures improbables, mais toujours enrichissantes d'une manière ou d'une autre. J'ai énormément appris avec toi, et grâce à toi. Merci de m'avoir supportée pendant ces presque quatre ans, merci pour tout.

Un énorme merci, évidemment à tous les membres de l'équipe LPM du LPCV, qui rassemble à elle seule une impressionnante concentration de gens adorables au mètre carré. Vous avez tous largement contribué d'une façon ou d'une autre à rendre ces quelques années plus belles. Mille mercis pour tous les gentils mots que j'ai pu recevoir de votre part pendant la rédaction. Merci Cécile, pour ta douceur et ta gentillesse, et pour avoir toujours été présente, à l'écoute, et de bon conseil. Merci Jojo, pour les longues discussions, les pauses café, et les chouette moments passés à nous raconter nos vies (toutes nos vies) au bureau. Je ne serai plus là pour ta dernière année de thèse, mais je n'ai aucun doute quant au fait tu vas vraiment bien t'en sortir ! Merci Mathilde, pour ta bonne humeur et ton sourire qui nous rendent à tous la journée plus belle. Thank you, Serena, for always being kind, warm, and helpful to me. Merci Gilles, pour être un tel puit de connaissances et pour aimer à ce point partager ce que tu sais. J'ai toujours beaucoup apprécié nos échanges. Merci Florence, pour ta gentillesse, pour les discussions et les conseils, ainsi que pour la gentillesse que tu m'as toujours témoignée (et pour les raclette parties, évidemment). Merci Dimitri, pour ta gentillesse à toute épreuve, et pour nous avoir toujours aidés au pied-levé Guillaume et moi quand on en avait besoin (et pour m'avoir gavée de viennoiseries quand c'était nécessaire). Je voulais également vous remercier spécialement,

Florence et Dimitri, pour avoir pris de votre temps pour relire et corriger mon manuscrit, alors même que la doctorante désordonnée que j'étais vous le demandait au dernier moment.

Merci également à tous celles qui ont quitté l'équipe en cours de route, mais que je prends toujours autant de plaisir à revoir : Claire, Clarisse, et Erika et Chloé bien sûr. Merci Claira pour toujours avoir pris des petites nouvelles et essayé de me changer les idées. Merci Cloclo pour ton immense contribution au projet, et pour toujours avoir été à l'écoute et de bon conseil quand le besoin s'en faisait sentir. Erika, mon p'tit, tu sais déjà tout je pense ! Juste merci d'être la belle personne que tu es.

I would also like to thank all the interns who contributed to this project: Emma, Celeste, and Eva, you did a lot!

Un grand merci également à toute l'équipe MetalStress, qui m'a mis le pied à l'étrier au LPCV. Et plus particulièrement à Stéphane qui, en plus d'avoir été mon mentor en master, a également continué d'être présent et de m'accompagner tout au long de ma thèse. Merci pour ton écoute et tes bons conseils, mais aussi pour ton humour et ton autodérision ! Encore une fois, je me sens privilégiée d'avoir pu te côtoyer ces dernières années.

Je n'oublie pas bien sûr toutes autres les personnes qui m'ont rendu la vie plus joyeuse au labo : Manon, Camille, Sébastien, Fabien, Charlotte, Caroline, Daniel, Andrea, Yiorgos, Antonin, Loïc, Elise, Fabien, Johan, Benoît, Manu, Gaëlle, Laetitia, Yannick, Damien, Louise, Yizhong, Vangeli, Laura, Denis, ... et tous ceux que j'aurais pu oublier de citer. Et un énorme merci à notre team admin, sans qui tout le labo tournerait à l'envers et marcherait sur la tête. Tiffany, Sophie, et Corinne merci pour tout ce que vous faites, et merci de garder le sourire même quand on vous rend chèvres !

Of course, a big thanks also to all the members of Roman's lab, for their always warm welcome. In particular Richard, and Manu, thanks for your kindness, and also Zhoubo and Neha, I look forward to attending another conference together someday!

Et enfin, je voudrais terminer en remerciant mes proches du fond du cœur. Vous êtes tous plus formidables les uns que les autres, et si vous n'avez pas participé directement à cette thèse, votre contribution a été tout aussi importante sachez-le.

Merci à tous mes petits corréziens, qui sont toujours là de près ou de loin, et sur qui je sais que je peux toujours compter : Anaïs, Gaspard, Gabriel, Clémence, Ludivine, Myriam,

Brandon, Baptiste, Clément, mais aussi Marion, Mélanie, Marine, et Pauline. Merci à Noémie, toujours.

Merci à toutes les belles personnes que Grenoble a apportées dans ma vie au cours de ces six dernières années. Merci à Marie, et Marie, qui ont été mes deux piliers ici. On s'est soutenue dans l'avancement de nos thèses respectives, dans les bons comme dans les mauvais moments. Merci à Belinda aussi, tu as toujours été là même de loin, et tu as toujours fait de ton mieux pour amener du soleil dans nos quotidiens. Merci à vous trois pour les rires, pour votre chaleur, pour tous ces moments de joies partagés.

Merci également à Mathieu et Kévin, vous avez été de jolies rencontres en master et je ne vous ai plus vraiment lâchés depuis. Ça a toujours été un plaisir de se revoir, de rire avec vous, et se soutenir dans nos thèses respectives !

Merci à mes parents et à mon frère, pour m'avoir toujours soutenue dans les moments difficiles ces dernières années, pour m'avoir patiemment supportée quand je râlais, et pour avoir toujours su m'encourager. Merci de m'avoir suivie dans mon choix de faire cette thèse, je ne regrette rien.

# Regulation and function of the LHL4 protein, a new actor of photoprotection in the green microalga *Chlamydomonas reinhardtii*.

**Abstract** – Light is a primary source of energy allowing photosynthetic organisms to meet their metabolic needs. For them, keeping photosynthesis functional is crucial. Consequently, to thrive with light fluctuations in their natural environment, they dispose of a large panel of acclimation processes. Among these, photoprotection mechanisms such as Non Photochemical Quenching (NPQ) increase their tolerance to high light intensities. In the model organism for green microalga *Chlamydomonas reinhardtii*, NPQ is controlled by specific proteins whose expression is induced by light, depending on its intensity and/or quality. It was recently discovered that UV-B radiations from the solar spectrum, detected by the UVR8 photoreceptor, are a master regulator of NPQ protein induction.

The objective of this project was to identify and characterise new actors involved in the UV-B-induced acclimation and photoprotection in *C. reinhardtii*. Using transcriptome and proteome analyses of UV-B-exposed cells, we decided to investigate the role of LHL4, a photosystem II protein of the ELIP family that was highly, but transiently, induced under these conditions. In a similar way to NPQ proteins, we showed that LHL4 was also induced by exposure to high light. We used this feature to study in more details the convergence of UV-B and high light signalling pathways in *C. reinhardtii* and we established that the expression of LHL4 was dependent on the UVR8 photoreceptor but also on the phototropin and cryptochromes blue light photoreceptors. We finally demonstrated that at the onset of high light exposure, LHL4 helps cells to attenuate the harmful effect of light, while NPQ proteins are not yet accumulated to effectively protect the photosynthetic machinery. This protective effect is even more important when cells are exposed to natural sunlight or under extreme light intensity where the presence of LHL4 becomes mandatory for cells survival.

Overall, the work presented in this manuscript bring new insights into the acclimation of photosynthesis to high light. Our results also decipher and highlight the convergence and cooperation of blue and UV-B signalling in *C. reinhardtii*, raising new questions about the exact nature of the synergies between different colour-induced signalling pathways within photosynthetic organisms.

# **Régulation et fonction de la protéine LHL4, un nouvel acteur de la photoprotection chez la microalgue verte *Chlamydomonas reinhardtii*.**

**Résumé** — La lumière est une source d'énergie primaire dont les végétaux dépendent pour répondre à leurs besoins métaboliques. Chez ces organismes, le maintien de l'activité photosynthétique est donc crucial pour leur survie. De ce fait, pour s'adapter aux fluctuations de la lumière dans leur environnement naturel, ils disposent d'un large panel de processus d'acclimatation. Parmi eux, des mécanismes de photoprotection tels que le Non-Photochemical Quenching (NPQ) augmentent leur tolérance à de fortes intensités de lumières. Chez la micro-algue verte modèle *Chlamydomonas reinhardtii*, le NPQ est contrôlé par des protéines spécifiques dont l'expression est induite par la lumière, en fonction de son intensité et/ou de sa qualité. Il a récemment été découvert que les radiations UV-B du spectre solaire, détectées par le photorécepteur UVR8, sont un régulateur majeur pour l'induction des protéines NPQ.

L'objectif de ce projet était d'identifier et caractériser de nouveaux acteurs impliqués dans l'acclimatation et la photoprotection induites par les UV-B chez *C. reinhardtii*. En nous basant sur des analyses du transcriptome et du protéome de cellules exposées aux UV-B, nous avons décidé d'étudier le rôle de LHL4, une protéine du photosystème II de la famille des ELIP qui était fortement induite dans ces conditions, mais de manière transitoire. D'une manière similaire aux protéines NPQ, nous avons montré que LHL4 était aussi induite par une exposition à de la forte lumière. Nous avons utilisé cette caractéristique pour étudier plus en détails la convergence des voies de signalisation de l'UV-B et de la forte lumière chez *C. reinhardtii*, et nous avons établi que l'expression de LHL4 était dépendante du photorécepteur UVR8 mais aussi de la phototropine et des cryptochromes, des photorécepteurs à la lumière bleue. Nous avons finalement démontré qu'au début d'une exposition à de la forte lumière, LHL4 aide les cellules à atténuer l'effet nocif de la lumière, alors que les protéines NPQ ne sont pas encore accumulées pour protéger efficacement la machinerie photosynthétique. Cet effet protecteur est encore plus important lorsque les cellules sont exposées à la lumière naturelle du soleil ou à une

intensité lumineuse extrême, où la présence de LHL4 devient obligatoire pour la survie des cellules.

Dans l'ensemble, les résultats présentés dans ce manuscrit apportent de nouvelles connaissances sur l'acclimatation de la photosynthèse à la forte lumière. De plus, nos résultats décryptent et mettent également en évidence la convergence et la coopération des signalisations bleue et UV-B chez *C. reinhardtii*, soulevant ainsi de nouvelles questions sur la nature exacte des synergies entre les différentes voies de signalisation induites par la couleur au sein des organismes photosynthétiques.

# TABLE OF CONTENT

<b>ACKNOWLEDGEMENTS/REMERCIEMENTS .....</b>	<b>1</b>
<b>ABSTRACT (English) .....</b>	<b>6</b>
<b>RESUME (Français) .....</b>	<b>7</b>
<b>LIST OF ABBREVIATIONS.....</b>	<b>15</b>
<b>CHAPTER 1: GENERAL INTRODUCTION .....</b>	<b>17</b>
<b>1. BIODIVERSITY OF GREEN PHOTOSYNTHETIC ORGANISMS .....</b>	<b>17</b>
<b>1.1. Emergence of the green lineage.....</b>	<b>17</b>
<b>1.2. The model green microalga <i>Chlamydomonas reinhardtii</i> .....</b>	<b>18</b>
<b>2. FROM LIGHT TO LIFE: THE USE OF LIGHT IN PLANTS.....</b>	<b>20</b>
<b>2.1. The photosynthetic process .....</b>	<b>21</b>
<b>2.2. Photoinhibition (qI).....</b>	<b>23</b>
<b>2.3. Photoprotection to cope with excess light.....</b>	<b>24</b>
<b>2.3.1. Non-photochemical quenching (NPQ).....</b>	<b>24</b>
<b>2.3.1.1. Energy-dependant NPQ (qE) .....</b>	<b>24</b>
<b>2.3.1.2. State transition (qT).....</b>	<b>26</b>
<b>2.3.1.3. Zeaxanthin-dependent quenching (qZ) .....</b>	<b>27</b>
<b>2.3.1.4. Other components of NPQ.....</b>	<b>27</b>
<b>2.3.2. The family of LHC-like proteins and its variants.....</b>	<b>27</b>
<b>2.3.3. Long-term responses.....</b>	<b>30</b>
<b>3. LIVING UNDER THE LIGHT: NOT ONLY A MATTER OF LIGHT QUANTITY, BUT ALSO A MATTER OF LIGHT COLOR .....</b>	<b>31</b>
<b>3.1. A brief overview of photoreceptor diversity in photosynthetic organisms</b>	<b>31</b>
<b>3.2. Focus on the green lineage photoreceptors currently identified in <i>C. reinhardtii</i>.....</b>	<b>32</b>
<b>3.2.1. Channelrhodopsins (ChRs) .....</b>	<b>32</b>

3.2.2.	<i>UV-A and blue-light photoreceptors</i> .....	33
3.2.2.1.	Phototropin (PHOT).....	33
3.2.2.2.	Cryptochromes (CRYs) .....	36
3.2.2.3.	Cryptochromes DASH (CRY-DASHs).....	38
3.2.3.	<i>The UV-B photoreceptor: UVR8</i> .....	40
<b>3.3.</b>	<b>Common photoreceptor signaling components</b> .....	<b>44</b>
3.3.1.	<i>The COP1/SPA1 complex</i> .....	44
3.3.2.	<i>bZIP transcription factors HY5 and HYH</i> .....	46
3.3.3.	<i>CONSTANS (CO) transcription factor</i> .....	48
<b>3.4.</b>	<b>Cross-talk between different light signalling pathways in plants</b> .....	<b>49</b>
<b>4.</b>	<b>PHOTORECEPTOR REGULATION OF PHOTOPROTECTION IN <i>C. REINHARDTII</i></b>	<b>50</b>
<b>5.</b>	<b>PROJECT PRESENTATION &amp; AIMS OF THE THESIS</b> .....	<b>51</b>
	<b>CHAPTER 2: LHL4, A THYLAKOID ELIP INDUCED BY UV-B AND HIGH LIGHT IN <i>C. REINHARDTII</i></b> .....	<b>52</b>
<b>1.</b>	<b>IDENTIFICATION OF LHL4 UPON UV-B EXPOSURE</b> .....	<b>52</b>
1.1.	Proteomics analysis of <i>C. reinhardtii</i> cells exposed to UV-B.....	52
1.2.	Structure of LHL4.....	55
<b>2.</b>	<b>LOCALIZATION OF LHL4 WITHIN THE CELL</b> .....	<b>58</b>
2.1.	Localization of LHL4 in the ultrastructure of the cell .....	58
2.2.	LHL4 comigrates with PSII in non-denaturing conditions .....	60
<b>3.</b>	<b>LHL4 ACCUMULATION IS STRONGLY AND RAPIDLY INDUCED UPON UV-B AND HIGH LIGHT IN <i>C. REINHARDTII</i></b> .....	<b>61</b>
3.1.	LHL4 expression and accumulation in cells over time and under different light conditions .....	61
3.2.	The LHL4 protein is rapidly degraded once the light treatment is stopped	64
<b>4.</b>	<b>SUMMARY</b> .....	<b>65</b>

<b>CHAPTER 3: LHL4 IS AT THE CONVERGENCE OF TWO PHOTORECEPTOR-MEDIATED PATHWAYS IN <i>C. REINHARDTII</i>.....</b>	<b>66</b>
<b>1. REGULATION OF LHL4 EXPRESSION BY UV-B AND HIGH LIGHT SIGNALLING PATHWAYS .....</b>	<b>66</b>
<b>1.1. Regulation of LHL4 by blue and UV-B photoreceptors .....</b>	<b>66</b>
1.1.1. <i>Generation and characterization of blue and UV-B photoreceptor mutants .....</i>	66
1.1.2. <i>Control of LHL4 expression by blue and UV-B photoreceptors.....</i>	69
<b>1.2. LHL4 is mainly regulated by the CONSTANS (CO) transcription factor and the COP1 ubiquitin ligase in both UV-B and high light .....</b>	<b>71</b>
<b>2. REGULATION OF NPQ-RELATED PROTEINS BY UV-B AND HIGH LIGHT SIGNALLING PATHWAYS.....</b>	<b>73</b>
<b>3. TRANSCRIPTOME ANALYSIS OF <i>C. REINHARDTII</i> <i>uvr8</i>, <i>constans</i>, <i>hy5</i> MUTANTS EXPOSED TO UV-B.....</b>	<b>75</b>
<b>4. SUMMARY .....</b>	<b>79</b>
<b>CHAPTER 4: LHL4 PREVENTS SHORT-TERM PHOTOINHIBITION AND INCREASES TOLERANCE TO LIGHT CHANGES IN <i>C. REINHARDTII</i> .....</b>	<b>80</b>
<b>1. GENERATION AND MOLECULAR CHARACTERISATION OF STRAINS IMPAIRED IN LHL4 EXPRESSION .....</b>	<b>80</b>
<b>2. LHL4 PROTECTS PSII FROM PHOTOINHIBITION .....</b>	<b>81</b>
2.1. <b>LHL4 is not an NPQ actor.....</b>	<b>81</b>
2.2. <b>LHL4 is involved in photoprotection, prior to the establishment of NPQ .</b>	<b>82</b>
2.3. <b>The absence of LHL4 decreases the cell’s ability to regulate photooxidative stress.....</b>	<b>85</b>
<b>3. THE IMPORTANCE OF LHL4 DEPENDS ON THE LIGHT INTENSITY .....</b>	<b>87</b>
3.1. <b>The stronger the high light is, the more important LHL4 becomes .....</b>	<b>87</b>
3.2. <b>The <i>lhl4</i> mutant is not able to cope with extreme light intensities, despite UV-B acclimation .....</b>	<b>88</b>
<b>4. PHOTOPROTECTIVE ROLE OF LHL4 UNDER NATURAL SUNLIGHT EXPOSURE</b>	

91	
5. SUMMARY .....	92
<b>CHAPTER 5: GENERAL DISCUSSION AND CONCLUSIONS.....</b>	<b>94</b>
1. LHL4 IS A NON-CANONICAL ELIP .....	94
2. LHL4 IS AN ELIP THAT LIMITS THE PSII PHOTOINHIBITION IN <i>C. REINHARDTII</i>	95
2.1. LHL4 limits PSII photoinhibition by limiting photooxidative stress regulation.....	95
2.1.1. Hypothesis 1: LHL4 may regulate pigment biosynthesis.....	95
2.1.2. Hypothesis 2: LHL4 may bind free chlorophylls to prevent <sup>1</sup> O <sub>2</sub> formation .....	97
2.2. Physiological role of LHL4 in natural light conditions .....	98
3. NEW INSIGHTS ON THE REGULATION OF UV-B- AND HL-INDUCED SIGNALLING PATHWAYS IN <i>C. REINHARDTII</i> .....	99
3.1. Relative importance of the HY5 and CO transcription factors in the UV-B response .....	99
3.2. Involvement of CO and the COP1 E3 ubiquitin ligase in the UV-B and high light-induced cellular responses in <i>C. reinhardtii</i> .....	100
3.3. Regulation of the HL response by SPA1 in <i>C. reinhardtii</i> .....	101
3.4. Existence of secondary signalling pathways involved in HL response .....	102
3.4.1. Potential role of another photoreceptor(s).....	102
3.4.2. Alternative pathway for LHCSR3 induction in high light.....	103
4. CONCLUSIVE REMARKS.....	104
<b>CHAPTER 6: MATERIALS AND METHODS.....</b>	<b>107</b>
1. <i>C. REINHARDTII</i> STRAINS AND CULTURE CONDITIONS.....	107
1.1. Provenance of the different genotypes .....	107
1.2. Chlamydomonas liquid cultures and storage .....	107
2. LIGHT ACCLIMATIONS & TREATMENTS.....	108
2.1. UV-B and high light (HL) treatments.....	108

2.2.	<b>Bleaching experiments</b> .....	<b>110</b>
2.3.	<b>Outdoor experiments</b> .....	<b>110</b>
3.	<b>GENETIC ENGINEERING OF CHLAMYDOMONAS BY CRISPR-CAS9</b> .....	<b>110</b>
3.1.	<b>Donor DNA design and paromomycin resistance plasmid</b> .....	<b>110</b>
3.2.	<b>Preparation and assembly of the CRISPR/Cas9 complex</b> .....	<b>111</b>
3.3.	<b>Cell transformation</b> .....	<b>111</b>
4.	<b>NUCLEIC ACID ANALYSIS</b> .....	<b>112</b>
4.1.	<b>Quick genomic DNA extraction</b> .....	<b>112</b>
4.2.	<b>PCR analysis</b> .....	<b>113</b>
4.3.	<b>Purification and sequencing of PCR products</b> .....	<b>114</b>
4.4.	<b>RNA extraction</b> .....	<b>114</b>
4.5.	<b>RT-qPCR analysis</b> .....	<b>115</b>
4.6.	<b>RNA-seq analysis</b> .....	<b>117</b>
5.	<b>PROTEIN ANALYSIS</b> .....	<b>118</b>
5.1.	<b>Protein extraction</b> .....	<b>118</b>
5.1.1.	<i>Total protein extraction</i> .....	118
5.1.2.	<i>Protein quantification</i> .....	118
5.1.3.	<i>Membrane-enriched protein extraction</i> .....	119
5.2.	<b>Western blots</b> .....	<b>119</b>
5.2.1.	<i>Sample preparation</i> .....	119
5.2.4.	<i>Immunodetection of proteins</i> .....	122
5.3.	<b>Blue-native (BN)-PAGE and second dimension (2D)</b> .....	<b>122</b>
5.3.1.	<i>Sample preparation</i> .....	122
5.3.2.	<i>Separation of complexes by electrophoresis under non-denaturing conditions (Blue-native-PAGE)</i> .....	124
5.3.3.	<i>Analysis of complexes by 2D electrophoresis under denaturing conditions</i> .....	125
5.4.	<b>List of antibodies</b> .....	<b>126</b>

5.5. Mass spectrometry (MS)-based proteomic analyses .....	126
6. PHYSIOLOGICAL MEASUREMENTS OF PHOTOSYNTHESIS .....	128
6.1. Principle of chlorophyll fluorescence measurements.....	128
6.2. Estimation of photosynthetic parameters <i>in vivo</i> .....	130
7. PIGMENT ANALYSIS .....	130
7.1. Pigment extractions.....	130
7.2. HPLC analysis .....	131
8. SINGLET OXYGEN ( $^1O_2$ ) MEASUREMENTS.....	131
9. EXPANSION MICROSCOPY .....	131
<b>TABLE OF FIGURES .....</b>	<b>133</b>
<b>TABLE OF TABLES .....</b>	<b>136</b>
<b>BIBLIOGRAPHY .....</b>	<b>137</b>
<b>SYNTHESE EN FRANÇAIS.....</b>	<b>160</b>

# LIST OF ABBREVIATIONS

**ADP/ATP:** Adenosine di/triphosphate

**BN:** Blue native

**CBB:** Calvin-Benson-Bassham cycle

**Chl:** Chlorophyll

**ChR:** Channelrhodopsin

**CHS:** Chalcone synthase

**CO:** CONSTANS

**COL:** CONSTANS-like

**COP1:** Constitutively photomorphogenic 1

**CP43:** Core Antenna Protein 43

**CPF:** Cryptochrome Photolyase Family

**CRY:** Cryptochrome

**CRY-DASH:** Drosophila Arabidopsis Synechocystis Homo

**CUL4-DDB1:** Cullin4-Damaged DNA Binding protein 1

**Cyt b<sub>6</sub>f:** Cytochrome *b<sub>6</sub>f*

**DEG:** Degradation of periplasmic proteins

**ELIP:** Early light-induced protein

**FAD:** Falvin Adenin Dinucleotide

**FC:** Fold change

**Fd:** Ferredoxin

**FMN:** Flavin mononucleotide

**FNR:** Ferredoxin NADP<sup>+</sup> reductase

**GPXH:** Gluthatione peroxidase

**HCF:** High chlorophyll fluorescence

**hit:** High light tolerant

**HL:** High light

**HY5:** Elongated hypocotyl 5

**HYH:** HY5 homologue

**LHC:** Light harvesting complex

**LHCI:** PSI antenna complex

**LHCII:** PSII antenna complex

**LHCSR:** Light harvesting complex stress-related

**LHL4:** LHC-like 4

**LIL/SEP:** Light harvesting like/Stress-enhanced protein

**LL:** Low light

**LOV:** Light, oxygen, or voltage domain

**MTHF:** Methenyltetrahydrofolate

**NAD:** Nicotinamide adenine dinucleotide

**NADPH:** Nicotinamide adenine dinucleotide phosphate

**NPQ:** Non-photochemical quenching

**OHP/HLIP:** One-helix protein/High light induced protein

**PBCP:** PSII core phosphatase

**PC:** Plastocyanin

**PHOT:** Phototropin

**PHR:** Photolyase Homologous Region

**PIF:** Phytochrome interactive factor

**PPH1/TAP38:** Protein phosphatase 1/Thylakoid associated phosphatase 38

**PQ:** Plastoquinone

**PQH<sub>2</sub>:** Plastoquinol

**PSBS:** Photosystem II subunit S

**PSI:** Photosystem I

**PSII:** Photosystem II

**qE:** Energy-dependant quenching

**qH:** sustained quenching

**qI:** Photoinhibition

**qM:** Chloroplast movement-dependant

**qT:** State transition

**qZ:** Zeaxanthin-dependant quenching

**RING:** Really Interesting New Gene motif

**ROS:** Reactive oxygen species

**RUP:** Repressor of UV-B photomorphogenesis

**SOSG:** Singlet oxygen sensor green

**SPA:** Suppressor of PHYA

**STT7:** State transition 7

**U-ExM:** Ultrastructure expansion microscopy

**UV-A/B:** Ultraviolet A/B

**VDE:** Violaxanthin de-epoxidase

**WT:** Wild type

**ZEP:** Zeaxanthin epoxidase

**<sup>1</sup>O<sub>2</sub> :** Singlet oxygen

# **CHAPTER 1:**

## **GENERAL INTRODUCTION**

---

### **1. BIODIVERSITY OF GREEN PHOTOSYNTHETIC ORGANISMS**

#### **1.1. Emergence of the green lineage**

Photosynthesis in eukaryotes takes place in a dedicated organelle called a plastid. Plastids have evolved from a primary endosymbiosis event that occurred 1.5 billions years ago, involving a heterotrophic host and a photosynthetic cyanobacterium (McFadden 2001). Later during evolution, a secondary endosymbiosis event occurred, involving a heterotrophic host which established a symbiosis with a primary endosymbiont, reducing the latter to a plastid state (e.g. in diatoms), (Falconet 2012).

Here, we will focus on the "green" lineage, or "Viridiplantae", which is a lineage of organisms derived from a primary endosymbiosis, as well as the "red" (Rhodophytes) and "blue" (Glaucophytes) lineages. The green lineage refers to all plants (plants and algae) with a green plastid, i.e. a plastid with a pigment content rich in chlorophyll, resulting from primary endosymbiosis (all green plants and most green algae) or secondary endosymbiosis with a green alga (other green algae: Chlorarachniophytes and Euglenophytes). It includes, among others, some organisms used as model system by plant biologists: the flowering plant *Arabidopsis thaliana*, the bryophyte *Physcomitrella (Physcomitrium) patens*, or the green microalga *Chlamydomonas reinhardtii* (**Fig. 1.1**).

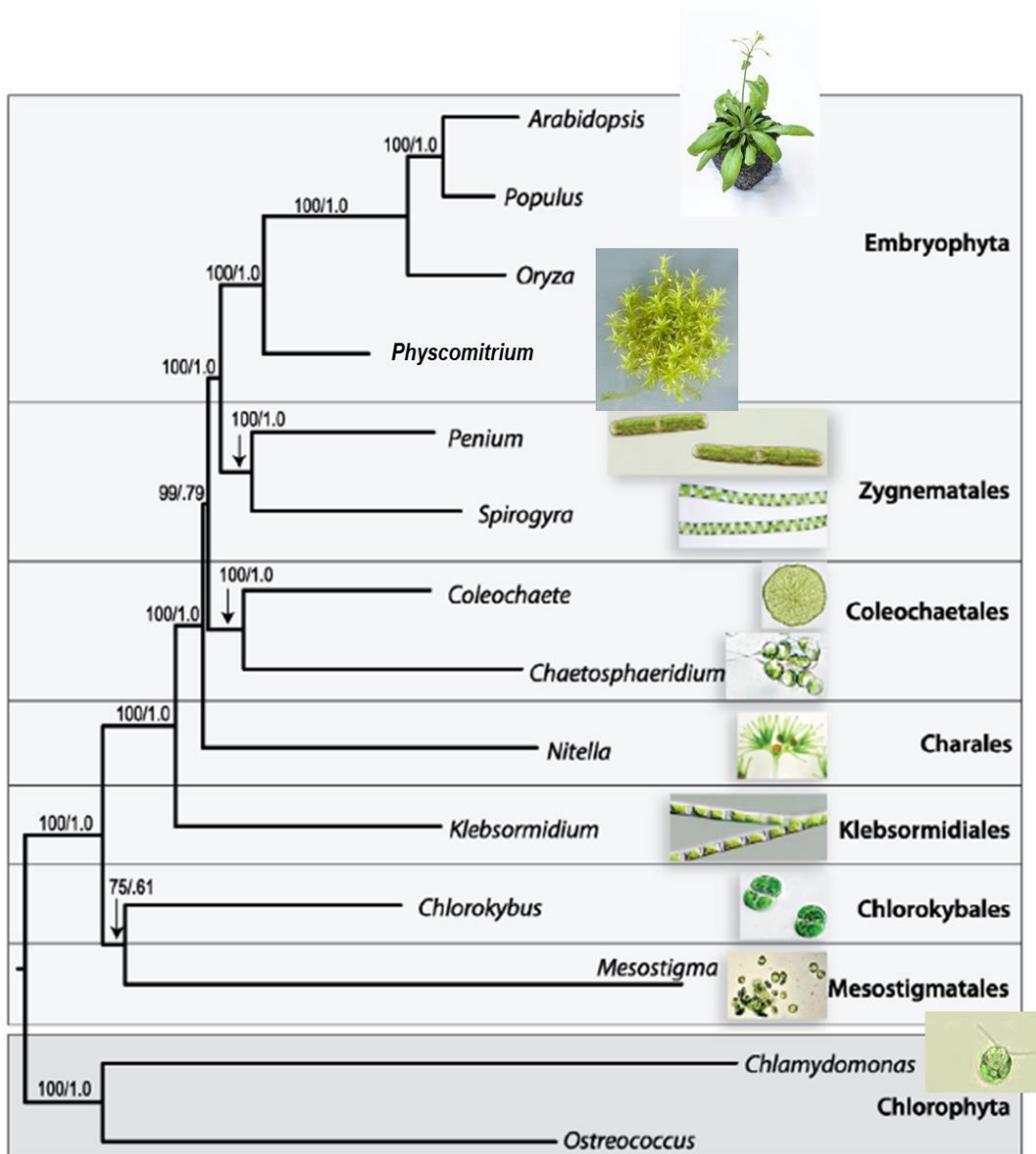


Figure 1.1: Phylogenetic relationships of 14 Viridiplantae taxa. Adapted from Timme et al., 2012

## 1.2. The model green microalga *Chlamydomonas reinhardtii*

The thesis work presented in this manuscript focuses on *Chlamydomonas reinhardtii*, which was the organism used in this PhD project.

*C. reinhardtii* is the most studied photosynthetic unicellular organism. It belongs to the green lineage, phylum Chlorophyta, and consists in a biflagellated microalga that has a diameter of approximately 10  $\mu\text{m}$  and is often found in freshwater environments such as ponds and lakes (Sasso et al. 2018). This alga has two equal apical flagella which allow it to swim, and a cell wall composed of glycoproteins. A single chloroplast containing a pyrenoid occupies a large volume of the cytoplasm (up to 50%). Near the chloroplast, a

primitive eye, the eye-spot, mediates the perception of some light. This eye is essential for phototaxis (the ability to swim towards or away from a light source) (Schmidt et al. 2006) **(Fig. 1.2)**.

One of the most significant advantages of using *C. reinhardtii* as a model organism is its relatively small and fully sequenced genome. The genome of *C. reinhardtii* is approximately 120 000 kbp, and it has been completely sequenced since 2007 (Merchant et al. 2007), which makes it a good organism for genetic studies. *C. reinhardtii* is also amenable to genetic engineering, which has enabled the creation of various genetically modified strains that are now available for specific research purposes (<https://www.chlamycollection.org/>). These modified strains have been used to investigate various aspects of metabolism, cell signaling pathways, and photosynthesis. Indeed, *C. reinhardtii* has been studied widely for its ability to carry out photosynthesis and adapt to various environmental conditions, due to its ability to grow under a range of light intensities and the ability to perform mixotrophy.

In addition to its scientific significance, *C. reinhardtii* has many applied research. It is a valuable source of biomass, and its lipid content can be used to produce biofuels (Scranton et al., 2015; Banerjee, Ray et al., 2021). It is also being investigated as a potential food supplement for human consumption (Masi et al. 2023). The use of *C. reinhardtii* as a model organism has also provided transferable knowledge to use other green microalgae for similar applications.

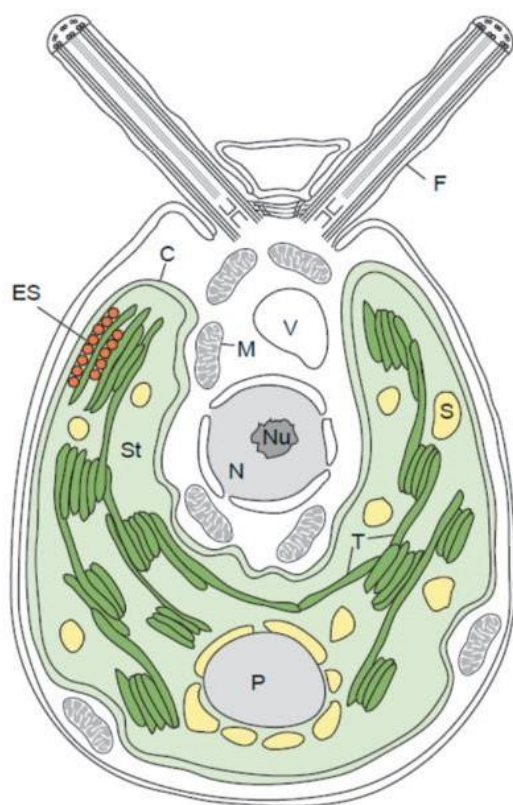


**Figure 1.2: The morphology of *Chlamydomonas reinhardtii*.** The scheme shows the nucleus (N) with the nucleolus (Nu) in the center. It is surrounded by the large cup- shaped chloroplast (C) with the thylakoid membranes (T), stroma (St), starch grains (S) and the pyrenoid (P) inside. The pyrenoid inside the chloroplast houses large amounts of RuBisCo and is the place of CO<sub>2</sub> assimilation into starch. The eye-spot (ES) is located beside the inner envelope membrane of the chloroplast. Two flagella (F) branch from the apical region where is also the contractile vacuole (V) located. In the cytoplasm several mitochondria (M) are situated. From Volgusheva et al., 2017

## 2. FROM LIGHT TO LIFE: THE USE OF LIGHT IN PLANTS

Light is a primary energy source for photosynthetic organisms. Indeed, it is thanks to the energy of photons that photosynthesis can fulfil its function. The functioning of photosynthesis is based on the excitability by photons of the pigments (in particular chlorophylls) present in the photosynthetic apparatus. When chlorophyll (Chl) is excited by light energy, it passes to singlet-state of excitation ( $^1\text{Chl}^*$ ). To return to a fundamentally stable state, the chlorophyll seeks to transfer this excess energy either by i. using it to fuel photosynthesis (photochemistry), ii. relaxing it in the form of fluorescence, or iii. dissipating it as heat, which is the basis of the process called Non-Photochemical Quenching (NPQ). These three regulatory pathways occur in competition with each other, and their rapid regulation is an essential component for the successful acclimation of photosynthetic organisms to their environment (Müller et al. 2001).

## 2.1. The photosynthetic process

In photosynthetic eukaryotes, photosynthesis takes place in a particular organelle, the chloroplast. The chloroplast contains an internal membrane system called thylakoids, in which photosynthetic electron transfer takes place, and an aqueous matrix, the stroma, where CO<sub>2</sub> is fixed in the form of carbohydrates.

Photosynthesis is generally summarised by the equation:  $6\text{H}_2\text{O} + 6\text{CO}_2 \rightarrow \text{C}_6\text{H}_{12}\text{O}_6 + 6\text{O}_2$  and takes place in two phases: light-dependent reactions, which allow the collection of photons and the formation of energy molecules (NADPH and ATP), and light-independent reactions, which convert CO<sub>2</sub> into carbohydrates for cellular metabolism. Four main protein complexes embedded in thylakoid membranes are involved in light-dependent reactions: photosystem II (PSII), cytochrome b<sub>6</sub>f (Cyt b<sub>6</sub>f), photosystem I (PSI), and ATP synthase (ATPase). PSI and II are protein supercomplexes, and the two main actors in the photosynthetic process. Their structure is divided into two distinct units: the antenna complex, which is dedicated to light harvesting, and the core complex where electron transfer takes place. The two PS are different but have some similarities, such as certain chlorophyll binding proteins and a particular pair of chlorophylls in the core complex that conduct electron transfer (Whitmarsh and Govindjee 1999). The core complexes of the photosystems are well conserved in evolution, and consist of a reaction centre and internal antennae. The PSII core complex contains the D1 and D2 proteins that directly bind the special chlorophyll a pair of PSII (P680), electron transport cofactors, and two internal antenna proteins. In the green lineage, the PSI core complex contains 14 subunits, including three main subunits PSAA, PSAB, and PSAC and their cofactors, as well as the special chlorophyll pair P700 for photochemical conversion (Nelson and Yocum 2006).

All the photosynthetic organisms of the green lineage possess antenna complexes composed of proteins of the Light-Harvesting Complexes (LHC) superfamily (**Table 1.1**). These proteins bind a large amount of light-harvesting pigments (i.e. chlorophylls *a* and *b*, and carotenoids), in varying proportions (Green and Durnford, 1996; Nelson and Ben-Shem, 2005). These antenna complexes are encoded in the nuclear genome, transported to the chloroplast and associated with PSI (LHC1 complex composed of LHCA proteins) or PSII (LHCII complex composed of LHCB proteins). In *A. thaliana*, 4 LHCA are associated with PSI, and 6 LHCB are associated with PSII (Jansson 1999). In *C. reinhardtii*, the antenna complexes are larger, with 9 subunits for LHCI and LHCII (Büchel 2015). Interestingly, as

mentioned above, photosystem core-complexes also contain internal antennae, such as CP43 and CP47 for PSII.

The light phase of photosynthesis begins with the absorption of photon by the pigments of the LHCI and LHCII antenna complexes. This energy is then transferred to the neighbouring pigment, and eventually excites a chlorophyll pair in the reaction centre (P680 or P700), which initiates electron transfer. The energy of the excited chlorophyll is used for charge separation to fuel a chain of redox reactions. This reaction chain enables the reduction of the plastoquinone (PQ) pool to plastoquinol (PQH<sub>2</sub>). PQH<sub>2</sub> then binds to Cyt b<sub>6</sub>f and reduces its cofactors, releasing two protons (H<sup>+</sup>) into the lumen. The electrons are then transferred to plastocyanin (PC) when it reoxidises the Cyt b<sub>6</sub>f complex, and it transfers them to PSI. When PSI is excited by light, it is able to reduce ferredoxin (Fd) resulting in the generation of nicotinamide adenine dinucleotide phosphate (NADPH) molecules via the action of ferredoxin NADP<sup>+</sup> reductase (FNR) (**Fig 1.3**) (Whitmarsh and Govindjee 1999).

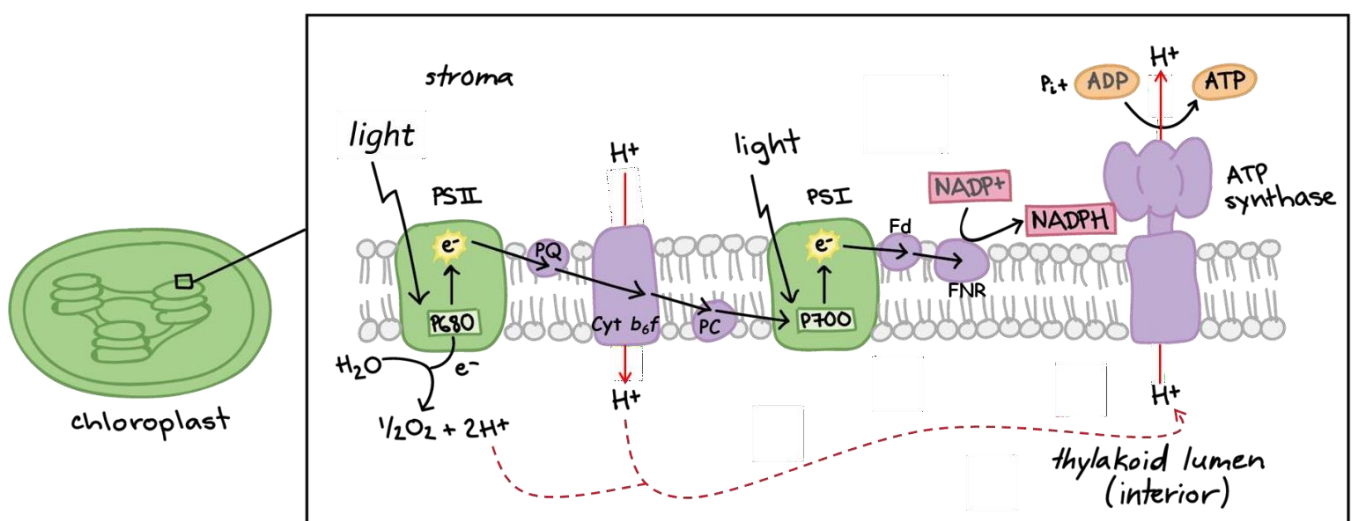


**Figure 1.3: Schematic representation of the photosynthetic linear electrons and protons flows.** Black arrows represent the electrons pathway through the major components of the photosynthetic electron flow chain: photosystem II (PSII), the plastoquinone (PQ) the cytochrome b<sub>6</sub>f complex (Cyt b<sub>6</sub>f) the plastocyanin (PC), the light harvesting complex of the photosystems I (LHCI), the photosystems I (PSI), the ferredoxin (Fd), the enzyme Fd-NADP<sup>+</sup>-oxidoreductase (FNR) and the ATP synthase. Red arrows represent the protons pathway. Green structures contain chlorophyll, purple structures do not. Adapted from <https://www.khanacademy.org/science/ap-biology/cellular-energetics/photosynthesis/a/light-dependent-reactions>

In parallel to the charge separations in photosystems, protonation/deprotonation reactions occur on both sides of the thylakoid membrane during electron transfer leading to the formation of a proton gradient across the membrane ( $\Delta$ pH), between the stroma

and the lumen. This gradient is used to phosphorylate adenosine diphosphate (ADP) to adenosine triphosphate via the action of ATPase.

The NADPH and ATP produced during the light phase of photosynthesis are then used during the light-independent phase to fix atmospheric CO<sub>2</sub> in the form of carbohydrates via the Calvin-Benson-Bassham Cycle (CBB; Benson and Calvin, 1950).

## **2.2. Photoinhibition (qi)**

The light environment in which photosynthetic organisms live is extremely variable, and can lead to dangerous situations affecting their growth and performance. While low light (LL) can limit growth by restricting photosynthetic productivity, excessive light can lead to the production of Reactive Oxygen Species (ROS), thus generating photooxidative stress within cells (e.g., Niyogi and Truong, 2013).

In the most extreme cases, during prolonged light stress, photoinhibition (qi) of the photosynthetic apparatus can occur. Photoinhibition corresponds to the degradation and disassembly of the PSII core complex due to light stress, leading to a general decrease in photosynthetic quantum yield (Aro et al., 1993; Long et al., 1994). The degree of photoinhibition depends on the balance between degradation and repair of PSII (Murata et al. 2007). Furthermore, the degradation of these proteins leads to the release of chlorophylls which then become an important source of ROS (singlet oxygen in particular), which in turn can increase the degradation of core proteins of photosystems, thus increasing photoinhibition in a kind of chain reaction (Krieger-Liszkay 2005; Murata et al. 2007).

However, this critical stage of photoinhibition is usually reached within an hour (Eberhar et al., 2008), which gives photosynthetic organisms time to activate photoprotective mechanisms to protect themselves from the deleterious effects of high light (HL) (Demarsy et al., 2018) (**Fig 1.4**).

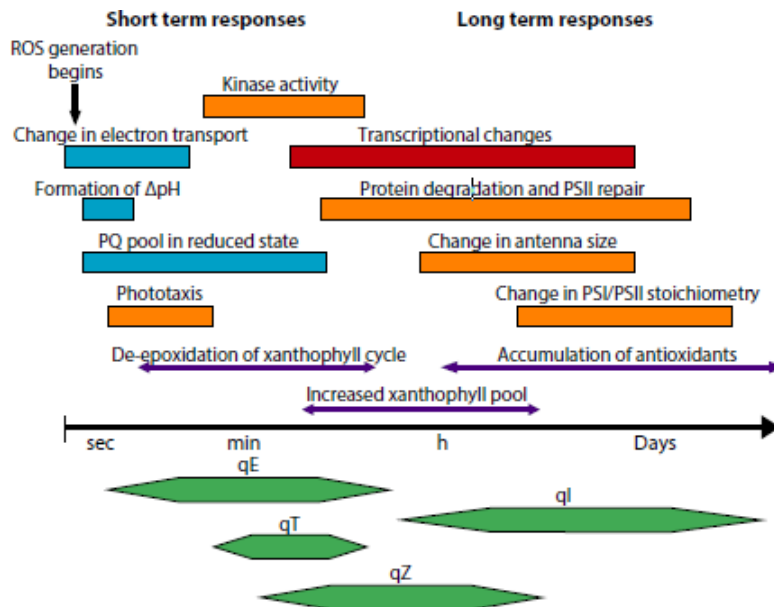


**Figure 1.4: Relative time scales of short-term and long-term responses to excess light.** Non-photochemical quenching processes (qE, qZ, qT, and qI) are shown in green. Changes in protein expression or activity are shown in orange. Transcriptional responses, like the up-regulation of high-light-induced and stress-response genes and the down-regulation of LHCII genes, are shown in red. Changes in the chloroplast energetic state are shown in blue, and changes in pigment properties and accumulation are shown in purple. From Erickson et al., 2015.

## 2.3. Photoprotection to cope with excess light

### 2.3.1. Non-photochemical quenching (NPQ)

NPQ is the major short-term response to excess light energy. In plants, several components of NPQ have been identified based on the rates of their relaxation (Horton, et al., 1996; Dall'Osto et al., 2005; Joliot and Finazzi, 2010; Sohbat, 2022). The fastest component is the energy-dependent quenching, qE, which is activated and relaxed in less than a minute in plants. This is followed by the qT state transition, and zeaxanthin-dependent (qZ) quenching, which relaxes within min (Erickson et al., 2015) (**Fig 1.4**).

#### 2.3.1.1. Energy-dependant NPQ (qE)

The qE is the major component of NPQ, and basically is the dissipation of excess light energy in the form of heat. qE mainly takes place at the LHCII level (Horton et al., 1996). The qE is triggered by i. the acidification of the lumen, caused by a large pH gradient across the thylakoid membrane as a consequence of the saturation of the electron flow in HL, ii. the activation of specific qE effector proteins (Niyogi and Truong 2013).

Effector proteins exist in all photoautotrophic eukaryotes organisms. This is the case for the LHCSR3s (LIGHT-HARVESTING COMPLEX STRESS-RELATED) whose expression is inducible in green algae such as *C. reinhardtii*, and also in mosses (Peers et al. 2009; Alboresi et al. 2010; Niyogi and Truong 2013; Tokutsu and Minagawa 2013). Three genes encoding three isoforms of LHCSR3s are present in the *C. reinhardtii* genome (Merchant et al. 2007). Two of them, *LHCSR3.1* (Cre08.g367500) and *LHCSR3.2* (Cre08.g367400) code for LHCSR3 proteins that show 99% identity (259 aa). The third gene is a paralogue of *LHCSR3.1* and *3.2* and code for LHCSR1 protein (256 aa; Cre08.g365900). LHCSR1 and LHCSR3 share 80% identity (Bonente et al. 2011) and are LHC-like proteins with three transmembrane helices, which contain binding sites for chlorophylls a/b and for carotenoids. LHCSR3s are nucleus-encoded and then addressed to the chloroplast, where they insert in the membrane of thylakoids (Bonente et al. 2011). In 2009, Peers et al. showed that *npq4*, a double mutant of *LHCSR3.1* and *LHCSR3.2* exhibits a greatly reduced qE capacity compared to a WT, demonstrating that LHCSR3 is the main player in qE in *C. reinhardtii* (Peers et al. 2009). Petroustos et al. have also shown that LHCSR3 accumulation requires active photosynthesis, as well as Ca<sup>2+</sup> binding protein CAS (CALCIUM SENSOR) and Ca<sup>2+</sup> ion-induced signalling (Petroustos et al. 2011). A secondary function in qE has been assumed for LHCSR1 for a long time due to its high percentage identity with LHCSR3, but the essential contribution of LHCSR1 to qE has only recently been shown in the context of UV-B induced photoprotection in *C. reinhardtii* (Allorent et al. 2016). Moreover, it seems that both LHCSR3s act possibly as quenching sites (Tokutsu and Minagawa 2013) and as sensors of luminal acidification, thanks to several residues at their C-terminal end (aspartate and glutamate) essential for NPQ induction (Ballottari et al. 2016). While many studies have been done on LHCSR3, relatively little data exists on the mechanics of LHCSR1. However, it appears that both proteins mediate qE via different mechanisms, and that LHCSR1 might be more related to PSI (Kosuge et al. 2018).

In diatoms, LHCX proteins play a similar role to green lineage LHCSR3s in qE activation (Zhu and Green 2010; Bailleul et al. 2010; Lepetit et al. 2013). Among the four LHCX isoforms identified in the diatom *Phaeodactylum tricornotum*, it is interesting to note that one of them (LHCX1) is constitutively present in the cells and maintains a basal level of qE (Bailleul et al. 2010).

This is also the case for the PSBS (PHOTOSYSTEM II SUBUNIT S) protein which is always present in *A. thaliana* and essential for the establishment of qE in this plant (Li et al. 2000).

PSBS is composed of four transmembrane helices and not three, and does not bind pigments (Fan et al. 2015). In *C. reinhardtii*, two genes encoding orthologs of *AtPSBS* have been identified: *PSBS1* (Cre01.g016600), and *PSBS2* (Cre01.g016750) which encode a single PSBS protein (only one amino acid is different between the two). Unlike the *A. thaliana* protein, CrPSBS is not constitutively present in cells, and is induced by various stress conditions: UV-B exposure (Allorent et al. 2016), high light (Tibiletti et al. 2016), or low CO<sub>2</sub> (Correa-Galvis et al. 2016). So far, only a few studies have shown that PSBS may slightly modify qE capacity in *C. reinhardtii* but its precise role remains to be clarified, even if these data suggest that PSBS would be of less importance for qE than LHCSR proteins (Allorent et al. 2016; Correa-Galvis et al. 2016; Redekop et al. 2020). Although PSBS has residues that sense luminal acidification like LHCSRs, it does not bind pigments, indicating that it is not the direct quenching site in HL.

#### 2.3.1.2. State transition (qT)

State transition consists of the migration of PSII antennae between PSII and PSI, thus optimising light absorption by the two photosystems. (Bellafiore et al. 2005; Sohbat 2022). Under light conditions favouring PSII excitation over PSI, the reduced state of the PQ pool activates the protein kinase STT7 (STATE-TRANSITION 7, in *C. reinhardtii*)/STN7 (flowering plants) by binding to Cyt b<sub>6</sub>f (Dumas et al. 2017). The kinase then phosphorylates some antennae of the LHCII complex which then migrate to the PSI, increasing its light absorption capacity. This mechanism is referred to as state 2 transition (Krause and Weis 1991; Ruban and Johnson 2009; Sohbat 2022). The reverse process is catalysed by the phosphatases PPH1/TAP38 (PPH1 PROTEIN PHOSPHATASE 1/THYLAKOID ASSOCIATED PHOSPHATASE 38, in flowering plants) and PBCP (PHOTOSYSTEM II CORE PHOSPHATASE, in *C. reinhardtii*) which dephosphorylates the LHCII antennae associated with PSI, which return to PSII (state 1 transition) (Cariti et al., 2020; Goldschmidt-Clermont, 2023).

The amplitude of qT is low in plants (Niyogi 1999) but it has been proposed that up to 80% of antennae can migrate between the two photosystems in *C. reinhardtii* (Delosme et al., 1996). qT is involved in photoprotection under HL in the algae and can also modulate the level of qE (Allorent et al. 2013; Cariti et al. 2020)

#### 2.3.1.3. Zeaxanthin-dependent quenching (qZ)

Analysis of the relaxation kinetics of NPQ showed that qZ is set up after 10-15 min, which corresponds to the time required for the accumulation of zeaxanthin pigment via the xanthophyll cycle. The qZ was therefore identified as zeaxanthin dependent (Nilkens et al. 2010).

Xanthophylls are carotenoids present in the antenna complexes of photosystems and play a major role in photoprotection by facilitating the dissipation of excess light energy as heat. In green lineage organisms, this cycle consists of the two-step conversion of zeaxanthin to violaxanthin via the antheraxanthin intermediate. It is a cycle because this reaction is reversible in the dark or in LL. The conversion are catalysed by VDE (VIOLAXANTHIN DE-EPOXIDASE) and ZEP (ZEAXANTHIN EPOXIDASE) (Hieber et al., 2000). ZEP is associated with the membrane of thylakoids on the stroma side, and VDE is located in the lumen (Schubert et al. 2002). In diatoms, another xanthophyll cycle is also present and predominant, which consists in the conversion of diadinoxanthin to diatoxanthin. The level of NPQ in diatoms has been shown to be proportional of the diatoxanthin level accumulated in the cell (Lohr and Wilhelm 1999; Lavaud et al. 2002).

#### 2.3.1.4. Other components of NPQ

Additional forms of NPQ have also been identified in recent years in *A. thaliana*. In particular, sustained quenching (qH), which protects the photosynthetic apparatus in HL (Malnoë et al. 2018; Malnoë 2018). The qH is a slow component of NPQ that involves PLASTID LIPOCALIN (LCNP) and is repressed by SUPPRESSOR OF QUENCHING 1 (SOQ1) in the absence of light stress. qM, which corresponds to the chloroplast movement-dependent quenching, is dependent on blue light and the phototropin blue light receptor (PHOT). qM was observed in a *phot2* mutant of *A. thaliana*, which is impaired in chloroplast movement and a missing part in the relaxation kinetics of chlorophyll fluorescence (Cazzaniga et al. 2013). However, the consideration of chloroplast movement as a component of NPQ remains controversial at present (Sohbat 2022).

#### 2.3.2. *The family of LHC-like proteins and its variants*

In green lineage, light energy is collected by LHC proteins in the antennae, which thus power fuel photosynthesis by transferring this energy to photosystems. LHCs form a large

multigene family in which most members generally consist of three transmembrane helices proteins that can bind chlorophyll a and b, as well as carotenoids (Kühlbrandt et al., 1994; Liu et al., 2004). Moreover, LHC-distant relative proteins called "LHC-like" proteins also exist, and are found in a wide range of organisms, from cyanobacteria to land plants, algae and mosses. These LHC-like proteins consist of one to four transmembrane helices with chlorophyll *a/b* binding sites that contain conserved amino acid sequences considered as "LHC motifs": E\*\*NGR\*AM\*G or E\*\*HAR\*AM\*G (Rochaix and Bassi 2019). These LHC-like proteins consist in the one-helix proteins (OHPs or HLIPs, HIGH LIGHT-INDUCED PROTEINS) originated from cyanobacteria, and the two- and three-helix proteins involved in various light responses, including: SEPs (STRESS-ENHANCED PROTEINS) also called LILs (LIGHT-HARVESTING-LIGHT), LHCSRs, and ELIPs (EARLY LIGHT-INDUCED PROTEINS). They also include the PSBS protein, which is the only one to contain four helices and does not bind pigments (**Tableau 1.1**, Rochaix and Bassi 2019).

Protein	Organism	Number of helices	Function
PSBS	Land plants, mosses, algae	4	qE-NPQ (land plants, mosses) acclimation to UV-B
LHCSR1	Green and brown algae, non-vascular plants, diatoms	3	qE-NPQ
LHCSR3	Green and brown algae, non-vascular plants, diatoms	3	qE-NPQ
CrLHCBM1	<i>C. reinhardtii</i>	3	qE-NPQ
CrLHCBM9	<i>C. reinhardtii</i>	3	Acclimation to high light
ELIP	Land plants, mosses, algae	3	Response to high light
MSF1	<i>C. reinhardtii</i>	3	Assembly of photosynthetic complexes
SEP/LIL	Land plants, algae	2	Acclimation to stress, chlorophyll biosynthesis
OHP1, HLIP	Land plants, algae, cyanobacteria	1	Acclimation to stress, assembly of photosynthetic complexes
OHP2	Land plants, algae, cyanobacteria	1	Acclimation to stress, assembly of photosynthetic complexes

**Table 1.1: LHC-like proteins involved in stress responses and assembly of photosynthetic complexes, from Rochaix et Bassi, 2019.**

On the basis of structural analyses, an evolutionary link between cyanobacterial OHPs and the green lineage proteins LHCS and ELIPs has been postulated (Green et Kühlbrandt 1995; **Fig. 1.5**). Indeed, the basic structure of these two protein families suggests that they may have originally been two prokaryotic OHPs (A and B). The genes encoding these OHPs would have fused during evolution, resulting in an intermediate protein with two helices (AB; Heddad and Adamska 2002). A further duplication and fusion step would then have resulted in the appearance of the PSBS family (four transmembrane helices;

ABAB). This hypothesis is supported by the fact that in the PSBS proteins, helices 1 and 3 (black in **Fig. 1.5**) are very similar in their amino acid sequences, as helices 2 and 4 (white in **Fig. 1.5**). Finally, helix 4 has been lost by deletion, resulting in proteins with three transmembrane helices (ABAs) in which the amino and carboxyl ends are on opposite sides of the thylakoid membrane, as is the case in LHCs and ELIPs (**Fig. 1.5**) (Green and Kühlbrandt 1995). However, while these two groups of proteins are similar in structure and have conserved amino acid sequences in the transmembrane helices, it is important to note that they differ in the size and composition of the connecting loops between the helices (longer in LHC than in ELIPs, see **Fig. 1.5**). Their binding to pigments is also different, since in the case of ELIPs, the exact composition of the pigments bound by the proteins is unknown (Montané and Kloppstech 2000).

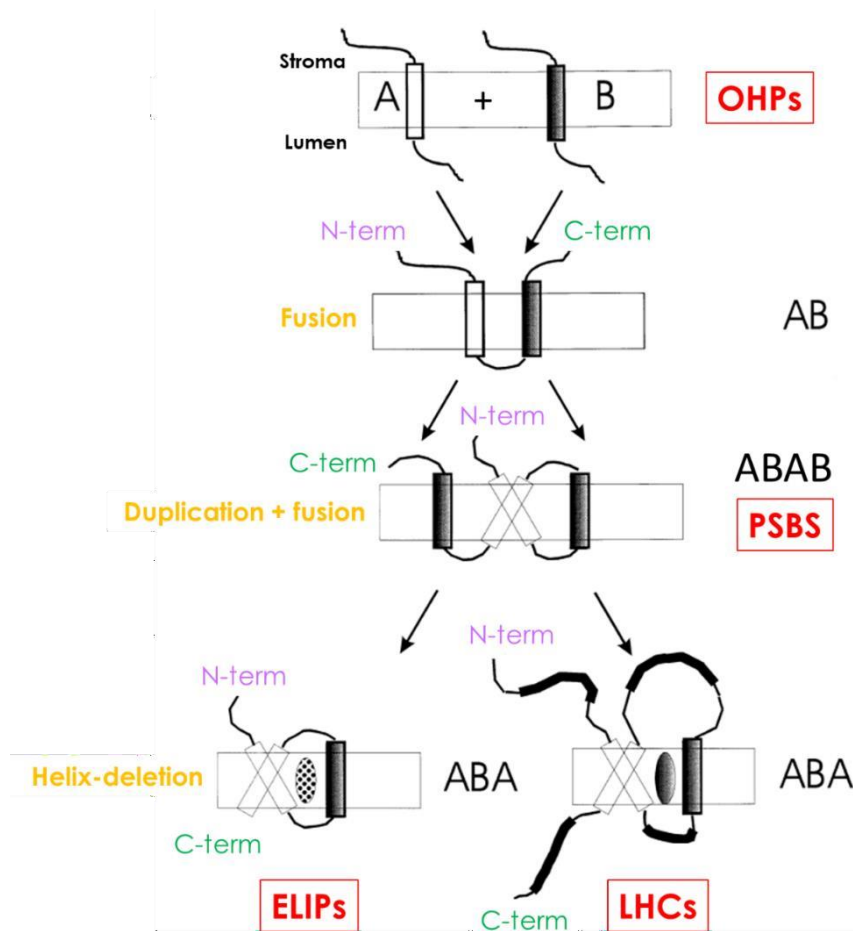


**Figure 1.5: Schematic representation of the evolution of OHPs to LHCs and ELIPs proteins.** Two gene fusion and duplication steps of two Ohps genes (A and B) gave rise to a four-helix form (ABAB), that resembles the modern PSBS protein. Proteins that may represent an intermediate (AB) were detected in Heddad et Adamska, 2000. Then the evolutionary process diverges to give rise to the three-helix ELIPs and LHCs. The ellipses represent pigments bound by these proteins. Adapted from Montané et Kloppstech, 2000.

Thus, as a result of this process, two groups of proteins with complementary functions would have been generated: LHCs are highly accumulated in photosynthetic cells to allow light collection under non-saturating conditions, and ELIPs are induced in response to

high light intensities when LHCs are repressed, and predicted to have a photoprotective function (Montané and Kloppstech 2000; Hutin et al. 2003; Rochaix and Bassi 2019).

The inducibility of ELIPs is the main difference with LHCs. Unlike LHCs, which are very abundant structural components of photosynthetic membranes (Jansson 1999), ELIPs accumulate in plant cells transiently and in substoichiometric amounts (1 ELIP per 10-20 PSII reaction centres in pea, Adamska 1997). In addition to light stress, other conditions can induce *ELIP* genes expression such as dehydration (Adamska and Kloppstech 1994; Xiao et al. 2015; Challabathula et al. 2018; Marks et al. 2021), or low temperature (Shimosaka et al., 1999; Pedron et al., 2009; Lee et al., 2020). However, the exact function and importance of ELIPs in the response to these various stresses remains debated.

In *C. reinhardtii*, 10 genes have been identified as belonging to the ELIP family. One of them, ELIP3, is a homolog of AtELIPs and has been studied in the context of resistance to cold-induced photooxidative stress, suggesting a protective function of CrELIPs (Lee et al. 2020). However, the other 9 CrELIPs are not characterised and *C. reinhardtii* remains poorly studied within this context.

### 2.3.3. Long-term responses

Exposure of photosynthetic organisms to high light intensities induces multiple responses within the cells that modify the photosynthetic apparatus. Over the long term, the photoprotective responses involve the activation/repression of certain genes responsible for a diverse range of responses in the cell. For example, long-term acclimation control changes in the PSII/PSI ratio, chloroplast movements, and even the compression and decompression of thylakoid membranes to optimise the efficiency of photosynthesis according to environmental conditions (Raven and Geider 2003; Erickson et al. 2015). The ultimate relevance of all these responses is to prevent photoinhibition under chronic HL exposure (**Fig 1.4**).

In addition to being a source for the cell's energy metabolism, light is also an essential source of information for plant organisms. Indeed, plants are able, via an elaborate set of photoreceptors, to perceive the colour of light and induce corresponding physiological responses. The photoreceptors found in the green lineage, as well as the functions they regulate, are presented in the next part of this introduction.

### 3. LIVING UNDER THE LIGHT: NOT ONLY A MATTER OF LIGHT QUANTITY, BUT ALSO A MATTER OF LIGHT COLOR

#### 3.1. A brief overview of photoreceptor diversity in photosynthetic organisms

Plants use numerous and varied photoreceptors to cover a wide spectrum of wavelengths (from UV-B to far-red), and thus detect and respond efficiently to changes in light. These photoreceptors have chromophores capable of sensing light, which is then converted into biological signals controlling various processes (gene expression, photo-orientation, circadian rhythm training, development, ...). In flowering plants, photoreceptors can be divided into five major families: phytochromes which mainly absorb red and far-red light; flavoproteins: cryptochromes, phototropins, zeaxanthin family proteins which are activated by UV-A and blue light; and the UV-B photoreceptor, UVR8 (Galvão and Fankhauser 2015; Allorent and Petroustos 2017) (**Fig. 1.6A**). Phytochromes and the blue light photoreceptors bind different chromophores (phytochromobilin and flavin-containing chromophore, respectively) (Chaves et al. 2011; Suetsugu and Wada 2013; Burgie and Vierstra 2014; Galvão and Fankhauser 2015). In contrast, UVR8 photoactivation relies on intrinsic properties of its sequence and structure, specifically on a triad of tryptophan residues, and not on a chromophore cofactor (Rizzini et al. 2011; Christie et al. 2012; Wu et al. 2012).

Among these five families, only three are found in the microalgae *C. reinhardtii*: cryptochromes, phototropins, and UVR8, with slight differences with photoreceptors characterised in flowering plants. In addition, *C. reinhardtii* also possesses blue-green light photoreceptors found only in algae: channelrhodopsins (**Fig. 1.6B**) (Flori 2016; Allorent and Petroustos 2017).

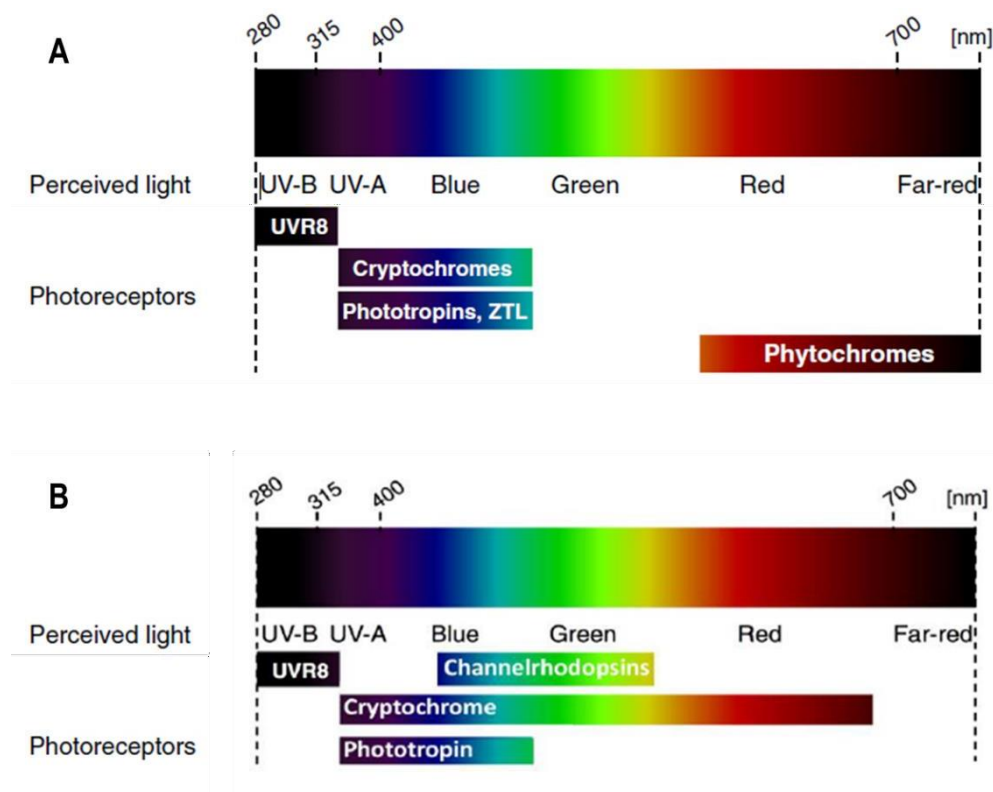


**Figure 1.6: Photoreceptor proteins with their spectral specificities.** (A) Five photoreceptor families found in flowering plants. Adapted from Heijde and Ulm, 2012. (B) Photoreceptors in *C. reinhardtii*. From Flori 2016.

### 3.2. Focus on the green lineage photoreceptors currently identified in *C. reinhardtii*

#### 3.2.1. Channelrhodopsins (ChRs)

Rhodopsins are a family of photoreceptors involved in vision in animals, and in mobility in both eukaryotic and prokaryotic microorganisms (Kateriya et al. 2004). In contrast, channelrhodopsins (ChRs) are found only in algae, and were originally identified in *C. reinhardtii* (Nagel et al. 2002).

*C. reinhardtii* has two ChRs (ChR1 and ChR2), which are located in the eye spot, a carotenoid-rich sensory organ that allows the alga to "see" light, and act as photoreceptors sensitive to blue-green light (maximum absorption at 500 nm) thanks to an ATR (all-trans retinylidene, an aldehyde derivative of vitamin A) chromophore (Kateriya et al. 2004). They are proton and calcium channels consisting of seven transmembrane domains. The channels open when excited by light, which depolarises the membrane and initiates a transducer signal triggering activation of the flagellar motors (Kateriya et al. 2004; Lin 2011). In this way, ChRs control a process called phototaxis (or

directed movement), which enables flagellated algae to move towards or away from a light source in order to find optimal light conditions for growth. In the case of sudden strong illumination, the cells also show a photophobic response by moving away from the light source (Witman 1993; Allorent and Petroustos 2017). In *C. reinhardtii*, phototaxis is controlled by both ChRs while the photophobic response appears to depend mainly on ChR1 as well as partially on the phototropin blue light photoreceptor (Hegemann 1997; Govorunova et al. 2004).

### 3.2.2. *UV-A and blue-light photoreceptors*

*C. reinhardtii* can sense UV-A (315-400 nm) and blue light (400-500 nm) by using two families of photoreceptors: phototropins and cryptochromes.

#### 3.2.2.1. Phototropin (PHOT)

Phototropins are blue light photoreceptors present in the entire green lineage. PHOTs structure consists in N-terminal photosensory region composed of two flavin mononucleotide (FMN) chromophore-binding light oxygen voltage (LOV1 and LOV2) domains, and one C-terminal Serine/Threonine protein kinase domain (Suetsugu and Wada 2013). At the molecular level, blue light induces the covalent binding of the FMN to LOV1 and LOV2 domains, which induces conformational changes leading to the release of the kinase domain (C-terminal) previously inhibited by the photosensory domain (N-terminal) (Suetsugu and Wada 2013). The following signalling events differ depending on the physiological response, but unfortunately only few substrates of PHOT protein kinase activity are known (e.g. the NONPHOTOTROPIC HYPOCOTYL 3 (NPH3) for phototropism) (Christie et al. 2011; Demarsy et al. 2012; Takemiya et al. 2013; Sullivan et al. 2021).

The flowering plants, like *A. thaliana*, possess two independent phototropins encoded by *PHOT1* and *PHOT2* (Okajima 2016). PHOTs are localized to the plasma membrane, but blue light mediates the partial internalization of PHOT1 to the cytoplasm, and PHOT2 is addressed to the Golgi apparatus (Suetsugu and Wada 2013).

PHOT1 and PHOT2 present various and partially overlapping physiological functions. For example, both of them regulate hypocotyl phototropism in response to high light intensities (Sakai et al. 2001) but, under low light, hypocotyl growth is only mediated by PHOT1 (Liscum and Briggs 1995; Sakai et al. 2001; Sakamoto and Briggs 2002). In

addition, the blue light rapid inhibition of hypocotyl elongation of dark-grown seedlings requires PHOT1 only (Folta and Spalding 2001).

They both promote cotyledon (Ohgishi et al. 2004) and leaf (Sakamoto and Briggs 2002) expansion in *A. thaliana*, and have a role in light-induced leaf movement in kidney bean (Inoue *et al.*, 2005). The two PHOTs mediate other light responses in *A. thaliana*, like blue light-induced stomatal opening (Kinoshita et al. 2001) in leaves and stem, which allows plants to regulate CO<sub>2</sub> uptake to fuel photosynthesis and water loss.

Under low blue light intensity, PHOT1 (and to a lesser extent PHOT2) induces the chloroplast accumulation to the upper cell surface in order to improve light capture for photosynthesis (Sakai et al. 2001). In high light conditions, chloroplasts move away from light (Wada *et al.*, 2003) to prevent photodamage (Kasahara et al. 2002), and this avoidance movement is mediated by PHOT2 only (Kagawa et al. 2001; Jarillo et al. 2001). Altogether, the PHOT-mediated blue-light responses serve to improve photosynthesis and enhance plant growth (Takemiya et al. 2005). Gene expression analysis show that PHOTs have a minor function in transcriptional regulation in Arabidopsis seedlings (Ohgishi et al. 2004). However, it was proposed that PHOT1 is required to destabilize specific nuclear transcripts (the LIGHT HARVESTING CHLOROPHYLL-BINDING (*LHCB*) gene family) and chloroplast transcripts *RCBL* (RIBULOSE-1,5-BIPHOSPHATE CARBOXYLASE) in response to high blue light intensity (Folta and Kaufman 2003).

The **Figure 1.7** summarizes all the above mentioned functions of PHOTs in *A. thaliana*.

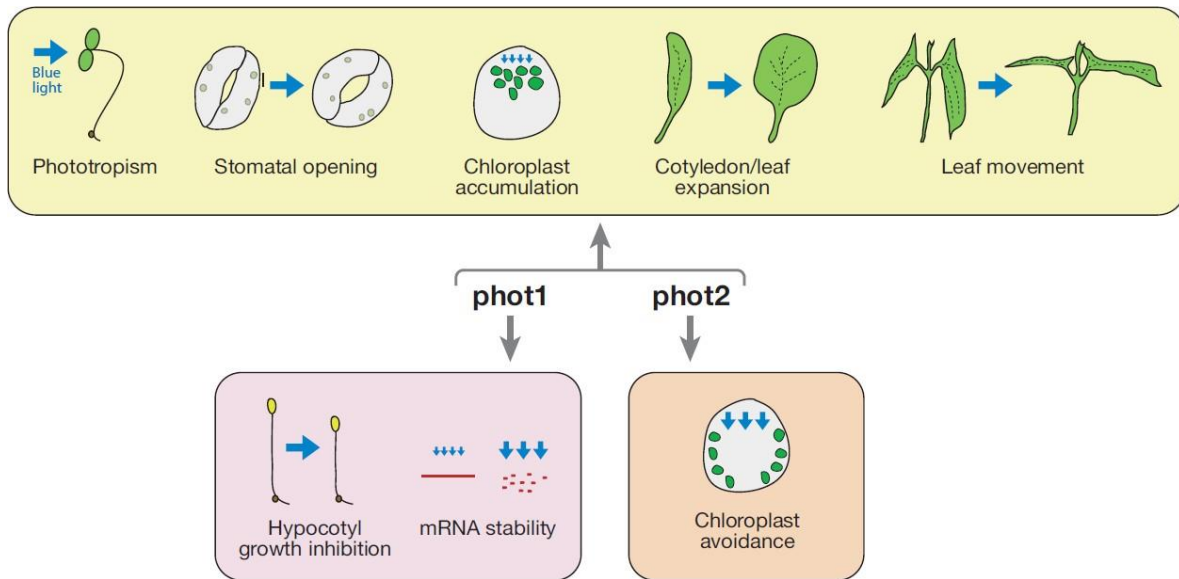


**Figure 1.7: Summary of phototropin-mediated responses in flowering plants.** From Christie, 2007.

*PHOT* genes can also be found in non-flowering plants. Ferns, like *Adiantum capillus-veneris*, have two phototropins and AcPHOT2 is involved in chloroplast avoidance movement, as in *A. thaliana* (Kagawa et al. 2001). *A. capillus-veneris* also have a neochrome photoreceptor, which is a chimeric protein containing a phytochrome photosensory domain fused to the N-terminal of an entire PHOT receptor (Nozue et al. 1998; Suetsugu et al. 2005; Christie 2007). However, fern species present a lack in blue light stomatal responses despite having PHOTs (Doi et al. 2006).

In the moss *Physcomitrella (Physcomitrium) patens* four PHOTs have been identified and mediate the chloroplast movements (Kasahara et al. 2004). On the algae side, the filamentous green alga *Mougoetia scalaris* owns two PHOTs like *Arabidopsis*, but also two neochromes, which seem to have arisen independently of the ferns (Suetsugu et al. 2005). In contrast, the green microalga *C. reinhardtii* has only one *PHOT* gene, which induces blue light-dependant sexual differentiation, photosynthetic gene expression, and influences eyespot parameters and phototactic response (Huang and Beck 2003; Im et al. 2006; Trippens et al. 2012). Furthermore, PHOT plays a key role in the regulation of photoprotection as it controls the induction of the key NPQ player LHCSR3 when cells are exposed to high light (Petroutsos et al. 2016). CrPHOT is targeted to the plasma membrane and the flagella, whereas other photoreceptors are mainly localized in the nucleus (Huang et al., 2004; Schmidt et al., 2006). Unlike flowering plant phototropins, the blue light-mediated activation of CrPHOT induces major changes at the transcriptomic

level, especially for the *GLE* gene encoding the GAMETIC LYTIC ENZYME responsible of the cell wall digestion of gametes before cell fusion in *C. reinhardtii* sexual reproduction (Huang and Beck 2003). However, even if the function of CrPHOT is different from its flowering plant counterparts, the *PHOT* gene in *C. reinhardtii* can restore PHOT signaling pathway in the double mutant *phot1phot2* of *A. thaliana* (Onodera et al. 2005), suggesting that the mechanism of action of this photoreceptor is highly conserved between flowering and non-flowering plants. Nevertheless, the substrates of PHOT in *C. reinhardtii* have not been identified yet.

### 3.2.2.2. Cryptochromes (CRYs)

Cryptochromes (CRYs) are a large family of photoactive molecules present in a wide variety of animals and plants (which we will focus on in this manuscript), but also in some prokaryotes. From a structural point of view, CRYs are close to photolyases, which are enzymes that use light energy to repair UV damage to DNA. CRYs, on the other hand, function primarily as signalling molecules that regulate various biological responses (Lin and Todo 2005; Chaves et al. 2011). The N-terminal PHR (Photolyase-Homologous Region) part of CRYs is highly conserved in the living kingdom and non-covalently binds up to two chromophores capable of absorbing light: a flavin adenine dinucleotide (FAD) and a methenyltetrahydrofolate (MTHF). In contrast, the C-terminal parts are variable, even among cryptochromes of the same species (e.g. AtCRY1 and AtCRY2 of *A. thaliana*) (Lin et al. 1995; Malhotra et al. 1995; Liu et al. 2011).

CRYs are consistently present in plant cell and, as soluble proteins, they accumulated in the nucleus and/or cytosol (Imaizumi *et al.*, 2000; Yang *et al.*, 2000; Wu and Spalding, 2007; Jourdan *et al.*, 2015). Photoactivation of plant CRYs begins with photoreduction of the FAD chromophore, which changes its phosphorylation status and induces conformational changes. These changes lead to the release of the C-term end of the PHR (Lin et al. 1995; Wang and Lin 2020), allowing the formation of the CRYs homodimer/tetramer, which constitutes the active form of the photoreceptor (Shao et al. 2020; Fraikin 2022).

CRYs are involved in many aspects of life cycle regulation in flowering plants like *A. thaliana*, in particular via the E3 ubiquitin ligase AtCOP1/SPA complex. For examples, CRYs promote deetiolation, circadian rhythm entrainment, biotic and abiotic stress response, inhibition of hypocotyl elongation, initiation of flowering, regulation of shade

avoidance, high light acclimation, ... (Wang and Lin 2020; Ponnu and Hoecker 2022). The main physiological functions regulated by AtCRY are presented below, in the **Figure 1.8**.

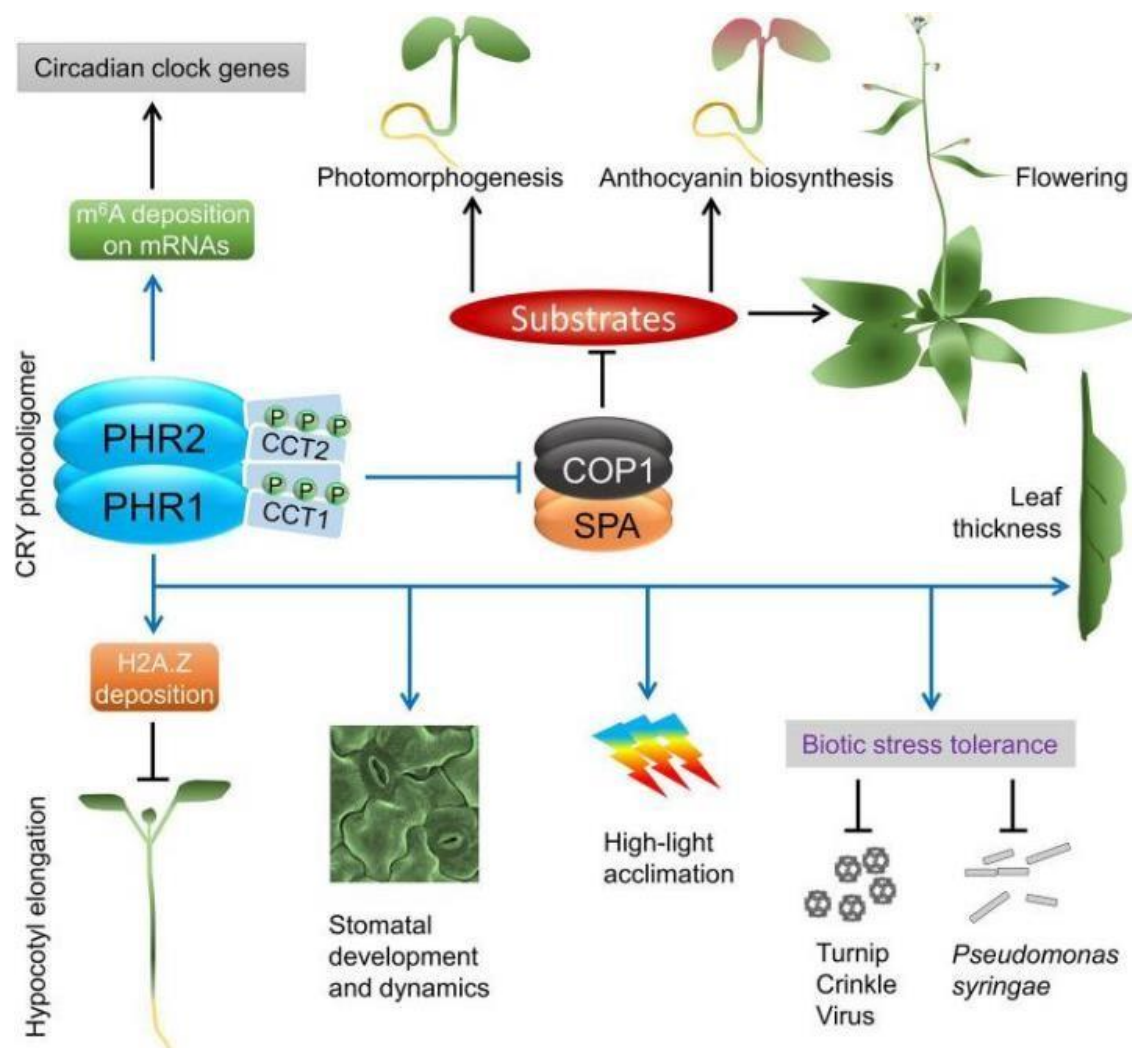


**Figure 1.8: An overview of cryptochrome signaling in *A. thaliana*.** Blue lines and arrows represent the direct involvement of CRYs. Abbreviations: PHR, photolyase homology region; CCT, CRY carboxy terminus; COP1; SPA; m<sup>6</sup>A, methylation of N6 adenosine; H2A.Z, a variant of histone H2A. From Ponnu and Hoecker, 2022.

Moreover, in bryophytes such as *Physcomitrella (Physcomitrium) patens* and *Marchantia polymorpha*, it appears that CRYs are also involved in plant development, via the repression of phytohormone signals (Imaizumi et al. 2002; Liao et al. 2023).

Green algae, on the other hand, possess a more diverse array of cryptochromes (plant-like cryptochromes, animal-like, and CPFs in addition to the plant cryptochrome) (Essen et al. 2017; Kottke et al. 2017; König et al. 2017). In algae, members of the Cryptochrome Photolyase Family (CPF1) also retain photolyase activity, as is the case for the CPF1s present in the diatom *Phaeodactylum tricornutum* and the green alga *Ostreococcus tauri* (Coesel et al. 2009; Heijde et al. 2010; Kottke et al. 2017).

In addition, the CRYs of algae perceive a wider part of the light spectrum than those of land plants. For example, the microalga *C. reinhardtii* has an animal-like cryptochrome (aCRY) that responds to red and yellow light in addition to blue light, and is mainly present in the nucleus (day time), and in the cytosol (night time) (Beel et al. 2012; Zou et al. 2017; Kottke et al. 2017). CraCRY influences transcripts encoding proteins in the chlorophyll and carotenoid biosynthetic pathway, light harvesting complexes, nitrogen metabolism, the sexual cycle, and the circadian rhythm (Beel et al. 2012; Kottke et al. 2017). In addition, some studies suggest that CraCRY is the photoreceptor that compensates for the absence of phytochromes in *C. reinhardtii* by controlling the response to red light (Mittag et al., 2005; Beel et al., 2012, 2013; Kottke et al., 2017). *C. reinhardtii* also possesses a plant cryptochrome (pCRY), which is a blue light photoreceptor localized in the nucleus of the cell (Kottke et al. 2017). CrpCRY plays a central role in the regulation of circadian rhythm (Müller et al. 2017). In addition, like CraCRY, CrpCRY plays a key role in the sexual reproduction of *C. reinhardtii* and influences the regulation of zygote germination (positive regulation), gamete mating ability, and mating maintenance (negative regulations). Depending on the stage of the sexual cycle, CrCRYs act in concert or antagonistically with CrPHOT (Huang and Beck 2003; Müller et al. 2017; Zou et al. 2017; Kottke et al. 2017).

### 3.2.2.3. Cryptochromes DASH (CRY-DASHs)

CRY-DASHs (*Drosophila*, *Arabidopsis*, *Synechocystis*, *Homo*) are a subfamily of cryptochromes (Brudler et al. 2003), identified in at least 140 genomes of very diverse organisms (cyanobacteria, fungi, plants, vertebrates,...) (Chaves et al. 2011), and exhibiting DNA repair activity (Selby and Sancar 2006; Pokorny et al. 2008). The first CRY-DASH characterised in plants was identified in *A. thaliana* and named CRY3. AtCRY3 was detected in the chloroplasts and mitochondria of cells, as well as in the nucleus (Kiontke et al. 2020) and its photolyase activity has been confirmed (Kleine et al., 2003).

CRY-DASHs identified in microorganisms additionally display photoreceptor activity (Kiontke et al. 2020; Wang and Lin 2020). In some fungi, CRY-DASHs are involved in light-regulated development and secondary metabolism (Castrillo *et al.*, 2013) and regulate the UV-A response (Veluchamy and Rollins 2008). This photoreceptor function to UV-A has also been confirmed in the cyanobacterium *Synechocystis* PCC 6803 where CRY-DASH mediates, among other things, the repair of PSII under light stress (Vass et al. 2014).

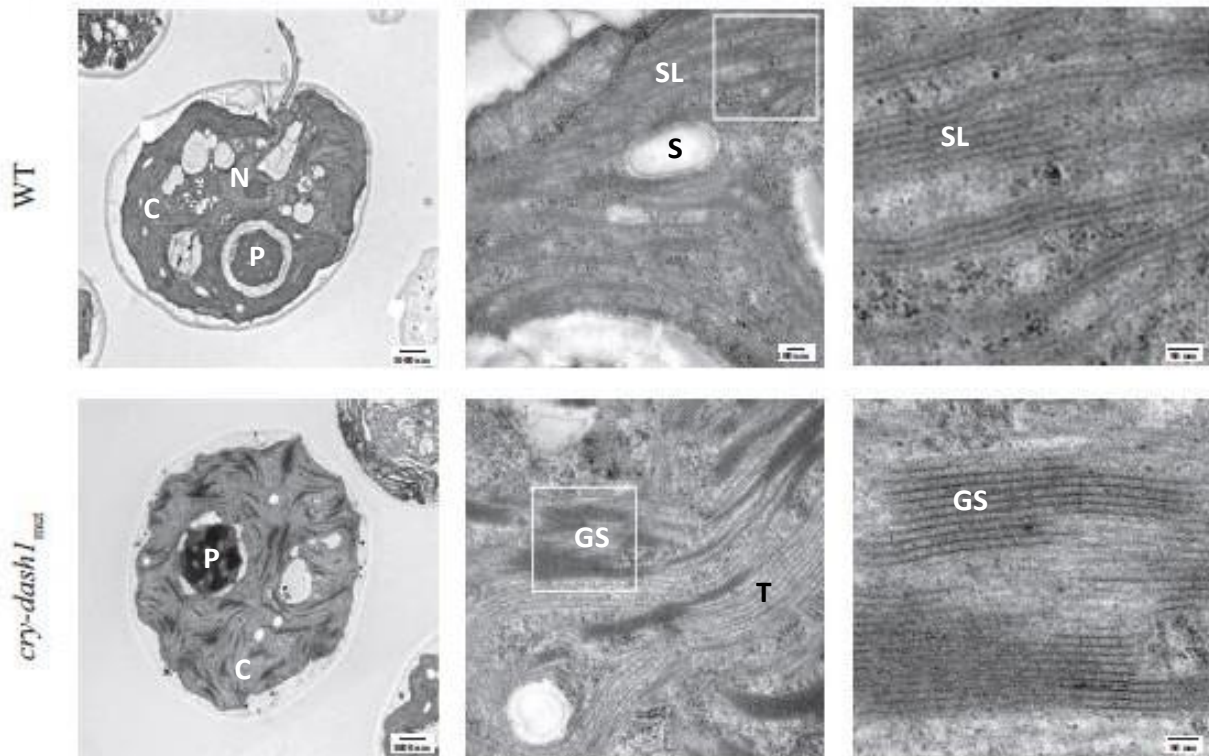


**Figure 1.9: Grana stacking of *C. reinhardtii* is increased in *cry-dash1*<sub>mut</sub> (*CRY-DASH1*, *DASH* cryptochrome 1).** Electron microscopy. Ultrastructure of *C. reinhardtii* wild-type (WT) and *cry-dash1*<sub>mut</sub> cells. It was found that hyper-stacking occurs in the grana part of the thylakoid membranes in *cry-dash1*<sub>mut</sub>. C: chloroplast; N: nucleus; P: pyrenoid; S: starch; SL: stroma lamellae; GS: grana stacks. Adapted from Rredhi et al., 2021.

Kottke et al. showed that out of 9 green algal genomes analysed, all of them contain at least one gene encoding a CRY-DASH1-like protein, and in some of them a more distant CRY-DASH2-like protein can additionally be found (Kottke et al. 2017). In *C. reinhardtii*, two CRY-DASHs have been identified in the genome, CrCRY-DASH1 and CrCRY-DASH2 (Beel et al. 2012). CrCRY-DASH1 was recently studied and identified as a UV-A photoreceptor. CrCRY-DASH1 is located in the chloroplast, and uses light as a source of information to regulate the alga's photoautotrophic growth and photosynthetic machinery (Rredhi et al. 2021). The *Crcry-dash1* mutant shows significant alterations in its photosynthetic apparatus, with hyper-stacking of grana (**Fig. 1.9**), as well as an

increase in the amount of PSII core proteins, demonstrating the importance of CrCRY-DASH1 in the regulation of photosynthesis. Interestingly, the absorption maximum of CrCRY-DASH1 in the UV-A (388 nm) corresponds exactly to the area of the spectrum where the absorption of blue light photoreceptors (CraCRY, CrpCRY, CrPHOT) is minimal, indicating that in *C. reinhardtii* this area of the light spectrum is extremely well covered and probably of high importance (Rredhi et al. 2021).

### 3.2.3. The UV-B photoreceptor: UVR8

Plants perceive and respond to UV-B via the UVR8 photoreceptor, and acclimate themselves to the harmful effects of these wavelengths through genetic and morphological changes (Favory et al. 2009; Rizzini et al. 2011; Jenkins 2014). UVR8 is a highly conserved photoreceptor in plants, present in a large number of species belonging to the green lineage. (Rizzini et al. 2011; Di Wu et al. 2012; Fernández et al. 2016).

UVR8 is a 440 amino acid protein fold into a seven-bladed  $\beta$ -propeller (Christie et al. 2012; Wu et al. 2012) and it presents a singular light perception mechanism since it does not depend on an exogenous chromophore. Instead, UVR8 uses a tryptophan triade (W233, W285, and W337) formed by three packed Gly-Trp-Arg-His-Thr motifs (GWRHT) to sense UV-B light, with a major role of W285 (Rizzini et al. 2011; Christie et al. 2012; Wu et al. 2012). In cell, UVR8 is present as an inactive homodimer, which is converted in an active monomer after UV-B irradiation (Rizzini et al. 2011; Christie et al. 2012; Wu et al. 2012). After UV-B absorption, the salts bridges flanking the tryptophan residues are disrupted, which leads to a UV-B-dependent reversible monomerization of UVR8 and initiates UV-B molecular signalling (Rizzini et al. 2011; Christie et al. 2012; Wu et al. 2012; Heijde and Ulm 2013).

The UVR8 receptor of the model organism *A. thaliana* was identified by screening mutants with a UV-B hypersensitivity. *UVR8* mutation results in a necrosis of the first true leaves and cotyledons (Kliebenstein et al. 2002a) (**Fig. 1.10A**), a decrease in stomatal movement (**Fig 1.10B**), a decrease in photosynthetic capacity (Davey et al. 2012), and an impairment of UV-B-induced suppression of hypocotyl elongation (Favory et al. 2009) (**Fig. 1.10C**). The mutation of *UVR8* in *A. thaliana* also blocks the expression of hundreds UV-induced genes, including the chalcone synthase (CHS), that causes a lack of UV-induced flavonoids and anthocyanin (Kliebenstein et al., 2002; Brown et al., 2005; Favory et al., 2009).

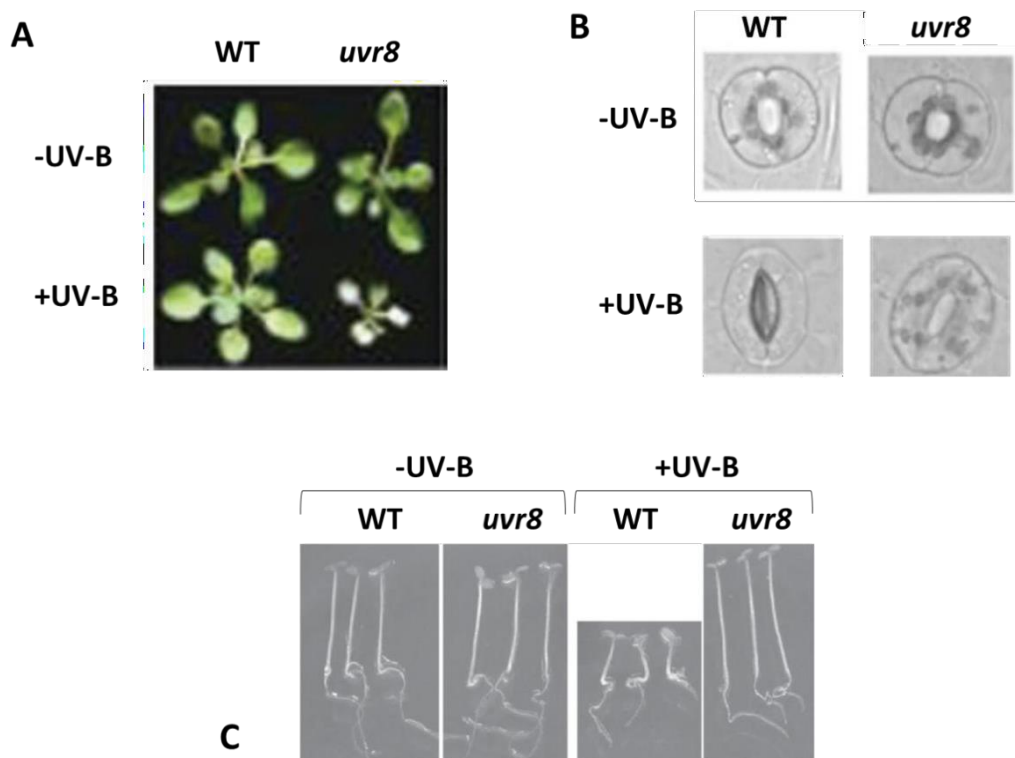


**Figure 1.10:** Impact of the *uvr8* mutation in *A. thaliana* on growth (A), stoma closure (B), and hypocotyl elongation (C) compared to the wild type (WT) before and after a UV-B exposure. Adapted from Kliebenstein et al. 2002, Tossi et al. 2014, and Favory et al. 2009 respectively.

In addition, UVR8 is involved in phototropic bending, and circadian clock, in flowering plants (Fehér et al. 2011; Tossi et al. 2014; Vandenbussche et al. 2014).

In *A. thaliana*, UVR8 signalling has been well described (**Fig. 1.11**) (Podolec et al. 2021). Once monomerized, UVR8 binds to the E3 ubiquitin ligase CONSTITUTIVELY PHOTOMORPHOGENIC 1 (COP1), thereby repressing the activity of the complex that COP1 forms with the SUPPRESSOR OF PHYA (SPA). This repression leads to the stabilisation of the key transcription factor ELONGATED HYPOCOTYL 5 (HY5). A negative regulatory loop is also active in this signalling pathway, in order to prevent deleterious effects of constitutive UVR8 signalling that could affect plant growth and development. Signalling pathways usually have a negative regulatory loop to control the response. The importance of such a regulatory pathway in the case of UV-B signalling is underlined by the dwarf phenotype observed in the UVR8 overexpressor in *A. thaliana* (Favory et al. 2009). The negative regulators of UVR8 signalling pathway has been identified as the REPRESSOR OF UV-B PHOTOMORPHOGENESIS (RUP1 and RUP2 in *A. thaliana*) proteins.

RUP interacts directly with UVR8 and facilitates its redimerisation and thus inactivation (Gruber et al. 2010; Heijde and Ulm 2013; Tilbrook et al. 2013).

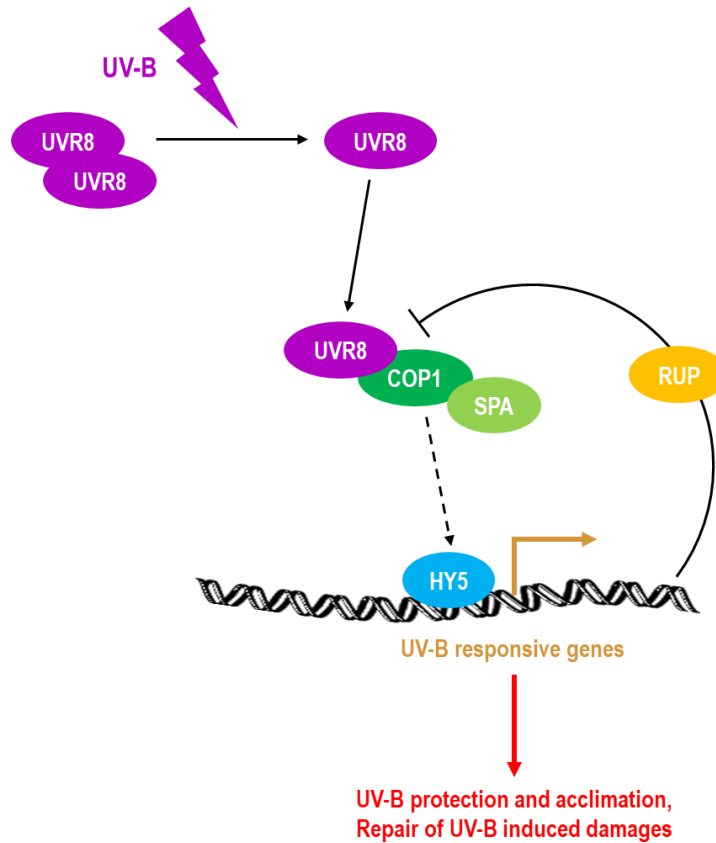


**Figure 1.11: Model of the UVR8 signalling pathway in *A. thaliana*.** When it senses UV-B radiation, UVR8 monomerises and interacts with COP1. Therefore, the activity of the COP1/SPA complex is inhibited and the bZIP transcription factor HY5 is stabilised and UV-B-responsive genes are activated. Based on Heijde and Ulm, 2012.

In bryophytes, such as the moss *Physcomitrella (Physcomitrium) patens* or the liverwort *Marchantia polymorpha* (Mp), UVR8 is also present. On the one hand, according to Soriano et al. 2018, two *UVR8* genes that encode both functional proteins are found in *P. patens* while *A. thaliana* has only one *UVR8* gene encoding one protein. Moreover, in *Physcomitrella*, UVR8 monomerizes in the presence of UV-B, but in white light both dimers and monomers are detected. On the other hand, the single *uvr8* gene of *M. polymorpha* expresses two transcripts by alternative splicing, which code for two functional proteins found in the nucleus. In addition, in *M. polymorpha*, UVR8 is accumulated as monomer independently of UV-B treatment, and the homodimer is weakly present (Soriano et al. 2018).

In the green micro alga *C. reinhardtii*, CrUVR8 dimers monomerize after UV-B exposure and re-form when the cells go back to white light as in *A. thaliana* (Tilbrook et al. 2016). It has also been shown that CrUVR8 is a key regulator of photoprotection in *C. reinhardtii*, and triggers the accumulation of NPQ players LHCSR1 and PSBS (and LHCSR3 to a lesser extent) upon UV-B exposure (Allorent et al. 2016). It is also of note that an ortholog of *AtRUP1/RUP2* has been identified in *C. reinhardtii* (Cre01.g053850). *CrRUP* expression is induced by UV-B exposure in *C. reinhardtii*, and is dependent on UVR8, further demonstrating that the UV-B signalling pathway has been evolutionarily conserved within the green lineage (Tilbrook et al. 2016).

In all the species mentioned, as well as in angiosperms species (e.g. *Chrysanthemum morifolium*, *Populus euphratica*, and *Malus domestica*), the heterologous expressions of their UVR8 proteins rescued the UV-B-deficient phenotype of *uvr8* mutants in *A. thaliana* (Mao et al. 2015; Tilbrook et al. 2016; Zhao et al. 2016; Yang et al. 2018; Soriano et al. 2018). These data provide evidences that these different UVR8 receptors are functional and similar to the one described for *A. thaliana*. This also suggests the existence of UVR8 in green lineage ancestral organisms, that could be related to the elevated UV-B dose in the primitive atmosphere from which the first photosynthetic plants required protection (Jenkins 2017).

Finally, UVR8 homologues can also be found in photosynthetic organisms that are not part of the green lineage. For example, a putative UVR8 has been identified in diatoms based on their sequence homology with AtUVR8 (identity below 40%) (Fernández et al. 2016). However, despite the fact that the "GWSHS" motif containing the tryptophan W337 important for AtUVR8 activity is present, no studies have yet shown that this diatom "UVR8" has photoreceptor activity or is even involved in the UV-B response. As another example, UVR8 presents structural similarities with the human REGULATOR OF CHROMATIN CONDENSATION1 (RCC1), without presenting any homology of function with the latter (Brown et al. 2005; Jenkins 2009). Note also that the key motif for UVR8 activity, "GWRHT", is missing from the RCC1 sequence.

The photoreceptors currently identified in *C. reinhardtii* and their functions are summarized in the figure below (**Fig. 1.12**).

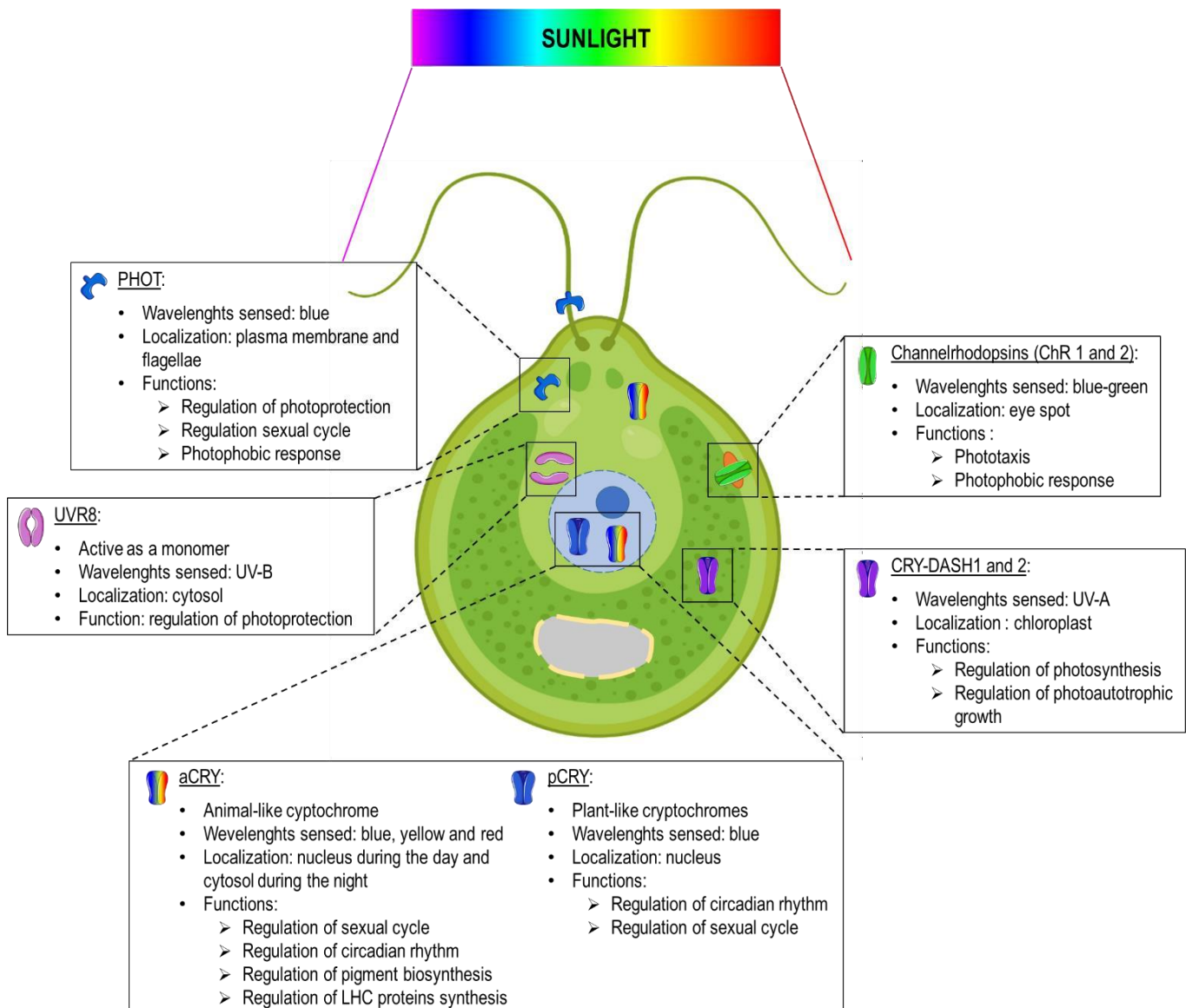


**Figure 1.12: A schematic summary of the different photoreceptors of *C. reinhardtii*, with their intracellular location and identified functions.**

### 3.3. Common photoreceptor signaling components

In plants, downstream of the photoreceptors, different actors are shared between the different light signalling pathways.

#### 3.3.1. The COP1/SPA1 complex

The COP1 protein is widely conserved in animals and plants (Han et al. 2020), whereas SPAs are only found in the green lineage (Ranjan et al. 2014).

The COP1/SPA E3 ubiquitin ligase complex is a key repressor of photomorphogenesis in flowering plants (Lau and Deng 2012; Hoecker 2017). Indeed, the knockdown mutant (KO is seedling lethal) *Atcop1* showed in *A. thaliana* constitutive photomorphogenesis, as did the quadruple mutant *Atspa1234* (McNellis et al. 1994; Laubinger et al. 2004; Podolec and Ulm 2018).

COP1 is composed of three functional domains: a Really Interesting New Gene (RING)-finger motif required for ligase activity at the N-terminus, a coiled-coil domain for dimerization, and a domain containing seven WD40 repeats at the C-terminus that is involved in binding to target proteins (Yi and Deng 2005; Podolec and Ulm 2018). The SPA proteins are part of a small family of four members (SPA1, SPA2, SPA3, and SPA4) all sharing similar structures, including a coiled-coil domain, a domain containing four WD40 repeats similar to that of COP1, and a kinase-like region (Hoecker et al. 1999; Laubinger et al. 2004). It has been shown *in vivo* that the accessory SPA proteins are required for the E3 ubiquitin ligase activity of COP1, although their exact role remains unclear (Laubinger et al. 2004; Ordoñez-Herrera et al. 2015). Indeed, COP1 and the SPA proteins physically interact via their respective coiled-coil domains to form a tetrameric complex consisting of two COP1 and two SPA, with any of the SPA proteins (Zhu et al. 2008). This tetramer also acts as a substrate adaptor for the CULLIN4-DAMAGED DNA BINDING PROTEIN 1 (CUL4-DDB1)-based E3 ubiquitin ligase complex, which has been proposed to enhance the COP1/SPA-dependent E3 ubiquitin ligase activity (Lau and Deng 2012). Subsequently, the COP1/SPA complex, which is localized in the nucleus, targets a wide range of transcription factors (including HY5 and CO) involved in photomorphogenesis. Many of these transcription factors contain a conserved valine-proline domain that interacts directly with the WD40 domain of COP1. These transcription factors are then ubiquitinated by the COP1/SPA complex and degraded (Holm et al. 2001, 2002; Jang et al. 2005; Uljon et al. 2016).

In *A. thaliana*, the activity of the AtCOP1/SPA complex is required for seedling etiolation in the dark. This process must then be inhibited in the light, and this inhibition is mediated by phytochrome, cryptochrome, and UVR8 photoreceptors (Hoecker 2017; Yin and Ulm 2017; Podolec and Ulm 2018). Exposure to UV-B leads to activation of the UVR8 photoreceptor via its monomerization. AtUVR8 monomers then interact directly with AtCOP1 at the WD40 repeat domain. However, unlike other photoreceptors, AtUVR8 does not interact with the SPA part of the AtCOP1/SPA complex (Favory et al. 2009; Heijde and

Ulm 2012, 2013; Huang et al. 2013; Podolec and Ulm 2018). Two distinct domains of AtUVR8 enable its interaction with AtCOP1, one at the  $\beta$ -helices and the other in its C-terminus. The latter contains a valine-proline domain similar to that detected by the AtCOP1/SPA complex in its targets, suggesting that AtUVR8 may repress AtCOP1/SPA activity by competing with the targets of this complex (Lau et al. 2019). Indeed, this competition would prevent the ubiquitination and degradation by the proteasome of the target transcription factors of the AtCOP1/SPA complex. Binding of AtUVR8 to AtCOP1 also induces dissociation of AtCOP1/SPA from CUL4-DDB1, thereby inactivating this complex to create a stable UVR8-COP1/SPA complex that could promote the stabilisation of downstream transcription factors (Huang et al. 2013, 2014).

In *C. reinhardtii*, CrCOP1 (Cre02.g085050) an orthologue of AtCOP1 was identified. In contrast to *A. thaliana*, mutations in genes involved in light response is not lethal in *C. reinhardtii*, because this alga can grow in the presence of an external carbon source (mixotrophy). A mutant of CrCOP1 was generated in *C. reinhardtii* and named *hit1* (High Light Tolerant) because of its phenotype showing tolerance to high light and an increased NPQ capacity (Schierenbeck et al. 2015). CrCOP1 is much longer than AtCOP1 (1444 aa and 675 aa, respectively), but still has the three functional domains described above (a RING-finger motif, a coiled-coil domain, and a WD40 repeats domain). Furthermore, CrUVR8 interacts with both AtCOP1 and CrCOP1 (originally designated as LRS1, LIGHT RESPONSE SIGNALING PROTEIN 1), and this interaction is specifically induced by UV-B, suggesting that the UVR8 signalling pathway is conserved between *A. thaliana* and *C. reinhardtii* (Tilbrook et al. 2016). In contrast to *A. thaliana*, only one SPA protein has been identified in *C. reinhardtii* (Cre13.g602700), and it is an ortholog of AtSPA1. The study of CrCOP1 and CrSPA1 has so far shown that the two proteins function also as a complex in *C. reinhardtii*. The complex is active in LL, and repressed following exposure to UV-B or HL, allowing CrCOP/SPA1 to regulate the activity of the transcription factor CO under both conditions. Thus, the CrCOP1/SPA1 complex appears to have the same type of function as in *A. thaliana*. Moreover, given its function in UV-B- and HL-induced photoprotection, it is proposed to be regulated by CrUVR8 and CrPHOT (Gabilly et al. 2019; Tokutsu et al. 2019).

### 3.3.2. *bZIP* transcription factors HY5 and HYH

HY5 is a basic leucine-zipper transcription factor (bZIP) that plays a major role in de-etiolation in plants. In the dark, HY5 is one of the targets of the COP1/SPA complex, and is

therefore ubiquitinated and degraded by the proteasome. In the light, however, COP1/SPA activity is inhibited, resulting in the stabilisation of HY5, which then acts as a promoter of photomorphogenesis (Osterlund et al. 2000; Saijo et al. 2003). In this context, HY5 activity is regulated by several photoreceptors: UVR8, CRY, and phytochromes depending on the colour of the perceived light (UV-B, blue, or red respectively) (Gangappa and Botto 2016).

In *A. thaliana*, mutation of *AtHY5* inhibits the transcription of several genes involved in UV-B tolerance, and the *Athy5* mutant exhibits lower tolerance to UV-B than the WT (Ulm et al. 2004; Brown et al. 2005; Favory et al. 2009; Heijde and Ulm 2012). A homolog of *AtHY5*, named *AtHYH* (*HY5 HOMOLOG*), has been identified in *A. thaliana* and shows partial functional redundancy with *AtHY5*. Both transcription factors control the expression of genes targeted by AtUVR8 in UV-B exposure, with a predominant role for *AtHY5* (Brown and Jenkins 2008; Stracke et al. 2010). *AtHY5* and *AtHYH* genes are activated in a UVR8-dependent manner, and the *AtHY5* and *AtHYH* proteins are stabilised by UV-B exposure (Holm et al. 2002; Favory et al. 2009).

*AtHY5* and *AtHYH* form homodimers and heterodimers, and *AtHY5* binds to a T/G-box cis-element of its own promoter and thus induces its own expression in response to UV-B, demonstrating the key role of these transcription factors in the UV-B-induced signalling pathway (Ulm et al. 2004; Heijde and Ulm 2012; Binkert et al. 2014). In addition, *AtHY5* and *AtHYH* also bind to the promoters of other UV-B regulated genes such as *RUP1*, *RUP2*, *COP1*, and *BBX24* (*B-BOX24*) (Binkert et al. 2014).

It has been shown that HY5 functions are conserved in the green lineage. Several *AtHY5* orthologs have been reported such as *LONG1* in *Pisum sativa*, *LeHY5* in tomato, *STF1* in *Glycine max*, *VfBZIPZF* in *Vicia faba*, and *BZF/ASTRAY* in *Lotus japonicus*. All of them seem to be controlled by an ortholog of *AtCOP1* and to perform a similar function to *AtHY5*, although differences exist between their structures (e.g. *LONG1* has an additional RING-finger motif at its N-terminus). Two orthologs have also been identified in the moss *P. patens*, *PpHY5a* and *PpHY5b*, and overexpression of *PpHY5a* in *A. thaliana* causes a short hypocotyl phenotype similar to that observed in the *Athy5* mutant (Gangappa and Botto, 2016; Yamawaki et al., 2011). In *C. reinhardtii*, an ortholog of *AtHY5* has also been identified. As in the other species mentioned, CrHY5 appears to have functional homology with *AtHY5*, and to be the main target of CrCOP1 (Tilbrook et al. 2016; Lämmermann et al. 2020). Like CrCOP1 (Schierenbeck et al. 2015), CrHY5 appears to play a prominent role

in HL-induced photoprotection in *C. reinhardtii* (Lämmermann et al. 2020). *CrHY5* expression is also induced by UV-B exposure and under the control of CrUVR8 under these conditions (Tilbrook et al. 2016). However, there are currently no studies confirming the function of the CrHY5 protein upon UV-B exposure of cells.

### 3.3.3. *CONSTANS (CO) transcription factor*

*CO* is a circadian rhythm regulated gene encoding a transcription factor central to flowering in flowering plants. It mediates photoperiodic flowering by positively regulating FLOWERING LOCUS T (FT) transcription. *CO* encodes a zinc finger-type B-box transcription factor (Putterill et al. 1995; Suárez-López et al. 2001; Song et al. 2015). Blue light stabilises *CO* in a CRY-dependent manner, in particular CRY2 in *A. thaliana*. Once photoactive, CRY2 forms a complex with SPA, thereby fortifying the binding between CRY2 and COP1 in response to blue light. The CRY2-COP1/SPA complex results in the loss of COP1/SPA activity, which then allows *CO* to accumulate in cells and FT transcription to occur (Zuo et al. 2011). Conversely, *CO* is degraded in red light, via phytochromes (Valverde 2011). The importance of this mechanism has been studied in various species other than *A. thaliana* such as wheat, barley, or rice, demonstrating that *CO*- and FT-mediated flowering is conserved between different species (Song et al. 2015).

A family of proteins closely related to *CO* has also been identified in *A. thaliana* (Robson et al. 2001) and named *CO*-like or *COL*. In total, in *A. thaliana* 32 members of the B-box protein family have been identified, and are involved in flowering-independent regulatory pathways (Kumagai et al., 2008; Ledger et al., 2001; Shin et al., 2004). Three *COLs* have been identified in *P. patens*, and appear to be related to the regulation of circadian rhythm (Zobell et al. 2005). In *C. reinhardtii*, although the flowering process does not occur, three *COLs* genes have also been identified: *CrCO* (Cre06.g278159), *ROC66* (RHYTHM OF CHLOROPLAST 66; Cre06.g278200), and Cre03.g182700. *CrCO* is an ortholog of *AtCOL3* and has recently been studied for its key role in UV-B and HL-induced photoprotection in *C. reinhardtii* (Gabilly et al. 2019; Tokutsu et al. 2019).

### 3.4. Cross-talk between different light signalling pathways in plants

In nature, concerted action of photoreceptors is necessary for integrative/appropriate response to ever changing light environment. For example, the response mediated by CRYs is often co-regulated (redundant, coordinated, or antagonistic) by other photoreceptors such as phytochromes (Mockler et al. 2003; Rockwell et al. 2006; Quail 2010; Xu et al. 2015), phototropins (Christie 2007), or UVR8 (Heijde and Ulm 2012; Jenkins 2014; Rai et al. 2019; Tissot and Ulm 2020) in flowering plants. This is partly due to the fact that CRYs mediate the response to blue light by interacting with cryptochrome-interacting proteins that may also interact with other photoreceptors, such as the E3 ubiquitin ligase COP1/SPA complex (part of the UVR8, CRYs, and phytochromes signalling pathways), or the PHYTOCHROME-INTERACTING FACTORS PIF4 and PIF5 (part of CRYs and phytochromes signalling pathways) (Ponnu and Hoecker 2022). Indeed, these interactions may compete with or increase the signalling process of these other photoreceptors. In addition, CRYs can induce the expression of RUPs, which are the negative regulator of UVR8 in flowering plants (Tissot and Ulm 2020).

These concerted actions are more often controlled by molecular actors downstream of the photoreceptors, than by the photoreceptors themselves. Earlier in this manuscript (**section 3.3.1.**), for example, we presented the E3 ubiquitin ligase COP1/SPA complex which is a central regulator of photomorphogenesis in *A. thaliana*. The COP1/SPA complex is involved in UV-B, red light, and blue light responses via its interactions with five different photoreceptors (UVR8, phytochromes A and B, cryptochromes 1 and 2, and the zeitlupe protein FKF1) (Podolec and Ulm 2018). Similarly, the transcription factors mentioned above, in particular HY5, also respond to different colours of light (UV-B, blue, red) as they are regulated directly by COP1/SPA (or other ubiquitin ligase, in the case of CO upon red light) (Jakoby et al. 2002; Valverde 2011; Podolec and Ulm 2018).

In *C. reinhardtii*, recent observations on the CO transcription factor suggest that CrCO is also involved in several signalling pathways in this alga, since it regulates photoprotection in both UV-B and HL, which depend on different photoreceptors (Gabilly et al. 2019; Tokutsu et al. 2019). However, a real convergence of the UVR8 (UV-B) and PHOT (HL) signalling pathways has not yet been demonstrated in *C. reinhardtii*, and therefore remains hypothetical.

#### **4. PHOTORECEPTOR REGULATION OF PHOTOPROTECTION IN *C. REINHARDTII***

UV-B (280-315 nm) is a highly energetic wavelength. Therefore, although the majority of UV-B in the solar spectrum is filtered out by the stratosphere, the amount of UV-B that reaches the Earth's surface is still a danger to living organisms. UV-B can damage the macromolecules that absorb it, such as proteins or DNA, and can also induce the accumulation of cell-damaging ROS and consequent damage to PSII (Jansen et al. 1998; Britt 2004; Takahashi and Badger 2011; Demarsy et al. 2018). As a result, plants have developed mechanisms to prevent, limit and repair damages caused by UV-B: synthesis of specific phenylpropanoid "sunscreens" are accumulated in terrestrial plants, production of antioxidants to scavenge ROS induced by UV-B (violaxanthin, vitamin B6, ...), repair of damage induced at the DNA by photolyases, repair or degradation of damaged photosystems, etc. (Demarsy et al. 2018). In plants, all these responses are mediated by the UVR8 photoreceptor.

In *C. reinhardtii*, UVR8 enables the transcription of genes involved in PSII repair as well as in the regulation of photosynthesis in response to UV-B (Tilbrook et al. 2016). In addition to this, and contrary to observations in flowering plants, the UVR8 photoreceptor is also a key regulator of NPQ in *C. reinhardtii* since it controls the UV-B induction of the NPQ proteins LHCSR1 and PSBS, and LHCSR3 to a lesser extent (Allorent et al. 2016).

In addition to UV-B, white light is also probably one of the most damaging parameter when provided at high doses and can lead to photodamage of the photosynthetic apparatus and photooxidative stress (Demarsy et al. 2018). In land plants, as in *C. reinhardtii*, HL is the main inducer of NPQ. In *C. reinhardtii*, HL-induced NPQ is regulated by the blue light photoreceptor, PHOT, allowing the accumulation of NPQ proteins, predominantly LHCSR3 (and low accumulation of LHCSR1 and PSBS), in the cells (Allorent et al. 2013; Petroutsos et al. 2016). In addition, in *C. reinhardtii*, PHOT also enables the photophobic response to be set up, allowing the cells to move away from the source of light stress (Trippens et al. 2012). Similarly, in *A. thaliana*, chloroplast avoiding response to HL is also triggered by PHOT (AtPHOT2) (Jarillo et al. 2001; Kasahara et al. 2004).

Interestingly, UVR8 and PHOT mediated induction of photoprotection in *C. reinhardtii* seems to be mediated by the same transcription factor CrCO, in contrast with *A. thaliana*, in which AtCO is not part of either the AtPHOT or the AtUVR8 signalling pathway. This

suggests some major differences between the UV-B and HL induced responses in these two organisms.

## **5. PROJECT PRESENTATION & AIMS OF THE THESIS**

Photosynthetic cells are able to mitigate the harmful effect of light by activating NPQ mechanisms, which probably also contributes to the ability of photosynthetic organisms to grow under a wide variety of light conditions. Until recently, NPQ was thought to be only regulated by light intensity. However, several recent works, including in the two host labs, have suggested an unexpected link between light colours and the establishment of photoprotection in *C. reinhardtii*. In particular, UVR8 (Allorent et al. 2016) and PHOT (Petroutsos et al. 2016) photoreceptors have been demonstrated to control the expression of genes involved in NPQ (*LHCSR1*, *LHCSR3*, *PSBS*), and allow cells survival under high light exposure.

Whereas high light acclimation in *C. reinhardtii* has already been extensively studied (Allorent et al., 2013; Govorunova et al., 2004; McKim and Durnford, 2006; Meagher et al., 2021; Zones et al., 2015), UV-B-induced acclimation remains much less characterized in this alga. A transcriptome of *C. reinhardtii* exposed to UV-B was performed in the host lab a few years ago to identify genes induced by exposure to low UV-B level (Tilbrook et al. 2016). The results of this study showed that UV-B exposure induces changes in the expression of more than 2000 genes, whose the vast majority was under the control of UVR8. This experiment demonstrates that UV-B also controls a large variety of cell functions in *C. reinhardtii*. The most-induced genes by UV-B are related to the light harvesting and regulation of photosynthesis: qE actors, ELIPs, PSII assembly, ... This suggests that the impact of UV-B on the photosynthetic process goes beyond the induction of NPQ-related proteins and probably involves a more global reorganization of the architecture of the photosynthetic apparatus and its intrinsic capacity to absorb, utilize and/or dissipate light energy.

In this context, my PhD project aimed at identifying new actors involved in the UV-B acclimation of photosynthesis in *C. reinhardtii*. Using complementary and multidisciplinary laboratory approaches, this manuscript describes the identification, regulation, and the function of one of this actor that modifies the light stress response of *C. reinhardtii*: the LHL4 protein (LHC-LIKE 4 aka ELIP6).

## **CHAPTER 2:**

# **LHL4, A THYLAKOID ELIP INDUCED BY UV-B AND HIGH LIGHT IN *C. REINHARDTII***

---

## **1. IDENTIFICATION OF LHL4 UPON UV-B EXPOSURE**

### **1.1. Proteomics analysis of *C. reinhardtii* cells exposed to UV-B**

A proteomic analysis was performed on *C. reinhardtii* cells exposed to UV-B in order to identify new actors involved in the regulation of photosynthesis by this type of radiation. WT 137C cultures were simultaneously exposed to low light (20  $\mu\text{mol.photons.m}^{-2}.\text{s}^{-1}$ ) and UV-B (0.08  $\text{mW.cm}^{-2}$ ) for 16 hours, a time required to provide the UV-B protective effect to the algae (Allorent et al. 2016). The protein content of the cells was then analysed by mass spectrometry and compared to the proteome of cells only exposed to the visible part of the light spectrum. The results of this analysis are represented as a volcano plot in **Figure 2.1**. Each point corresponded to a protein detected at the time of analysis, and was placed on the graph according to its fold change (FC) and its p-value. The  $\log_2(\text{FC})$  was the parameter that quantified the enrichment ( $\log_2(\text{FC}) > 0$ ) or depletion ( $\log_2(\text{FC}) < 0$ ) of a protein compared to the control condition. In our study, we decided to focus on the 46 proteins that were significantly over-accumulated following UV-B exposure (**Fig. 2.1**, green dots) compared to the control condition (low light, 30  $\mu\text{E}$ ). Among them, 28% were related to i. photoprotection or ii. PSII repair and synthesis (**Table 2.1**, in pink).

i. The two main NPQ proteins, LHCSR1 (1st rank;  $\log_2(\text{FC}) = 5.91$ ) and LHCSR3 (5th rank;  $\log_2(\text{FC}) = 3.15$ ), were highly accumulated, which was consistent with their demonstrated role in the UV-B-induced protection of the photosynthetic machinery (**Table 2.1**). Although known to also be strongly induced by UV-B, PSBS (the third NPQ protein in *C. reinhardtii*) was absent from the dataset (Allorent et al. 2016). This is probably due to the fact that PSBS might be transiently accumulated in the cells during the first few hours of exposure but almost disappears on a longer time scale, such as the one we used (16 hours) for our proteomic analysis (Tibiletti et al. 2016).

ii. The UV-B intensity used in the experiment was low to prevent damage at PSII (Fv/Fm was similar between UV-B and low light-exposed cells). Several proteins involved in the turnover of PSII were nevertheless largely enriched in the UV-B treated samples. This included proteases (FTSH-like and DEG) which act first in the repair cycle of PSII by degrading the damaged proteins (Malnoë et al. 2014), but also proteins involved in the PSII biogenesis, assembly and stability (HCF136, HCF173, HCF244, SRRP1) (Plücken et al. 2002; Link et al. 2012) (**Table 2.1**). The over accumulation of these proteins suggested that, even at low doses, exposure to UV-B could damage PSII and/or promotes its protection. Thus, the accumulation of these PSII repair proteins in *C. reinhardtii* could contribute to its resistance towards light stress and the maintenance of photosynthetic activity under more stressful conditions.

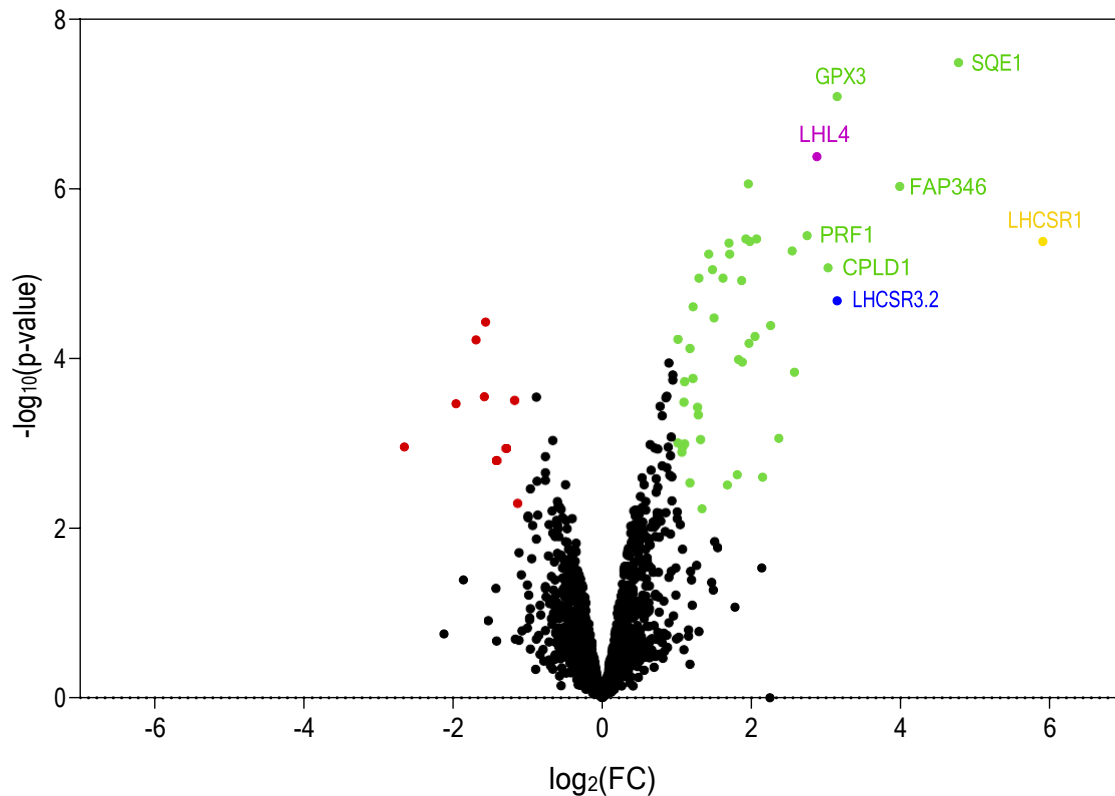


**Figure 2.1: LHL4 and the NPQ proteins LHC3R1 and LHC3R3 are significantly induced by UV-B exposure.** Proteomic analysis of *C. reinhardtii* WT 137C after 16h exposure to low UV-B and low light ( $0.08 \text{ mW}\cdot\text{cm}^{-2}$  and  $30 \mu\text{mol photons m}^{-2} \text{ s}^{-1}$ ) or low light ( $30 \mu\text{mol photons m}^{-2} \text{ s}^{-1}$ ; control condition). After 16h, the cells were harvested and the proteins extracted for mass spectrometry analysis ( $n=3-4$ ). The results are represented by a volcano plot where each dot represents a protein. Green dots correspond to proteins whose accumulation is significantly enriched in UV-B samples compared to the control, and red dots to proteins significantly repressed by UV-B exposure ( $\log_2(\text{FC}) \geq 1$  and  $-\log_{10}(\text{p-value}) \geq 2.11$ , leading to a Benjamini-Hochberg FDR < 0.01).

Besides these two groups of protein, one protein in particular stood out in this dataset (in purple on the volcano plot, **Fig 2.1**), as the only LHC-like protein with NPQ actors, and the only ELIP. This protein was identified as LHL4 (LHC-LIKE PROTEIN 4; Cre17.g740950), also annotated as ELIP6 in *C. reinhardtii* (*C. reinhardtii* genome v5 from Phytozome 10; Merchant et al., 2007), and was the 7<sup>th</sup> most UV-B induced protein ( $\log_2(\text{FC}) = 2.108$ ) in our proteomic analysis (**Table 2.1**). We decided therefore to focus on this protein to further decipher its expression and function in *C. reinhardtii*.

Gene identifier	Log2(FC)	Annotation (Phytozome 13)	Gene identifier	Log2(FC)	Annotation (Phytozome 13)
Cre08.g365900	5,91	Photosynthesis. Chlorophyll a/b binding protein. LHC- stress related protein 1, LHCSR1	Cre06.g294450	1,71	Aldo/keto reductase
Cre17.g734644	4,78	Squalene epoxidase, SQE1	Cre08.g358540	1,70	No annotation available
Cre12.g492600	3,99	FAS Domain Flagellar Associated Protein 346, FAP346	Cre06.g290350	1,68	No annotation available
Cre03.g197750	3,15	Glutathione peroxidase 3, GPX3	Cre10.g439000	1,62	Putative ABC transporter
Cre08.g367400	3,15	Photosynthesis. Chlorophyll a/b binding protein. LHC- stress related protein 3, LHCSR3.2	Cre10.g444550	1,50	Signal peptide peptidase, SPP1A
Cre03.g145587	3,03	Conserved in the Plant Lineage and Diatoms, CPLD1	Cre13.g562850	1,48	Chloroplast-localized protein similar to Arabidopsis Thylakoid Formation1, THF1
Cre17.g740950	2,88	<b>Photosynthesis. Chlorophyll a/b binding protein. High-intensity light-inducible LHC-like protein, LHL4 (alias ELIP6)</b>	Cre17.g720050	1,43	Photosynthesis. PSII repair. FtsH-like membrane AAA-metalloprotease, FTSH2
Cre16.g673617	2,75	Peptide chain release factor, PRF1	Cre02.g088400	1,34	Photosynthesis. PSII repair. Deg protease, DEG1A
Cre13.g587500	2,58	Flavin-containing amine oxidase, AOF8	Cre06.g286350	1,31	UbiE/COQ5 methyltransferase family protein, UMM6
Cre01.g028600	2,55	Short-chain dehydrogenase/reductase	Cre12.g485800	1,30	Photosynthesis. PSII repair. FtsH-like membrane ATPase/metalloprotease, FTSH1
Cre09.g395650	2,37	No annotation available	Cre02.g142146	1,28	Photosynthesis. PSII biogenesis protein, HCF244
Cre10.g466850	2,26	Peptidyl-prolyl cis-trans isomerase, FKBP18	Cre03.g148950	1,27	Photosynthesis. Ortholog of PSII biogenesis protein SRRP1, SRRP1
Cre17.g715000	2,15	Heat shock protein 33, HSP33	Cre03.g195200	1,22	Conserved in the Green Lineage, CGL76
Cre12.g501050	2,07	Aldehyde/histidinol dehydrogenase, ALD6	Cre13.g565650	1,21	No annotation available
Cre14.g624350	2,05	Tocopherol O-methyltransferase, VTE6	Cre06.g273700	1,17	Photosynthesis. PSII stability/assembly factor, HCF136
Cre02.g088500	1,98	No annotation available	Cre06.g279850	1,17	Putative dehydrogenase
Cre05.g241655	1,97	No annotation available	Cre13.g578650	1,10	Photosynthesis. PSII biogenesis protein, HCF173 homolog
Cre04.g221550	1,96	Xanthophyll cycle. Chlorophycean Violaxanthin De-epoxidase, CVDE1	Cre03.g184550	1,10	Photosynthesis. Low Photosystem II Accumulation 3, LPA3
Cre09.g407801	1,93	ABC1/COQ8 ser/thr kinase, AKC1	Cre10.g458450	1,09	Glutathione peroxidase 5, GPX5
Cre09.g401701	1,88	No annotation available	Cre05.g232150	1,07	Glutamate dehydrogenase, GDH2
Cre17.g697050	1,87	No annotation available	Cre12.g517900	1,06	Chloroplast-associated SecA protein, SECA1
Cre09.g411200	1,83	Photosynthesis. PSII assembly protein, PSBS3	Cre14.g617300	1,01	Signal peptide peptidase-like protein
Cre02.g078507	1,81	No annotation available	Cre09.g397250	1,01	Palmitate delta-7 desaturase, FAD5A

**Table 2.1: List of the proteins significantly induced by UV-B in *C. reinhardtii*, and their functional annotations ( $\log_2(\text{FC}) \geq 1$  ;  $-\log_{10}(\text{p-value}) \geq 2.11$  ; Benjamini\_Hochberg  $\text{FDR} \leq 0.01$ ). A gene identifier in pink corresponds to a protein possibly involved in the regulation photosynthesis or photoprotection.**

## 1.2. Structure of LHL4

The sequence analysis of the LHL4 protein with the TargetP webtool (<http://www.cbs.dtu.dk/services/TargetP/>) indicated that LHL4 contained a transit peptide (aa 1-39) with 50% probability of being addressed to the chloroplast. As all LHC-like proteins (Teramoto et al. 2006), LHL4 was predicted to insert into the thylakoid membrane. Moreover, models generated by the AlphaFold Protein Structure Database (<https://alphafold.ebi.ac.uk/>) and the PHYRE2 server (<http://www.sbg.bio.ic.ac.uk/~phyre2/html/page.cgi?id=index>) (**Fig. 2.2A and 2.2B**) predicted that LHL4 has three transmembrane helices (in blue in both panels): between amino acids 64-80; 95-117; and 245-260, that are expected to insert into the thylakoid membrane as shown in **Figure 2.2B**. Predictions based on the amino acid sequence of this protein (**Fig. 2.2C**, Teramoto et al., 2006) also show that LHL4 contains two LHC motifs with chlorophyll-binding residues (in red and green respectively in **Fig. 2.2C**). LHL4 is therefore a three-helix transmembrane protein, similar to the other ELIPs described in the literature (Adamska 2001; Rochaix and Bassi 2019).

The two LHC motifs (in green, **Fig. 2.3A**) are conserved in the 10 ELIPs identified in *C. reinhardtii*. In contrast, the extramembrane loop between helices 2 and 3 of LHL4 was much longer and was markedly different from that of other ELIPs (**Fig. 2.3A**, red arrow). On the other hand, the sequence of LHL4 was very different from the LHCSR3 proteins that are involved in NPQ in *C. reinhardtii*, although they also harbor 3 transmembrane helices including one LHC motif (**Fig. 2.3B**). In addition, LHL4 lacked the acidic residues (glutamates - E) in its C-terminal part (exposed in the lumen) that are required for LHCSR3 for NPQ establishment (Camargo et al. 2021). Overall, these observations suggest that LHL4 displays the canonical structures of ELIP proteins but is not a NPQ protein.

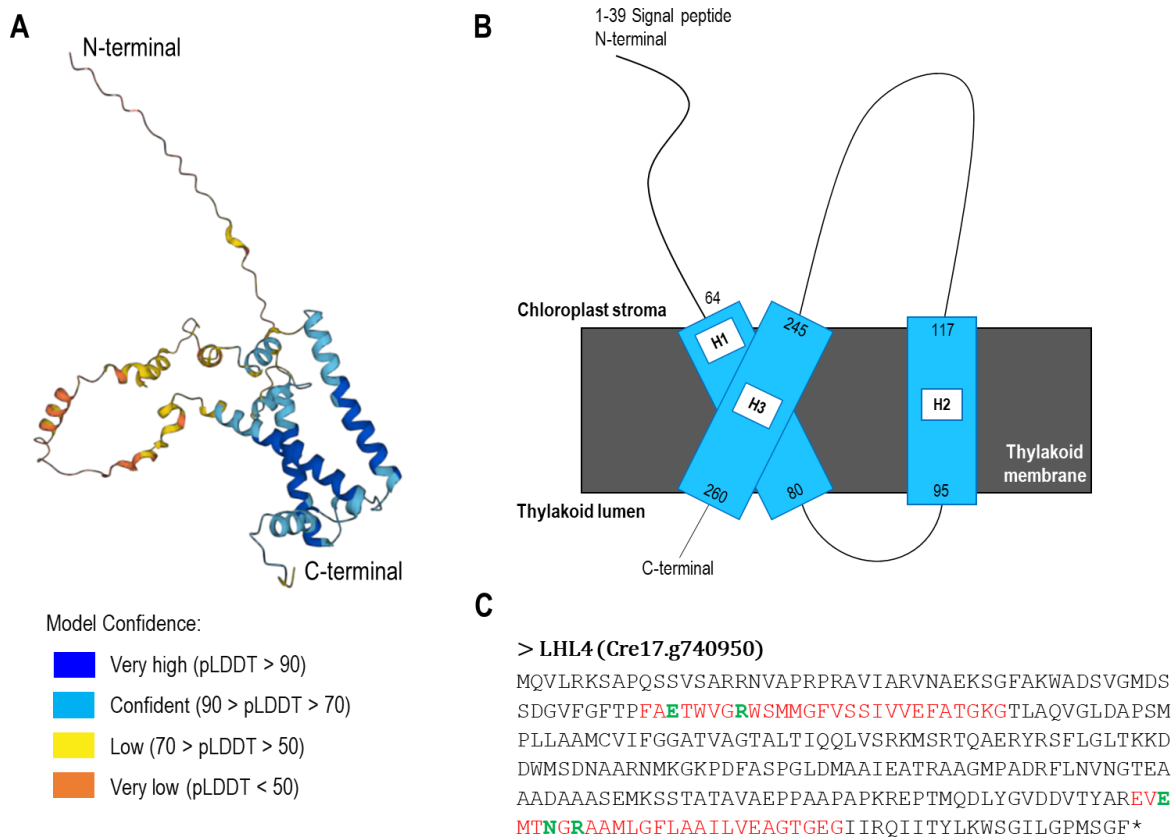


**Figure 2.2: Prediction of the LHL4 structure.** (A) Three-dimensional structure prediction of LHL4 generated by the AlphaFold Protein Structure Database. AlphaFold produces a per-residue confidence score (pLDDT) between 0 and 100. Structures of regions below 50 pLDDT are uncertain. (B) Prediction of the insertion of LHL4 in the thylakoid membranes by the PHYRE2 server. The blue rectangles H1, H2, H3 represent the predicted transmembrane helices based on the amino acid sequence. The numbers indicate the position of the amino acids at the beginning and end of the helices. (C) Amino acid sequence of LHL4 protein. Red: LHC motifs in helices 1 and 3; green: residues identified as putative chlorophyll ligands in LHC proteins (Teramoto et al. 2006).

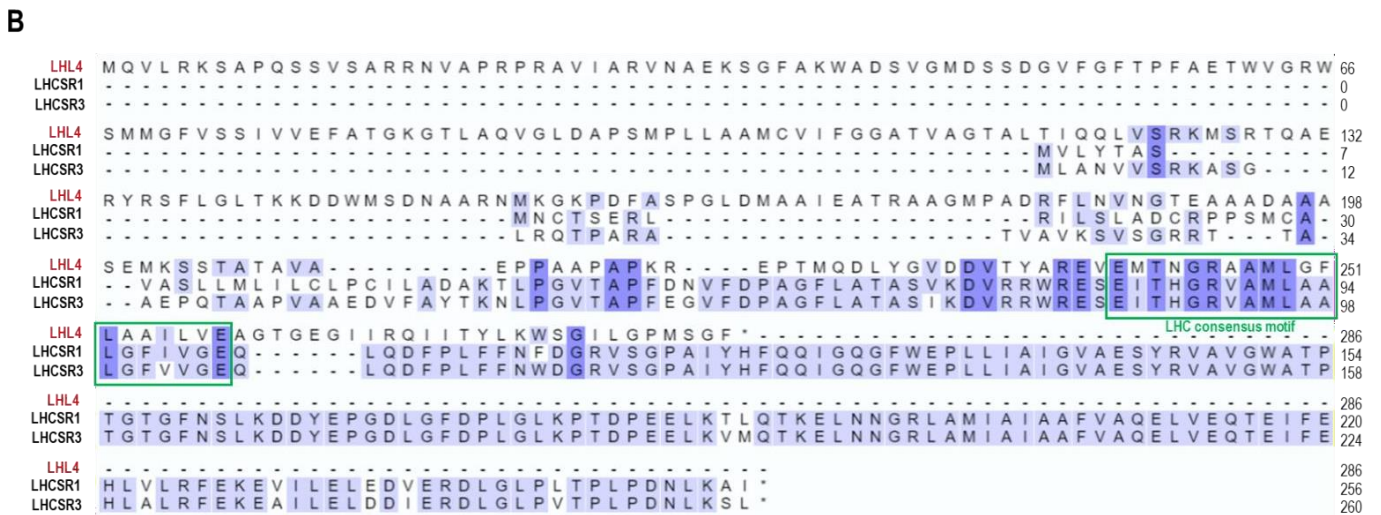
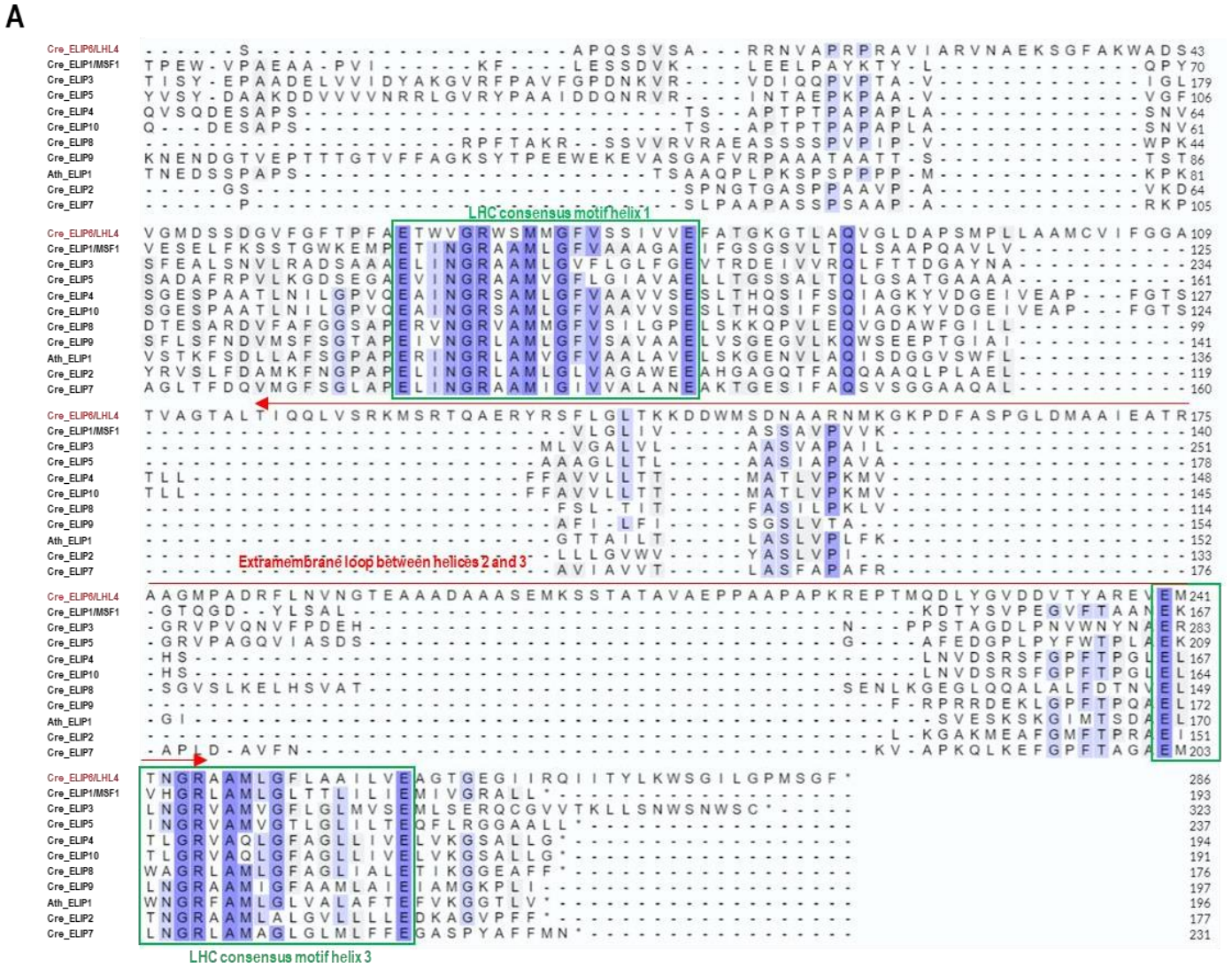


**Figure 2.3: Comparison of LHL4 protein sequence with other CrELIPs and LHCSRs. (A) Alignment of the partial amino acid sequences of the 10 ELIPs from *C. reinhardtii*, and ELIP1 from *A. thaliana*. Red arrow: LHL4 specific extramembrane loop; green frame: conserved LHC motifs (B) Alignment of the amino acid sequences of LHL4 and LHCSR proteins.**

## 2. LOCALIZATION OF LHL4 WITHIN THE CELL

The localization of a protein can give important clues about its function. We therefore decided to confirm but also to refine the chloroplast localization of LHL4 by different and complementary experimental approaches: ultrastructure expansion microscopy and 2D BN-PAGE.

### 2.1. Localization of LHL4 in the cell ultrastructure

Ultrastructure expansion microscopy (U-ExM) is a relatively recent technique that allows the visualization of different structures in cells at the nanoscale, while using conventional microscopes (e.g. confocal microscope), by physically enlarging the size of the sample (up to 4.2-fold ; Faulkner et al., 2020; Hamel and Guichard, 2021; Laporte et al., 2022). In the context of these experiments, we collaborated with the laboratory of Prof. Guichard/Dr Hamel (University of Geneva, Switzerland) who are experts in this technique (Gambarotto et al. 2021). This technique had already been applied to *C. reinhardtii* cell wall-less strain to visualise the centriole and the assembly of intraflagellar transport trains at the ciliary base (Hamel and Guichard 2021; van den Hoek et al. 2022). However, the organisation of the proteins of the photosynthetic apparatus with U-ExM has not yet been investigated. Using this new approach, we aimed to: 1) confirm that LHL4 was localized in the chloroplast as predicted by the presence of a transit peptide; 2) to refine the localization of LHL4 within the thylakoid network by using specific photosystem antibodies.

We first decided to localize the two photosystems (which are very abundant in chloroplasts) using highly specific, and already well characterised, commercial antibodies: anti-PsbA (PSII; **Fig. 2.4A**) and anti-PsaH (PSI; **Fig. 2.4B**). The two antibodies were produced in different animals to allow the co-detection of both photosystems in the same cell using two different secondary antibodies coupled to two different chromophores (**Fig. 2.4C**). Confocal microscopy images showed that the size of the algae cells was now ~50  $\mu\text{m}$  (five times bigger than its original size). Both PSI and PSII signals clearly delimited the characteristic cup-shaped chloroplast of *C. reinhardtii* (**Fig. 2.4A,B,C**) and confirmed that the signals detected are indeed localised in the chloroplast. By merging the two images (**Fig. 2.4C**), we also demonstrated that the resolution was high enough to discriminate between the location of both photosystems in the chloroplast

since the two signals did not overlap. A zoom-in on some specific region of the chloroplast revealed that the architecture of the thylakoid network can be observed using this approach (**Fig. 2.4D**) as well as the presence of sub-cellular structures like the pyrenoid (**Fig. 2.4E**). The results of these first tests constituted a proof of concept of this method in our *C. reinhardtii* WT 137C model. This experiment demonstrated that U-ExM was suitable to investigate, in the chloroplast, the architecture of the thylakoid membranes and provided sufficient spatial resolution to estimate the distribution of proteins of interest within the network.

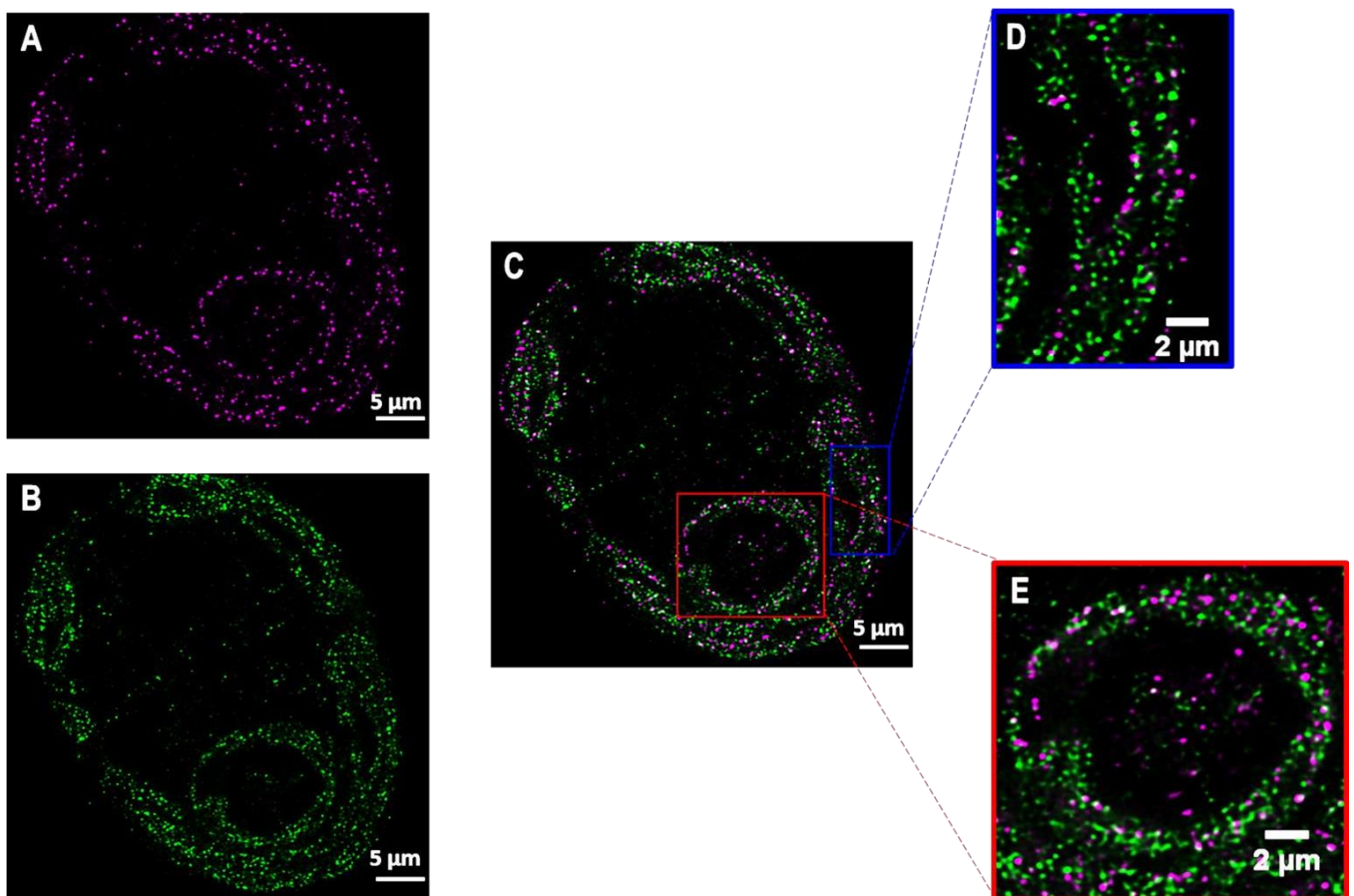


**Figure 2.4: Localisation of photosystems I and II in *C. reinhardtii* using ultrastructure expansion microscopy (U-ExM).** (A) to (E) Images were obtained using a confocal microscope. Photosystems are detected using specific PSI and PSII antibodies labelled with two different fluorophores (Alexa 488 and Alexa 568). The signal is then artificially colorized in pink for PSII and green for PSI. (A) PSBA staining (PSII) ; (B) PSAH staining (PSI); (C) Merge channels showing the locations of both photosystems in the cell; (D) Zoom-in on thylakoid membranes; (E) Zoom-in on pyrenoid.

We therefore decided to investigate the localization of LHL4 in the cell using the same approach. WT 137C cultures were exposed for 3h to UV-B to induce LHL4 accumulation. However, the labelling of LHL4 was detected throughout the cell in a non-specific manner. Consequently, we were unable to conclude about the localisation of LHL4 from these

images (**Fig. 2.5A**). This could be explained by the lack of specificity of the LHL4 antibody (**Fig. 2.5B**), which was not an issue when used for western blots (the band corresponding to LHL4 can then be identified thanks to its size), but became problematic when a high specificity is required as in the case of U-ExM.

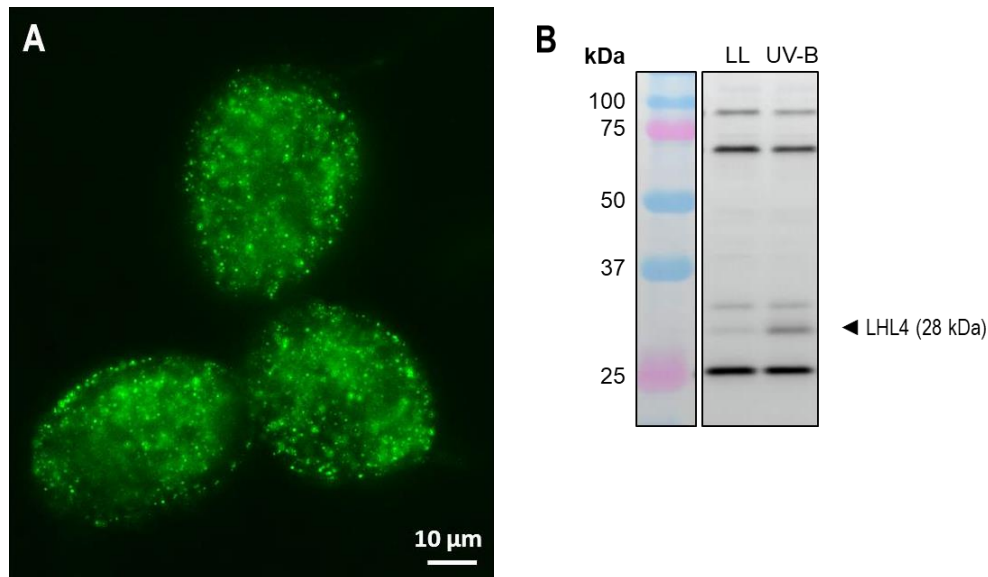


**Figure 2.5: U-ExM localisation of LHL4 protein.** (A) U-ExM images of *C. reinhardtii* WT137C cell exposed to UV-B (3h, LL 30  $\mu\text{mol photon m}^{-2} \text{s}^{-1}$  + 0.2  $\text{mW.cm}^{-2}$  UV-B) to induce LHL4 accumulation. Images were obtained using a widefield fluorescence microscope. Cells were stained using anti-LHL4 antibody coupled to Alexa 488-labeled secondary antibody. (B) Blot control showing the non-specificity of the anti-LHL4 antibody.

## 2.2. LHL4 comigrates with PSII in non-denaturing conditions

Since the detection of LHL4 was not possible using expansion microscopy, we investigated its localisation by 2D Blue Native (BN)-PAGE analysis (**Fig. 2.6**). The WT strain was exposed for 6h to UV-B to induce LHL4 accumulation in the cells. Membrane proteins were then extracted from the cells under non-denaturing conditions. Photosynthetic complexes were then separated by electrophoresis on a polyacrylamide gel, and their composition was investigated by running the lanes in a second denaturing dimension (SDS-PAGE), which allowed the separation of the different subunits of the complexes by their apparent molecular weight. Finally, the presence of PSI, PSII and LHL4 was identified by immunodetection using specific antibodies. Our results showed that LHL4 was detected in two spots (**Fig. 2.6A**) that were absent in not UV-B-treated samples (**Fig. 2.6B**). Each spot appeared to be located on either side of the PSII monomer/Cyt *b<sub>6</sub>f* band. Since LHL4

was predicted to be located into the thylakoid membrane and displays chlorophyll-binding (Adamska and Kloppstech 1991), it seemed therefore more plausible that LHL4 interacted with PSII monomers rather than Cyt *b6f*, that did not contain chlorophyll. This result suggests that LHL4 is likely associated with PSII, as predicted or demonstrated for the other NPQ and ELIP proteins.

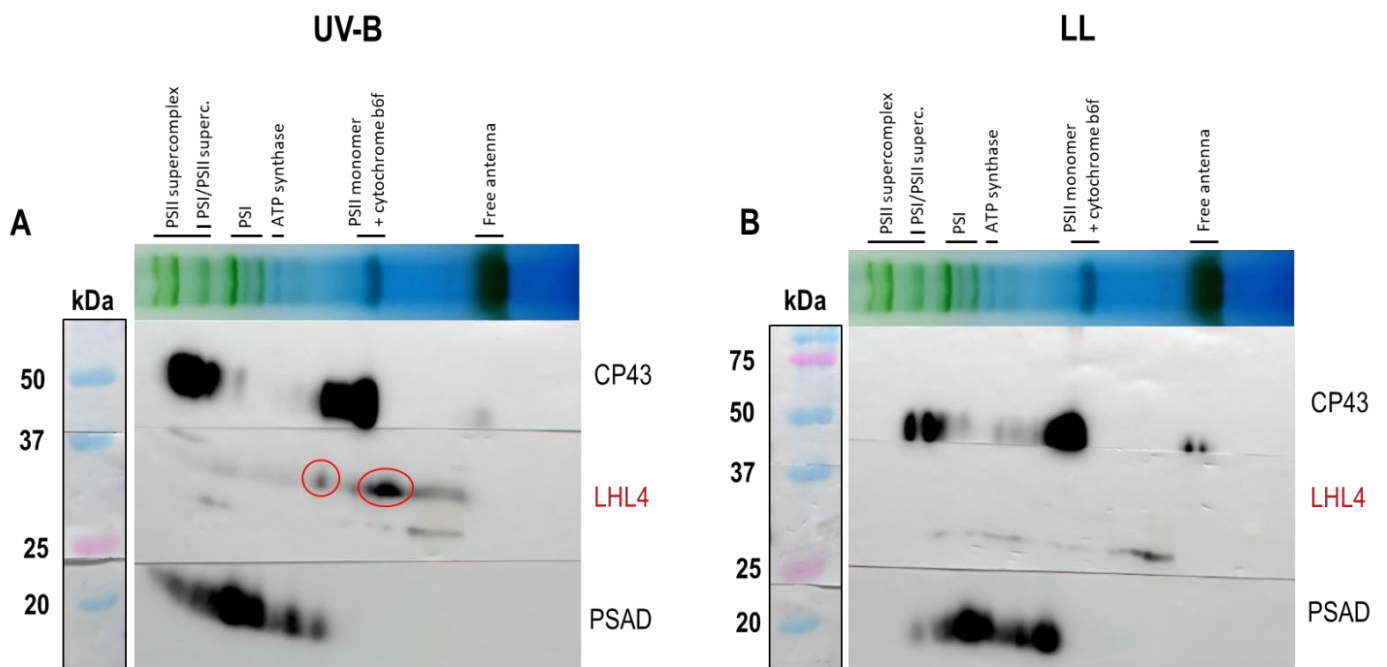


**Figure 2.6: Localization of LHL4 by analysis of the composition of different photosynthetic complexes by 2D-BN-PAGE.** WT cells were exposed for (A) 6h to UV-B (LL  $30\mu\text{mol photons.m}^{-2}.s^{-1} + 0.2 \text{ mW.cm}^{-2}$  UV-B) or (B) to low light only ( $30\mu\text{mol photons.m}^{-2}.s^{-1}$ .) The cells were then harvested, lysed and the membrane proteins extracted. After solubilisation with a mild detergent, photosynthetic complexes were separated on a gel in native conditions (top part). The native gel was then cut and proteins were separated in a second dimension under denaturing conditions. The localization of PSI (PSAD) and PSII (CP43) and LHL4 were finally determined by immunodetection (bottom part). The membranes are representative of the 5 biological replicates tested.

### 3. LHL4 ACCUMULATION IS STRONGLY AND RAPIDLY INDUCED UPON UV-B AND HIGH LIGHT IN *C. REINHARDTII*

#### 3.1. LHL4 expression and accumulation in cells over time and under different light conditions

Our previous results showed that LHL4 was enriched in cells exposed for several hours to UV-B (3 to 16h, see above). In contrast, ELIPs were usually known to be rapidly and strongly induced upon different stresses, including high light exposure (Adamska et al.

1992b; Pötter and Kloppstech 1993; Bruno and Wetzel 2004). This feature is of particular importance to rapidly limit the level of stress and to avoid any long term deleterious effects. The same holds true for NPQ actors, that are massively accumulated upon light stress conditions (when they are not constitutively present as in *C. reinhardtii*). We decided therefore to investigate the dynamics of *LHL4* expression in WT cells to determine whether it also shares these characteristics (i.e. rapid induction and induction upon high light). Cultures were exposed up to 8h to UV-B or HL and the expression of *LHL4* was investigated both at the transcript (**Fig. 2.7A**) and protein levels (**Fig. 2.7B**).

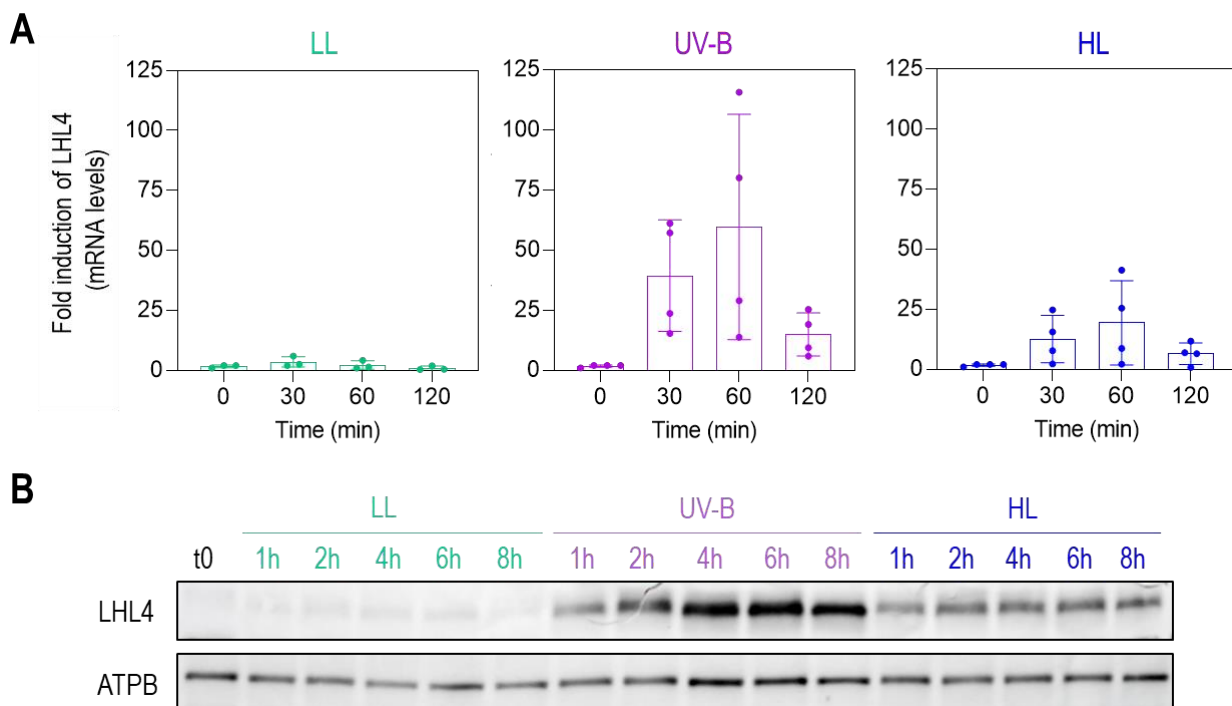


**Figure 2.7: *LHL4* is not constitutively present in the cells but is rapidly accumulated during both UV-B and HL exposures. (A) and (B).** WT137C cells were exposed to LL (green -  $30 \mu\text{mol photons m}^{-2} \text{s}^{-1}$ ; control condition), UV-B (purple -  $30 \mu\text{mol photons m}^{-2} \text{s}^{-1}$  LL +  $0.2 \text{ mW.cm}^{-2}$  UV-B) or HL (blue -  $300 \mu\text{mol photons m}^{-2} \text{s}^{-1}$ ) for 8h and the accumulation of *LHL4* transcripts were analyzed by RT-qPCR. Error bars represent standard deviation ( $n=3$  biological replicates and 2 technical replicates) (A) or the level of protein by immunodetection (B). ATPB (Beta subunits of ATP synthase) is used as a loading control for western blots. The membrane is representative of the 3 biological replicates tested.

Exposure to UV-B or HL induced *LHL4* gene transcription within 30 min, with a transient peak of mRNA accumulation at 1h that decreased thereafter (**Fig. 2.7A**). The level of accumulation was 3 times stronger after UV-B exposure than after HL, demonstrating that *LHL4* was preferentially induced by UV-B. However, it showed that *LHL4* transcription was also activated under HL, which was consistent with the observations made by Teramoto et al. 2006. This pattern of transcription was very similar to the one described

for the NPQ actors (LHCSR1, 3 and PSBS) when cells were suddenly exposed to stress light conditions (Strenkert et al. 2019).

At the protein level (**Fig 2.7B**), LHL4 did not appear to be constitutively expressed under standard growth conditions (LL) but accumulated rapidly in the cells since the protein was already detectable after 1h under UV-B or HL. The maximum expression level was reached after 4 hours and remained stable for 8 hours. Moreover, LHL4 was also slightly more accumulated under UV-B light than under HL, which was in accordance with the trend observed at the transcript level (**Fig. 2.7A**). However, although the transcript level dropped after 1 hour, the accumulation of the protein persisted for several more hours, which may suggest a high stability of LHL4. This parameter will be further investigated in the next section (3.2).

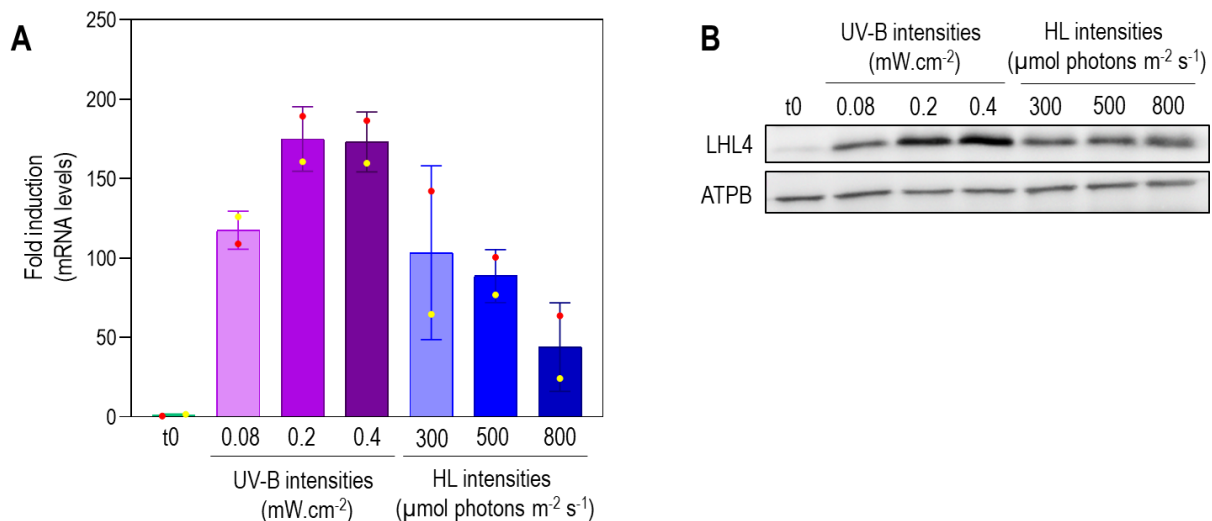


**Figure 2.8: LHL4 expression upon different light intensity.** WT137C cells were exposed to different UV-B (LL 30 μmol photons m<sup>-2</sup> s<sup>-1</sup> + 0.08/0.2/0.4 mW.cm<sup>-2</sup>) or HL (300/500/800 μmol photons m<sup>-2</sup> s<sup>-1</sup>) intensities. **(A)** Cells were harvested after 1h and the level of LHL4 transcript was determined by RT-qPCR. Each color of dot corresponds to a biological replicate. Error bars represent standard deviation (n=3 biological replicates and 2 technical replicates) **(B)** Proteins were extracted from cells exposed for 6h and the accumulation of LHL4 was evaluated by immunodetection. ATPB is used as a loading control. The membrane is representative of the 4 biological replicates tested.

In samples exposed for 1h to UV-B, the level of LHL4 transcripts slightly increased with the intensity (**Fig. 2.8A**) but reached a maximum for an intensity of 0.2 mW.cm<sup>-2</sup>. In contrast, the accumulation of LHL4 protein in the WT increased with UV-B intensity (**Fig. 2.8B**) up to 0.4 mW.cm<sup>-2</sup>. When the cells were exposed to HL, the level of LHL4 transcripts decreased as the intensity increased whereas the protein level remained stable (**Fig. 2.8A and B**). Altogether, our results indicate that the expression level of LHL4 does not strictly depend on the light intensity but also on the quality. These results also suggest a strong

post-transcriptional regulation of the *LHL4* gene or/and its stability in HL, which would be responsible of the constant level of protein independent of the level of transcripts induced. The stability of the *LHL4* transcripts was previously demonstrated to be low in this context ( $t_{1/2} = 8$  min in the dark and 12 min in HL ; Teramoto et al., 2006), so we cannot also exclude the possibility that for higher light intensities (500 and 800  $\mu\text{mol photons m}^{-2} \text{s}^{-1}$ ), the peak of transcription occurred before 1h.

### 3.2. The LHL4 protein is rapidly degraded once the light treatment is stopped

As the kinetic of induction of LHL4, at both mRNA and protein levels, was similar to that of NPQ proteins (Allorent et al. 2016; Petroutsos et al. 2016), we decided to investigate the stability of the protein by comparison with that of two other main actors of the light response: LHCSR1 (mainly induced by UV-B) and LHCSR3 (mainly induced by HL).

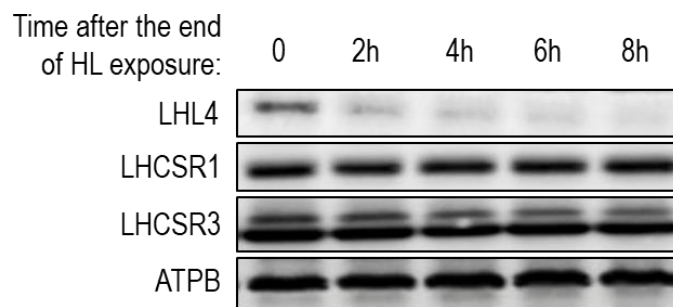


**Figure 2.9: LHL4 protein accumulation decreases quickly after the end of light treatment.** *WT137C* cultures were acclimated overnight to low doses of UV-B (LL 30  $\mu\text{mol photons m}^{-2} \text{s}^{-1} + 0.08 \text{ mW.cm}^{-2}$ ) and then exposed for 4h to 300  $\mu\text{mol photons m}^{-2} \text{s}^{-1}$  HL. The combination of these two treatments induced the accumulation of LHL4 and NPQ proteins at a high level (0). The induction of proteins was then stopped by switching the cells to LL (30  $\mu\text{mol photons m}^{-2} \text{s}^{-1}$ ) for 8 h, and samples were harvested after 2/4/6/8h. Accumulation of LHL4 and LHCSRs proteins were then estimated by immunodetection using the corresponding antibodies. The upper band in the LHCSR3 blot corresponds to the phosphorylated form of the protein (Scholz et al., 2019). ATPB was used as loading control. The membranes are representative of the 2 biological replicates tested.

To do this, *C. reinhardtii* cultures were sequentially exposed to both UV-B and HL to induce a high level of LHL4, LHCSR1, and LHCSR3 (time “0”, **Fig 2.9**). The algae were then transferred to LL in order to stop the light signal inducing the expression of the three proteins. Cells were finally collected at regular intervals over time and the accumulation of the three proteins was monitored (**Fig. 2.9**). Our results showed that LHCSR1 and LHCSR3 accumulation levels remained stable during at least 8h whereas LHL4 was no more detectable after 2 hours (only a faint band was still visible on the blot). The results of this experiment showed therefore a much lower stability over time of LHL4 compared

to LHCSRs. This may also suggest a more transient role in the response to light stress compared to NPQ proteins that remain stable for longer periods. These hypotheses will be investigated in further details in the **Chapter 4**.

#### **4. SUMMARY**

In this chapter, we have:

- Identified by proteomics that the LHL4 protein as the only ELIP overaccumulated in *C. reinhardtii* cells exposed to UV-B
- Showed that LHL4 has the structural characteristics of ELIPs but was very different from the LHCSRs proteins involved in NPQ
- Demonstrated that LHL4 co-localized with PSII in thylakoid membranes
- Proved that LHL4 is preferentially induced by UV-B but can also be induced by HL treatment
- Showed that the induction of LHL4 at the transcript and protein level was dose-dependent under UV-B but was rather stable under different visible light intensities
- Highlighted the fact that LHL4 was not very stable after cessation of light treatment (UV-B or HL), unlike NPQ proteins

# **CHAPTER 3:**

## **LHL4 IS AT THE CONVERGENCE OF TWO PHOTORECEPTOR-MEDIATED PATHWAYS IN *C. REINHARDTII***

---

### **1. REGULATION OF LHL4 EXPRESSION BY UV-B AND HIGH LIGHT SIGNALLING PATHWAYS**

#### **1.1. Regulation of LHL4 by blue and UV-B photoreceptors**

In the previous chapter, we demonstrated that *LHL4* expression was induced by UV-B and HL in *C. reinhardtii*, which is really similar to the one described for NPQ effector proteins that are under the control of distinct photoreceptors. Indeed, UV-B signalling is mediated by the UVR8 photoreceptor and triggers the expression of *LHCSR1* and *PSBS* in *C. reinhardtii* (Allorent et al. 2016; Tilbrook et al. 2016). In parallel, the blue light photoreceptor PHOT is involved in the induction of the expression of *LHCSR3* under HL exposure (Petroustos et al., 2016). In addition, two blue cryptochromes, an animal-like one (aCRY) and a plant-like one (pCRY), were also found in the *C. reinhardtii* genome (Kottke et al. 2017). In this chapter, we deciphered the light signalling pathway responsible for the induction of LHL4, from the photoreceptor to the transcription factor. We also investigated the possible convergence and synergy between the UV-B and HL signalling pathways for LHL4, as well as for the NPQ proteins.

##### *1.1.1. Generation and characterization of blue and UV-B photoreceptor mutants.*

To study how the expression of *LHL4* was regulated, we decided to generate *uvr8*, *phot*, *acry*, and *pcry* knock-out (KO) mutants in the WT137C. These mutants were obtained by inserting, after cleavage by the Cas9, an exogenous donor DNA into an exon of the genes targeted. The donor DNA contained a stop codon, thus blocking the translation of mRNAs and inhibiting the expression of the genes of interest. The mutants were first genotyped

by PCR and the region of the gene where the Cas9 cut was sequenced to confirm the insertion of the exogenous donor DNA (**Fig. 3.1**). The absence of protein was eventually verified by immunodetection after western blot.

For the *uvr8* mutant, we confirmed the absence of UVR8 by exposing cultures of WT 137C and *uvr8* to UV-B and HL and checked the accumulation of NPQ proteins, since UVR8 is responsible for the induction of LHCSR1 and PSBS under UV-B (Allorent et al. 2016). The results showed that LHCSR1 and PSBS were accumulated in both LL and HL conditions in WT but not in UV-B in *uvr8*, which confirmed that the photoreceptor was indeed absent in this strain (**Fig. 3.1A**). Concerning *phot* and *acry* (**Fig. 3.1B and C**), two KO mutants were obtained for each gene. Western blots of *phot* mutants showed a residual band detected at the expected size for PHOT, as the one observed in a KO mutant previously published (Greiner et al. 2017). The residual band observed was thus probably due to a non-specific binding of the antibodies (**Fig. 3.1B**). Concerning *acry* mutants, the western blot clearly confirmed that both strains are KO for the *aCRY* gene (**Fig. 3.1C**). The *pcry* mutant was only sequenced, as the anti-pCRY antibody developed in the lab did not give any specific signal (**Fig. 9D**). According to the sequencing of the strain which confirmed the insertion of an exogenous DNA in the second exon, it was clear that the mutant is KO for *pCRY*.

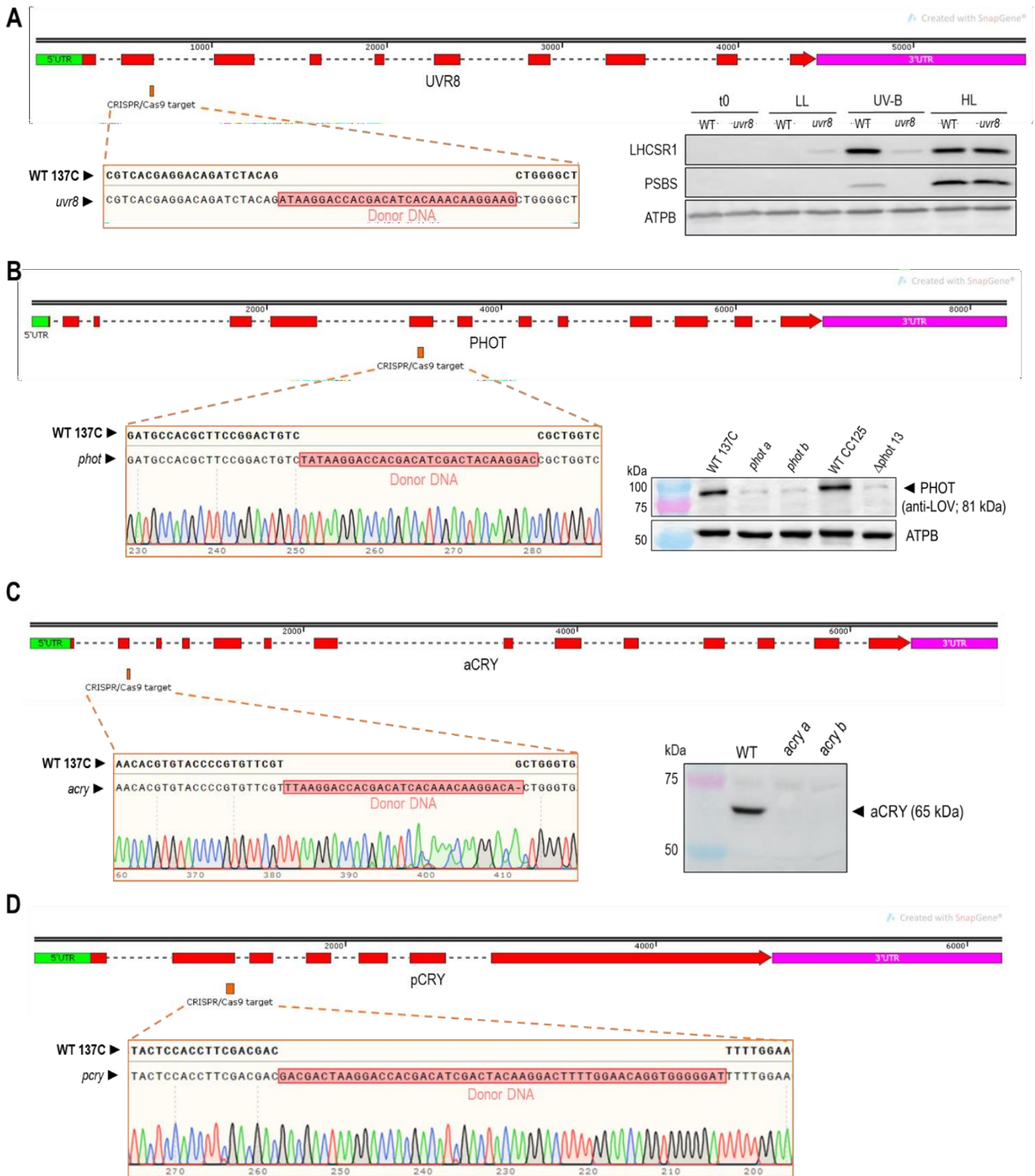


**Figure 3.1: Characterisation of *uvr8* (A), *phot* (B), *acry* (C), and *pcry* (D) photoreceptor mutants.** The mutants were all generated from WT 137C by CRISPR/Cas9. The insertion of an exogenous DNA in one of the first exons was verified by PCR and the absence of the corresponding protein was evaluated by immunodetection using a specific antibody. (A) the cells were exposed for 6h to LL ( $30 \mu\text{mol photons m}^{-2} \text{s}^{-1}$ ), UV-B (LL  $30 \mu\text{mol photons m}^{-2} \text{s}^{-1}$  +  $0.2 \text{ mW.cm}^{-2}$  UV-B), or HL ( $300 \mu\text{mol photons m}^{-2} \text{s}^{-1}$ ) before protein extraction. ATPB is used as a loading control for western blots. Data kindly provided by Chloé Bertin.

### 1.1.2. Control of *LHL4* expression by blue and UV-B photoreceptors

We then used these different mutants to check the expression of *LHL4* at both mRNA and protein levels. Cultures of the mutants were placed under UV-B or HL for few hours, i.e. conditions known to induce *LHL4* expression in the WT (**Fig. 3.2**).

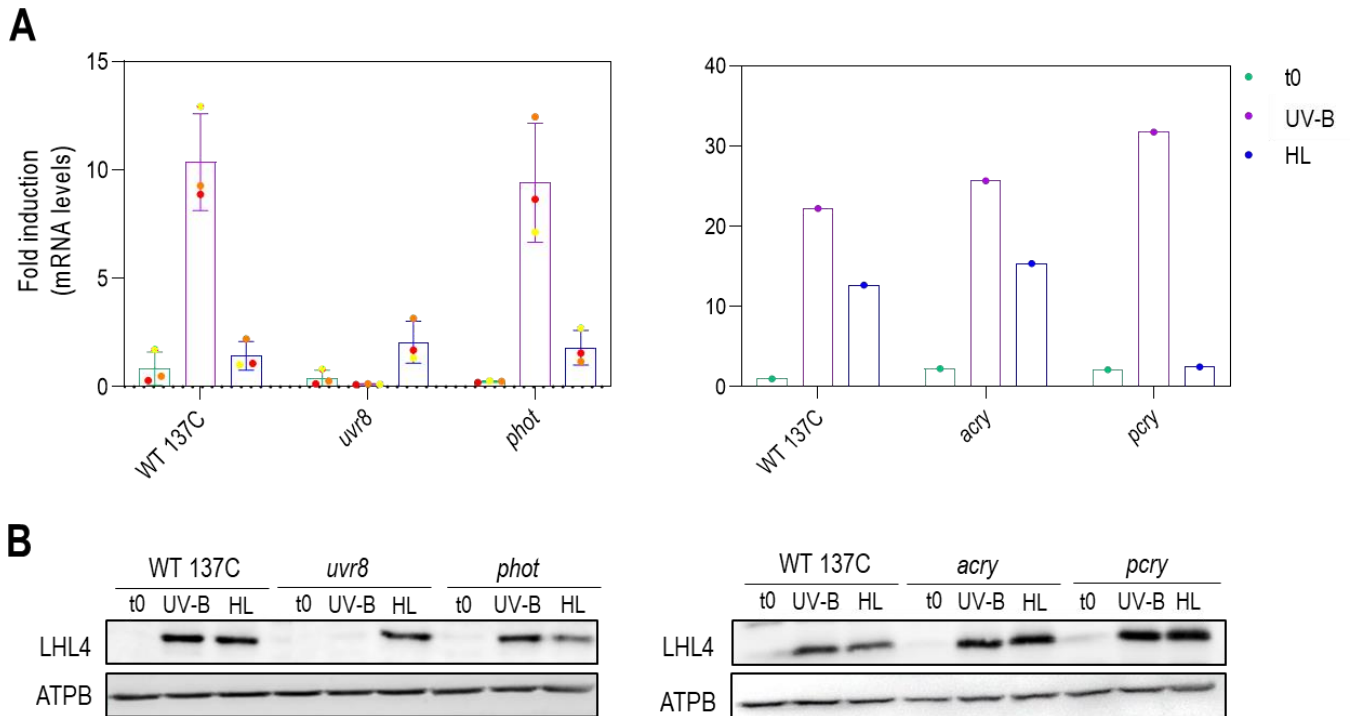


**Figure 3.2: *LHL4* gene expression and protein accumulation in photoreceptor mutants after exposure to UV-B or HL.** (A) RT-qPCR analysis of *LHL4* gene expression in photoreceptor mutants *uvr8*, *phot*, *acr1*, and *pcry*. Cells were exposed for 1 h to UV-B (LL 30  $\mu\text{mol photons m}^{-2} \text{s}^{-1}$  + UV-B 0.2  $\text{mW.cm}^{-2}$ ) or HL (300  $\mu\text{mol photons m}^{-2} \text{s}^{-1}$ ). Each dot colour corresponds to a biological replicate. Error bars represent standard deviations ( $n=3$  biological replicates and 2 technical replicates) (B) Immunodetection of *LHL4* protein accumulation in the different genotypes. Cells were exposed for 6 h to the UV-B or HL treatments as described for panel A. ATPB is used as a loading control. The membranes are representative of the 3 biological replicates tested.

As described in the previous chapter, the expression of *LHL4* was induced by HL and more strongly by UV-B (**Fig3.2.A**). Transcript analysis by qRT-PCR showed that *LHL4* expression was repressed in the *uvr8* mutant exposed to UV-B, but was induced at a similar level as the WT in *phot* and *acr1*. In contrast, *LHL4* was slightly more accumulated in *pcry* exposed to UV-B (**Fig. 3.2A**) even if it should be noticed that the qRT-PCR were performed only once in the case of *pcry* and *acr1* and must be therefore confirmed. The accumulation of *LHL4* protein in the same exposure conditions showed that *LHL4* was no more detected in *uvr8*, but over-accumulated in *pcry* and maybe slightly also in *acr1* (**Fig. 3.2B**). Overall, these results demonstrated that upon UV-B exposure, *LHL4* transcription

is mainly controlled by the UV-B specific UVR8 photoreceptor but also partly by the blue light photoreceptor pCRY.

On the other hand, the accumulation of *LHL4* transcripts in response to HL showed no significant change in the *uvr8*, *phot* and *acry* mutants compared to the WT. However, *LHL4* was 3 times less accumulated than in WT in *pcry* (**Fig. 3.2A**). In contrast with UV-B exposure, the accumulation of LHL4 in HL-treated cells did not exactly follow the observations made at the transcript level. Indeed, *phot* accumulated 2 times less LHL4 than in the WT whereas LHL4 was over accumulated in *acry* and *pcry* at a similar level to the one previously observed under UV-B (**Fig. 3.2B**). Taken together, these results show that *LHL4* expression under HL appears to be controlled by several different blue photoreceptors that do not always directly modulate its transcriptional level but modify the accumulation of the protein. This observation demonstrates that the regulation of *LHL4* expression under HL may be different from that described for the LHCSR3 NPQ effector (mainly under the control of PHOT; Petroutsos et al. 2016), although the role of pCRY in its induction remains to be analysed. We cannot also exclude the possibility that the expression of *LHL4* under these conditions depends on another recently characterized UV-A/blue photoreceptor, CRY-DASH1 (Rredhi et al. 2021).

**1.2. LHL4 is mainly regulated by the CONSTANS (CO) transcription factor and the COP1 ubiquitin ligase in both UV-B and high light**

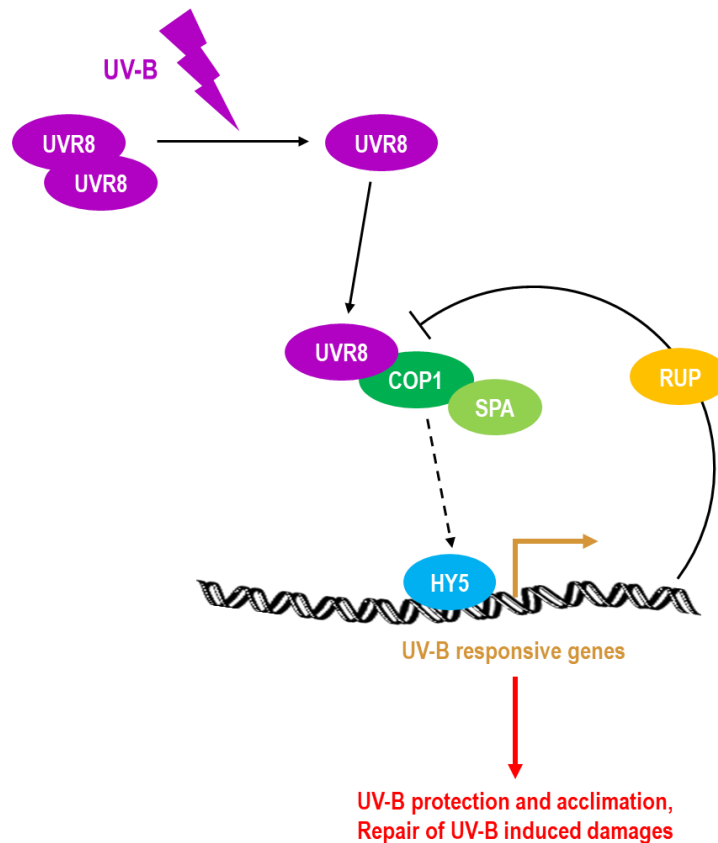


**Figure 1.11: Model of the UVR8 signalling pathway in *A. thaliana*.** Based on Heijde and Ulm, 2012.

We showed that *LHL4* expression is regulated upon UV-B and HL, via different photoreceptors. Next, we tested which downstream factors were involved in this regulation. The UVR8 signalling pathway starts with the monomerization of the UVR8 photoreceptor following UV-B perception (Favory et al. 2009; Tilbrook et al. 2016). Then, the monomers (active form of the photoreceptor) interact with the COP1/SPA1 complex (Favory et al. 2009). In the absence of UV-B, this complex ubiquitinates the transcription factors HY5 and CO (in *C. reinhardtii*; Tokutsu et al. 2019), which are then degraded and downstream gene expression is repressed (Osterlund et al. 2000; Jang et al. 2008; Podolec and Ulm 2018) (**Fig. 1.11**). In contrast, in the presence of UV-B, the activity of COP1/SPA1 is inhibited by its interaction with UVR8, which in the end activates gene transcription. In addition, in *A. thaliana* the RUP proteins facilitate the redimerisation of UVR8 and

participates to the regulation of the UVR8 signalling pathway by this negative feed-back. Concerning the transcription factor, CO has been shown to be involved in the induction of NPQ actors both in UV-B and HL, suggesting that it is also involved in both signalling pathways (Gabilly et al. 2019; Tokutsu et al. 2019). These results suggest the existence of a cross-talk of the PHOT and UVR8 pathways in *C. reinhardtii* that has not been further investigated yet. In this context, we thought of using *LHL4* as a tool to assess the convergence of these two pathways. Therefore, we used KO mutants of actors already characterized in the UVR8 and/or PHOT pathways, that were available in the CLiP library (*constans*, *hy5*, *rup*, and *spa1* from the CLiP library (Li et al. 2016); *hit1* (CrCOP1) from Schierenbeck et al., 2015). These mutants were treated by UV-B or HL to induce *LHL4* expression as determined previously, and we then analysed the accumulation of *LHL4* transcripts by qRT-PCR, and the accumulation of the protein by immunodetection in all these strains (**Fig. 3.3**) to assess which genes were part of the UV-B and/or HL signalling pathways.

We first focused on RUP, a negative regulator of UVR8 in *A.thaliana*. *LHL4* transcript was similarly accumulated in *rup* compared to the WT in both UV-B and HL (**Fig. 3.3A**). At the protein level, *LHL4* accumulation was comparable to the WT under HL but slightly more abundant in *rup* under UV-B exposure (**Fig. 3.3B**). Our results therefore suggest that UVR8 signalling is overactivated upon UV-B in a *rup* mutant, leading to a higher induction of target genes (here *LHL4*), which is consistent with the role of RUP in *A. thaliana*.

Concerning the transcriptions factors HY5 and CO, we observed that *LHL4* gene expression was not induced upon UV-B and HL in *constans*, but was similarly regulated in *hy5* compared to the WT (**Fig. 3.3A**). For these two strains, exactly the same trend was observed in the accumulation of the *LHL4* protein (**Fig. 3.3B**). It must be noted that a minor induction of *LHL4* was still detected in *constans*, which could indicate that the protein induction was partially independent on CO under these conditions. Despite this observation, our results indicate that CO is clearly the key transcription factor for *LHL4* regulation in *C. reinhardtii*, both in UV-B and HL.

We then tested the effect of *COP1* and *SPA1* mutations on the regulation of *LHL4* expression. The *hit1* mutant, affected in *CrCOP1* expression, showed largely reduced induction of *LHL4* transcript and the corresponding protein in both UV-B and HL compared to WT (**Fig. 3.3A and B**). In contrast, in *spa1*, the expression of *LHL4* was not affected under UV-B but was overexpressed under HL, which was also confirmed at the

protein level. From this experiment, we can conclude that the ubiquitin ligase COP1 is part of both UVR8 and HL signalling pathways, whereas SPA1 only controls the HL part of the *LHL4* expression.

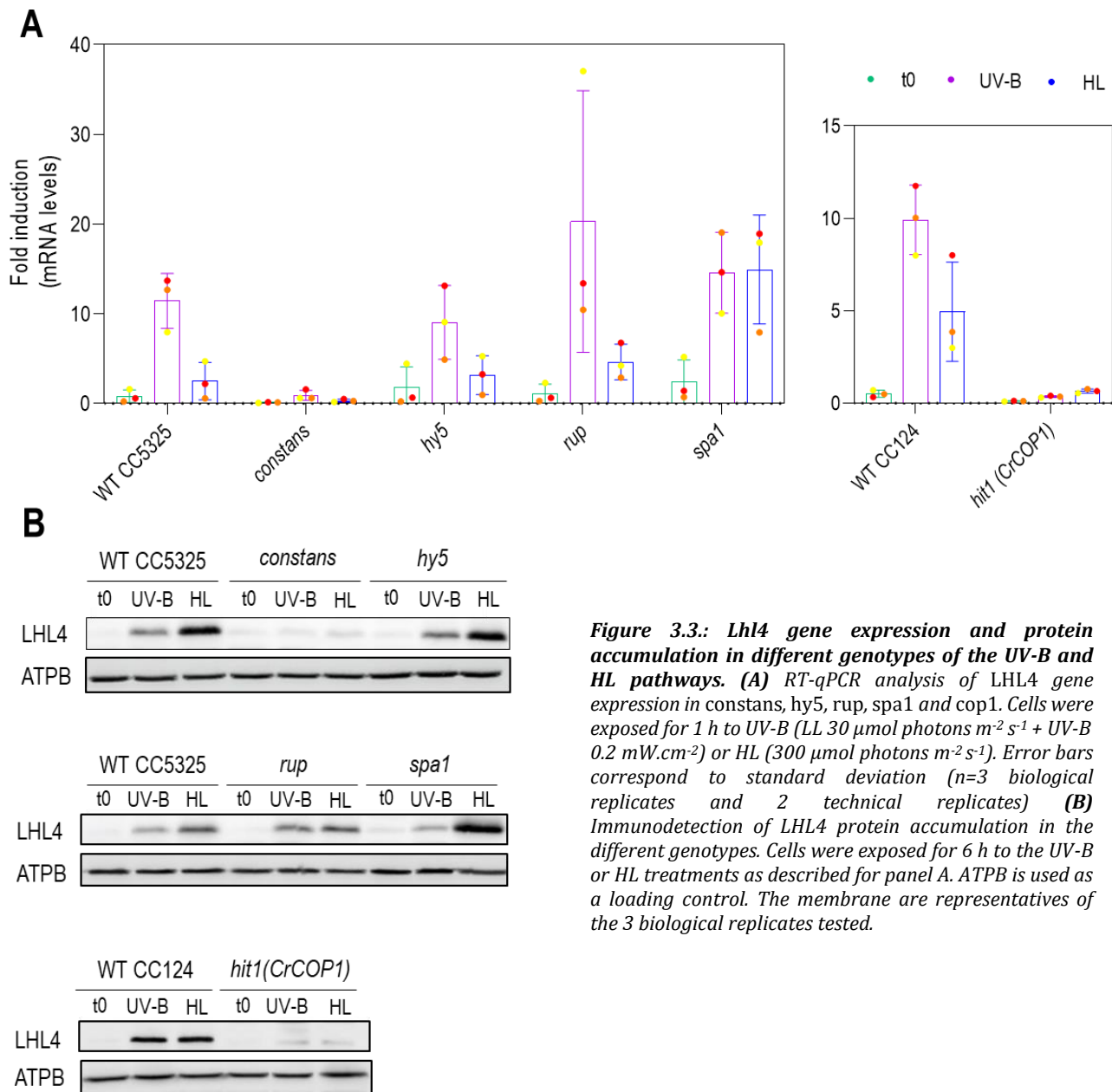


**Figure 3.3.: Lhl4 gene expression and protein accumulation in different genotypes of the UV-B and HL pathways.** (A) RT-qPCR analysis of LHL4 gene expression in *constans*, *hy5*, *rup*, *spa1* and *cop1*. Cells were exposed for 1 h to UV-B (LL 30  $\mu\text{mol photons m}^{-2} \text{s}^{-1}$  + UV-B 0.2  $\text{mW.cm}^{-2}$ ) or HL (300  $\mu\text{mol photons m}^{-2} \text{s}^{-1}$ ). Error bars correspond to standard deviation ( $n=3$  biological replicates and 2 technical replicates) (B) Immunodetection of LHL4 protein accumulation in the different genotypes. Cells were exposed for 6 h to the UV-B or HL treatments as described for panel A. ATPB is used as a loading control. The membrane are representatives of the 3 biological replicates tested.

## 2. REGULATION OF NPQ-RELATED PROTEINS BY UV-B AND HIGH LIGHT SIGNALLING PATHWAYS

In a similar way to LHL4, NPQ proteins were previously shown to be regulated by both UV-B light and HL intensity (Allorent et al. 2016; Petroutsos et al. 2016). We decided

therefore to analyse the accumulation of LHCSR1, LHCSR3, and PSBS proteins by western blot in the strains affected in the photoreceptor-mediated response (*uvr8*, *phot*, *hy5*, *constans*, *hit1*, *spa1*, *rup*) (**Fig. 3.4**) to determine whether the control of their induction was similar to LHL4.

At the level of photoreceptors, our results showed that in *uvr8*, the three proteins studied are no longer accumulated following UV-B exposure, as previously observed (Allorent et al. 2016). In *phot*, a similar accumulation of LHCSR1 as in the WT was observed, but the levels of LHCSR3 (Petroutsos et al. 2016) and PSBS were decreased under HL. These data support our previous results concerning LHL4 (**Fig 3.2**) and suggest that PHOT is probably not the only photoreceptor involved in the regulation of photoprotection-related genes under HL (**Fig. 3.4**). In this context, we planned to decipher the role of aCRY and pCRY but data concerning the expression of the NPQ proteins in the *acry* and *pcry* mutants had not been yet obtained at the time of writing this thesis manuscript.

Unexpectedly, in the *rup* mutant, no difference was detected in UV-B but an overaccumulation of LHCSR3 and PSBS in HL was observed compared to the WT.

*constans* showed no longer accumulation of LHCSR1 nor PSBS, either after UV-B or HL treatment. In contrast, LHCSR3 was still detected in both light conditions, although at a lower level than in the WT. These data suggest that CO is the main transcription factor for *LHCSR1* and *PSBS* (as *LHL4*) but *LHCSR3* may be also controlled by other(s) transcription factor(s) in both UV-B and HL. We also cannot exclude the possible involvement of an independent signalling pathway in the regulation of *LHCSR3* expression. In contrast, the induction of NPQ proteins was slightly upregulated in *hy5*, which was not observed in the case of LHL4 (**Fig. 3.4**).

The analysis of *hit1* (CrCOP1) showed a large decrease in the accumulation of NPQ proteins compared to WT, both in UV-B and HL. However, it should be noted that a residual protein was still detected for LHCSR3 under HL, confirming the existence of a COP1-independent induction of some stress-related proteins under HL. In contrast, the expression of the three proteins (LHCSR1, LHCSR3, and PSBS) was not affected in *spa1*, both in UV-B and HL (**Fig. 3.4**). This data confirmed the observations made in the previous paragraph, which showed that only COP1 in the COP1/SPA1 complex was involved in the two signalling pathways.

Altogether, our data demonstrate that the UV-B and HL pathways converge at the level of COP1 during the photoprotective response in *C. reinhardtii*. In addition, our data confirm that CO is the main transcription factor, although HY5 could be involved in the HL response. Finally, our data also suggest that this regulation may also be controlled by other transcription factors and/or inducing signals that are not identified yet (but had already been hypothesized in Gabilly et al. 2019).

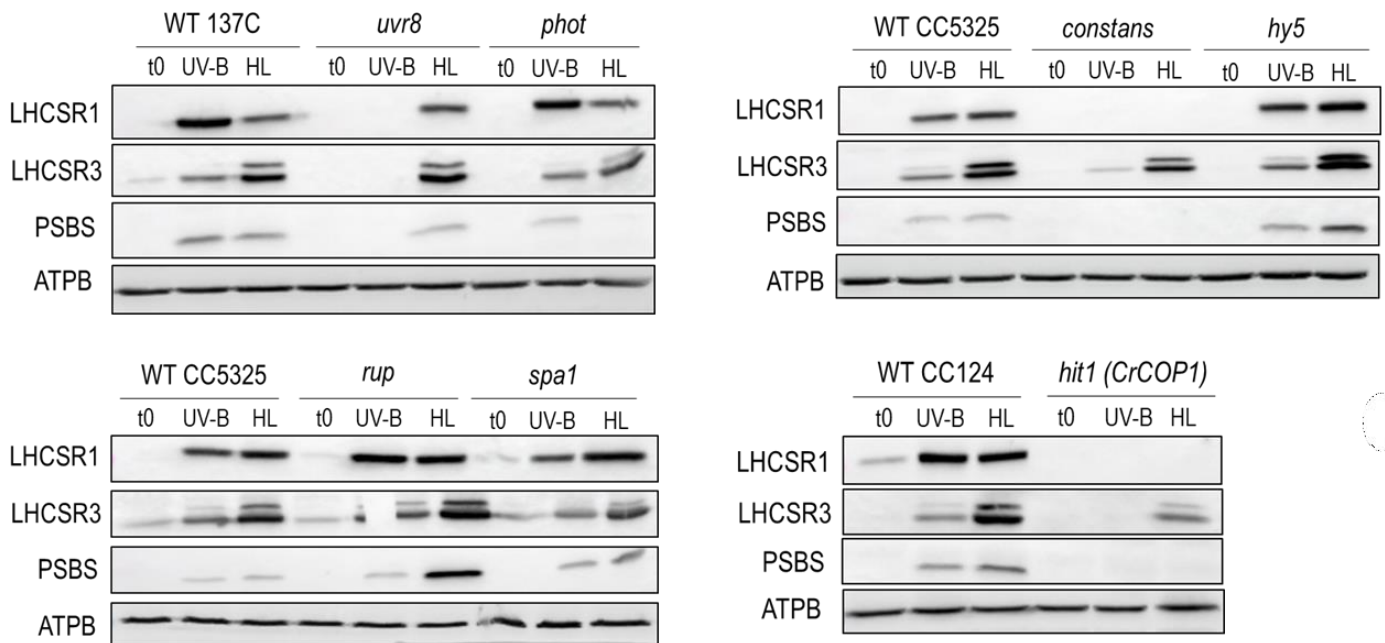


**Figure 3.4: Accumulation of NPQ proteins in the different genotypes investigated after UV-B or HL exposure.** Western blot analysis of all genotypes and corresponding WTs: WTCC5325 for *constans* and *hy5*; WT137C for *uvr8*, and *phot*; and WTCC124 for *hit1*(CrCOP1). Cells were exposed for 6h to UV-B ( $0.2 \text{ mW.cm}^{-2}$ ) or HL ( $300 \mu\text{mol photons m}^{-2} \text{ s}^{-1}$ ), and then harvested for protein analysis. ATPB is used as a loading control for western blots. The upper band in the LHCSR3 blot corresponds to the phosphorylated form of the protein. The membranes are representative of the 3 biological replicates tested.

### 3. TRANSCRIPTOME ANALYSIS OF *C. REINHARDTII* *uvr8*, *constans*, *hy5* MUTANTS EXPOSED TO UV-B

Our previous results demonstrated that HY5 is not involved in the transcription of LHL4 upon UV-B exposure, which mainly relies on CO as also demonstrated for LHCSR proteins (Tokutsu et al., 2019, see also **Fig 3.3 and 3.4** above). Although based on a limited number of genes, these results suggested that HY5 might play only a minor role in the UVR8 signalling pathway in *C. reinhardtii*, in stark contrast to *A. thaliana* where its role was preponderant in the transcription of UV-B-induced genes. Thus, while the UV-B signalling pathway appeared to be well conserved between flowering plants and green algae, these

observations raised the question of the functional role of HY5 in *C. reinhardtii*. To answer this question, a comparative transcriptome analysis using total mRNA extracted from WT, *uvr8* (LMJ.RY0402.156289 from Allorent et al., 2016), *constans* and *hy5* was performed after UV-B exposure. The analysis of the RNA-seq revealed that UV-B induces changes (up- or down-regulation compared to the control low light condition devoid of UV-B radiation) in the expression of more than 1000 genes in the WT (**Fig. 3.5A**).

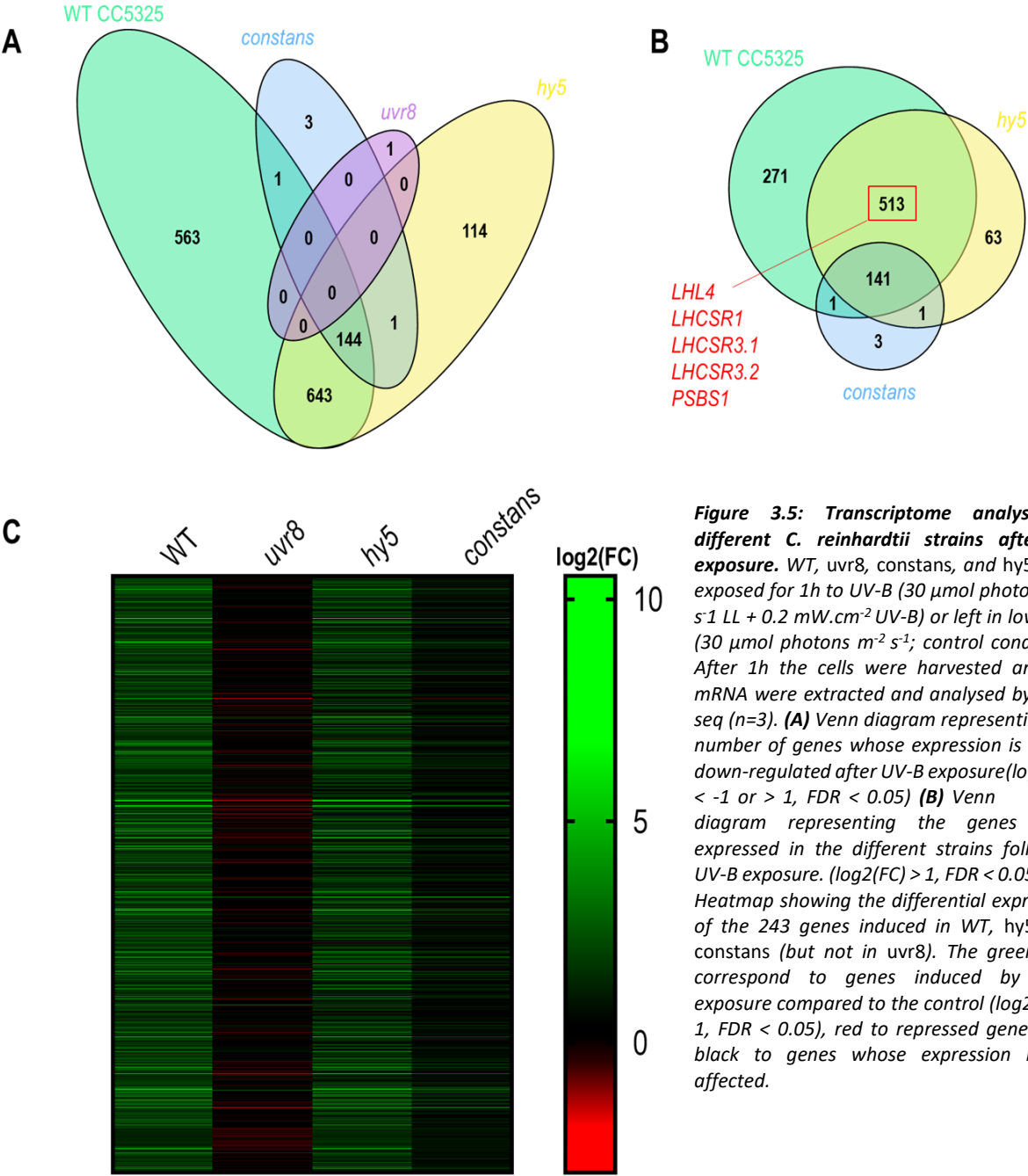


**Figure 3.5: Transcriptome analysis of different *C. reinhardtii* strains after UV exposure.** WT, *uvr8*, *constans*, and *hy5* were exposed for 1h to UV-B (30  $\mu\text{mol photons m}^{-2} \text{s}^{-1}$  LL + 0.2  $\text{mW.cm}^{-2}$  UV-B) or left in low light (30  $\mu\text{mol photons m}^{-2} \text{s}^{-1}$ ; control condition). After 1h the cells were harvested and the mRNA were extracted and analysed by RNA-seq (n=3). **(A)** Venn diagram representing the number of genes whose expression is up- or down-regulated after UV-B exposure ( $\log_2(\text{FC}) < -1$  or  $> 1$ ,  $\text{FDR} < 0.05$ ) **(B)** Venn diagram representing the genes over-expressed in the different strains following UV-B exposure. ( $\log_2(\text{FC}) > 1$ ,  $\text{FDR} < 0.05$ ). **(C)** Heatmap showing the differential expression of the 243 genes induced in WT, *hy5*, and *constans* (but not in *uvr8*). The green bars correspond to genes induced by UV-B exposure compared to the control ( $\log_2(\text{FC}) > 1$ ,  $\text{FDR} < 0.05$ ), red to repressed genes, and black to genes whose expression is not affected.

The Venn diagram in **Figure 3.5A** illustrated these changes. Each ellipse represented a genotype (WT, *uvr8*, *constans*, or *hy5*), and the numbers indicated the number of transcripts whose expression was altered by UV-B ( $\log_2(\text{FC}) < -1$  or  $> 1$ ,  $\text{FDR} < 0.05$ ) in one (e.g. 563 corresponds to transcripts differentially regulated only in WT) or more genotypes if the ellipses overlapped (e.g. 144 corresponds to the number of transcripts whose regulation was significantly altered in WT, *constans*, and *hy5* but not in *uvr8*).

The results of this transcriptomic analysis revealed that 1351 genes were up- or downregulated under UV-B in the WT. Almost all were under the control of UVR8, and 89% were also dependent on CO, but only 42% on HY5. A small proportion of genes found in the transcriptome (144 out of 1351, 10%) was not regulated by any of these transcription factors, but the majority (563 of 1351, 58%) was regulated by both (**Fig. 3.5A**). This indicates that under UV-B exposure, HY5 also contributes to gene transcription, but to a lesser extent than CO.

Among genes impacted by UV-B in the WT, 926 (69%) of them were overexpressed compared to the control condition ( $\log_2(\text{FC}) > 1$ ,  $\text{FDR} < 0.05$ ) (**Fig. 3.5B**). 18 were found to be highly induced ( $> 5$ -fold). Of these, half were related to photoprotection (**Table 3.1**) and included mainly ELIPs (5 of the 10 ELIPs identified in *C. reinhardtii*), as well as the genes coding PSBS and the zeaxanthin epoxidase (ZXE) involved in the xanthophyll cycle (qZ). *LHL4* and NPQ genes (*LHCSR1*, *LHCSR3*, and *PSBS*) were found in the cluster of 513 genes overexpressed in the WT and the *hy5* mutant, confirming the CO transcription dependency of these genes, as previously demonstrated (Gabilly et al. 2019; Tokutsu et al. 2019).

The heat map presented in **Figure 3.5C** showed that the gene expression profile between *hy5* and WT was comparable, although the expression level was lower for some genes in the mutant. In stark contrast, most of the genes were completely repressed or much less induced in *constans*. It was also interesting to note that while most of the genes were no longer induced in *uvr8* compared to WT, some of them were also repressed, which might suggest a state of stress in the mutant.

This result demonstrates once again that UVR8 is the key photoreceptor in the UV-B induced signalling pathway in *C. reinhardtii*, and that without it, the signalling cascade cannot take place (Tilbrook et al. 2016). We can also conclude that CO is the key regulator in the UVR8 signalling pathway in contrast with what is known from *A. thaliana*, in which HY5 is predominant. This had already been showed for NPQ genes, but this RNA-seq

clearly revealed that CO is also essential at the level of the overall UV-B response of the cell in *C. reinhardtii*.

Gene identifier	Log2(FC)	Annotation (Phytozome 13)	Gene identifier	Log2(FC)	Annotation (Phytozome 13)
Cre07.g320400	10,52	Photosynthesis. Chlorophyll a/b binding protein. Early light-inducible protein 4, <i>ELIP4</i>	Cre08.g372200	4,61	No annotation available
Cre07.g333050	9,88	Serine/threonine protein kinase	Cre03.g145567	4,35	Conserved in the Green Lineage
Cre07.g320450	8,86	Photosynthesis. Chlorophyll a/b binding protein. Early light-inducible protein 10, <i>ELIP10</i>	Cre03.g144184	4,31	No annotation available
Cre01.g016600	8,62	Photosynthesis. PSII-associated 22 kDa protein, <i>PSBS1</i>	Cre03.g145587	4,29	Conserved in the Plant Lineage and Diatoms, <i>CPLD1</i>
Cre01.g016750	8,45	Photosynthesis. PSII-associated 22 kDa protein, <i>PSBS2</i>	Cre13.g571580	4,29	Probable transposon-derived protein of Chlamydomonas-Specific family B
Cre12.g496402	7,22	No annotation available	Cre06.g310500	4,25	bZIP transcription factor, <i>HYS</i>
Cre02.g077976	6,55	No annotation available	Cre05.g242502	4,24	No annotation available
Cre09.g394325	6,51	Photosynthesis. Chlorophyll a/b binding protein. Early light-inducible protein 9, <i>ELIP9</i>	Cre16.g686350	4,20	No annotation available
Cre01.g021800	5,79	Histone-lysine N-methyltransferase	Cre03.g207489	4,20	No annotation available
Cre07.g349700	5,74	Putative dehydrogenase	Cre03.g197750	4,19	Glutathione peroxidase, <i>GPX3</i>
Cre08.g384650	5,71	Photosynthesis. Chlorophyll a/b binding protein. Early light-inducible protein 7, <i>ELIP7</i>	Cre02.g143450	4,17	No annotation available
Cre12.g493700	5,56	Xanthophyll cycle. Zeaxanthin epoxidase, <i>ZXE2</i>	Cre09.g393953	4,12	No annotation available
Cre12.g501702	5,50	No annotation available	Cre13.g588150	3,98	GDP-L-galactose phosphorylase, <i>VTC2</i>
Cre10.g460326	5,46	No annotation available	Cre17.g731050	3,97	No annotation available
Cre16.g686400	5,06	FAD-dependent oxidoreductase	Cre13.g579650	3,95	No annotation available
Cre17.g740950	5,05	Photosynthesis. Chlorophyll a/b binding protein. High-intensity light-inducible LHC-like protein, <i>LHL4</i> (alias <i>ELIP6</i> )	Cre13.g571560	3,95	No annotation available
Cre09.g392097	5,04	No annotation available	Cre17.g733174	3,91	No annotation available
Cre08.g360850	5,03	No annotation available	Cre12.g519300	3,88	Conserved expressed protein, possible chloroplast localization, <i>TEF9</i>
Cre11.g467627	4,93	$\beta$ -amyryn 11-oxidase	Cre16.g681100	3,86	No annotation available
Cre13.g587500	4,86	Flavin-containing amine oxidase	Cre17.g703000	3,84	No annotation available
Cre08.g376250	4,86	Antifreeze protein, type I	Cre09.g407200	3,83	Putative all-trans-retinol 13,14-reductase
Cre07.g333100	4,84	No annotation available	Cre10.g428000	3,79	No annotation available
Cre03.g190250	4,82	Subtilisin-like protease	Cre14.g626750	3,77	Photosynthesis. Chlorophyll a/b binding protein. Maintenance factor for PSI, <i>MSF1</i> (alias <i>ELIP1</i> )
Cre15.g634650	4,71	No annotation available	Cre06.g258600	3,77	No annotation available
Cre08.g365900	4,62	Photosynthesis. Chlorophyll a/b binding protein. LHC- stress related protein 1, <i>LHCSR1</i>	Cre01.g028600	3,76	Short-chain dehydrogenase/reductase
			Cre14.g624350	3,76	Tocopherol O-methyltransferase, <i>VTE6</i>

**Table 3.1: 50 genes whose expression is most induced by UV-B exposure in *C. reinhardtii* WT CC5325, and their functional annotations. (FDR 0,05). The identifiers in green correspond to actors of photosynthesis or photoprotection. The shaded lines correspond to genes also identified in the proteomic analysis presented in Chapter 2 (Table 2.1).**

## 4. SUMMARY

In this second chapter, we have:

- Established that under UV-B, the expression of *LHL4* was controlled by the UV-B specific photoreceptor UVR8 but might also be slightly dependent on the blue light photoreceptors pCRY and aCRY
- Showed that under HL, LHL4 protein accumulation was controlled by the three blue light photoreceptors aCRY, pCRY and PHOT which acted in different ways: PHOT promoted its induction while aCRY and pCRY repressed its accumulation. This control was not necessarily exercised at the level of the transcription of the *LHL4* gene.
- Highlighted that CO was the main transcription factor of *LHL4* in both UV-B and HL while HY5 played no role in this process.
- Demonstrated that in contrast to LHL4, HY5 might modulate the level of NPQ proteins in response to HL
- Explored the role of HY5 and CO by transcriptomic and showed that gene expression under UV-B was mainly under the control of CO, but that HY5 was also involved in the transcription of few genes, similar or not to those induced by CO

# **CHAPTER 4:**

## **LHL4 PREVENTS SHORT-TERM PHOTOINHIBITION AND INCREASES TOLERANCE TO LIGHT CHANGES IN *C. REINHARDTII***

---

In the two first chapters of the manuscript, we identified the LHL4 proteins and characterized its expression upon both UV-B and HL. In this last result chapter, we will focus on its function in the light acclimation process of *Chlamydomonas reinhardtii*.

### **1. GENERATION AND MOLECULAR CHARACTERISATION OF STRAINS IMPAIRED IN LHL4 EXPRESSION**

In order to understand the function of the LHL4 protein in *C. reinhardtii*, we investigated the photoprotective response in mutants affected in LHL4 expression. One insertion mutant was available in the CLiP mutant library: LMJ.SG0182.003906 whose donor DNA cassette is inserted in the second intron of the *LHL4* gene (**Fig. 4.1A**). Characterisation of this mutant showed that the protein was still present in the mutant, although at a lower level than in the WT (~20 % of the WT level, data not shown). However, we could not exclude the possibility that a small amount of LHL4 was sufficient to maintain its role within the cell. Indeed, it had been shown for example that a small amount of LHCSR1 was sufficient to induce NPQ in *C. reinhardtii* (Dinc et al. 2016). Therefore, we chose to generate a KO mutant by CRISPR/Cas9 in the laboratory. An exogenous donor DNA containing a stop codon was inserted at the end of the first exon of the *LHL4* gene (**Fig. 4.1A**). The positive transformants were identified by PCR and were sequenced to confirm the correct insertion of the donor DNA. Two candidate mutants were identified. We then confirmed that in these two strains, *LHL4* gene expression was abolished (**Fig. 4.1B**), and that the corresponding protein was not detectable after both HL or UV-B exposure. These two KO mutants were named *lhl4a* and *lhl4b* (**Fig. 4.1C**). For the remainder of this

manuscript, all experiments were performed with the *lhl4a* mutant (referred to as '*lhl4*' below).

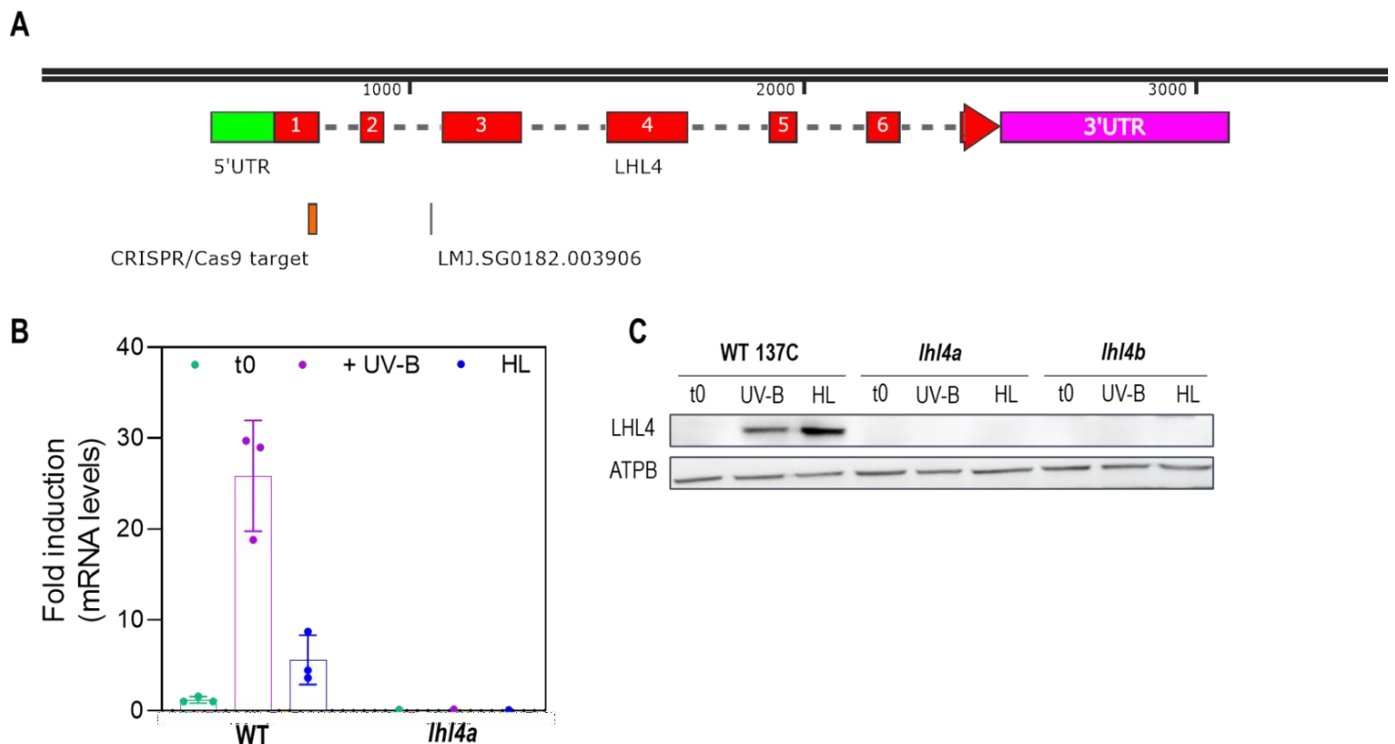


**Figure 4.1: Characterisation of the *lhl4* mutant.** (A) Map of the LHL4 gene: 5'UTR (green), 3'UTR (pink), exons (red), introns (dotted). The localization of the DNA insertion of the *Clp* mutant (LMG.SG0182.003906) and of the mutant generated by CRISPR/Cas9 in B and C are shown below the map. (B) and (C) Expression of the LHL4 gene and protein in the *lhl4* mutants compared to the WT 137C in growth conditions (t0) or after exposure to UV-B (30  $\mu\text{mol photons m}^{-2} \text{s}^{-1}$  + 0.2  $\text{mW.cm}^{-2}$  UV-B) or HL (300  $\mu\text{mol photons m}^{-2} \text{s}^{-1}$ ). The level of gene expression is analysed by RT-qPCR (1h exposure) and the protein accumulation by immunodetection (6h exposure). ATPB was used as a loading control. The membranes are representatives of the 3 biological replicates tested. Error bars correspond to standard deviation (SD; n=3 biological replicates and 2 technical replicates).

## 2. LHL4 PROTECTS PSII FROM PHOTOINHIBITION

### 2.1. LHL4 is not an NPQ actor

As demonstrated earlier in **chapter 2**, LHL4 belongs to the ELIP family, a family of proteins whose role had not yet been clearly identified but which was probably involved in photoprotection. Still, despite its differences in terms of sequence, LHL4 shared similarities with the NPQ actors already identified in *C. reinhardtii* (LHCSR1, LHCSR3, and PSBS) due to its intrinsic characteristics (inducible, UV-B and HL responsive, light intensity dependent accumulation). Therefore, we first decided to investigate whether LHL4 was able to modulate NPQ capacity. NPQ was measured via chlorophyll fluorescence in WT137C and in *lhl4* under LL (control condition; non-acclimated cells), or after a 6h

exposure to UV-B or HL to induce LHL4. (**Fig. 4.2A**). Our data indicated that there was no difference in NPQ level between WT and *lhl4*, regardless of the light treatment to which the cells were exposed. The NPQ capacity did not depend on LHL4, but mainly on the accumulation of the three NPQ proteins, which was similar in the mutant and in the WT (**Fig. 4.2B**). This strongly suggests that the LHL4 protein does not directly modulate NPQ extent, at least when the NPQ effectors are present.

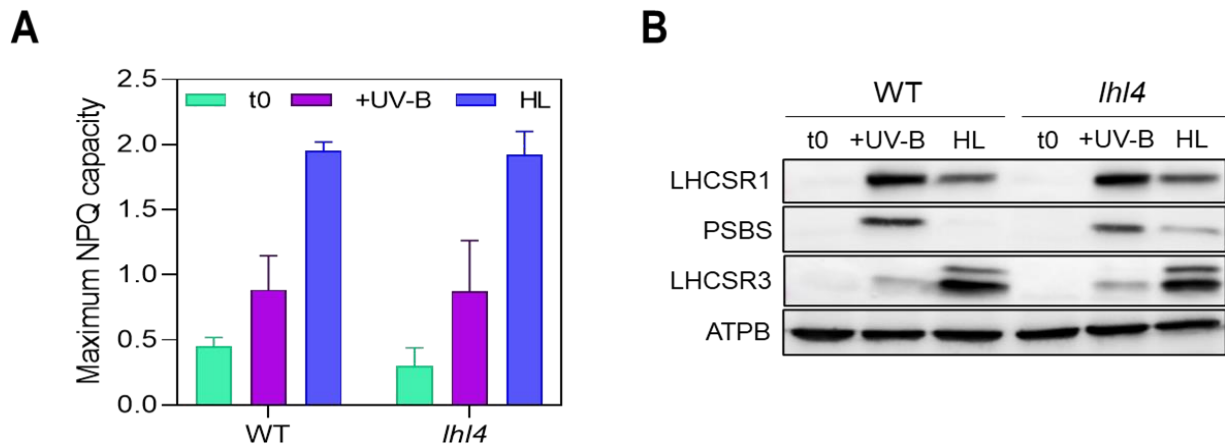


**Figure 4.2: LHL4 is not a NPQ actor. (A)** Maximum NPQ capacity of WT 137C and the *lhl4* mutant in growth conditions (t0) and after exposure to moderate UV-B ( $30 \mu\text{mol photons m}^{-2} \text{s}^{-1} + 0.2 \text{ mW.cm}^{-2} \text{ UV-B}$ ) or HL ( $300 \mu\text{mol photons m}^{-2} \text{s}^{-1}$ ) for 6h. Error bars represent standard deviations ( $n=3$ ). **(B)** Accumulation of NPQ proteins in each strain after 6h of UV-B ( $30 \mu\text{mol photons m}^{-2} \text{s}^{-1} + 0.2 \text{ mW.cm}^{-2} \text{ UV-B}$ ) and or HL ( $300 \mu\text{mol photons m}^{-2} \text{s}^{-1}$ ). ATPB is used as a loading control for western blots. The membrane is representative of the 4 biological replicates tested.

## 2.2. LHL4 is involved in photoprotection, prior to the establishment of NPQ

We decided to investigate the potential effect of light treatment on photosynthetic apparatus physiology by monitoring the Fv/Fm parameter, which is commonly used to assess the integrity of the PSII and its photoinhibition/degradation in stress conditions. Cultures of WT 137C, *lhl4* and *uvr8* mutants were acclimated overnight to low doses of UV-B. The acclimation induced the accumulation of NPQ proteins that protected the cell against the subsequent exposure to light stress, but also of LHL4 (**Fig. 4.3**).

First of all, a drastic decrease (30 to 60%) of the Fv/Fm was observed during the first hour of treatment compared to the initial level (t0), regardless of the cultures and the acclimation considered (**Fig. 4.3A2**). This decrease was more pronounced in non-acclimated samples compared to cultures acclimated to UV-B which exhibits a 30% higher Fv/Fm. This observation confirmed the photoprotective effect induced by UV-B (**Fig. 4.3**,

Allorent et al., 2016). The *uvr8* strain, used as a control in this experiment, did not show a significant difference in Fv/Fm between acclimated or not samples confirming that the protection provided by UV-B against HL was controlled by the UVR8 photoreceptor. Moreover, the *uvr8* acclimated strain was even already affected at the beginning of the experiment (t0), probably because of a deleterious effect of UV-B during acclimation on this mutant, which was known to be highly sensitive to this radiation, as already observed in *A. thaliana* (Kliebenstein et al. 2002b).

In non-acclimated cells, a defect in the accumulation of LHL4 led to a higher photoinhibition (**Fig. 4.3A2 and A3**), which demonstrated that LHL4 mitigated the extent of photodamage during the first two hours of exposure to HL (**Fig. 4.3A3**). On the other hand, this difference was suppressed on a longer time scale (3h; **Fig. 4.3A4**) and in UV-B acclimated samples, where both WT and *lhl4* were similar throughout the experiment.

These findings suggest that LHL4 plays a crucial role in the preservation of PSII function in the absence of protection conferred by UV-B acclimation. This protection was transient and disappeared after three hours of HL exposure. This timing coincided with the time required to fully induce the NPQ proteins that protected cells against the damaging effects of HL exposure (Allorent et al. 2013). This NPQ capacity was also provided by UV-B acclimation, i.e. condition where the WT and *lhl4* were similar in our dataset. These observations may suggest that LHL4 is required for PSII protection when the NPQ capacity has not been yet acquired by the cells. To explore this hypothesis, we monitored the NPQ capacity of the different strains during the same experiment (**Fig 4.3B**). Our result showed that acclimated samples were already able to develop NPQ response when the HL exposure starts. In contrast, NPQ capacity was only detectable after 2 hours of HL exposure in non-acclimated samples. The NPQ capacity in these cells only reached the initial level of UV-B acclimated cells after 3h. Overall, these data support our hypothesis that LHL4 helps cells to cope with high light stress when their NPQ capacity is not high enough to effectively protect the photosynthetic apparatus from photodamage.

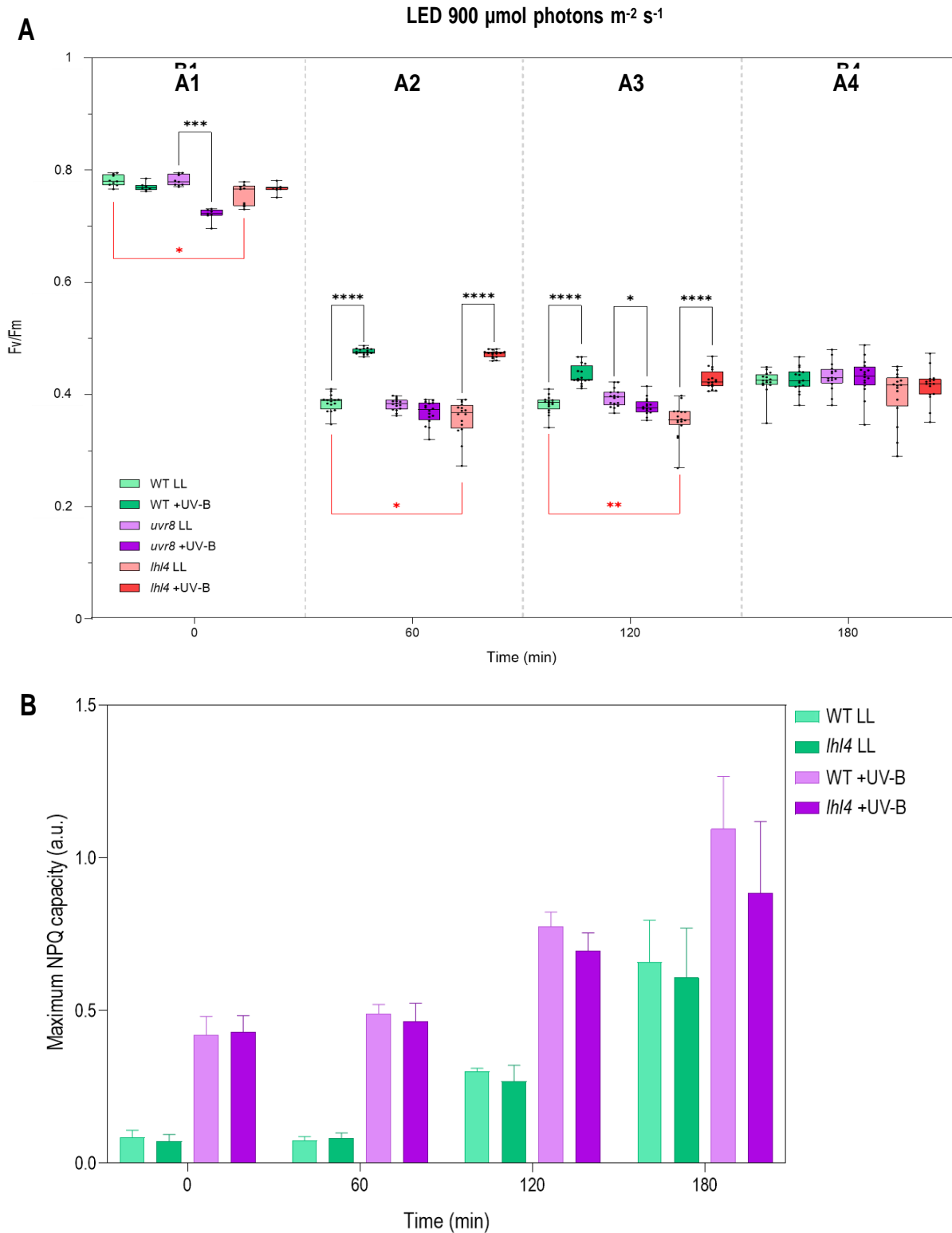


**Figure 4.3: LHL4 alleviates PSII photoinhibition. (A)** WT137C, *uvr8* and *lh14* cells were acclimated (+UV-B) or not (LL) to low doses of UV-B ( $30 \mu\text{mol photons m}^{-2} \text{s}^{-1}$  LL +  $0.08 \text{ mW.cm}^{-2}$  UV-B) for 16h (0). The cultures were then exposed to HL ( $900 \mu\text{mol photons m}^{-2} \text{s}^{-1}$  of white light) for 3h. The Fv/Fm was then monitored every hour. The statistical differences in Fv/Fm at each time point are shown in the corresponding box plots. The differences between the strains (red stars) and the effect of the different acclimations (black stars) were evaluated by a Kolmogorov-Smirnov test (\* p-value<0.05; \*\* p-value<0.01; \*\*\* p-value<0.001, \*\*\*\*p-value<0.0001; n=4 biological replicates). **(B)** Maximum NPQ capacity of the WT137C and *lh14* in the experimental conditions tested in A).

We therefore correlated these observations with the accumulation of NPQ proteins by comparing in the different strains their induction during the first hour of HL (**Fig. 4.4**). In the WT, NPQ proteins and LHL4 were absent when cells were not acclimated to UV-B. The exposition under 1h of HL led to the induction of the four proteins. In contrast, cells acclimated already contained LHCSR1, LHCSR3 and LHL4. After 1h of HL exposure, the level of LHCSR3 increased but the level of LHCSR1 remained stable. In stark contrast with non-acclimated cells, LHL4 induction was largely repressed, despite the HL exposure. These data show that the induction of LHL4 is inhibited when cells had already acquired the full capacity (through both LHCSRs) to mitigate the damaging consequences of high light exposure. This observation was confirmed in *uvr8*, which exhibited a high induction of LHL4 even after UV-B acclimation, because the NPQ proteins were not present when the HL treatment has started.

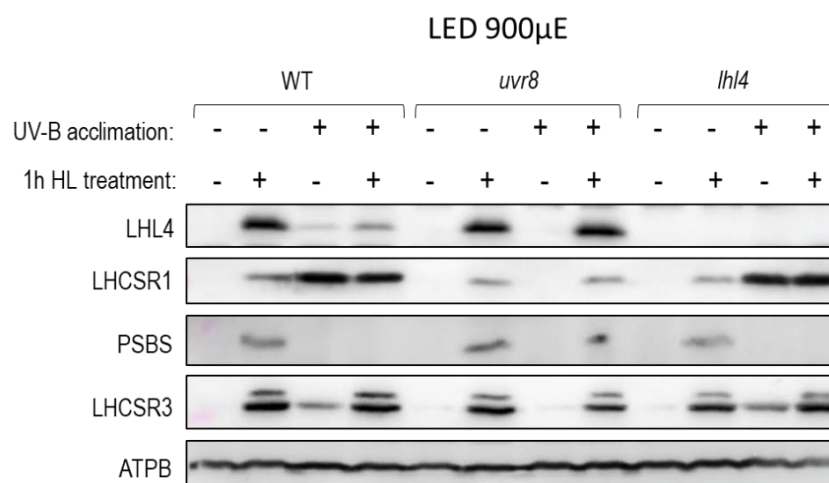


**Figure 4.4: LHL4 induction is repressed when NPQ proteins are present** Accumulation of NPQ and LHL4 proteins in cultures of WT137C, *lhl4* and *uvr8*. Cells were acclimated (UV-B acclimation +) or not (UV-B acclimation -) to low doses of UV-B ( $30 \mu\text{mol photons m}^{-2} \text{s}^{-1}$  LL +  $0.08 \text{ mW.cm}^{-2}$  UV-B) for 16h. The cultures were then exposed to  $900 \mu\text{mol photons m}^{-2} \text{s}^{-1}$  for 1h. ATPB is used as a loading control. The membrane is representative of the 2 biological replicates tested.

### 2.3. The absence of LHL4 decreases the cell's ability to regulate photooxidative stress

The photoinhibition phenotype of *lhl4* (**Fig. 4.3**) might result from an excessive accumulation of ROS (Reactive Oxygen Species) in the cell. This hypothesis was consistent with the predicted role of the ELIP proteins (to which LHL4 belongs) in the protection against photooxidative stress. Indeed, during the photosynthetic process, the chlorophylls

(Chl) of photosystems are excited by the light energy of photons and enter an excited state (Chl\*). In order to return to their ground state, Chl must dissipate this energy, which normally occurs via three different pathways: photochemistry, fluorescence, and NPQ. However, during prolonged exposure to HL, the excess light energy leads to the degradation of photosystems and the release of their pigments. Among these pigments, free chlorophylls are highly reactive and excitable by light, with no possibility to transfer this excess energy. Under these conditions, chlorophylls can remain excited and form a chlorophyll triplet ( $^3\text{Chl}^*$ ). This triplet can react with the oxygen present and lead to the formation of highly reactive singlet oxygen ( $^1\text{O}_2$ ), which generates a strong photooxidative stress for the cell, particularly at the level of the PSII (**Fig. 4.5A**; Krieger-Liszkay, 2005). ELIPs, due to their structure, could play a role in trapping free chlorophylls under such conditions (Adamska 2001). Furthermore, LHL4 is predicted to contain at least two chlorophyll a/b binding sites (**Fig 2.2, chapter 2**), which could therefore be involved in this type of function. We were therefore interested in the singlet oxygen production of the *lhl4* mutant, compared to WT 137C using a  $^1\text{O}_2$ -specific fluorescent dye, SOSG (Singlet Oxygen Sensor Green). The use of SOSG was controversial for certain reasons (unevenness of cell penetration, photosensitivity), but it remained a reference dye for the quantification of singlet oxygen in photosynthetic organisms (Prasad et al. 2016, 2018; Virtanen et al. 2021) In the experiment, cells were exposed for 30 min to moderate HL ( $300 \mu\text{mol photons m}^{-2} \text{s}^{-1}$ ) with SOSG. The fluorescence was then measured to estimate the relative amount of  $^1\text{O}_2$  in the cells (**Fig. 4.5B**). Cells were not preacclimated in this experiment, since we had previously established that the difference between WT and *lhl4* was more important in this condition (**Fig. 4.3**).

Our results indicated that *lhl4* accumulated 2 times more singlet oxygen than the WT under these conditions, which confirmed its higher sensitivity when exposed to high light and was probably responsible of the photoinhibition previously observed (**Fig 4.3**). This experiment could be confirmed using alternative strategies such as electron paramagnetic resonance spin-trapping spectroscopy, or RT-qPCR on marker genes of  $^1\text{O}_2$  accumulation such as *GPXH* (Glutathione peroxidase; Fischer et al. 2006).

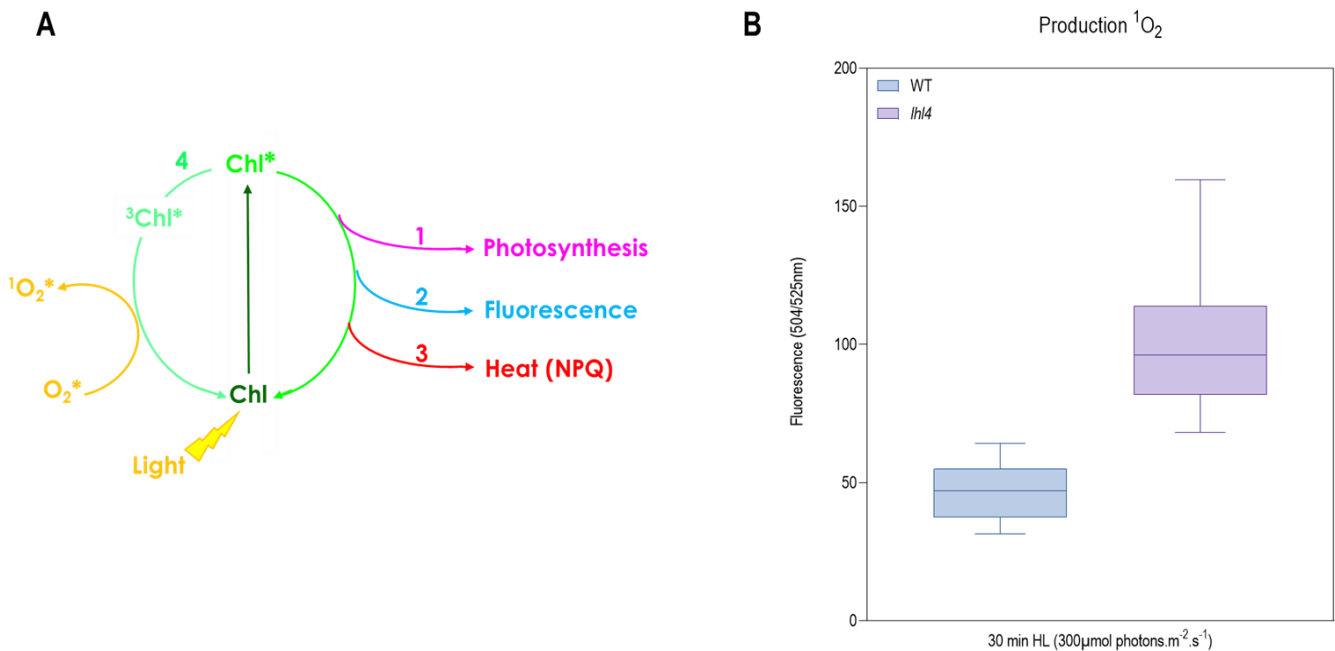


**Figure 4.5: LHL4 is involved in photooxidative stress regulation. (A)** Schematic representation of singlet oxygen generation via the formation of chlorophyll triplets. **(B)** The level of singlet oxygen in cells was measured using the SOSG dye (0.5 μM). WT137C and *lhl4* were exposed for 30 min to 300 μE HL in the presence of the dye. 100 μL of each culture was then collected. The green fluorescence of the dye was then measured with a TECAN plate reader (Em: 504 nm; Ex: 525 nm). This experiment was performed on 5 biological replicates, and each replicate allowed 21 technical replicates, for a total of n=105 measurements, error bars correspond to SD. Data kindly provided by Dr Dimitri Tolleter.

### 3. THE IMPORTANCE OF LHL4 DEPENDS ON THE LIGHT INTENSITY

#### 3.1. The stronger the high light is, the more important LHL4 becomes

We had clearly established that the *lhl4* mutant was photosensitive when exposed to high light. In order to draw a more global view on the role of LHL4 in response to light stress, we decided to investigate the light intensity dependency of this phenomenon. The Fv/Fm was measured in the WT and *lhl4* after exposure for one hour to different HL intensities. In non-acclimated cells, the difference between the WT and *lhl4* increased when the light

intensity became stronger suggesting a more preponderant role of LHL4 in the protection of PSII when the stress became severe (**Fig. 4.6**).

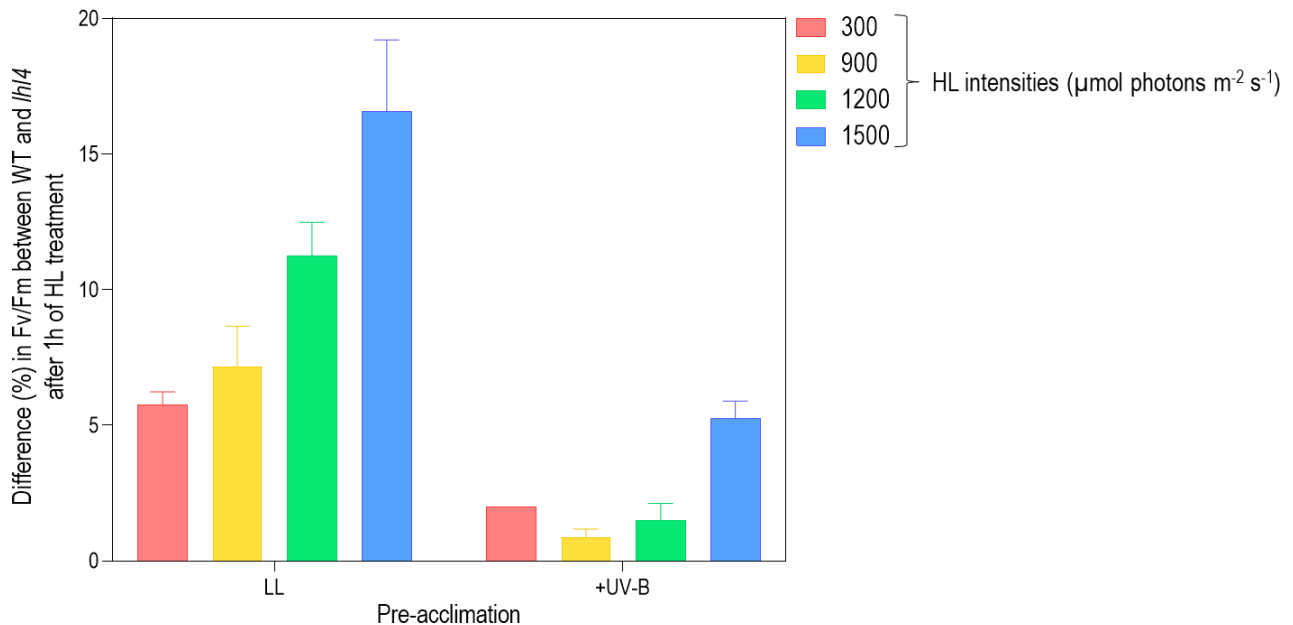


**Figure 4.6: LHL4 is more important with increasing light intensity.** WT 137C and *lhl4* cells were acclimated (+UV-B) or not (LL) to low doses of UV-B ( $0.08 \text{ mW.cm}^{-2}$  UV-B +  $30 \mu\text{mol photons m}^{-2} \text{ s}^{-1}$  LL) for 16h. The cultures were then exposed to different HL intensities ( $300/900/1200/1500 \mu\text{mol photons m}^{-2} \text{ s}^{-1}$ ) for 1h. The difference of Fv/Fm after 1h between the WT and *lhl4* at each intensity is presented. Error bars represent standard deviations ( $n=3$  to 6 biological replicates depending on the experiments and 2 technical replicates).

For cultures acclimated to UV-B, the experiment confirmed that the WT and *lhl4* were similar, as previously shown (**Fig 4.3**). However, at the highest light intensity tested ( $1500 \mu\text{mol photons m}^{-2} \text{ s}^{-1}$ ) the Fv/Fm became significantly different between the two strains (**Fig. 4.6**), despite the UV-B acclimation and the presence of NPQ proteins (**Fig. 4.4**). Therefore, it seems that beyond a certain HL intensity, the UV-B-induced NPQ proteins alone are no longer sufficient to effectively protect the photosynthetic apparatus, which make LHL4 even more essential in these conditions to limit photoinhibition.

### 3.2. The *lhl4* mutant is not able to cope with extreme light intensities, despite UV-B acclimation

While our first results (**Fig. 4.3, 4.4, and 4.5**) showed that the role of LHL4 was limited to cells in which NPQ proteins were not yet present and active, this latest result suggested that LHL4 might also play an important role when NPQ effectors were present (**Fig 4.4**), when the cells had to cope with a very high irradiance (**Fig. 4.7**;  $1500 \mu\text{mol photons m}^{-2}$

s<sup>-1</sup>). To test what were the consequences on this difference at very high intensity on a longer term, we performed photobleaching experiments on WT 137C and *lhl4* mutant cultures, acclimated or not to UV-B as described above, and then exposed to extreme light stress (2000  $\mu\text{mol photons m}^{-2} \text{s}^{-1}$ ). These conditions were expecting to mimic that faced by photosynthetic organisms during summer in Europe. The cell fitness was monitored by following pigment density in the culture, either by a visual inspection of the colour culture (**Fig. 4.7A**) or by pigment quantification (**Fig. 4.7B**) In parallel, the NPQ protein accumulation was also evaluated by immunodetection (**Fig. 4.7C**).

Cultures not acclimated to UV-B bleached much more rapidly than those protected by UV-B light exposure, for both WT and *lhl4*. After 2h of HL, the *lhl4* was already completely bleached, whereas the WT strain was still slightly green before it was also bleached after 3h. This observation confirmed by another experimental approach the photosensitivity of *lhl4* observed in the previous experiments (**Fig. 4.3 and 4.6**). In UV-B acclimated cultures, both cultures remained green for a few hours. This observation was probably related to the protection provided by the NPQ proteins. However, this protection was not sufficient over the long term in *lhl4* which bleached after 5 hours (**Fig. 4.7A**). This result underlines the crucial role of LHL4, which added an extra mandatory layer of photoprotection in the cell exposed at this very high light intensity, i.e. conditions in which NPQ proteins cannot handle all the excess light energy absorbed to protect the photosynthetic apparatus. This experiment demonstrates that in addition to its transitory role under moderate light, the absence of LHL4 could have dramatic long-term consequences when cells are exposed to extreme light stress.

The bleaching phenotype of the *lhl4* mutant was supported by HPLC analysis of the pigment content (total chlorophylls and xanthophylls) of the WT and *lhl4* under these conditions. (**Fig. 4.7B**). Indeed, the non-acclimated cells showed a drastic decrease (5 times less in both cultures) in their pigment content after 1h of HL (2000  $\mu\text{mol photons m}^{-2} \text{s}^{-1}$ ). In UV-B acclimated cultures, the chlorophyll and xanthophyll content decreased more rapidly over time in *lhl4* than in WT, which was consistent with the bleaching phenotype.

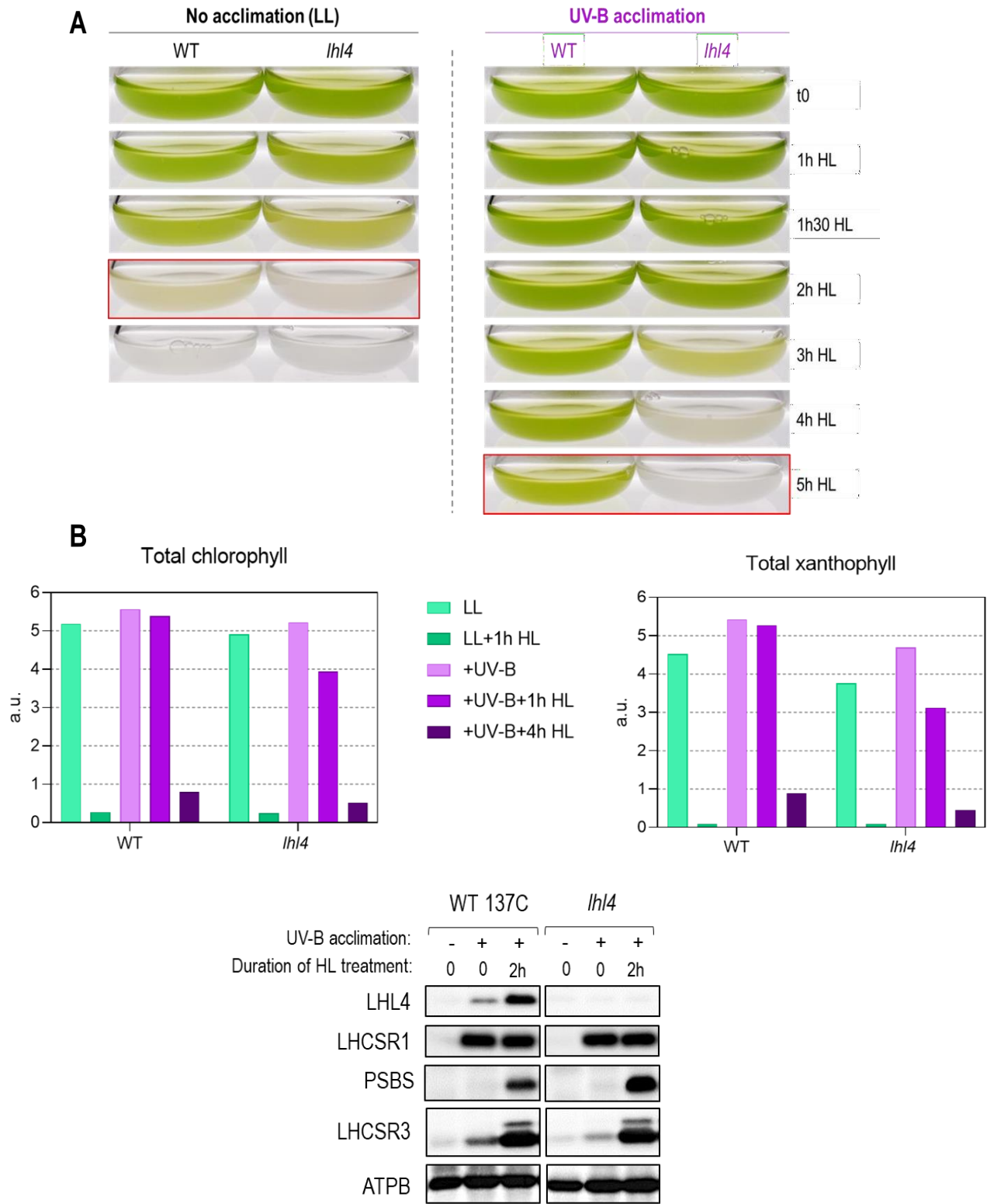


**Figure 4.7: The *lhl4* mutant is photosensitive.** (A) Photobleaching experiment performed on *Chlamydomonas* WT137C and *lhl4* acclimated (+UV-B) or not (LL) to low doses of UV-B ( $30 \mu\text{mol photons m}^{-2} \text{s}^{-1}$  LL +  $0.08 \text{ mW.cm}^{-2}$  UV-B) for 16h and then exposed for 4h to a strong HL treatment ( $2000 \mu\text{mol photons m}^{-2} \text{s}^{-1}$ ). Photos were taken regularly during the exposure to HL. Red frame: time point where the *lhl4* culture is bleached and not the WT (B) Total xanthophyll and chlorophyll contents of the strains after strong HL exposure. Cells were prepared as in A and harvested after LL or UV-B acclimation and after 1h of HL ( $2000 \mu\text{mol photons m}^{-2} \text{s}^{-1}$ ) or 4h (UV-B acclimated cells only). Pigment content was estimated by HPLC analysis. (C) Accumulation of LHL4 and NPQ proteins in cells acclimated or not to UV-B ( $30 \mu\text{mol photons m}^{-2} \text{s}^{-1}$  LL +  $0.08 \text{ mW.cm}^{-2}$  UV-B) and after 2h of HL ( $2000 \mu\text{mol photons m}^{-2} \text{s}^{-1}$ ). ATPB is used as a loading control. *The membranes are representatives of the 2 biological replicates tested*

Finally, we collected cells throughout the bleaching process and analysed by immunodetection the accumulation of LHL4 and NPQ proteins over time in the two strains (**Fig. 4.7C**). Thanks to these results, we were able to confirm that the photobleaching was only due to the absence of LHL4 in the mutant, and not to a defect in the induction of NPQ proteins which accumulated in the same way in *lhl4* during the early steps of the experiment.

#### **4. PHOTOPROTECTIVE ROLE OF LHL4 UNDER NATURAL SUNLIGHT EXPOSURE**

We finally decided to challenge the role of LHL4 in natural sunlight conditions. At the difference with our experimental setup, sunlight combines both HL and UV-B in fluctuating proportions that are hardly reproducible in laboratory conditions, which may in turn exacerbate the photoprotective role of LHL4 (**Fig. 4.8**). We decided therefore to monitor the photoinhibition by measuring the Fv/Fm (as in **Fig 4.3**) in cells acclimated or not to UV-B and exposed for few hours to natural sunlight. During the experiment, the HL intensity varied from 500 to 1000  $\mu\text{mol photons m}^{-2} \text{s}^{-1}$  (similar to the one used in the previous experiment), and UV-B from 0.1 to 0.5  $\text{mW.cm}^2$  (much higher than the one used for the acclimation). The setup was built so that the other parameters (agitation, temperature) were controlled to ensure that the putative differences between the WT and *lhl4* could only be attributed to the effects of light. The results showed that in non-acclimated cells, the difference between the WT and *lhl4* was higher compared to the stress using LED panels, suggesting that the combination of HL and UV-B was more deleterious for the cells and that under this condition, the presence of LHL4 was even more important to limit photoinhibition (**Fig. 4.8**). This finding was also supported by the fact that under natural sunlight, acclimated cells of both strains were also significantly different, in stark contrast to the experiment performed in lab-controlled conditions. Overall, this experiment underlines the preponderant role of LHL4 in the protection of PSII, which may be of even greater relevance when the algae has to cope with multiple light stress in natural environment.

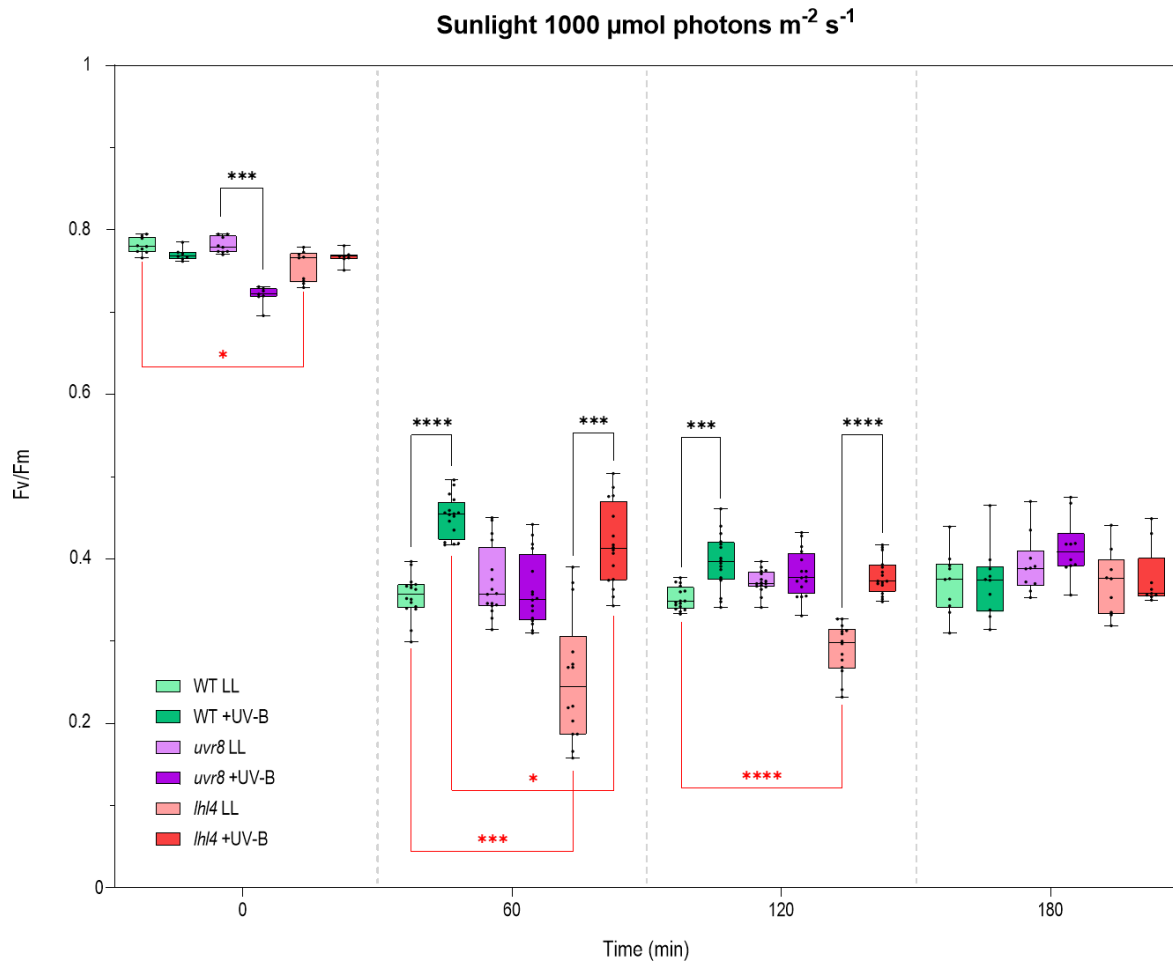


**Figure 4.8: LHL4 is of primary importance for the protection of PSII in natural light.** WT137C, *uvr8* and *lhl4* cells were acclimated (+UV-B) or not (LL) to low doses of UV-B ( $30 \mu\text{mol photons m}^{-2} \text{s}^{-1}$  LL +  $0.08 \text{ mW.cm}^{-2}$  UV-B) for 16h (0). The cultures were then exposed to sunlight ( $1000 \mu\text{mol photons m}^{-2} \text{s}^{-1}$  of white light +  $0.5 \text{ mW.cm}^{-2}$  UV-B) for 3h. The Fv/Fm was monitored every hour. The statistical differences in Fv/Fm at each time point are shown in the corresponding box plots. The differences between the strains (red stars) and the effect of the different acclimations (black stars) were evaluated by a Kolmogorov-Smirnov test (\* p-value<0.05; \*\* p-value<0.01; \*\*\* p-value<0.001, \*\*\*\*p-value<0.0001; n=4 biological replicates and 2 technical replicates).

## 5. SUMMARY

In this chapter we have demonstrated that:

- LHL4 did not modulate the extent of NPQ in *C. reinhardtii* and that the accumulation of the NPQ-related proteins was not impaired in the *lhl4* mutant
- LHL4 protected non-acclimated cells from damage caused by high light exposure during the first hours of the stress, when NPQ was not yet active in the cells.
- The protective effect of LHL4 was higher when the light intensity increased and limited the production of  $^1\text{O}_2$  to help the cells to cope with high light

- The induction of LHL4 during the stress was repressed when NPQ proteins were already present in the cells
- The presence of LHL4 was mandatory for the survival of *C. reinhardtii* under extreme HL exposure
- The requirement of LHL4 to protect the cells from the damaging effect of light stress was exacerbated under natural sunlight

# **CHAPTER 5:**

## **GENERAL DISCUSSION AND CONCLUSIONS**

---

The aim of my PhD project was to provide new insights into the regulation of UV-B-induced photoprotection in *C. reinhardtii*, by identifying new actors and possibly new mechanisms. Our proteomic and transcriptomic analyses led us to focus on the LHL4 protein, which until now has only been slightly studied in *C. reinhardtii*, and never in the context of UVR8-mediated photoprotection. Moreover, LHL4 displays a unique induction pathway, controlled by both UV-B and HL, which made this protein an interesting tool to study these two signalling pathways and their possible convergence in *C. reinhardtii*.

### **1. LHL4 IS A NON-CANONICAL ELIP**

ELIPs are proteins conserved in all members of the green lineage. They have been extensively studied in other species, especially in flowering plants, since their discovery in pea and barley in the 1980s (Meyer and Kloppstech 1984; Grimm and Kloppstech 1987). In contrast, few studies have been published on ELIPs and their function in *C. reinhardtii*, although 10 members of this protein family have been identified in this organism. Unlike the two ELIPs of *A. thaliana* (AtELIP1 and AtELIP2) whose amino acid sequences are extremely similar, the CrELIPs are quite different from each other (**Fig. 2.3, chapter 2**).

The LHL4 protein characterised in this thesis work is one of these 10 CrELIPs, identified as ELIP6 (*C. reinhardtii* genome v5 from Phytozome 10; Merchant et al., 2007). Nevertheless, based on the sequences of the different CrELIPs, LHL4 stands out from the others, which led us to question the relevance of its classification as an ELIP. From an evolutionary point of view, homologs of the LHL4 gene appear to be present in all unicellular green microalgae (*Chlamydomonas*, *Volvox*, *Dunaliella*, *Micromonas*, *Botryococcus*) but this gene has subsequently not been conserved in mosses and land plants (data obtained from Phytozome 13). In *C. reinhardtii*, the accumulation of LHL4 in cells is inducible and transient (**Fig. 2.3, chapter 2**), which are two main characteristics of ELIPs

compared to LHC proteins (Adamska et al. 1993; Adamska 1997, 2001; Rochaix and Bassi 2019). Other characteristics of ELIPs are the LHC motifs highly conserved in helices 1 and 3, as well as the residues involved in chlorophyll binding, that are all found in the LHL4 sequence (**Fig. 2.6, chapter 2**; Adamska 2001; Teramoto et al. 2006). The particularity of LHL4 compared to other ELIPs is that the extramembrane loop connecting helices 2 and 3 is very long (128 aa) in this protein compared to what is observed in ELIPs in general (about 20 aa) (Montané and Kloppstech 2000). This is the only notable difference between LHL4 and the other nine *C. reinhardtii* ELIPs, which provides support that LHL4 has been classified in this family. However, it must be noted that in the latest annotated version of the *C. reinhardtii* genome (v6.1, published in February 2023), the *LHL4* gene (Cre17.g740950) is no longer annotated as an ELIP, and the *ELIP6* designation now corresponds to a new gene: Cre13.g576760 (Craig et al. 2023) which may reopen the debate on its membership in this gene family.

## **2. LHL4 IS AN ELIP THAT LIMITS THE PSII PHOTOINHIBITION IN *C. REINHARDTII***

### **2.1. LHL4 limits PSII photoinhibition by limiting photooxidative stress regulation**

Our results (**Fig. 4.6, chapter 4**) showed that the *LHL4* gene mutation prevents photoinhibition of PSII by regulating  $^1\text{O}_2$  production of the cell upon exposure to HL.  $^1\text{O}_2$  is produced mainly in PSII, via the formation of highly reactive chlorophyll triplets from free chlorophyll (Krieger-Liszkay 2005). Currently, two hypotheses have been raised concerning the regulation of free chlorophyll (and as a consequence, of  $^1\text{O}_2$  level) by proteins of the ELIP family: i. ELIPs would act directly on the chlorophyll biosynthetic pathway; and ii. ELIPs would be able to bind and quench chlorophylls released by the degradation of photosystems during light stress (Adamska 2001; Tzvetkova-Chevolleau et al. 2007; Rochaix and Bassi 2019).

#### *2.1.1. Hypothesis 1: LHL4 may regulate pigment biosynthesis*

The first hypothesis would be a regulation of the chlorophyll biosynthetic pathway by LHL4. Indeed, in *A. thaliana*, constitutive expression of ELIP2 leads to a 50% decrease in

the amount of chlorophyll and subsequently diminishes the proportion of functional photosystems in the leaves (Tzvetkova-Chevolleau et al. 2007). Analysis of the chlorophyll synthesis pathway in this transgenic line showed that two important steps in the pathway were affected (decreases in GLUTAMYL tRNA REDUCTASE and Mg CHELATASE proteins leading to a slowing down of the flow of the chlorophyll synthesis pathway) by the constitutive presence of ELIP2 (red circles, **Fig. 5.1**). These results suggest that ELIP2 modulates chlorophyll synthesis to prevent the accumulation of free chlorophylls in thylakoids and thus oxidative stress (Tzvetkova-Chevolleau et al., 2007). However, it has been shown that the null mutation of both *ELIP1* and *ELIP2* in *A. thaliana* has no effect on the photosensitivity of the mutant or on its ability to recover from light stress. This suggests that the chlorophyll synthesis pathway is still regulated despite the missing ELIPs (Rossini et al., 2006). Therefore, it is difficult to conclude from these data on the role of ELIPs in the regulation of chlorophyll biosynthesis. The analysis of the chlorophyll biosynthetic pathway in the *lhl4* mutant (e.g. quantifying chlorophyll metabolic intermediates by HPLC) would definitely be an avenue to investigate this hypothesis and to explore for further work.

On the other hand, the same study (Rossini et al. 2006) also showed a decrease in the level of zeaxanthin in the double mutant *elip1 elip2* in HL, suggesting that ELIPs might rather be involved in the modulation of the pigments of the xanthophyll cycle, which had already been hypothesised in the past (Adamska 2001; Zarter et al. 2006). Our preliminary pigment analysis shows that, however still constitutive, the accumulation level of xanthophylls is lower in the *lhl4* mutant than in the WT (**Fig. 4.8, chapter 4**). Taken all together, these results may therefore support the idea that LHL4, and possibly ELIPs in general, are involved in the regulation of the xanthophyll cycle, which may increase the cell capacity to cope with excess light energy.

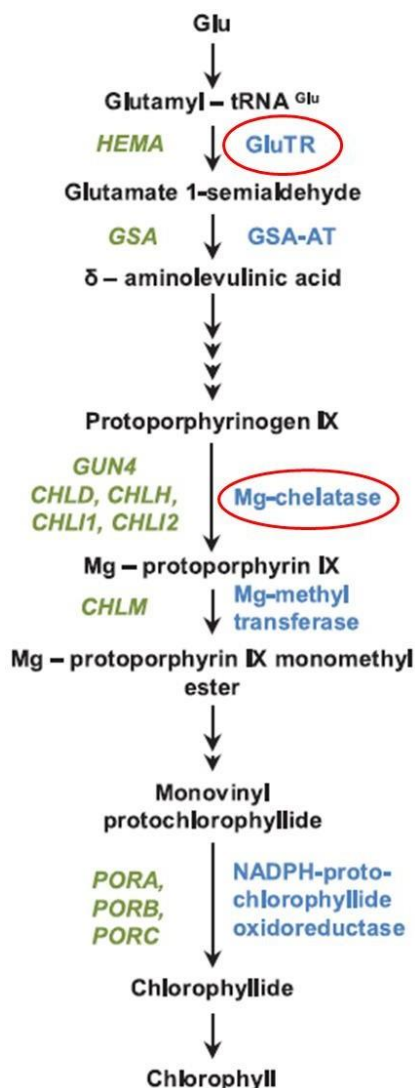


**Figure 5.1: Simplified scheme of chlorophyll biosynthesis pathway.** Genes and the corresponding enzymes catalysing distinct reactions of chlorophyll synthesis are indicated in green and blue, respectively. Red circles indicate the enzymes whose level is decreased when ELIP2 is constitutively expressed in *A. thaliana* (Tzvetkova-Chevolleau et al. 2007). Adapted from Cortleven and Schmölling, 2015.

### 2.1.2. Hypothesis 2: LHL4 may bind free chlorophylls to prevent <sup>1</sup>O<sub>2</sub> formation

The second hypothesis is that LHL4 may bind chlorophylls released by PSII degradation during HL exposure. Indeed, the sequence of LHL4 contains residues predicted to bind chlorophyll in the first and third transmembrane helix. The role of LHL4 could therefore be to scavenge free chlorophylls thus prevent oxidative stress by avoiding formation of chlorophyll triplets. In addition, given the low abundance of ELIPs in the membranes of thylakoids compared to that of the LHC proteins, it seems more likely that the ELIPs allow the scavenging of chlorophylls released by the core proteins of the photosystem (less abundant) than by the antennae (Montané and Kloppstech 2000). This hypothesis has been put forward concerning the function of ELIPs in flowering plants (Adamska et al. 1992b, a; Adamska 2001), as well as in the green microalga *Dunaliella* (Lers et al. 1991),

in which a LHL4 homolog is also present. In *C. reinhardtii*, our data show that LHL4 is associated to PSII (**Fig. 2.6, chapter 2**). On a native gel, the PSII band with which LHL4 colocalizes also corresponds to the PSII repair/degradation zone, where protein involved in PSII biogenesis (like HCF136) are located (unpublished data from the host lab). Thus, LHL4 could play a role in scavenging chlorophyll released from PSII at the time of their degradation. In addition, photosystem degradation occurs in about 1h, which is the time at which photoinhibition is measured (Erickson et al. 2015). We can therefore consider that it is at this time that a scavenger would be necessary for the chlorophylls released at that moment, which is consistent with the induction rate of LHL4, which is also of 1h (**Fig. 2.7, chapter 2 and 4.3 and 4.8, chapter 4**). The development of complementary approach such as in-gel cross-linking mass-spectrometry (IGX-MS) analysis, which consists in the use of small chemical cross-linkers, to allow the study of the structures and interactions of large protein assemblies, would precisely identify the main proteins that interact with LHL4 and therefore would bring insights of its mechanistic role in the protection of the photosynthetic apparatus (Hevler et al. 2021).

## **2.2. Physiological role of LHL4 in natural light conditions**

Our results show that LHL4 mitigates PSII photoinhibition upon exposure to HL in *C. reinhardtii*, preceding the accumulation of NPQ proteins, which later ensure a complete photoprotection (**Chapter 4**). Once synthesized, LHL4 is not stable and is rapidly degraded in the absence of light stimulus (UV-B or HL), which is also the case for PSBS (preliminary data from the host lab). In contrast, the NPQ proteins LHCSR1 and LHCSR3 remain detectable in the cells 8h after the end of the inducing signal (**Fig. 2.9, chapter 2**; and up to 2 days in Nawrocki et al., 2020). Furthermore, under natural light conditions, we have shown that the absence of the LHL4 protein is more deleterious to *C. reinhardtii* than under artificial laboratory light conditions (**Fig. 4.8, chapter 4**). This difference is probably due to the additive effect of HL and UV-B under natural conditions, whereas we usually study the two types of irradiation separately in the laboratory. In this context, our work provides new experimental evidences of the importance of the light spectrum, and in particular UV-B, for the acclimation of the photosynthetic apparatus.

Recent work (Sasso et al. 2018; Nawrocki et al. 2020) has emphasised the importance of moving to more physiological conditions than those usually used in the laboratory, with

the important limitation that UV-B radiations were not considered in both studies. Nevertheless, they show that high stability of LHCSR1 and LHCSR3 means that they are almost always present in the cells once they have been induced. In these conditions, NPQ can be rapidly activated at any time (Nawrocki et al. 2020) and protect the cells from photodamages. Our results (**Fig. 2.5, chapter 2 and 4.4, chapter 4**) demonstrate that in such conditions, LHL4 is not or less accumulated in the cells.

However, on a longer time scale, the level of NPQ proteins may become not sufficient to ensure PSII protection. Our results suggest that, in natural conditions, LHL4 could be quickly induced (within an hour ; **Fig. 4.4 chapter 4**) to protect the photosynthetic machinery, when the NPQ actors have been degraded and need to be synthesised again (e.g. in winter after long periods without high light intensity). It can also be synthesized when UV-B or white light exceed a certain intensity above which NPQ alone is no longer able to protect the photosynthetic apparatus (**Fig. 4.6, chapter 4**). Consequently, LHL4 would function as a sort of "emergency system" in the cell, and this model could explain its low stability and high inducibility upon UV-B and HL.

### **3. NEW INSIGHTS ON THE REGULATION OF UV-B- AND HL-INDUCED SIGNALLING PATHWAYS IN *C. REINHARDTII***

#### **3.1. Relative importance of the HY5 and CO transcription factors in the UV-B response**

In *A. thaliana*, the bZIP transcription factors AtHY5 and its homolog AtHYH are key transcription factors involved in the UVR8 signalling pathway (Ulm et al. 2004; Brown et al. 2005; Oravecz et al. 2006; Favory et al. 2009), whereas the B-box transcription factor like AtCO and AtCOL are involved in the blue and red light responses via cryptochromes and phytochromes (Liu et al. 2008; Song et al. 2020). However, our RNA-seq analysis of *hy5* and *constans* mutants exposed to UV-B revealed a dominant role of CrCO in the regulation of the UV-B response in *C. reinhardtii*. Indeed, 89% of the genes whose expression is altered by UV-B exposure (up- or down-regulated) are controlled by CrCO, whereas it is 42% for CrHY5 (**Fig. 2.2, chapter 2**). It was already shown that CrCO regulates the expression of genes involved in UV-induced photoprotection (*LHCSR1*, *LHCSR3*, *PSBS*) (Tokutsu et al. 2019). However, no global assessment of the UV-B

responsive transcriptome mediated by CrCO has been described as far. Furthermore, recent data show in *C. reinhardtii* that the regulation of genes involved in NPQ induction in HL are controlled by CrCO (Gabilly et al. 2019). Nevertheless, as mentioned earlier in this paragraph, induction of 42% of the genes involved in the UVR8-mediated UV-B response in *C. reinhardtii* depends on CrHY5. Together with the results presented in **Chapter 3** of this thesis, we conclude that CrCO is a major transcription factor in both photoreceptor-mediated UV-B and HL responses.

However, it is important to note that out of the total number of genes affected by UV-B exposure, the regulation of the expression of 58% of them depends on both CrCONSTANS and CrHY5, thus suggesting that both transcription factors are required for the regulation of these genes in *C. reinhardtii*. To understand this regulation pathway, several *co hy5* double mutants have recently been generated by crossing in our laboratory, but have not yet been characterised. A comparative RNA-seq analysis of these mutants with WT could in the future provide additional information on the role of CO and/or HY5 in the regulation of individual genes expression upon exposure to UV-B.

Furthermore, as these two transcription factors are involved in two distinct signalling pathways in *A. thaliana* (mainly UV-B via UVR8 for AtHY5; and mainly blue light via CRY2 for AtCONSTANS), it is likely that that the major role of CO has been lost in *A. thaliana*, and taken over by HY5. Then, the neofunctionalized CO and COL families have become major players in blue light-induced flowering in flowering plants such as *A. thaliana* (Putterill et al. 1995; Suárez-López et al. 2001).

### **3.2. Involvement of CO and the COP1 E3 ubiquitin ligase in the UV-B and high light-induced cellular responses in *C. reinhardtii***

Our results showed that LHL4 protein accumulates following exposure to UV-B or HL, at similar levels. Therefore, LHL4 represented an interesting tool to study the convergence between the UV-B- and HL-induced signalling pathways controlled by the UVR8 and PHOT photoreceptors in *C. reinhardtii*. We have shown that the two signalling pathways converge early in their signalling cascade, at the level of the CrCOP1/SPA1 complex. These results were subsequently confirmed with the NPQ proteins, LHCSR1, LHCSR3, and PSBS (**Fig. 3.3 and 3.4, chapter 3**).

Our analysis of mutants affected in UV-B and/or HL signalling pathways confirmed the key role of the CrCO transcription factor in the regulation of gene expression upon exposure to UV-B and HL, which had already been recently indicated for genes involved in photoprotection through NPQ (Gabilly et al. 2019; Tokutsu et al. 2019). Furthermore, these studies showed that CrCO stability is controlled at the level of protein stability by the E3 ubiquitin ligase complex CrCOP1/SPA1, as in *A. thaliana* (Liu et al. 2008). Our results support these observations since the studied proteins (LHL4, LHCSR1, LHCSR3, and PSBS) have the same accumulation pattern in *hit1* (*CrCOP1*) and *constans* mutants of *C. reinhardtii*. Moreover, the parallel study of these mutants in UV-B and HL allowed us to establish that, for proteins involved in photoprotection (here LHL4, LHCSR1, PSBS), CrCOP1 are involved in both signalling pathways.

CrCOP1 and CrCO are therefore part of both the UV-B and HL pathways. However, it is not clear whether there is crosstalk between the two pathways (one pathway regulates the other), or if the regulation of the target genes remains independent, although the pathways involve CrCOP1 and CrCO as common components. To clarify this point, it would be relevant to replicate this study under light that combine UV-B and HL, such as in natural light conditions (UV-B + HL) to investigate whether one pathway affects the other when both are active.

### **3.3. Regulation of the HL response by SPA1 in *C. reinhardtii***

Our results suggest that CrSPA1 is only involved in the HL response, and not in the UV-B response (as well as in *A. thaliana*, see Oravecz et al., 2006), at least with respect to the regulation of *LHL4* (**Fig. 3.3, chapter 3**). This observation seems consistent with recently published results on the study of two CrSPA1 mutants in *C. reinhardtii* (Gabilly et al. 2019; Tokutsu et al. 2019). Indeed, these studies showed no difference in the accumulation of NPQ proteins (LHCSR1, LHCSR3, PSBS) in the *spa1* mutant exposed to UV (UV-A 30% + UV-B 10%), compared to the WT (Tokutsu et al. 2019) but an over-accumulation of LHCSR1 and PSBS in the cells following HL in the *spa1-1* mutant (Gabilly et al. 2019). However, we were not able to confirm the constitutive accumulation of all three NPQ proteins in the *spa1* mutant as observed by Tokutsu et al. (2019)

In *C. reinhardtii*, it is already established that in the context of photoprotection, the response to HL is controlled by PHOT (Petroutsos et al. 2016), that is localized at the

plasma membrane (Huang et al. 2002) and flagella (Huang et al. 2004). The COP1/SPA1 complex is located in the cytosol and nucleus. As mentioned above, the *spa1* mutant exhibits an over-accumulation of LHL4 in HL, which means that under these conditions the CrCOP1/SPA1 complex no longer regulates the activity of downstream transcription factors (here, CrCO). It is conceivable that a competition between PHOT and SPA1 for binding to COP1 (e.g. as is the case between UVR8 and COP1) exists. Therefore, the absence of CrSPA1 would strengthen the CrPHOT-CrCOP1 interaction, thus preventing the relocation of CrCOP1 to the nucleus, and *a fortiori* the regulation of CrCO activity. On the other hand, CrSPA1 could also be regulated by another photoreceptor in HL, or there could be one or more intermediates in the CrPHOT-induced signalling cascade in HL (as suggested in Redekop et al., 2021) that would allow an indirect regulation of CrSPA1 activity (and thus of the CrCOP1/SPA1 complex) by CrPHOT. In the case of this second hypothesis, such intermediates have still to be identified.

In *A. thaliana*, the physical interaction of AtSPA proteins with AtCRY1 and AtCRY2 (Kleiner et al. 1999) has already been shown to regulate the activity of the AtCOP1/SPA complex by blue light (Lian et al. 2011; Liu et al. 2011a; Zuo et al. 2011; Podolec and Ulm 2018). The mechanism of CrCOP1/SPA1 complex regulation via the CrSPA1 subunit has not yet been investigated, but three photoreceptors of the cryptochrome family have been identified (aCRY, pCRY, CRY-DASH1). The CrCRY/CrSPA1 interaction could therefore also exist in *C. reinhardtii* and play a role similar to that characterised in *A. thaliana*.

### **3.4. Existence of secondary signalling pathways involved in HL response**

#### *3.4.1. Potential role of another photoreceptor(s)*

Previous research has shown that PHOT controls the HL-induced photoprotective response in *C. reinhardtii* (Petroutsos et al. 2016). Nevertheless, in our study, the analysis of the *phot* mutant still shows a strong HL-responsive accumulation of the NPQ proteins LHCSR1 and LHCSR3, as well as LHL4. It is also worth noting that the amount of *LHL4* transcripts in HL is at the same level in *phot* mutants as in WT (**Fig. 3.2, chapter 3**), indicating that PHOT does not affect *LHL4* expression. Taken together, our results suggest the existence of one or more PHOT-independent signalling pathways induced by HL in *C. reinhardtii*.

Other blue photoreceptors are present in *C. reinhardtii*: the cryptochromes (CRY) aCRY and pCRY. It has already been shown in diatoms, that cryptochromes are involved in photoprotection by controlling the induction of LHCX proteins (Juhas et al. 2014; Allorent and Petroustos 2017). Furthermore, the involvement of any of these cryptochromes in the HL response would also be consistent with the hypothesis of regulation of CrCOP1/SPA1 complex activity by CrCRYs, mentioned in the previous paragraph. In the *acry* and *pcry* mutants, the accumulation of LHL4 is higher than in the WT, both after UV-B and HL exposure. For the UV-B part, these results seem consistent with a recent study in *A. thaliana*, which showed that the activity of the UVR8 signalling pathway is regulated by AtCRYs (Tissot and Ulm 2020). Indeed, in that study, the UVR8 signalling pathway is hyperactivated in the *cry1 cry2* double mutant of *A. thaliana*. In a similar way, an overaccumulation of LHL4 is observed in *acry* and *pcry* mutants (**Fig. 3.2, chapter 3**) of *C. reinhardtii*, both in UV-B and HL, suggesting that CrCRYs might modulate indirectly photoprotection via the regulation of UVR8 and PHOT.

In order to gain a more complete understanding of the mechanisms that control photoprotection in HL, it might be relevant to generate and study a mutant of all blue photoreceptors. An *acry pcry phot* triple mutant, and possibly *acry phot*, *pcry phot*, *acry pcry* double mutants, would allow us to investigate the relative contribution of these photoreceptors to the regulation of photoprotection in HL in *C. reinhardtii*. Another option would be to study a mutant of the chloroplastic CRY-DASH1 photoreceptor, which is a member of the CRYs family recently studied in *C. reinhardtii* (Beel et al. 2012; Rredhi et al. 2021). The blue/UV-A part of the light spectrum is very important in *C. reinhardtii*, and the absorption spectra of the blue light photoreceptors (aCRY, pCRY, PHOT) and UV-A photoreceptor (CRY-DASH1) overlap to ensure optimal coverage of these irradiations (Rredhi et al. 2021). Thus, in HL, photoprotection could be regulated in parallel by PHOT and/or CRYs and CRY-DASH1.

#### 3.4.2. Alternative pathway for LHCSR3 induction in high light

Our results also show a different accumulation pattern of LHCSR3 in the HL-exposed signalling mutants (*hit1*(CrCOP1), *constans*, *hy5*) (**Fig. 3.4, Chapter 3**), compared to LHCSR1, PSBS, and LHL4. Indeed, whereas the induction of LHCSR1, PSBS, and LHL4 in HL seems to be totally controlled by CrCO and CrCOP1, a substantial accumulation of LHCSR3 can still be observed in the two respective mutants suggesting the existence of

another HL-responsive pathway for *LHCSR3* expression (see also Gabilly et al., 2019). This accumulation of *LHCSR3* could very well be photoreceptor-independent and rather the result of retrograde signals like those generated by ROS during light stress (Roach et al. 2017, 2020). Furthermore, it has already been shown in *C. reinhardtii* that the *LHCSR3* induction is only partially dependent on photosynthetic activity, since the addition of DCMU (inhibits electron transfer in PSII) to the cultures decreases *LHCSR3* intracellular accumulation but does not inhibit it (Petroutsos et al. 2016). Recent results have shown that it is strongly regulated by CO<sub>2</sub> level via the regulatory factor CIA5 (Ruiz-Sola et al. 2021; Redekop et al. 2021). The hypothesis brought forward by Ruiz-Sola et al. (2021) and Redekop et al. (2021) is that exposure to HL increases the rate of CO<sub>2</sub> fixation, which leads to a decrease in the amount of intracellular CO<sub>2</sub> that results in the activation via CIA5 of the expression of the CCM (Carbon Concentration Mechanism)-related genes, *LHCSR3*, and to a lesser extent *PSBS*, whereas *LHCSR1* is repressed. This regulation was shown to not be directly dependent of light and could explain our results that clearly show that *LHCSR3* expression is not exclusively controlled by CONSTANS and COP1, unlike *LHCSR1*, *LHL4*, and *PSBS*.

Although CrPHOT is currently considered to be the key photoreceptor in the HL signalling pathway in *C. reinhardtii*, our results therefore do not allow us to exclude the existence of one or more other photoreceptors involved in the HL response (e.g. CrCRYs). The accumulation of *LHCSR3* in HL in the mutants of signalling also suggests that another pathway, not directly dependent on light, might be involved (via CIA5), as well as retrograde signals (ROS). Thus, in HL, the induced intracellular signalling is clearly more complex and less cleaved than in UV-B, where everything is under the control of CrUVR8.

#### **4. CONCLUSIVE REMARKS**

*C. reinhardtii* is a widely used model organism for the study of photosynthesis and associated mechanisms in green lineage organisms. In recent years, numerous studies have been carried out on photoprotection in *C. reinhardtii*, highlighting the role of HL- and UV-B-perception in the establishment of photoprotection.

In this work, we wanted to identify new actors of UV-B-mediated photoprotection in *C. reinhardtii*. Omics studies carried out on *C. reinhardtii* cultures exposed to UV-B allowed

identification of LHL4, a protein that accumulates highly in response to UV-B. In addition, LHL4 was also found to be induced by HL. LHL4 belongs to the family of ELIPs, which are involved in photoprotection and include proteins conserved throughout the green lineage; however, their precise function is not yet understood. LHL4 itself is found in other green microalgae, but not in mosses or land plants, indicating that it was lost during evolution. LHL4 inserts into the thylakoid membrane and appears to be associated with PSII. It also appears from its structure that it can bind chlorophylls.

We constructed KO mutants of the *LHL4* gene and then used them to study the role of this protein in *C. reinhardtii*. By studying the *lhl4* mutant under physiological (sunlight) and laboratory (artificial light) conditions, we were able to establish that the LHL4 protein limits photoinhibition of PSII when cells are exposed to HL stress. From our results, it appears that LHL4 regulates HL-induced photooxidative stress by preventing  $^1O_2$  formation at PSII.

On the other hand, as LHL4 is induced by both UV-B and HL, we chose to use it as a tool to study the convergence between the signalling pathways controlled by the UVR8 (UV-B) and PHOT (high light) photoreceptors. In *C. reinhardtii*, the hypothesis of a convergence of the two signalling pathways is underlying the recent studies published (Gabilly et al. 2019; Tokutsu et al. 2019), but the exact point of convergence has not been clearly established. In our work, we established that the point of convergence of the UVR8- and PHOT-induced signalling pathways is at the E3 ubiquitin ligase COP1/SPA1 complex. We then extended this study to NPQ proteins (LHCSR1, LHCSR3, PSBS) in the context of these two signalling pathways, which allowed us to confirm this result. Surprisingly, this work also allowed us to establish the existence of an additional signalling pathway involved in the response to HL, which is PHOT-independent. However, it remains to be established whether this other pathway is under the control of a photoreceptor or a retrograde signal (e.g. the ROS-induced retrograde signal). These results are summarised in **Figure 5.2**.

In addition, we were able to generate new information on the UVR8 signalling pathway in *C. reinhardtii*, although it has already been well characterised. In particular, our study confirmed that the main transcription factor in this pathway is CO and not HY5, contrary to what seems the case in *A. thaliana*. Initial results had already been published concerning the key role of CO in the regulation of photoprotection in *C. reinhardtii*, but here we were able to show that CO is a key UV-B transcription factor on a genome wide scale, although some of the UV-B regulated genes are still controlled by HY5.

LHL4 is the first ELIP characterised in the context of the UV-B response in *C. reinhardtii*, and has broadened our knowledge of both UV-B induced photoprotection in this microalgae, and that induced by HL. Furthermore, this work has improved our understanding of the regulation of intracellular signalling cascades induced by UV-B and HL in *C. reinhardtii*, and thus opened up new questions concerning the exact nature of the synergies existing between the different signalling pathways induced by the different colours within photosynthetic organisms.

All the results presented in this manuscript will be summarised in a publication that is currently being written.

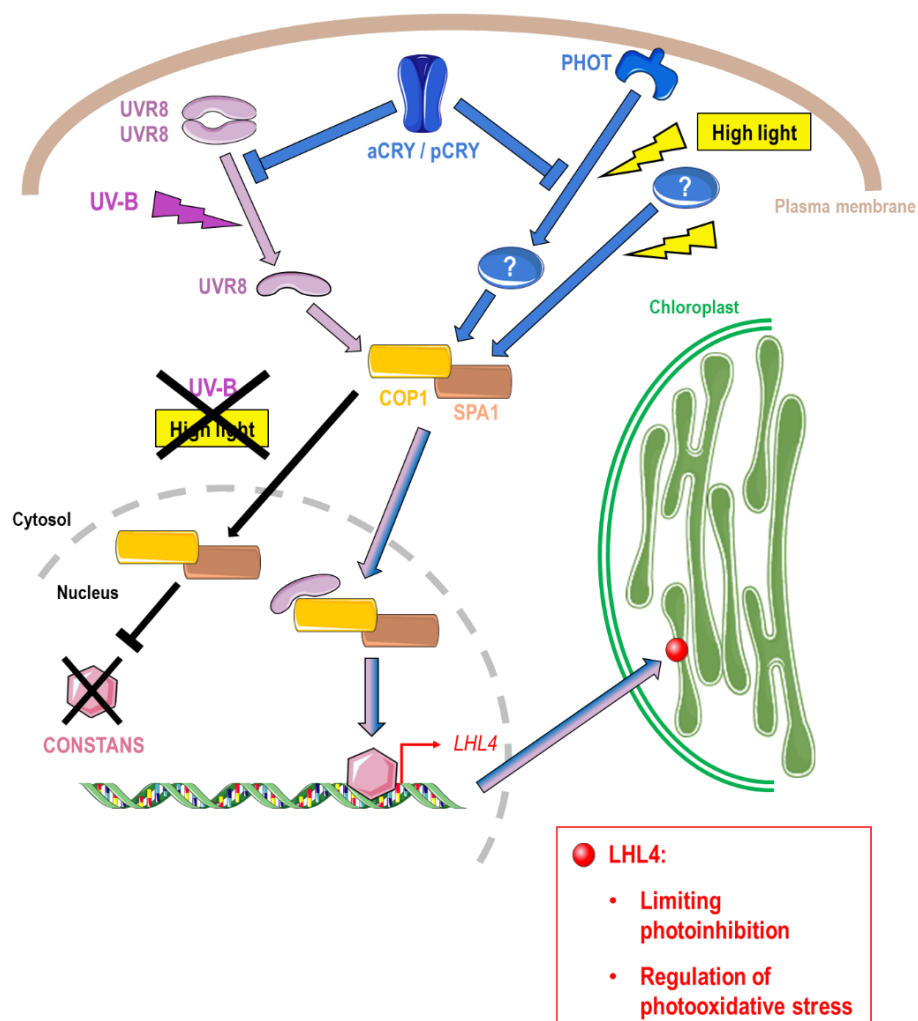


**Figure 5.2: Proposed model for the regulation of LHL4 expression in *C. reinhardtii*.** The UVR8 signalling pathway controls the induction of LHL4 when UV-B is sensed by the cell. In HL, LHL4 is partially under the control of PHOT, as well as a secondary blue signalling pathway whose photoreceptor has yet to be identified (indicated as ? on the scheme). The UV-B and HL-induced signalling cascades then converge at the COP1/SPA1 complex, before transcription of the LHL4 gene is initiated by the CONSTANS transcription factor. Once the mRNAs have been translated, the newly synthesised LHL4 protein is transported to the chloroplast, where it inserts into the thylakoid membrane. Once in place, LHL4 can play its role in regulating photooxidative stress. In the absence of an inducing signal (no UV-B or HL), LHL4 induction is repressed via the COP1/SPA1 complex which degrades CONSTANS and thus inhibits LHL4 gene expression. In parallel to these mechanisms, negative regulation of UV-B and HL induced signalling takes place and is mediated by cryptochrome photoreceptors.

# **CHAPTER 6:**

## **MATERIALS AND METHODS**

---

### **1. *C. REINHARDTII* STRAINS AND CULTURE CONDITIONS**

#### **1.1. Provenance of the different genotypes**

The *C. reinhardtii* mutant strains *lhl4* (*lhl4a* and *lhl4b* generated in our lab, and LMJ.SG0182.003906), *uvr8* (*uvr8* generated in our lab, and LMJ.RY0402.156289 (Allorent et al. 2016)), *phot*, *acry*, *pcry*, *hit1*(CrCOP1) (Schierenbeck et al. 2015), *spa1* (LMJ.RY0402.060340) (Tokutsu et al. 2019), *constans* (LMJ.RY0402.149321), *hy5* (LMJ.RY0402.194448) (Li et al. 2019), and *rup* (LMJ.RY0402.078413) were used with their respective WT background strains: CC-124 (137C mt-) for *hit1*; CC-5325 (cw15 mt-) for the strains *spa1*, *constans*, *hy5*, and *rup* provided by the CLiP mutant library (<https://www.chlamylibrary.org/>) (Li et al. 2016); and WT137C (mt+) for *lhl4*, *uvr8*, *phot*, *acry*, and *pcry*. The *lhl4*, *uvr8*, *acry*, *pcry* and *phot* mutated strains were generated in WT137C (mt+) using CRISPR-Cas9 technology (cf chapter 6, part 3. « Genetic engineering of Chlamydomonas »).

#### **1.2. Chlamydomonas liquid cultures and storage**

Cells were cultivated in Tris Acetate Phosphate mixotrophic medium (TAP) under continuous low white light provided by LED (30  $\mu\text{mol photons m}^{-2} \text{s}^{-1}$ ) at 25°C and 110 rpm shaking (Multitron pro, INFORS HT).

For storage, the strains were grown for a month on agar plates (agar (Plant culture agar, CarlRoth) 1,6 % (w/v) in TAP medium), supplemented with an antibiotic if necessary, at light intensity of 20  $\mu\text{mol photons m}^{-2} \text{s}^{-1}$  provided by fluorescent tubes at 25°C in a vertical light chamber (Sanyo plant growth chamber, Sanyo Japan).

<b>TAP medium</b>	<b>Final concentration (mM)</b>
Tris	800 mM
KPO <sub>4</sub> 1M pH7	40 mM
Acetic Acid to pH 7	-
NH <sub>4</sub> Cl	274 mM
CaCl <sub>2</sub> *2H <sub>2</sub> O	14 mM
MgSO <sub>4</sub> *2H <sub>2</sub> O	26 mM
<b>Trace Elements</b> (Kropat et al. 2011)	
EDTA-Na <sub>2</sub>	58 μM
(NH <sub>4</sub> ) <sub>6</sub> Mo <sub>7</sub> O <sub>24</sub>	0.2 μM
Na <sub>2</sub> SeO <sub>3</sub>	0.1 μM
ZnSO <sub>4</sub> ·7H <sub>2</sub> O	2.5 μM
MnCl <sub>2</sub> ·4H <sub>2</sub> O	6 μM
FeCl <sub>3</sub> ·6H <sub>2</sub> O	20 μM
Na <sub>2</sub> CO <sub>3</sub>	22 μM
CuCl <sub>2</sub> ·2H <sub>2</sub> O	2 μM
ddH <sub>2</sub> O to 1L	-

## **2. LIGHT ACCLIMATIONS & TREATMENTS**

### **2.1. UV-B and high light (HL) treatments**

For experiments, cells were quantified by measuring culture absorbance at 720 nm. They were then harvested during exponential phase ( $2-4 \cdot 10^6$  cells/mL) by centrifugation (6 min - 2934 g), washed, and resuspended at  $4,5 \cdot 10^6$  cells/mL in minimum medium (High Salt Medium, HSM) to enable NPQ proteins expression (Allorent et al. 2016) upon the

different light treatments. Cells were then exposed to light in 24-well plates (1,5 mL culture per well) with glass beads and a constant shaking (110 rpm) to allow the cells to remain in suspension in the medium.

UV-B treatment (0,2 mW/cm<sup>2</sup>, measured with the VLX-3W Uv Radiometer, Vilber Lourmat) was provided for 6h by Philips TL20W/01RS narrowband UV-B tubes (peak at 312 nm), and under a filter of the WG series (Schott Glaswerke) with half-maximal transmission at 311 nm. For the control samples without UV-B (LL), a 360 nm filter was used to block UV-B (<0.001 mW/cm<sup>2</sup>). In both cases (LL or +UV-B) cells were concomitantly exposed to low white light provided by fluorescent tubes (30 μmol photons m<sup>-2</sup> s<sup>-1</sup>; Osram L18W/30 white-light). For high-light treatment, cells were exposed under the indicated light intensity using the LED lights SL 3500-D system (Photon Systems Instruments) for 6h. Both LED and fluorescent tubes systems are devoid of any detectable UV-B radiation (<0.001 mW/cm<sup>2</sup>).

<b>HSM medium</b>	<b>Final concentration (mM)</b>
KPO <sub>4</sub> 1M pH7	6.5 mM
NH <sub>4</sub> Cl	274 mM
CaCl <sub>2</sub> *2H <sub>2</sub> O	14 mM
MgSO <sub>4</sub> *2H <sub>2</sub> O	26 mM
<b>Trace Elements (Kropat et al. 2011)</b>	
EDTA-Na <sub>2</sub>	58 μM
(NH <sub>4</sub> ) <sub>6</sub> Mo <sub>7</sub> O <sub>24</sub>	0.2 μM
Na <sub>2</sub> SeO <sub>3</sub>	0.1 μM
ZnSO <sub>4</sub> ·7H <sub>2</sub> O	2.5 μM
MnCl <sub>2</sub> ·4H <sub>2</sub> O	6 μM
FeCl <sub>3</sub> ·6H <sub>2</sub> O	20 μM
Na <sub>2</sub> CO <sub>3</sub>	22 μM

CuCl <sub>2</sub> ·2H <sub>2</sub> O	2 μM
ddH <sub>2</sub> O to 1L	-

## 2.2. Bleaching experiments

For the bleaching experiments, cells were prepared in HSM as indicated above and then treated for 16 h under low UV-B intensity (0,08 mW/cm<sup>2</sup>) in plant petri dishes (20 mL culture/plate) with a 100 rpm shaking. The cultures were then quantified, rediluted to 6.10<sup>6</sup> cells/mL, and transferred in 50 mL flasks (10 mL culture/flask) to be exposed 5h, under agitation (110 rpm) to strong high light intensities (2000 μmol photons m<sup>-2</sup> s<sup>-1</sup>) using the LED lights SL 3500-D system (Photo Systems Instruments).

## 2.3. Outdoor experiments

Outdoor experiments were performed using cells prepared as described above (**section 2.2, chapter 6**) and transferred in 24-well plates. Cells were then exposed to sunlight under constant shaking (110 rpm). Plates were partially immersed in water to maintain temperature at 25°C during the experiment using an external water bath (Dyneo, Julabo), light and UV-B intensities and ambient temperature were monitored every 30 min as well as the Fv/Fm photosynthetic parameter (**section 6.1, chapter 6**).

# 3. GENETIC ENGINEERING OF CHLAMYDOMONAS BY CRISPR-CAS9

The genetic engineering of the novel KO strains of *C. reinhardtii* was kindly performed by Chloé Bertin, engineer in our laboratory.

## 3.1. Donor DNA design and paramomycin resistance plasmid

The donor DNA, which contains a stop codon, was specifically designed for each gene of interest according to the protocol described in Greiner et al. 2017 to facilitate its insertion after cleavage by the CRISPR-Cas9 complex.

The pSL18 plasmid (provided by the Chlamydomonas resource center) was co-transferred into the cells to confer the resistance to paromomycin (10µg/mL) to the transformed cells and to facilitate the isolation of single colonies.

### **3.2. Preparation and assembly of the CRISPR/Cas9 complex**

The protocol used is adapted from the protocol published in Greiner et al. 2017. The complex consists of three parts: i. a common tracrRNA (trans-activating crRNA) sequence that binds to the Cas9 protein ii. a crRNA (CRISPR RNA) sequence that is specific to the gene of interest and iii. the Cas9 protein. The crRNA was designed using the CRISPRdirect webtool (<https://crispr.dbcls.jp/>) to ensure that the sequence is unique in the Chlamydomonas genome and limit the possibility of off-targets. Both tracrRNA and crRNA sequences were synthesized and purchased from the Ozyme company (<https://yris.ozyme.fr/fr>).

The sgRNA (single guide RNA) is formed by mixing 10 µM of crRNA and 10 µM of the trRNA, both resuspended in the duplex buffer (IDT - ref 11-01-03-01). The solution is then heated at 95°C for 2 min and cooled down at 22°C by decreasing the temperature by 2°C every minute in a thermal cycler (T100 - Biorad). The assembly of the sgRNA to the Cas9 protein is performed by mixing 10 µM of the sgRNA, 10 µM of the Cas9 protein (IDT - ref 1081058) and 3x of buffer O (Thermofisher - ref BO5) and incubating the mixture at 37°C for 15 min.

### **3.3. Cell transformation**

Cells were harvested in the exponential phase. The equivalent of 100 millions cells were centrifuged and resuspended in 1mL of the Max Efficiency Transformation buffer (Invitrogen - ref A24229) supplemented with 40 mM of Sucrose. 40 µL of cells were transferred in an electroporation cuvette (2 mm gap, Nepagene, ref EC-002S) and placed for 30 min at 40°C. A mix containing 3 µM of the in vitro assembled CRISPR-Cas9 complex, 30 pmol of the donor DNA and 300 ng of the pSL18 plasmid was then added to the culture. The cuvette was placed in the electroporation cuvette chamber (Nepagene - ref CU500) and electroporation was performed using the following parameters:

#### Poring pulse

- 300 Volts
- 8 ms length
- 50 ms interval
- 1 pulse
- 40 D.Rate polarity %

+ polarity

#### TransferPulse

- 20 Volt
- 50 Length ms
- 50 Interval ms
- 5 pulses
- 40 D.Rate %
- +/- polarity

After electroporation, cells were transferred in 1 mL of TAP Sucrose 40 mM and placed under agitation (110 rpm) and low light ( $30 \mu\text{mol of photons m}^{-2} \text{s}^{-1}$ ) for 20 hours. After this recovery period, cells were centrifuged (5 min - 3000 *g*), resuspended in 500  $\mu\text{L}$  of TAP sucrose and spread on an agar plate containing 10  $\mu\text{g/mL}$  of paromomycin. Single transformants usually appear within 1 week and are screened using the protocol described below (**sections 4.1 to 4.3, chapter 6**).

## 4. NUCLEIC ACID ANALYSIS

### 4.1. Quick genomic DNA extraction

This method was mainly used to screen mutants by PCR. Using a sterile toothpick, a small amount of biomass was collected from isolated colonies grown on agar plates. The collected cells were then placed in 20  $\mu\text{L}$  of extraction buffer. The mixture was vortexed 10 s and then centrifuged (5 min - 21130 *g*). The supernatant containing the DNA was then transferred (0.5  $\mu\text{L}$ ) directly in a ready-made PCR mix or stored at  $-20^\circ\text{C}$ .

## 4.2. PCR analysis

The transformants were genotyped by PCR. After DNA extraction, the sequences of interest were amplified by PCR with a primer in the gene of interest, and a primer in the exogenous DNA donor cassette (5'-GTCCTTGTAGTCGATGTCGTGG-3') likely inserted into the mutants after the Cas9 cleavage. A positive PCR control was performed using primers flanking the insertion site.

This method allowed to discriminate between mutated colonies from wild type. The amplicons were then mixed with the appropriate amount of orange G loading buffer, and visualized on 1% (w/v) agarose gel after electrophoresis. Migration was performed in 0.5x TAE buffer for 20 min at 120 V.

<b>TAE 50x</b>	<b>Final concentration</b>
Tris	2 M
Acetic acid 100%	5.7%
EDTA pH 8 0.5 M	50 mM
ddH <sub>2</sub> O to 1L	-

<b>Orange G 6x</b>	<b>Final concentration</b>
Orange G	3 mM
TAE 50x	1x
Glycerol 100%	60%
ddH <sub>2</sub> O to 100 mL	-

<b>Gene name</b>	<b>PCR primer sequence (5' - 3')</b>
<i>UVR8</i>	GGTCCTCCCATTCAATAGCGC
<i>PHOT</i>	GCAGCAGCTTCACCCGTAGG
<i>aCRY</i>	GCATCATATGGTGCGAGCGG
<i>pCRY</i>	ATGACTGCAAGCGCGGCCT
<i>LHL4</i>	CACACGTTTCCAGCCCCAGA

### **4.3. Purification and sequencing of PCR products**

PCR products of interest were cut, and DNA was extracted and purified from the gel with the NucleoSpin Gel and PCR Clean-up kit (Macherey-Nagel) according to the supplier's instructions, and then sequenced by MacroGen company (<https://dna.macrogen.com/>) to verify correct donor DNA insertion.

### **4.4. RNA extraction**

RNA extractions were performed as part of an RT-qPCR analysis of transcript levels of selected genes of interest.

Prior to the extraction,  $2 \cdot 10^7$  cells of *C. reinhardtii* were rapidly collected by centrifugation (1 min - 21300 *g*), frozen in liquid nitrogen, and stored at -80°C.

Total RNA was extracted using a commercial kit (RNeasy Plant Mini Kit, QIAGEN) including a DNase-treatment to remove residual genomic DNA, as recommended (RNase-Free DNase Set, QIAGEN).

RNA concentration was quantified using a NanoDrop Microvolume Spectrophotometer (absorbance measurements at 230, 260, and 280 nm), and RNA samples were diluted in RNase-free water to the lowest concentration in the series. Their quality was also checked by gel electrophoresis of 300 ng of RNA on a 1% agarose gel.

After dilution, the RNA samples were frozen in liquid nitrogen and stored in a -80°C freezer for at least one night.

#### 4.5. RT-qPCR analysis

RNAs were reverse transcribed (RT) to cDNA using the TaqMan Reverse Transcription Reagents kit (Applied Biosystems), and following the supplier's recommendations. Each RT was done on 480 ng of RNA.

An initial 10 min incubation at 25°C with 0.25 µL of oligo dT and random primers was performed to allow hybridization of the primers onto the RNAs (final volume = 5.3 µL). Then, 4.7 µL of RT mix is added to the samples (final volume = 10 µL) and polymerization is performed for 1h at 48°C. Finally, the enzyme is inactivated by heating at 95°C for 5 min. The resulting cDNAs are then diluted 20 times in 180 µL with ddH<sub>2</sub>O and stored at -20°C.

<b>Component</b>	<b>Final concentration</b>
RNA	48 ng/µL
Oligo dT	1.25 µM
Random primers	1.25 µM
ddH <sub>2</sub> O	-
<b>RT mix to 10 µL (4.7 µL/reaction):</b>	
10x RT buffer	1x
25 mM MgCl <sub>2</sub>	1.75 mM
10 mM dNTP mix (2.5 mM each)	0.5 mM each
RNase inhibitor (20 U/µL)	1 U/µL
MultiScribe RT (50 U/µL)	2.5 U/µL

Amplification by RT-qPCR was performed in 96-well plates using 6 µL of diluted cDNA (14.4 ng of equivalent RNAs) plus 8 µL of qPCR mix containing SYBR Green (Master Mix

PCR *Power SYBR™ Green*, Applied Biosystems, final concentration 1X) for amplification and detection, and the different primer pairs (10  $\mu$ M). The primers were designed for maximum amplification efficiency (amplicon between 50 and 150 bp, T<sub>m</sub> 60°C), and the efficiency of each primer pair was determined beforehand using different cDNA dilutions. To be used, the pair had to have an efficiency between 90 and 110%. For all genes of interest, the thermal cycler (CFX Connect Real-Time PCR Detection System, Bio-Rad) followed the following program: enzyme activation 10 min at 95°C, then 40 cycles of 15 s denaturation at 95°C and 1 min amplification at 60°C.

qPCR mix	Final concentration
Master Mix PCR <i>Power SYBR™ Green</i> 2x	1x
Forward primer 100 $\mu$ M	10 $\mu$ M
Reverse primer 100 $\mu$ M	10 $\mu$ M
ddH <sub>2</sub> O	-

Expression values were calculated using the  $\Delta\Delta$ Ct method (Livak and Schmittgen 2001), and using the two reference genes Cre06.g6364 (RACK1) and Cre13.g599400 (GBLP) for normalization.

Gene name	qPCR primer sequences (5' - 3')
<i>LHL4</i>	TACGGTGTGGATGACGTGAC
	AGGTGATAATCTGGCGGATG
<i>LHCSR1</i> (Allorent et al. 2016)	AAGACCCTGCCCCGGTGTAC
	TGGGTGATCTCAGACTCGCGC
<i>LHCSR3</i> (Allorent et al. 2016)	GGCCGTCAAGTCCGTGTCT
	GGGAAGGTCTTCGTGTATGCG
<i>PSBS</i> (Allorent et al. 2016)	CCGCCATCAACGGCAAGCAG
	CCACCATGGCCAGGCGACC
	CTTCTCGCCCATGACCAC

<i>RACK1</i> (Tilbrook et al. 2016)	CCCACCAGGTTGTTCTTCAG
<i>GBLP</i>	TGGCTTTCTCGGTGGACAAC
	CTCGCCAATGGTGTACTTGC

#### 4.6. RNA-seq analysis

Gene expression of *C. reinhardtii* in response to UV-B was analysed by RNA sequencing (RNA-Seq).

Four strains (WT cc5325, and *uvr8*, *constans*, and *hy5* mutants from the CLiP library) were grown for 5 days in low light and prepared for UV-B treatment as described in **sections 1.3. and 2.1 (chapter 6)** of this Materials & Methods. The cells were then exposed for 1 h to 0.2 mW/cm<sup>2</sup> of UV-B to induce gene expression. 4.5 mL of each culture (2.10<sup>7</sup> cells) were collected after UV-B exposure (centrifugation 1 min - 21130 *g*), and the cell pellets were immediately frozen in liquid nitrogen and stored at -80°C until RNA extractions. The same amount of cells were also sampled before exposure (t0) and after 1h of exposure with a 360 nm UV-B blocking filter (LL) as controls.

Total RNA was extracted from three biological replicates of each line and conditions using the Plant RNeasy Kit (Qiagen). The RNA quality control, library preparation using TruSeqUD Stranded mRNA (Illumina, <https://www.illumina.com/>) and sequencing on an Illumina HiSeq 4000 System using 100-bp single-end reads protocol were performed at the iGE3 genomics platform of the University of Geneva (<https://ige3.genomics.unige.ch/>).

Quality control was performed with FastQCv.0.11.5. Reads were mapped to the *C. reinhardtii* genome (PhytozomeV12.1 v5.5 assembly) using STARv.2.7.0f. software, with average alignment of 91.54%. Raw counts obtained using HTSeq v.0.9.1 were filtered for genes with low expression (15'125 genes with a count above 10 were kept) and normalized according to library size. Normalization and differential expression analysis were performed with the R/Bioconductor package edgeR 1.34.1, with a multiple testing Benjamini and Hochberg correction FDR of 5% and a fold change threshold of 2.

Annotations were obtained from *C. reinhardtii* V5.6 (Merchant et al. 2007).

Venn diagrams were generated using a webtool (<http://bioinformatics.psb.ugent.be/webtools/Venn/>).

## 5. PROTEIN ANALYSIS

### 5.1. Protein extraction

#### 5.1.1. Total protein extraction

For protein extraction,  $2 \cdot 10^7$  cells were collected by centrifugation and resuspended in 1 mL of 80% acetone (v/v) and stored at  $-20^{\circ}\text{C}$ .

The samples were then centrifuged at  $4^{\circ}\text{C}$ , and the supernatants were removed. The pellets were left for 5 min in air to allow the remaining acetone to evaporate. They were then resuspended in 50  $\mu\text{L}$  of 2x protease inhibitors (EDTA-free Protease Inhibitor Cocktail, Roche), to which 50  $\mu\text{L}$  of 2x lysis buffer was added to solubilize the proteins. After a 5 min incubation at room temperature, the samples were centrifuged and the supernatants containing proteins were collected in new tubes.

#### 5.1.2. Protein quantification

The amount of protein was estimated using the Pierce™ BCA Protein Assay Kit (Thermo Scientific). Protein samples were incubated 30 min at  $37^{\circ}\text{C}$  in a 96-well plate with 200  $\mu\text{L}$  of BCA reagents and the absorbance was then measured at 562 nm. The estimation of the concentration was based on a standard range made with different amounts of bovine serum albumin (BSA, 0-5-10-20  $\mu\text{g}/\mu\text{L}$ ).

Lysis buffer 2x	Final concentration
Tris-HCl 1M pH 6.8	100 mM
SDS 20%	4%
EDTA 0.5 M	20 mM
ddH <sub>2</sub> O to 10 mL	-

### 5.1.3. Membrane-enriched protein extraction

Some experiments required the preparation of extracts enriched in membrane proteins. For this purpose, a large quantity of cells ( $7 \cdot 10^7$  cells) of *C. reinhardtii* was pelleted and resuspended in 200  $\mu$ L of TAP + protease inhibitors in which 200 mg of glass microbeads were added. The cells were then broken in a cold room with a tissue grinder (Precellys evolution tissue grinder homogenizer, Bertin Technologies), performing 2 cycles of breaking at 10,000 rpm for 30 s, with 30 s pause between each cycle to avoid heating the samples.

The lysates were then transferred without the beads into new tubes, on ice. After a short centrifugation (4°C - 3 min - 21130 *g*), the supernatants were removed, and the pellets containing the membranes were gently resuspended in 40  $\mu$ L of 25BTH buffer, frozen in liquid nitrogen and stored at -80°C.

<b>25BTH buffer</b>	<b>Final concentration</b>
Anode buffer 1x ( <i>cf chapter 6, 5.4</i> )	0.5x
Glycerol 50%	20%
Protease inhibitors 50x	1x
NaF 1M	10 mM
ddH <sub>2</sub> O to 200 $\mu$ L	-

## 5.2. Western blots

### 5.2.1. Sample preparation

10 to 30  $\mu$ g of protein extract mixed with the blue loading buffer and denatured for 30 min at 37°C were loaded in a SDS-PAGE gel.

<b>Protein deposit blue 4x</b>	<b>Final concentration</b>
Tris-HCl 0.5 M pH 6.8	0.2 M
Glycerol 100%	40%
SDS 20%	4%
Bromophenol blue	0.1% (m/v)
DTT	1.54% (m/v)

*5.2.2. Separation of proteins by electrophoresis in denaturing conditions (SDS-PAGE)*

The SDS-PAGE gel was composed of a 15% acrylamide (v/v) separation gel topped with a 5% acrylamide (v/v) concentration gel. Migration was carried out in running buffer (Laemmli, 1970) at 20 mA per gel for 90 min and allow the separation of the proteins depending on their size.

After migration, the proteins were transferred to a nitrocellulose or PVDF membrane for immunodetection of the protein of interest.

<b>Separating gel</b>	<b>Final concentration</b>
Tris HCl pH 8.8 1.5 M	375 mM
Acrylamide/Bisacrylamide 30% / 0.8%	15% / 0.4%
ddH <sub>2</sub> O	-
SDS 20%	0.1%
APS 10% (m/v)	0.1%
Temed	0.001 % (v/v)

<b>Stacking gel</b>	<b>Final concentration</b>
Tris HCl pH 6.8 0.5 M	125 mM
Acrylamide/Bisacrylamide 30% / 0.8%	4.5% / 0.1 %
ddH <sub>2</sub> O	-
SDS 20%	0.3%
APS 10% (m/v)	0.05%
Temed	0.001% (v/v)

<b>Running buffer 10x</b>	<b>Final concentration</b>
Glycine	1.9 M
Tris	0.25 M
SDS 20%	0.5%
ddH <sub>2</sub> O to 1 L	-

### 5.2.3. Transfer

After separation on the SDS-PAGE gel, the proteins were transferred to either a nitrocellulose membrane or a PVDF membrane (previously activated for 1 min in methanol). The transfer was carried out at a constant voltage of 110V for 80 min in transfer buffer containing ethanol (in the case of transfer to a nitrocellulose membrane) or methanol (for a PVDF membrane). During the transfer, the system was cooled by an ice pack to avoid the degradation of the proteins.

<b>Transfer buffer</b>	<b>Final concentration</b>
Running buffer 10x	1x
Ethanol or Methanol	20%
ddH <sub>2</sub> O	-

#### 5.2.4. Immunodetection of proteins

After transfer, the membranes were incubated for at least 1h in TBS-Tween 0.1% (TBS-t, v/v) with 5% milk to block protein-free sites on the membrane.

The membrane was then incubated overnight at 4°C in a solution of TBS-t containing the diluted primary antibody (1/1'000 to 1/10'000 depending on the antibody used).

The membrane was then washed 3 x 10 min in TBS-t, then incubated for 1h at room temperature with the secondary antibody (diluted 1/10'000 in TBS-t). After 3 rinses in TBS-t, the membrane was placed in the presence of a chemiluminescent substrate (Clarity Western ECL Substrate, Bio-Rad) for horseradish peroxidase (HRP) which was coupled to the secondary antibody. The signal associated with the proteins was then detected and imaged (Fusion FX, Vilber Lourmat).

<b>TBS buffer 20x pH 7.5</b>	<b>Final concentration</b>
Tris	1 M
NaCl	3 M
HCl 12N (37%)	-
ddH <sub>2</sub> O to 1 L	-

### 5.3. Blue-native (BN)-PAGE and second dimension (2D)

#### 5.3.1. Sample preparation

The membrane-enriched protein extracts were prepared as described in **section 5.1.2, chapter 6**. The chlorophyll concentration of the sample was then measured by

spectrophotometric absorbance measurement at 652 nm using 4  $\mu\text{L}$  of sample diluted in 1 mL of 80% (v/v) acetone. Chlorophyll concentration was estimated by the following calculation:  $\text{Abs}_{652 \text{ nm}} \times 4.53 = x \mu\text{g Chl}/\mu\text{L}$  (Cariti 2018).

On ice, an aliquot of 16  $\mu\text{g}$  of chlorophyll for each sample was taken and the volume was adjusted to 20  $\mu\text{L}$  with 25BTH buffer. An equivalent volume of 2%  $\alpha$ -DM detergent (1% final) was added, to allow slight solubilisation of the membrane complexes. Samples with detergent were incubated for 5 min at 25°C with gentle agitation (300 rpm), centrifuged (4°C - 20 min - 21130  $g$ ). The supernatant, containing the proteins, was collected and 1/10 (v/v) of loading blue buffer 10x was added.

<b><math>\alpha</math>-DM 2%</b>	<b>Final concentration</b>
Anode buffer 10x	1x
Glycerol 50%	20%
$\alpha$ -DM stock 10% (m/v) <u>freshly prepared</u>	2%
Protease inhibitors 50x	1x
NaF 1 M	10 mM
ddH <sub>2</sub> O to 200 $\mu\text{L}$	-

<b>Blue loading buffer 10x for BN</b>	<b>Final concentration</b>
Aminocaproic acid	0.5 M
Sucrose	90 mM
Coomassie blue G-250	60 mM
Bis/Tris HCl pH 7.0 to 20 mL	-

5.3.2. *Separation of complexes by electrophoresis under non-denaturing conditions (Blue-native-PAGE)*

Sample migration was performed in cold room, in the dark, in a pre-cast acrylamide gradient gel (NativePAGE™ 3-12%, Bis-Tris, 1.0 mm, protein minigels, Invitrogen). First, separation of the different photosynthetic complexes is performed by native gel electrophoresis in a blue cathode buffer to negatively charge and stain the protein complexes. When the migration front reached half of the gel, the blue cathode buffer was replaced by white cathode to partially destain the gel to reveal the bands.

The migration was performed following this protocol:

<b>Voltage intensity</b>	<b>Duration</b>
75 V	30 min
100 V	30 min
125 V	30 min
Change cathode buffer	
150 V	60 min
175 V	30 min
200 V	until you see a good separation

<b>Anode buffer 10x</b>	<b>Final concentration</b>
Bis/Tris HCl pH 7	0.5 M
ddH <sub>2</sub> O to 1L	-

<b>White cathode buffer</b>	<b>Final concentration</b>
Tricine	50 mM
Bis/Tris HCl pH 7	15 mM
ddH <sub>2</sub> O to 1L	-

### 5.3.3. Analysis of complexes by 2D electrophoresis under denaturing conditions

This method separates individual proteins from the different protein complexes of the native gel (**section 5.3.2, chapter 6**), revealing some indications about their composition. The lanes containing the different samples were then cut from the native gel with a scalpel, and equilibrated twice for 15 min in the Equilibration buffer. They were then incubated for 1-2 min in the same buffer supplemented with 50% glycerol (v/v), which will allow it to shrink a little and so to fit the well.

A 15% acrylamide gel was prepared as described in **section 5.2.2, chapter 6** of this thesis, except that the stacking gel was only composed of two wells: a small one for the protein ladder and a large for the sample. A lane containing samples was then carefully inserted into the large well of the acrylamide gel, ensuring that the lane is in close contact with the well (1 sample/gel for the 2D). The strip was then sealed in the well by adding pre-heated 1x Running buffer + 0.8% agarose. Migration was then carried out for 90 min at 20 mA in 1x Running buffer. The proteins of interest were finally detected using the same approach as described above (5.2.3 and 5.2.4).

<b>Equilibration buffer</b>	<b>Final concentration</b>
Tris HCl pH 6.8 0.5 M	125 mM
SDS 20%	2%
ddH <sub>2</sub> O to 50 mL	-

#### 5.4. List of antibodies

Antibody name	Source	Dilution	2 <sup>nd</sup> antibody
LHL4	Agrisera AS07250	1/10 000	Anti-rabbit
LHCSR1	Agrisera AS142819	1/10 000	Anti-rabbit
LHCSR3	Agrisera AS142766	1/10 000	Anti-rabbit
PSBS	Allorent et al. 2016	1/1000	Anti-rabbit
CP43	Agrisera AS111787	1/10 000	Anti-rabbit
PSAD	Agrisera AS09461	1/10 000	Anti-rabbit
aCRY	Eurogentec (this work) Peptide : C+RRHPAHSQPPVSLRG (aCRY <sup>276-290</sup> )	1/10 000	Anti-rabbit
PHOT (LOV1 domain)	Petroutsos et al. 2016	1/2000	Anti-rabbit
ATPB	Agrisera AS05085	1/10 000	Anti-rabbit

#### 5.5. Mass spectrometry (MS)-based proteomic analyses

Protein expression of *C. reinhardtii* in response to UV-B was analysed by proteome mass spectrometry analysis. The analysis was performed by the EdyP proteomics platform of the CEA Grenoble (<http://www.edyp.fr/web/>).

WT137C was grown for 5 days in low light and prepared for UV-B treatment as described in Parts 1.3. and 2.1. of this Materials & Methods. The cells were then exposed for 16 h to 0.08 mW/cm<sup>2</sup> of UV-B to induce UV-B response, and so the accumulation of the corresponding proteins.

Proteins of thylakoids purified from three biological replicates of *C. reinhardtii* exposed or not to UV-B were solubilized in LaemmLi buffer and heated for 10 min at 95°C. They were then stacked in the top of a 4-12% NuPAGE gel (Invitrogen), stained with Coomassieblue R-250 (Bio-Rad) before in-gel digestion using modified trypsin (Promega,

sequencing grade) as previously described (Casabona et al. 2013). The resulting peptides were analyzed by online nanoliquid chromatography coupled to MS/MS (Ultimate 3000 RSLCnano and Q-Exactive HF, Thermo Fisher Scientific) using a 120-min gradient. For this purpose, the peptides were sampled on a precolumn (300  $\mu\text{m}$  x 5 mm PepMap C18, Thermo Scientific) and separated in a 75  $\mu\text{m}$  x 250 mm C18 column (Reprosil-Pur 120 C18-AQ, 1.9  $\mu\text{m}$ , Dr. Maisch). The MS and MS/MS data were acquired using Xcalibur 4.0 (Thermo Fisher Scientific).

Peptides and proteins were identified by Mascot (version 2.8.0, Matrix Science) through concomitant searches against the Chlre5\_6 database (downloaded from JGI Genome Portal, (Merchant et al. 2007), 19526 sequences), the mitochondrion and chloroplast protein sequences (downloaded from NCBI, respectively 69 and 8 proteins), and a homemade database containing the sequences of classical contaminant proteins found in proteomic analyses (human keratins, trypsin..., 126 sequences). Trypsin/P was chosen as the enzyme and two missed cleavages were allowed. Precursor and fragment mass error tolerances were set at respectively at 10 and 20 ppm. Peptide modifications allowed during the search were: Carbamidomethyl (C, fixed), Acetyl (Protein N-term, variable) and Oxidation (M, variable). The Proline software (Bouyssié et al. 2020), version 2.2.0) was used for the compilation, grouping, and filtering of the results (conservation of rank 1 peptides, peptide length  $\geq 6$  amino acids, false discovery rate of peptide-spectrum-match identifications  $< 1\%$  (Couté et al. 2020), and minimum of one specific peptide per identified protein group). Proline was then used to perform a MS1 label-free quantification of the identified protein groups based on razor and specific peptides.

Statistical analysis was performed using the ProStaR software (Wieczorek et al. 2017) based on the quantitative data obtained with the three biological replicates analyzed per condition. Proteins identified in the contaminant database, proteins identified by MS/MS in less than two replicates of one condition, and proteins quantified in less than three replicates of one condition were discarded. After  $\log_2$  transformation, abundance values were normalized using the variance stabilizing normalization (vsN) method, before missing value imputation (SLSA algorithm for partially observed values in the condition and DetQuantile algorithm for totally absent values in the condition). Statistical testing was conducted with limma, whereby differentially expressed proteins were selected using a  $\log_2$ (Fold Change) cut-off of 1 and a p-value cut-off of 0.00776, allowing to reach a false discovery rate inferior to 1% according to the Benjamini-Hochberg estimator.

Proteins found differentially abundant but identified by MS/MS in less than two replicates or detected in less than three replicates in the condition in which they were found to be more abundant were manually invalidated (p-value = 1).

## 6. PHYSIOLOGICAL MEASUREMENTS OF PHOTOSYNTHESIS

### 6.1. Principle of chlorophyll fluorescence measurements

In a plant cell, photons absorbed by chlorophylls can only be used in three ways: to fuel photosynthesis (photochemical pathway) or, in the case of excess energy, to be dissipated as heat (NPQ) or re-emitted as fluorescence. These three pathways are always in competition with each other, which means that an increase in one pathway leads to a decrease in the other two. Therefore, by measuring the fluorescence yield under a given light, it is possible to deduce information about the efficiency of photosynthesis and NPQ (Maxwell and Johnson 2000).

The basal level of fluorescence ( $F_0$ ) is measured when the measuring light is switched on after dark adaptation. This light condition is only enough to trigger photosynthesis, meaning that only a small part of the energy is reemitted as fluorescence. A short pulse (less than 1s) of saturating light is then applied to allow measurement of the maximum fluorescence level ( $F_m$ ), i.e. fluorescence level when photosynthesis is saturated. If cells are then exposed to actinic light for few min, NPQ starts to occur and part of the light energy is dissipated as heat. This leads to a decrease of the maximum fluorescence level from  $F_m$  to  $F_m(t)$ , maximum fluorescence level to light (with  $F_m > F_m(t)$ ).  $F_s$  corresponds to the steady-state fluorescence level, usually measured just before the dark adaptation allowing the NPQ to relax (**Fig. 6.1**, see also Seydoux 2020).

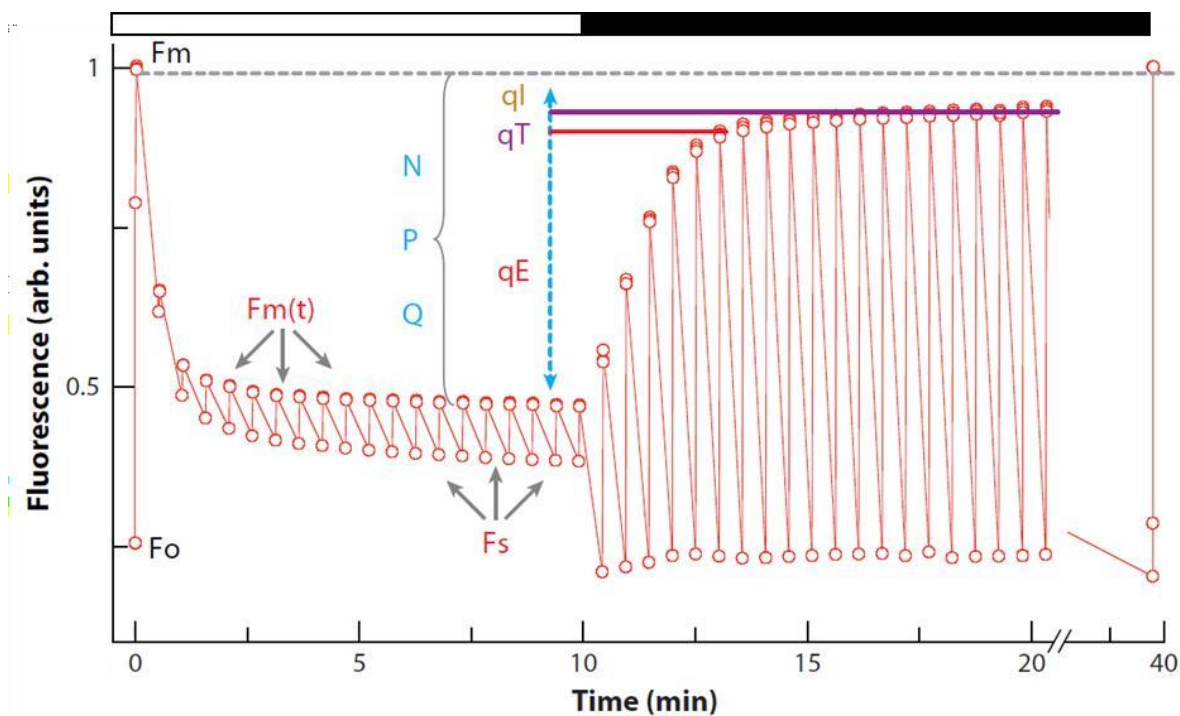


**Figure 6.1:** Kinetics of changes in fluorescence yield in a leaf subjected to continuous illumination saturating for photosynthesis ( $500 \mu\text{mol photons m}^{-2} \text{s}^{-1}$  of red light, white box on the figure) and then adapted to dark (dark box). Adapted from Eberhard, Finazzi, et Wollman 2008.

Illumination phase (white box, **Fig. 6.1**) causes a decrease in fluorescence that is quantified by measuring the NPQ. When the sample is switched to dark (dark box, **Fig. 6.1**), the NPQ relaxes in several phases which allow the identification of the different components of the NPQ: first the  $qE$  (energy-dependent quenching) and then the  $qT$  (state transition), and finally the  $qI$  (photoinhibition) can also be observed (Eberhard et al. 2008).

The different photosynthetic parameters can then be calculated on the basis of these different measurements:

Photosynthetic parameter	Fluorescence-based calculation
$\phi_{\text{PSII}}$	$(F_m(t) - F_s)/F_m(t)$
$F_v/F_m$	$(F_m - F_0)/F_m$
NPQ	$(F_m - F_m(t))/F_m(t)$

## **6.2. Estimation of photosynthetic parameters *in vivo***

All photosynthesis measurements in this thesis were performed *in vivo* with a fluorometer (Speedzen 3, JbeamBio) coupled to a highly sensitive camera (Orca 4-Flash, Hamamatsu) to record the fluorescence variation over time to estimate the photosynthetic properties of samples placed in 96-well plates.

200  $\mu\text{L}$  of *C. reinhardtii* cultures concentrated to  $4.5 \cdot 10^6$  cells/mL were added per well, after a dark recovery phase of about 30 min to establish the  $F_0$ . The plates were illuminated from above with red light of adjustable intensity, and chlorophyll fluorescence was then detected by short blue pulses. To avoid artefacts, the red light was switched off during the fluorescence measurement.

## **7. PIGMENT ANALYSIS**

The protocol was adapted from that of Dr. Marcel Kuntz (LPCV, Grenoble, France) (Allorent et al., 2013).

### **7.1. Pigment extractions**

$7 \cdot 10^7$  *C. reinhardtii* cells were centrifuged briefly ( $4^\circ\text{C}$  - 6 min -  $2934 g$ ) and then frozen in liquid nitrogen and stored at  $-80^\circ\text{C}$ .

Pigment extraction was carried out in the dark and on ice. The pellets were vortexed in 500  $\mu\text{L}$  of methanol buffered with HEPES/KOH pH 7.5 until the cells were completely resuspended, then centrifuged ( $4^\circ\text{C}$  - 5 min -  $21130 g$ ). The supernatants containing the pigments were transferred to opaque tubes, to prevent the degradation of the pigments by ambient light. This extraction step was repeated with 500  $\mu\text{L}$  of pure methanol until the pellet became colorless, and the different supernatants were combined in the same tube. The methanol was then completely evaporated under an argon flow, to avoid any oxidation of the pigments caused by the ambient air. These extracts were finally stored at  $-20^\circ\text{C}$  until they could be processed by HPLC.

## 7.2. HPLC analysis

Pigments were resuspended in 100  $\mu$ L DMF (Dimethylformamide) and injected on a HPLC (Varian ProStar 800, Varian), coupled to a diode detector. They were separated on a C30 column (Macherey-Nagel) and extracted in the following solvents, in order: (A) 80% methanol + 20% water (v/v) containing 0.2% of ammonium acetate (100 mM final); (B) 90% acetonitrile + 10% water (v/v); (C) 100% ethyl acetate. Pigments were identified according to their retention time and absorption spectrum as described in (Allorent et al, 2013).

## 8. SINGLET OXYGEN ( $^1O_2$ ) MEASUREMENTS

$^1O_2$  production was estimated using the dye SOSG (Singlet Oxygen Sensor Green, Invitrogen), which is a highly selective detection reagent for singlet oxygen in the presence of which it emits green fluorescence.

The stock (single use) SOSG was prepared in methanol at a concentration of 5 mM SOSG. The working solution was then prepared by diluting the stock to 500  $\mu$ M in ddH<sub>2</sub>O.

For these experiments, cultures were concentrated to  $4 \cdot 10^6$  cells/mL and plated in 24-well plates (1.5 mL/well; 115 rpm shaking). A final 0.5  $\mu$ M of SOSG was added to each well, and the cells were then exposed for 30 min to 300  $\mu$ mol photons  $m^{-2} s^{-1}$  to induce  $^1O_2$  production. 5 x 100  $\mu$ L of culture was then taken from each well and transferred in a 96-well plate. The fluorescence of each well was read with a plate reader (TECAN) (10 s of agitation - Ex: 504 nm; Em: 525 nm).

## 9. EXPANSION MICROSCOPY

Expansion microscopy images of *C. reinhardtii* were made following the "Initial U-ExM protocol" detailed in Gambarotto, Hamel, and Guichard 2021, after the cells had been exposed or not to 0.2 mW/cm<sup>2</sup> of UV-B for 4h. The tests were performed on cells with (WT 137C) and without (WT cw15) cell wall, to verify that it did not pose a problem for cell expansion.

<b>Antibody name</b>	<b>Source</b>	<b>Dilution</b>	<b>2<sup>nd</sup> antibody</b>
PSBA	Agrisera AS01016	1/500	Anti-chicken + Alexa 568
PSAD	Agrisera AS09461	1/500	Anti-rabbit + Alexa 488

# TABLE OF FIGURES

## CHAPTER 1

Figure 1. 1: Phylogenetic relationships of 14 Viridiplantae taxa.....	18
Figure 1. 2: The morphology of <i>Chlamydomonas reinhardtii</i> . Erreur ! Signet non défini.	20
Figure 1. 3: Schematic representation of the photosynthetic linear electrons and protons flows.....	22
Figure 1. 4: Relative time scales of short-term and long-term responses to excess light.....	24
Figure 1.5: Schematic representation of the evolution of OHPs to LHCs and ELIPs proteins .....	29
Figure 1. 6: Photoreceptor proteins with their spectral specificities .....	32
Figure 1.7: Summary of phototropin-mediated responses in higher plants.....	35
Figure 1.8: An overview of cryptochrome signaling in <i>A. thaliana</i> .....	37
Figure 1.9: Grana stacking of the <i>C. reinhardtii</i> is increased in <i>cry-dash1<sub>mut</sub></i> (CRY-DASH1, DASH cryptochrome 1).....	39
Figure 1.10: Impact of the <i>uvr8</i> mutation in <i>A. thaliana</i> .....	41
Figure 1.11: Model of the UVR8 signalling pathway in <i>A. thaliana</i> .....	42; 71
Figure 1.12: A schematic summary of the different photoreceptors of <i>C. reinhardtii</i> , with their intracellular location and functions.....	44

## CHAPTER 2

<b>Figure 2.1: LHL4 and the NPQ proteins LHCSR1 and LHCSR3 are significantly induced by UV-B exposure.....</b>	<b>53</b>
<b>Figure 2.2: Prediction of the LHL4 structure.....</b>	<b>56</b>
<b>Figure 2.3: Comparison of LHL4 protein with other CrELIPs and LHCSRs.....</b>	<b>57</b>
<b>Figure 2.4: Localisation of photosystems I and II in <i>C. reinhardtii</i> using ultrastructure expansion microscopy (U-ExM) .....</b>	<b>59</b>
<b>Figure 2.5: U-ExM localisation of LHL4 protein.....</b>	<b>60</b>
<b>Figure 2.6: Localization of LHL4 by analysis of the composition of different photosynthetic complexes by 2D-BNPAGE .....</b>	<b>61</b>
<b>Figure 2. 7: LHL4 is not constitutively present in the cells but is rapidly accumulated during both UV-B and HL exposures .....</b>	<b>62</b>
<b>Figure 2.8: LHL4 expression upon different light intensity .....</b>	<b>63</b>
<b>Figure 2.9: LHL4 protein accumulation decreases quickly after the end of light treatment.....</b>	<b>64</b>

## CHAPTER 3

<b>Figure 3.1: Characterisation of <i>uvr8</i>, <i>phot</i>, <i>acry</i>, and <i>pcry</i> photoreceptor mutants. ....</b>	<b>68</b>
<b>Figure 3. 2: <i>LHL4</i> gene expression and protein accumulation in photoreceptor mutants after exposure to UV-B or HL .....</b>	<b>69</b>
<b>Figure 3.3: <i>LHL4</i> gene expression and protein accumulation in different genotypes of the UV-B and HL pathways .....</b>	<b>73</b>

<b>Figure 3.4: Accumulation of NPQ proteins in the different genotypes investigated after UV-B or HL exposure</b> .....	75
---	----

<b>Figure 3.5: Transcriptome analysis of different <i>C. reinhardtii</i> strains after UV exposure</b> .....	76
--	----

## **CHAPTER 4**

<b>Figure 4. 1: Characterisation of the <i>lhl4</i> mutant</b> .....	81
--	----

<b>Figure 4. 2: LHL4 is not a NPQ actor</b> .....	82
---	----

<b>Figure 4. 3: LHL4 alleviates PSII photoinhibition</b> .....	84
--	----

<b>Figure 4. 4: LHL4 induction is repressed when NPQ proteins are present</b> .....	85
---	----

<b>Figure 4. 5: LHL4 is involved in photooxidative stress regulation</b> .....	87
--	----

<b>Figure 4. 6: LHL4 is more important with increasing light intensity</b> .....	88
--	----

<b>Figure 4. 7: The <i>lhl4</i> mutant is photosensitive</b> .....	90
--	----

<b>Figure 4. 8: LHL4 is of primary importance for the protection of PSII in natural light.</b> .....	92
---	----

## **CHAPTER 5**

<b>Figure 5. 1: Simplified scheme of chlorophyll biosynthesis pathway</b> .....	97
---	----

<b>Figure 5. 2: Proposed model for the regulation of <i>LHL4</i> expression in <i>C. reinhardtii</i>.</b> .....	106
--	-----

## CHAPTER 6

<b>Figure 6.1: Kinetics of changes in fluorescence yield in a leaf subjected to continuous illumination saturating for photosynthesis and then adapted to dark</b> .....	129
---	-----

## TABLE OF TABLES

<b>Table 1.1: LHC-like proteins involved in stress responses and assembly of photosynthetic complexes</b> .....	28
<b>Table 2.1: List of the proteins significantly induced by UV-B in <i>C. reinhardtii</i>, and their functional annotations</b> .....	54
<b>Table 3.1: 50 genes whose expression is most induced by UV-B exposure in <i>C. reinhardtii</i> WT CC5325, and their functional annotations</b> .....	78

## BIBLIOGRAPHY

- Adamska I (2001) The Elip Family of Stress Proteins in the Thylakoid Membranes of Pro- and Eukaryota. In: Regulation of Photosynthesis. Kluwer Academic Publishers, pp 487–505.
- Adamska I (1997) ELIPs – Light-induced stress proteins. *Physiol Plant* 100:794–805. <https://doi.org/10.1111/j.1399-3054.1997.tb00006.x>
- Adamska I, Kloppstech K (1994) Low temperature increases the abundance of early light-inducible transcript under light stress conditions. *J Biol Chem* 269:30221–30226. [https://doi.org/10.1016/S0021-9258\(18\)43800-8](https://doi.org/10.1016/S0021-9258(18)43800-8)
- Adamska I, Kloppstech K (1991) Evidence for an association of the early light-inducible protein (ELIP) of pea with photosystem II. *Plant Mol Biol* 16:209–223. <https://doi.org/10.1007/BF00020553>
- Adamska I, Kloppstech K, Ohad I (1993) Early light-inducible protein in pea is stable during light stress but is degraded during recovery at low light intensity. *J Biol Chem* 268:5438–5444. [https://doi.org/10.1016/S0021-9258\(18\)53340-8](https://doi.org/10.1016/S0021-9258(18)53340-8)
- Adamska I, Kloppstech K, Ohad I (1992a) UV light stress induces the synthesis of the early light-inducible protein and prevents its degradation. *J Biol Chem* 267:24732–24737
- Adamska I, Ohad I, Kloppstech K (1992b) Synthesis of the early light-inducible protein is controlled by blue light and related to light stress. *Proc Natl Acad Sci U S A* 89:2610–2613
- Alboresi A, Gerotto C, Giacometti GM, et al (2010) *Physcomitrella patens* mutants affected on heat dissipation clarify the evolution of photoprotection mechanisms upon land colonization. *Proc Natl Acad Sci* 107:11128–11133. <https://doi.org/10.1073/pnas.1002873107>
- Allorent G, Lefebvre-Legendre L, Chappuis R, et al (2016) UV-B photoreceptor-mediated protection of the photosynthetic machinery in *Chlamydomonas reinhardtii*. *Proc Natl Acad Sci U S A* 113:14864–14869. <https://doi.org/10.1073/pnas.1607695114>
- Allorent G, Petroutsos D (2017) Photoreceptor-dependent regulation of photoprotection. *Curr Opin Plant Biol* 37:102–108. <https://doi.org/10.1016/j.pbi.2017.03.016>
- Allorent G, Tokutsu R, Roach T, et al (2013) A Dual Strategy to Cope with High Light in *Chlamydomonas reinhardtii*[W]. *Plant Cell* 25:545–557. <https://doi.org/10.1105/tpc.112.108274>
- Aro EM, McCaffery S, Anderson JM (1993) Photoinhibition and D1 Protein Degradation in Peas Acclimated to Different Growth Irradiances. *Plant Physiol* 103:835–843. <https://doi.org/10.1104/pp.103.3.835>

- Bailleul B, Rogato A, de Martino A, et al (2010) An atypical member of the light-harvesting complex stress-related protein family modulates diatom responses to light. *Proc Natl Acad Sci* 107:18214–18219. <https://doi.org/10.1073/pnas.1007703107>
- Ballottari M, Truong TB, Re ED, et al (2016) Identification of pH-sensing Sites in the Light Harvesting Complex Stress-related 3 Protein Essential for Triggering Non-photochemical Quenching in *Chlamydomonas reinhardtii*\*. *J Biol Chem* 291:7334–7346. <https://doi.org/10.1074/jbc.M115.704601>
- Banerjee S, Ray A, Das D (2021) Optimization of *Chlamydomonas reinhardtii* cultivation with simultaneous CO<sub>2</sub> sequestration and biofuels production in a biorefinery framework. *Sci Total Environ* 762:143080. <https://doi.org/10.1016/j.scitotenv.2020.143080>
- Beel B, Müller N, Kottke T, Mittag M (2013) News about cryptochrome photoreceptors in algae. *Plant Signal Behav* 8:e22870. <https://doi.org/10.4161/psb.22870>
- Beel B, Prager K, Spexard M, et al (2012) A Flavin Binding Cryptochrome Photoreceptor Responds to Both Blue and Red Light in *Chlamydomonas reinhardtii*. *Plant Cell* 24:2992–3008. <https://doi.org/10.1105/tpc.112.098947>
- Bellaïfiore S, Barneche F, Peltier G, Rochaix J-D (2005) State transitions and light adaptation require chloroplast thylakoid protein kinase STN7. *Nature* 433:892–895. <https://doi.org/10.1038/nature03286>
- Benson AA, Calvin M (1950) Carbon Dioxide Fixation By Green Plants. *Annu Rev Plant Physiol* 1:25–42. <https://doi.org/10.1146/annurev.pp.01.060150.000325>
- Binkert M, Kozma-Bognár L, Terecskei K, et al (2014) UV-B-Responsive Association of the Arabidopsis bZIP Transcription Factor ELONGATED HYPOCOTYL5 with Target Genes, Including Its Own Promoter. *Plant Cell* 26:4200–4213. <https://doi.org/10.1105/tpc.114.130716>
- Bonente G, Ballottari M, Truong TB, et al (2011) Analysis of LhcSR3, a Protein Essential for Feedback De-Excitation in the Green Alga *Chlamydomonas reinhardtii*. *PLOS Biol* 9:e1000577. <https://doi.org/10.1371/journal.pbio.1000577>
- Bouyssié D, Hesse A-M, Mouton-Barbosa E, et al (2020) Proline: an efficient and user-friendly software suite for large-scale proteomics. *Bioinforma Oxf Engl* 36:3148–3155. <https://doi.org/10.1093/bioinformatics/btaa118>
- Britt AB (2004) Repair of DNA Damage Induced by Solar UV. *Photosynth Res* 81:105–112. <https://doi.org/10.1023/B:PRES.0000035035.12340.58>
- Brown BA, Cloix C, Jiang GH, et al (2005) A UV-B-specific signaling component orchestrates plant UV protection. *Proc Natl Acad Sci* 102:18225–18230. <https://doi.org/10.1073/pnas.0507187102>
- Brown BA, Jenkins GI (2008) UV-B Signaling Pathways with Different Fluence-Rate Response Profiles Are Distinguished in Mature Arabidopsis Leaf Tissue by Requirement for UVR8, HY5, and HYH. *Plant Physiol* 146:576–588

- Brudler R, Hitomi K, Daiyasu H, et al (2003) Identification of a New Cryptochrome Class: Structure, Function, and Evolution. *Mol Cell* 11:59–67. [https://doi.org/10.1016/S1097-2765\(03\)00008-X](https://doi.org/10.1016/S1097-2765(03)00008-X)
- Bruno AK, Wetzel CM (2004) The early light-inducible protein (ELIP) gene is expressed during the chloroplast-to-chromoplast transition in ripening tomato fruit. *J Exp Bot* 55:2541–2548. <https://doi.org/10.1093/jxb/erh273>
- Büchel C (2015) Evolution and function of light harvesting proteins. *J Plant Physiol* 172:62–75. <https://doi.org/10.1016/j.jplph.2014.04.018>
- Burgie ES, Vierstra RD (2014) Phytochromes: An Atomic Perspective on Photoactivation and Signaling. *Plant Cell* 26:4568–4583. <https://doi.org/10.1105/tpc.114.131623>
- Camargo FVA, Perozeni F, Valbuena G de la C, et al (2021) The Role of Acidic Residues in the C Terminal Tail of the LHCSR3 Protein of *Chlamydomonas reinhardtii* in Non-Photochemical Quenching. *J Phys Chem Lett* 12:6895–6900. <https://doi.org/10.1021/acs.jpcclett.1c01382>
- Cariti F (2018) Identification and characterization of chloroplast protein phosphatases involved in regulation of photosynthesis in *Chlamydomonas reinhardtii*. PhD thesis, University of Geneva
- Cariti F, Chazaux M, Lefebvre-Legendre L, et al (2020) Regulation of Light Harvesting in *Chlamydomonas reinhardtii* Two Protein Phosphatases Are Involved in State Transitions. *Plant Physiol* 183:1749–1764. <https://doi.org/10.1104/pp.20.00384>
- Casabona MG, Vandenbrouck Y, Attree I, Couté Y (2013) Proteomic characterization of *Pseudomonas aeruginosa* PAO1 inner membrane. *Proteomics* 13:2419–2423. <https://doi.org/10.1002/pmic.201200565>
- Castrillo M, García-Martínez J, Avalos J (2013) Light-Dependent Functions of the *Fusarium fujikuroi* CryD DASH Cryptochrome in Development and Secondary Metabolism. *Appl Environ Microbiol* 79:2777–2788. <https://doi.org/10.1128/AEM.03110-12>
- Cazzaniga S, Dall’Osto L, Kong S-G, et al (2013) Interaction between avoidance of photon absorption, excess energy dissipation and zeaxanthin synthesis against photooxidative stress in *Arabidopsis*. *Plant J* 76:568–579. <https://doi.org/10.1111/tpj.12314>
- Challabathula D, Zhang Q, Bartels D (2018) Protection of photosynthesis in desiccation-tolerant resurrection plants. *J Plant Physiol* 227:84–92. <https://doi.org/10.1016/j.jplph.2018.05.002>
- Chaves I, Pokorný R, Byrdin M, et al (2011) The Cryptochromes: Blue Light Photoreceptors in Plants and Animals. *Annu Rev Plant Biol* 335–64. <https://doi.org/10.1146/annurev-arplant-042110-103759>
- Christie JM (2007) Phototropin Blue-Light Receptors. *Annu Rev Plant Biol* 58:21–45. <https://doi.org/10.1146/annurev.arplant.58.032806.103951>

- Christie JM, Arvai AS, Baxter KJ, et al (2012) Plant UVR8 Photoreceptor Senses UV-B by Tryptophan-Mediated Disruption of Cross-Dimer Salt Bridges. *Science* 335:1492–1496. <https://doi.org/10.1126/science.1218091>
- Christie JM, Yang H, Richter GL, et al (2011) phot1 Inhibition of ABCB19 Primes Lateral Auxin Fluxes in the Shoot Apex Required For Phototropism. *PLOS Biol* 9:e1001076. <https://doi.org/10.1371/journal.pbio.1001076>
- Coesel S, Mangogna M, Ishikawa T, et al (2009) Diatom PtCPF1 is a new cryptochrome/photolyase family member with DNA repair and transcription regulation activity. *EMBO Rep* 10:655–661. <https://doi.org/10.1038/embor.2009.59>
- Correa-Galvis V, Redekop P, Guan K, et al (2016) Photosystem II Subunit PsbS Is Involved in the Induction of LHCSR Protein-dependent Energy Dissipation in *Chlamydomonas reinhardtii*\*. *J Biol Chem* 291:17478–17487. <https://doi.org/10.1074/jbc.M116.737312>
- Couté Y, Bruley C, Burger T (2020) Beyond Target-Decoy Competition: Stable Validation of Peptide and Protein Identifications in Mass Spectrometry-Based Discovery Proteomics. *Anal Chem* 92:14898–14906. <https://doi.org/10.1021/acs.analchem.0c00328>
- Craig RJ, Gallaher SD, Shu S, et al (2023) The *Chlamydomonas* Genome Project, version 6: Reference assemblies for mating-type plus and minus strains reveal extensive structural mutation in the laboratory. *Plant Cell* 35:644–672. <https://doi.org/10.1093/plcell/koac347>
- Dall’Osto L, Caffarri S, Bassi R (2005) A Mechanism of Nonphotochemical Energy Dissipation, Independent from PsbS, Revealed by a Conformational Change in the Antenna Protein CP26. *Plant Cell* 17:1217–1232. <https://doi.org/10.1105/tpc.104.030601>
- Davey MP, Susanti NI, Wargent JJ, et al (2012) The UV-B photoreceptor UVR8 promotes photosynthetic efficiency in *Arabidopsis thaliana* exposed to elevated levels of UV-B. *Photosynth Res* 114:121–131. <https://doi.org/10.1007/s11120-012-9785-y>
- Delosme R, Olive J, Wollman F-A (1996) Changes in light energy distribution upon state transitions: an in vivo photoacoustic study of the wild type and photosynthesis mutants from *Chlamydomonas reinhardtii*. *Biochim Biophys Acta BBA - Bioenerg* 1273:150–158. [https://doi.org/10.1016/0005-2728\(95\)00143-3](https://doi.org/10.1016/0005-2728(95)00143-3)
- Demarsy E, Goldschmidt-Clermont M, Ulm R (2018) Coping with ‘Dark Sides of the Sun’ through Photoreceptor Signaling. *Trends Plant Sci* 23:260–271. <https://doi.org/10.1016/j.tplants.2017.11.007>
- Demarsy E, Schepens I, Okajima K, et al (2012) Phytochrome Kinase Substrate 4 is phosphorylated by the phototropin 1 photoreceptor. *EMBO J* 31:3457–3467. <https://doi.org/10.1038/emboj.2012.186>

- Di Wu, Hu Q, Yan Z, et al (2012) Structural basis of ultraviolet-B perception by UVR8. *Nature* 484:214–219. <https://doi.org/10.1038/nature10931>
- Dinc E, Tian L, Roy LM, et al (2016) LHCSR1 induces a fast and reversible pH-dependent fluorescence quenching in LHClI in *Chlamydomonas reinhardtii* cells. *Proc Natl Acad Sci* 113:7673–7678. <https://doi.org/10.1073/pnas.1605380113>
- Doi M, Wada M, Shimazaki K-I (2006) The fern *Adiantum capillus-veneris* lacks stomatal responses to blue light. *Plant Cell Physiol* 47:748–755. <https://doi.org/10.1093/pcp/pcj048>
- Dumas L, Zito F, Blangy S, et al (2017) A stromal region of cytochrome b6f subunit IV is involved in the activation of the Stt7 kinase in *Chlamydomonas*. *Proc Natl Acad Sci* 114:12063–12068. <https://doi.org/10.1073/pnas.1713343114>
- Eberhard S, Finazzi G, Wollman F-A (2008) The Dynamics of Photosynthesis. *Annu Rev Genet* 42:463–515. <https://doi.org/10.1146/annurev.genet.42.110807.091452>
- Erickson E, Wakao S, Niyogi KK (2015) Light stress and photoprotection in *Chlamydomonas reinhardtii*. *Plant J* 82:449–465. <https://doi.org/10.1111/tpj.12825>
- Essen L-O, Franz S, Banerjee A (2017) Structural and evolutionary aspects of algal blue light receptors of the cryptochrome and aureochrome type. *J Plant Physiol* 217:27–37. <https://doi.org/10.1016/j.jplph.2017.07.005>
- Falconet D (2012) Origin, Evolution and Division of Plastids. In: Eaton-Rye JJ, Tripathy BC, Sharkey TD (eds) *Photosynthesis: Plastid Biology, Energy Conversion and Carbon Assimilation*. Springer Netherlands, Dordrecht, pp 35–61
- Fan M, Li M, Liu Z, et al (2015) Crystal structures of the PsbS protein essential for photoprotection in plants. *Nat Struct Mol Biol* 22:729–735. <https://doi.org/10.1038/nsmb.3068>
- Faulkner EL, Thomas SG, Neely RK (2020) An introduction to the methodology of expansion microscopy. *Int J Biochem Cell Biol* 124:105764. <https://doi.org/10.1016/j.biocel.2020.105764>
- Favory J-J, Stec A, Gruber H, et al (2009) Interaction of COP1 and UVR8 regulates UV-B-induced photomorphogenesis and stress acclimation in *Arabidopsis*. *EMBO J* 28:591–601. <https://doi.org/10.1038/emboj.2009.4>
- Fehér B, Kozma-Bognár L, Kevei É, et al (2011) Functional interaction of the circadian clock and UV RESISTANCE LOCUS 8-controlled UV-B signaling pathways in *Arabidopsis thaliana*. *Plant J* 67:37–48. <https://doi.org/10.1111/j.1365-313X.2011.04573.x>
- Fernández MB, Tossi V, Lamattina L, Cassia R (2016) A Comprehensive Phylogeny Reveals Functional Conservation of the UV-B Photoreceptor UVR8 from Green Algae to Higher Plants. *Front Plant Sci* 7:1698. <https://doi.org/10.3389/fpls.2016.01698>

- Fischer BB, Eggen RIL, Trebst A, Krieger-Liszkay A (2006) The glutathione peroxidase homologous gene Gpxh in *Chlamydomonas reinhardtii* is upregulated by singlet oxygen produced in photosystem II. *Planta* 223:583–590. <https://doi.org/10.1007/s00425-005-0108-9>
- Flori S (2016) Light utilization in microalgae : the marine diatom *Phaeodactylum tricornutum* and the green algae *Chlamydomonas reinhardtii*. Phdthesis, Université Grenoble Alpes
- Folta KM, Kaufman LS (2003) Phototropin 1 is required for high-fluence blue-light-mediated mRNA destabilization. *Plant Mol Biol* 51:609–618. <https://doi.org/10.1023/A:1022393406204>
- Folta KM, Spalding EP (2001) Unexpected roles for cryptochrome 2 and phototropin revealed by high-resolution analysis of blue light-mediated hypocotyl growth inhibition. *Plant J Cell Mol Biol* 26:471–478. <https://doi.org/10.1046/j.1365-313x.2001.01038.x>
- Fraikin GYa (2022) Photosensory and Signaling Properties of Cryptochromes. *Mosc Univ Biol Sci Bull* 77:54–63. <https://doi.org/10.3103/S0096392522020031>
- Gabilly ST, Baker CR, Wakao S, et al (2019) Regulation of photoprotection gene expression in *Chlamydomonas* by a putative E3 ubiquitin ligase complex and a homolog of CONSTANS. *Proc Natl Acad Sci* 116:17556–17562. <https://doi.org/10.1073/pnas.1821689116>
- Galvão VC, Fankhauser C (2015) Sensing the light environment in plants: photoreceptors and early signaling steps. *Curr Opin Neurobiol* 34:46–53. <https://doi.org/10.1016/j.conb.2015.01.013>
- Gambarotto D, Hamel V, Guichard P (2021) Chapter 4 - Ultrastructure expansion microscopy (U-ExM). In: Guichard P, Hamel V (eds) *Methods in Cell Biology*. Academic Press, pp 57–81
- Gangappa SN, Botto JF (2016) The Multifaceted Roles of HY5 in Plant Growth and Development. *Mol Plant* 9:1353–1365. <https://doi.org/10.1016/j.molp.2016.07.002>
- Goldschmidt-Clermont M (2023) Chapter 24 - State transitions. In: Grossman AR, Wollman F-A (eds) *The Chlamydomonas Sourcebook (Third Edition)*. Academic Press, London, pp 787–805
- Govorunova EG, Jung K-H, Sineshchekov OA, Spudich JL (2004) *Chlamydomonas* Sensory Rhodopsins A and B: Cellular Content and Role in Photophobic Responses. *Biophys J* 86:2342–2349. [https://doi.org/10.1016/S0006-3495\(04\)74291-5](https://doi.org/10.1016/S0006-3495(04)74291-5)
- Green BR, Kühlbrandt W (1995) Sequence conservation of light-harvesting and stress-response proteins in relation to the three-dimensional molecular structure of LHCII. *Photosynth Res* 44:139–148. <https://doi.org/10.1007/BF00018304>

- Greiner A, Kelterborn S, Evers H, et al (2017) Targeting of Photoreceptor Genes in *Chlamydomonas reinhardtii* via Zinc-Finger Nucleases and CRISPR/Cas9. *Plant Cell* 29:2498–2518. <https://doi.org/10.1105/tpc.17.00659>
- Grimm B, Kloppstech K (1987) The early light-inducible proteins of Barley °. *Eur J Biochem* 167:493–499. <https://doi.org/10.1111/j.1432-1033.1987.tb13364.x>
- Gruber H, Heijde M, Heller W, et al (2010) Negative feedback regulation of UV-B-induced photomorphogenesis and stress acclimation in *Arabidopsis*. *Proc Natl Acad Sci* 107:20132–20137. <https://doi.org/10.1073/pnas.0914532107>
- Hamel V, Guichard P (2021) Chapter 14 - Improving the resolution of fluorescence nanoscopy using post-expansion labeling microscopy. In: Guichard P, Hamel V (eds) *Methods in Cell Biology*. Academic Press, pp 297–315
- Han X, Huang X, Deng XW (2020) The Photomorphogenic Central Repressor COP1: Conservation and Functional Diversification during Evolution. *Plant Commun* 1:100044. <https://doi.org/10.1016/j.xplc.2020.100044>
- Heddad M, Adamska I (2002) The Evolution of Light Stress Proteins in Photosynthetic Organisms. *Int J Genomics* 3:504–510. <https://doi.org/10.1002/cfg.221>
- Hegemann P (1997) Vision in microalgae. *Planta* 203:265–274. <https://doi.org/10.1007/s004250050191>
- Heijde M, Ulm R (2013) Reversion of the *Arabidopsis* UV-B photoreceptor UVR8 to the homodimeric ground state. *Proc Natl Acad Sci* 110:1113–1118. <https://doi.org/10.1073/pnas.1214237110>
- Heijde M, Ulm R (2012) UV-B photoreceptor-mediated signalling in plants. *Trends Plant Sci* 17:230–237. <https://doi.org/10.1016/j.tplants.2012.01.007>
- Heijde M, Zabulon G, Corellou F, et al (2010) Characterization of two members of the cryptochrome/photolyase family from *Ostreococcus tauri* provides insights into the origin and evolution of cryptochromes. *Plant Cell Environ* 33:1614–1626. <https://doi.org/10.1111/j.1365-3040.2010.02168.x>
- Hevler JF, Lukassen MV, Cabrera-Orefice A, et al (2021) Selective cross-linking of coinciding protein assemblies by in-gel cross-linking mass spectrometry. *EMBO J* 40:e106174. <https://doi.org/10.15252/embj.2020106174>
- Hieber AD, Bugos RC, Yamamoto HY (2000) Plant lipocalins: violaxanthin de-epoxidase and zeaxanthin epoxidase. *Biochim Biophys Acta BBA - Protein Struct Mol Enzymol* 1482:84–91. [https://doi.org/10.1016/S0167-4838\(00\)00141-2](https://doi.org/10.1016/S0167-4838(00)00141-2)
- Hoecker U (2017) The activities of the E3 ubiquitin ligase COP1/SPA, a key repressor in light signaling. *Curr Opin Plant Biol* 37:63–69. <https://doi.org/10.1016/j.pbi.2017.03.015>

- Hoecker U, Tepperman JM, Quail PH (1999) SPA1, a WD-Repeat Protein Specific to Phytochrome A Signal Transduction. *Science* 284:496–499. <https://doi.org/10.1126/science.284.5413.496>
- Holm M, Hardtke CS, Gaudet R, Deng X-W (2001) Identification of a structural motif that confers specific interaction with the WD40 repeat domain of Arabidopsis COP1. *EMBO J* 20:118–127. <https://doi.org/10.1093/emboj/20.1.118>
- Holm M, Ma L-G, Qu L-J, Deng X-W (2002) Two interacting bZIP proteins are direct targets of COP1-mediated control of light-dependent gene expression in Arabidopsis. *Genes Dev* 16:1247–1259. <https://doi.org/10.1101/gad.969702>
- Horton P, Ruban AV, Walters RG (1996) Regulation of Light Harvesting in Green Plants. *Annu Rev Plant Physiol Plant Mol Biol* 47:655–684. <https://doi.org/10.1146/annurev.arplant.47.1.655>
- Huang K, Beck CF (2003) Phototropin is the blue-light receptor that controls multiple steps in the sexual life cycle of the green alga *Chlamydomonas reinhardtii*. *Proc Natl Acad Sci* 100:6269–6274. <https://doi.org/10.1073/pnas.0931459100>
- Huang K, Kunkel T, Beck CF (2004) Localization of the Blue-Light Receptor Phototropin to the Flagella of the Green Alga *Chlamydomonas reinhardtii*. *Mol Biol Cell* 15:3605–3614. <https://doi.org/10.1091/mbc.e04-01-0010>
- Huang K, Merkle T, Beck CF (2002) Isolation and characterization of a *Chlamydomonas* gene that encodes a putative blue-light photoreceptor of the phototropin family. *Physiol Plant* 115:613–622. <https://doi.org/10.1034/j.1399-3054.2002.1150416.x>
- Huang X, Ouyang X, Deng XW (2014) Beyond repression of photomorphogenesis: role switching of COP/DET/FUS in light signaling. *Curr Opin Plant Biol* 21:96–103. <https://doi.org/10.1016/j.pbi.2014.07.003>
- Huang X, Ouyang X, Yang P, et al (2013) Conversion from CUL4-based COP1–SPA E3 apparatus to UVR8–COP1–SPA complexes underlies a distinct biochemical function of COP1 under UV-B. *Proc Natl Acad Sci* 110:16669–16674. <https://doi.org/10.1073/pnas.1316622110>
- Hutin C, Nussaume L, Moise N, et al (2003) Early light-induced proteins protect Arabidopsis from photooxidative stress. *Proc Natl Acad Sci* 100:4921–4926. <https://doi.org/10.1073/pnas.0736939100>
- Im C-S, Eberhard S, Huang K, et al (2006) Phototropin involvement in the expression of genes encoding chlorophyll and carotenoid biosynthesis enzymes and LHC apoproteins in *Chlamydomonas reinhardtii*. *Plant J* 48:1–16. <https://doi.org/10.1111/j.1365-313X.2006.02852.x>
- Imaizumi T, Kadota A, Hasebe M, Wada M (2002) Cryptochrome Light Signals Control Development to Suppress Auxin Sensitivity in the Moss *Physcomitrella patens*. *Plant Cell* 14:373–386. <https://doi.org/10.1105/tpc.010388>

- Imaizumi T, Kanegae T, Wada M (2000) Cryptochrome Nucleocytoplasmic Distribution and Gene Expression Are Regulated by Light Quality in the Fern *Adiantum capillus-veneris*. *Plant Cell* 12:81–95. <https://doi.org/10.1105/tpc.12.1.81>
- Inoue S, Kinoshita T, Shimazaki K (2005) Possible involvement of phototropins in leaf movement of kidney bean in response to blue light. *Plant Physiol* 138:1994–2004. <https://doi.org/10.1104/pp.105.062026>
- Jakoby M, Weisshaar B, Dröge-Laser W, et al (2002) bZIP transcription factors in *Arabidopsis*. *Trends Plant Sci* 7:106–111. [https://doi.org/10.1016/S1360-1385\(01\)02223-3](https://doi.org/10.1016/S1360-1385(01)02223-3)
- Jang I-C, Yang J-Y, Seo HS, Chua N-H (2005) HFR1 is targeted by COP1 E3 ligase for post-translational proteolysis during phytochrome A signaling. *Genes Dev* 19:593–602. <https://doi.org/10.1101/gad.1247205>
- Jang S, Marchal V, Panigrahi KCS, et al (2008) *Arabidopsis* COP1 shapes the temporal pattern of CO accumulation conferring a photoperiodic flowering response. *EMBO J* 27:1277–1288. <https://doi.org/10.1038/emboj.2008.68>
- Jansen MAK, Gaba V, Greenberg BM (1998) Higher plants and UV-B radiation: balancing damage, repair and acclimation. *Trends Plant Sci* 3:131–135. [https://doi.org/10.1016/S1360-1385\(98\)01215-1](https://doi.org/10.1016/S1360-1385(98)01215-1)
- Jansson S (1999) A guide to the Lhc genes and their relatives in *Arabidopsis*. *Trends Plant Sci* 4:236–240. [https://doi.org/10.1016/S1360-1385\(99\)01419-3](https://doi.org/10.1016/S1360-1385(99)01419-3)
- Jarillo JA, Gabrys H, Capel J, et al (2001) Phototropin-related NPL1 controls chloroplast relocation induced by blue light. *Nature* 410:952–954. <https://doi.org/10.1038/35073622>
- Jenkins GI (2014) The UV-B Photoreceptor UVR8: From Structure to Physiology. *Plant Cell* 26:21–37. <https://doi.org/10.1105/tpc.113.119446>
- Jenkins GI (2017) Photomorphogenic responses to ultraviolet-B light. *Plant Cell Environ* 40:2544–2557. <https://doi.org/10.1111/pce.12934>
- Jenkins GI (2009) Signal transduction in responses to UV-B radiation. *Annu Rev Plant Biol* 60:407–431. <https://doi.org/10.1146/annurev.arplant.59.032607.092953>
- Joliot PA, Finazzi G (2010) Proton equilibration in the chloroplast modulates multiphasic kinetics of nonphotochemical quenching of fluorescence in plants. *Proc Natl Acad Sci* 107:12728–12733. <https://doi.org/10.1073/pnas.1006399107>
- Jourdan N, F Martino C, El-Esawi M, et al (2015) Blue-light dependent ROS formation by *Arabidopsis* cryptochrome-2 may contribute toward its signaling role. *Plant Signal Behav* 10:e1042647. <https://doi.org/10.1080/15592324.2015.1042647>
- Juhas M, von Zadow A, Spexard M, et al (2014) A novel cryptochrome in the diatom *Phaeodactylum tricornutum* influences the regulation of light-harvesting protein levels. *FEBS J* 281:2299–2311. <https://doi.org/10.1111/febs.12782>

- Kagawa T, Sakai T, Suetsugu N, et al (2001) Arabidopsis NPL1: A Phototropin Homolog Controlling the Chloroplast High-Light Avoidance Response. *Science* 291:2138–2141. <https://doi.org/10.1126/science.291.5511.2138>
- Kasahara M, Kagawa T, Oikawa K, et al (2002) Chloroplast avoidance movement reduces photodamage in plants. *Nature* 420:829–832. <https://doi.org/10.1038/nature01213>
- Kasahara M, Kagawa T, Sato Y, et al (2004) Phototropins mediate blue and red light-induced chloroplast movements in *Physcomitrella patens*. *Plant Physiol* 135:1388–1397. <https://doi.org/10.1104/pp.104.042705>
- Kateriya S, Nagel G, Bamberg E, Hegemann P (2004) “Vision” in Single-Celled Algae. *Physiology* 19:133–137. <https://doi.org/10.1152/nips.01517.2004>
- Kinoshita T, Doi M, Suetsugu N, et al (2001) phot1 and phot2 mediate blue light regulation of stomatal opening. *Nature* 414:656–660. <https://doi.org/10.1038/414656a>
- Kiontke S, Göbel T, Brych A, Batschauer A (2020) DASH-type cryptochromes – solved and open questions. *Biol Chem* 401:1487–1493. <https://doi.org/10.1515/hsz-2020-0182>
- Kleine T, Lockhart P, Batschauer A (2003) An Arabidopsis protein closely related to *Synechocystis* cryptochrome is targeted to organelles. *Plant J* 35:93–103. <https://doi.org/10.1046/j.1365-313X.2003.01787.x>
- Kleiner O, Kircher S, Harter K, Batschauer A (1999) Nuclear localization of the Arabidopsis blue light receptor cryptochrome 2. *Plant J* 19:289–296. <https://doi.org/10.1046/j.1365-313X.1999.00535.x>
- Kliebenstein DJ, Lim JE, Landry LG, Last RL (2002a) Arabidopsis UVR8 Regulates Ultraviolet-B Signal Transduction and Tolerance and Contains Sequence Similarity to Human Regulator of Chromatin Condensation 1. *Plant Physiol* 130:234–243. <https://doi.org/10.1104/pp.005041>
- Kliebenstein DJ, Lim JE, Landry LG, Last RL (2002b) Arabidopsis UVR8 Regulates Ultraviolet-B Signal Transduction and Tolerance and Contains Sequence Similarity to Human Regulator of Chromatin Condensation 1. *Plant Physiol* 130:234–243. <https://doi.org/10.1104/pp.005041>
- König S, Juhas M, Jäger S, et al (2017) The cryptochrome—photolyase protein family in diatoms. *J Plant Physiol* 217:15–19. <https://doi.org/10.1016/j.jplph.2017.06.015>
- Kosuge K, Tokutsu R, Kim E, et al (2018) LHCSR1-dependent fluorescence quenching is mediated by excitation energy transfer from LHCI to photosystem I in *Chlamydomonas reinhardtii*. *Proc Natl Acad Sci* 115:3722–3727. <https://doi.org/10.1073/pnas.1720574115>
- Kottke T, Oldemeyer S, Wenzel S, et al (2017) Cryptochrome photoreceptors in green algae: Unexpected versatility of mechanisms and functions. *J Plant Physiol* 217:4–14. <https://doi.org/10.1016/j.jplph.2017.05.021>

- Krause GH, Weis E (1991) Chlorophyll Fluorescence and Photosynthesis: The Basics. *Annu Rev Plant Physiol Plant Mol Biol* 42:313–349. <https://doi.org/10.1146/annurev.pp.42.060191.001525>
- Krieger-Liszkay A (2005) Singlet oxygen production in photosynthesis. *J Exp Bot* 56:337–346. <https://doi.org/10.1093/jxb/erh237>
- Kropat J, Hong-Hermesdorf A, Casero D, et al (2011) A revised mineral nutrient supplement increases biomass and growth rate in *Chlamydomonas reinhardtii*. *Plant J* 66:770–780. <https://doi.org/10.1111/j.1365-313X.2011.04537.x>
- Kühlbrandt W, Wang DN, Fujiyoshi Y (1994) Atomic model of plant light-harvesting complex by electron crystallography. *Nature* 367:614–621. <https://doi.org/10.1038/367614a0>
- KUMAGAI T, ITO S, NAKAMICHI N, et al (2008) The Common Function of a Novel Subfamily of B-Box Zinc Finger Proteins with Reference to Circadian-Associated Events in *Arabidopsis thaliana*. *Biosci Biotechnol Biochem* 72:1539–1549. <https://doi.org/10.1271/bbb.80041>
- Lämmermann N, Wulf D, Chang KS, et al (2020) Ubiquitin ligase component LRS1 and transcription factor CrHy5 act as a light switch for photoprotection in *Chlamydomonas*. *Plant Biology*
- Laporte MH, Klena N, Hamel V, Guichard P (2022) Visualizing the native cellular organization by coupling cryofixation with expansion microscopy (Cryo-ExM). *Nat Methods* 19:216–222. <https://doi.org/10.1038/s41592-021-01356-4>
- Lau K, Podolec R, Chappuis R, et al (2019) Plant photoreceptors and their signaling components compete for COP1 binding via VP peptide motifs. *EMBO J* 38:e102140. <https://doi.org/10.15252/embj.2019102140>
- Lau OS, Deng XW (2012) The photomorphogenic repressors COP1 and DET1: 20 years later. *Trends Plant Sci* 17:584–593. <https://doi.org/10.1016/j.tplants.2012.05.004>
- Laubinger S, Fittinghoff K, Hoecker U (2004) The SPA Quartet: A Family of WD-Repeat Proteins with a Central Role in Suppression of Photomorphogenesis in *Arabidopsis*. *Plant Cell* 16:2293–2306. <https://doi.org/10.1105/tpc.104.024216>
- Lavaud J, Rousseau B, van Gorkom HJ, Etienne A-L (2002) Influence of the Diadinoxanthin Pool Size on Photoprotection in the Marine Planktonic Diatom *Phaeodactylum tricornutum*. *Plant Physiol* 129:1398–1406. <https://doi.org/10.1104/pp.002014>
- Ledger S, Strayer C, Ashton F, et al (2001) Analysis of the function of two circadian-regulated CONSTANS-LIKE genes. *Plant J* 26:15–22. <https://doi.org/10.1046/j.1365-313x.2001.01003.x>
- Lee JW, Lee SH, Han JW, Kim GH (2020) Early Light-Inducible Protein (ELIP) Can Enhance Resistance to Cold-Induced Photooxidative Stress in *Chlamydomonas reinhardtii*. *Front Physiol* 11:. <https://doi.org/10.3389/fphys.2020.01083>

- Lepetit B, Sturm S, Rogato A, et al (2013) High Light Acclimation in the Secondary Plastids Containing Diatom *Phaeodactylum tricornutum* is Triggered by the Redox State of the Plastoquinone Pool. *Plant Physiol* 161:853–865. <https://doi.org/10.1104/pp.112.207811>
- Lers A, Levy H, Zamir A (1991) Co-regulation of a gene homologous to early light-induced genes in higher plants and beta-carotene biosynthesis in the alga *Dunaliella bardawil*. *J Biol Chem* 266:13698–13705. [https://doi.org/10.1016/S0021-9258\(18\)92755-9](https://doi.org/10.1016/S0021-9258(18)92755-9)
- Li X, Patena W, Fauser F, et al (2019) A genome-wide algal mutant library and functional screen identifies genes required for eukaryotic photosynthesis. *Nat Genet* 51:627–635. <https://doi.org/10.1038/s41588-019-0370-6>
- Li X, Zhang R, Patena W, et al (2016) An Indexed, Mapped Mutant Library Enables Reverse Genetics Studies of Biological Processes in *Chlamydomonas reinhardtii*. *Plant Cell* 28:367–387. <https://doi.org/10.1105/tpc.15.00465>
- Li X-P, Björkman O, Shih C, et al (2000) A pigment-binding protein essential for regulation of photosynthetic light harvesting. *Nature* 403:391–395. <https://doi.org/10.1038/35000131>
- Lian H-L, He S-B, Zhang Y-C, et al (2011) Blue-light-dependent interaction of cryptochrome 1 with SPA1 defines a dynamic signaling mechanism. *Genes Dev* 25:1023–1028. <https://doi.org/10.1101/gad.2025111>
- Liao J, Deng B, Yang Q, et al (2023) Insights into Cryptochrome Modulation of ABA Signaling to Mediate Dormancy Regulation in *Marchantia polymorpha*. *New Phytol n/a*: <https://doi.org/10.1111/nph.18815>
- Lin C, Robertson DE, Ahmad M, et al (1995) Association of flavin adenine dinucleotide with the Arabidopsis blue light receptor CRY1. *Science* 269:968–970. <https://doi.org/10.1126/science.7638620>
- Lin C, Todo T (2005) The cryptochromes. *Genome Biol* 6:220. <https://doi.org/10.1186/gb-2005-6-5-220>
- Lin JY (2011) A user's guide to channelrhodopsin variants: features, limitations and future developments. *Exp Physiol* 96:19–25. <https://doi.org/10.1113/expphysiol.2009.051961>
- Link S, Engelmann K, Meierhoff K, Westhoff P (2012) The Atypical Short-Chain Dehydrogenases HCF173 and HCF244 Are Jointly Involved in Translational Initiation of the *psbA* mRNA of Arabidopsis. *Plant Physiol* 160:2202–2218. <https://doi.org/10.1104/pp.112.205104>
- Liscum E, Briggs WR (1995) Mutations in the NPH1 locus of Arabidopsis disrupt the perception of phototropic stimuli. *Plant Cell* 7:473–485. <https://doi.org/10.1105/tpc.7.4.473>

- Liu B, Zuo Z, Liu H, et al (2011a) Arabidopsis cryptochrome 1 interacts with SPA1 to suppress COP1 activity in response to blue light. *Genes Dev* 25:1029–1034. <https://doi.org/10.1101/gad.2025011>
- Liu H, Liu B, Zhao C, et al (2011b) The action mechanisms of plant cryptochromes. *Trends Plant Sci* 16:684–691. <https://doi.org/10.1016/j.tplants.2011.09.002>
- Liu L-J, Zhang Y-C, Li Q-H, et al (2008) COP1-Mediated Ubiquitination of CONSTANS Is Implicated in Cryptochrome Regulation of Flowering in *Arabidopsis*. *Plant Cell* 20:292–306. <https://doi.org/10.1105/tpc.107.057281>
- Liu Z, Yan H, Wang K, et al (2004) Crystal structure of spinach major light-harvesting complex at 2.72 Å resolution. *Nature* 428:287–292. <https://doi.org/10.1038/nature02373>
- Livak KJ, Schmittgen TD (2001) Analysis of Relative Gene Expression Data Using Real-Time Quantitative PCR and the 2- $\Delta\Delta$ CT Method. *Methods* 25:402–408. <https://doi.org/10.1006/meth.2001.1262>
- Lohr M, Wilhelm C (1999) Algae displaying the diadinoxanthin cycle also possess the violaxanthin cycle. *Proc Natl Acad Sci* 96:8784–8789. <https://doi.org/10.1073/pnas.96.15.8784>
- Long SP, Humphries S, Falkowski PG (1994) Photoinhibition of Photosynthesis in Nature. *Annu Rev Plant Physiol Plant Mol Biol* 45:633–662. <https://doi.org/10.1146/annurev.pp.45.060194.003221>
- Malhotra K, Kim ST, Batschauer A, et al (1995) Putative blue-light photoreceptors from *Arabidopsis thaliana* and *Sinapis alba* with a high degree of sequence homology to DNA photolyase contain the two photolyase cofactors but lack DNA repair activity. *Biochemistry* 34:6892–6899. <https://doi.org/10.1021/bi00020a037>
- Malnoë A (2018) Photoinhibition or photoprotection of photosynthesis? Update on the (newly termed) sustained quenching component qH. *Environ Exp Bot* 154:123–133. <https://doi.org/10.1016/j.envexpbot.2018.05.005>
- Malnoë A, Schultink A, Shahrabi S, et al (2018) The Plastid Lipocalin LCNP Is Required for Sustained Photoprotective Energy Dissipation in *Arabidopsis*[OPEN]. *Plant Cell* 30:196–208. <https://doi.org/10.1105/tpc.17.00536>
- Malnoë A, Wang F, Girard-Bascou J, et al (2014) Thylakoid FtsH Protease Contributes to Photosystem II and Cytochrome b 6 f Remodeling in *Chlamydomonas reinhardtii* under Stress Conditions. *Plant Cell* 26:373–390. <https://doi.org/10.1105/tpc.113.120113>
- Mao K, Wang L, Li Y-Y, Wu R (2015) Molecular Cloning and Functional Analysis of UV RESISTANCE LOCUS 8 (PeUVR8) from *Populus euphratica*. *PloS One* 10:e0132390. <https://doi.org/10.1371/journal.pone.0132390>

- Marks RA, Smith JJ, VanBuren R, McLetchie DN (2021) Expression dynamics of dehydration tolerance in the tropical plant *Marchantia inflexa*. *Plant J* 105:209–222. <https://doi.org/10.1111/tpj.15052>
- Masi A, Leonelli F, Scognamiglio V, et al (2023) *Chlamydomonas reinhardtii*: A Factory of Nutraceutical and Food Supplements for Human Health. *Molecules* 28:1185. <https://doi.org/10.3390/molecules28031185>
- Maxwell K, Johnson GN (2000) Chlorophyll fluorescence—a practical guide. *J Exp Bot* 51:659–668. <https://doi.org/10.1093/jxb/51.345.659>
- McFadden GI (2001) Chloroplast Origin and Integration1. *Plant Physiol* 125:50–53. <https://doi.org/10.1104/pp.125.1.50>
- McKim SM, Durnford DG (2006) Translational regulation of light-harvesting complex expression during photoacclimation to high-light in *Chlamydomonas reinhardtii*. *Plant Physiol Biochem* 44:857–865. <https://doi.org/10.1016/j.plaphy.2006.10.018>
- McNellis TW, von Arnim AG, Araki T, et al (1994) Genetic and molecular analysis of an allelic series of cop1 mutants suggests functional roles for the multiple protein domains. *Plant Cell* 6:487–500. <https://doi.org/10.1105/tpc.6.4.487>
- Meagher E, Rangarikitphoti P, Faridi B, et al (2021) Photoacclimation to high-light stress in *Chlamydomonas reinhardtii* during conditional senescence relies on generating pH-dependent, high-quenching centres. *Plant Physiol Biochem* 158:136–145. <https://doi.org/10.1016/j.plaphy.2020.12.002>
- Merchant SS, Prochnik SE, Vallon O, et al (2007) The *Chlamydomonas* genome reveals the evolution of key animal and plant functions. *Science* 318:245–250. <https://doi.org/10.1126/science.1143609>
- Meyer G, Kloppstech K (1984) A rapidly light-induced chloroplast protein with a high turnover coded for by pea nuclear DNA. *Eur J Biochem* 138:201–207. <https://doi.org/10.1111/j.1432-1033.1984.tb07900.x>
- Mittag M, Kiaulehn S, Johnson CH (2005) The Circadian Clock in *Chlamydomonas reinhardtii*. What Is It For? What Is It Similar To? *Plant Physiol* 137:399–409. <https://doi.org/10.1104/pp.104.052415>
- Mockler T, Yang H, Yu X, et al (2003) Regulation of photoperiodic flowering by *Arabidopsis* photoreceptors. *Proc Natl Acad Sci* 100:2140–2145. <https://doi.org/10.1073/pnas.0437826100>
- Montané M-H, Kloppstech K (2000) The family of light-harvesting-related proteins (LHCs, ELIPs, HLIPs): was the harvesting of light their primary function? *Gene* 258:1–8. [https://doi.org/10.1016/S0378-1119\(00\)00413-3](https://doi.org/10.1016/S0378-1119(00)00413-3)
- Müller N, Wenzel S, Zou Y, et al (2017) A Plant Cryptochrome Controls Key Features of the *Chlamydomonas* Circadian Clock and Its Life Cycle. *Plant Physiol* 174:185–201. <https://doi.org/10.1104/pp.17.00349>

- Müller P, Li X-P, Niyogi KK (2001) Non-Photochemical Quenching. A Response to Excess Light Energy1. *Plant Physiol* 125:1558–1566. <https://doi.org/10.1104/pp.125.4.1558>
- Murata N, Takahashi S, Nishiyama Y, Allakhverdiev SI (2007) Photoinhibition of photosystem II under environmental stress. *Biochim Biophys Acta BBA - Bioenerg* 1767:414–421. <https://doi.org/10.1016/j.bbabbio.2006.11.019>
- Nagel G, Ollig D, Fuhrmann M, et al (2002) Channelrhodopsin-1: A Light-Gated Proton Channel in Green Algae. *Science* 296:2395–2398. <https://doi.org/10.1126/science.1072068>
- Nawrocki WJ, Liu X, Croce R (2020) Chlamydomonas reinhardtii Exhibits De Facto Constitutive NPQ Capacity in Physiologically Relevant Conditions. *Plant Physiol* 182:472–479. <https://doi.org/10.1104/pp.19.00658>
- Nelson N, Yocum CF (2006) Structure and Function of Photosystems I and II. *Annu Rev Plant Biol* 57:521–565. <https://doi.org/10.1146/annurev.arplant.57.032905.105350>
- Nilkens M, Kress E, Lambrev P, et al (2010) Identification of a slowly inducible zeaxanthin-dependent component of non-photochemical quenching of chlorophyll fluorescence generated under steady-state conditions in Arabidopsis. *Biochim Biophys Acta BBA - Bioenerg* 1797:466–475. <https://doi.org/10.1016/j.bbabbio.2010.01.001>
- Niyogi KK (1999) PHOTOPROTECTION REVISITED: Genetic and Molecular Approaches. *Annu Rev Plant Physiol Plant Mol Biol* 50:333–359. <https://doi.org/10.1146/annurev.arplant.50.1.333>
- Niyogi KK, Truong TB (2013) Evolution of flexible non-photochemical quenching mechanisms that regulate light harvesting in oxygenic photosynthesis. *Curr Opin Plant Biol* 16:307–314. <https://doi.org/10.1016/j.pbi.2013.03.011>
- Nozue K, Kanegae T, Imaizumi T, et al (1998) A phytochrome from the fern *Adiantum* with features of the putative photoreceptor NPH1. *Proc Natl Acad Sci U S A* 95:15826–15830. <https://doi.org/10.1073/pnas.95.26.15826>
- Ohgishi M, Saji K, Okada K, Sakai T (2004) Functional analysis of each blue light receptor, cry1, cry2, phot1, and phot2, by using combinatorial multiple mutants in Arabidopsis. *Proc Natl Acad Sci U S A* 101:2223–2228. <https://doi.org/10.1073/pnas.0305984101>
- Okajima K (2016) Molecular mechanism of phototropin light signaling. *J Plant Res* 129:149–157. <https://doi.org/10.1007/s10265-016-0783-6>
- Onodera A, Kong S-G, Doi M, et al (2005) Phototropin from *Chlamydomonas reinhardtii* is Functional in Arabidopsis thaliana. *Plant Cell Physiol* 46:367–374. <https://doi.org/10.1093/pcp/pci037>

- Oravecz A, Baumann A, Máté Z, et al (2006) CONSTITUTIVELY PHOTOMORPHOGENIC1 Is Required for the UV-B Response in Arabidopsis. *Plant Cell* 18:1975–1990. <https://doi.org/10.1105/tpc.105.040097>
- Ordoñez-Herrera N, Fackendahl P, Yu X, et al (2015) A cop1 spa Mutant Deficient in COP1 and SPA Proteins Reveals Partial Co-Action of COP1 and SPA during Arabidopsis Post-Embryonic Development and Photomorphogenesis. *Mol Plant* 8:479–481. <https://doi.org/10.1016/j.molp.2014.11.026>
- Osterlund MT, Hardtke CS, Wei N, Deng XW (2000) Targeted destabilization of HY5 during light-regulated development of Arabidopsis. *Nature* 405:462–466. <https://doi.org/10.1038/35013076>
- Pedron L, Baldi P, Hietala AM, La Porta N (2009) Genotype-specific regulation of cold-responsive genes in cypress (*Cupressus sempervirens* L.). *Gene* 437:45–53. <https://doi.org/10.1016/j.gene.2008.12.012>
- Peers G, Truong TB, Ostendorf E, et al (2009) An ancient light-harvesting protein is critical for the regulation of algal photosynthesis. *Nature* 462:518–521. <https://doi.org/10.1038/nature08587>
- Petroutsos D, Busch A, Janßen I, et al (2011) The Chloroplast Calcium Sensor CAS Is Required for Photoacclimation in *Chlamydomonas reinhardtii*. *Plant Cell* 23:2950–2963. <https://doi.org/10.1105/tpc.111.087973>
- Petroutsos D, Tokutsu R, Maruyama S, et al (2016) A blue-light photoreceptor mediates the feedback regulation of photosynthesis. *Nature* 537:563–566. <https://doi.org/10.1038/nature19358>
- Plücken H, Müller B, Grohmann D, et al (2002) The HCF136 protein is essential for assembly of the photosystem II reaction center in *Arabidopsis thaliana*. *FEBS Lett* 532:85–90. [https://doi.org/10.1016/S0014-5793\(02\)03634-7](https://doi.org/10.1016/S0014-5793(02)03634-7)
- Podolec R, Demarsy E, Ulm R (2021) Perception and Signaling of Ultraviolet-B Radiation in Plants. *Annu Rev Plant Biol* 72:793–822. <https://doi.org/10.1146/annurev-arplant-050718-095946>
- Podolec R, Ulm R (2018) Photoreceptor-mediated regulation of the COP1/SPA E3 ubiquitin ligase. *Curr Opin Plant Biol* 45:18–25. <https://doi.org/10.1016/j.pbi.2018.04.018>
- Pokorny R, Klar T, Hennecke U, et al (2008) Recognition and repair of UV lesions in loop structures of duplex DNA by DASH-type cryptochrome. *Proc Natl Acad Sci* 105:21023–21027. <https://doi.org/10.1073/pnas.0805830106>
- Ponnu J, Hoecker U (2022) Signaling Mechanisms by Arabidopsis Cryptochromes. *Front Plant Sci* 13:844714. <https://doi.org/10.3389/fpls.2022.844714>
- Pötter E, Kloppstech K (1993) Effects of light stress on the expression of early light-inducible proteins in barley. *Eur J Biochem* 214:779–786. <https://doi.org/10.1111/j.1432-1033.1993.tb17980.x>

- Prasad A, Ferretti U, Sedlářová M, Pospíšil P (2016) Singlet oxygen production in *Chlamydomonas reinhardtii* under heat stress. *Sci Rep* 6:20094. <https://doi.org/10.1038/srep20094>
- Prasad A, Sedlářová M, Pospíšil P (2018) Singlet oxygen imaging using fluorescent probe Singlet Oxygen Sensor Green in photosynthetic organisms. *Sci Rep* 8:13685. <https://doi.org/10.1038/s41598-018-31638-5>
- Putterill J, Robson F, Lee K, et al (1995) The CONSTANS gene of arabidopsis promotes flowering and encodes a protein showing similarities to zinc finger transcription factors. *Cell* 80:847–857. [https://doi.org/10.1016/0092-8674\(95\)90288-0](https://doi.org/10.1016/0092-8674(95)90288-0)
- Quail PH (2010) Phytochromes. *Curr Biol* CB 20:R504–R507. <https://doi.org/10.1016/j.cub.2010.04.014>
- Rai N, Neugart S, Yan Y, et al (2019) How do cryptochromes and UVR8 interact in natural and simulated sunlight? *J Exp Bot* 70:4975–4990. <https://doi.org/10.1093/jxb/erz236>
- Ranjan A, Dickopf S, Ullrich KK, et al (2014) Functional analysis of COP1 and SPA orthologs from *Physcomitrella* and rice during photomorphogenesis of transgenic *Arabidopsis* reveals distinct evolutionary conservation. *BMC Plant Biol* 14:178. <https://doi.org/10.1186/1471-2229-14-178>
- Raven JA, Geider RJ (2003) Adaptation, Acclimation and Regulation in Algal Photosynthesis. In: Larkum AWD, Douglas SE, Raven JA (eds) *Photosynthesis in Algae*. Springer Netherlands, Dordrecht, pp 385–412
- Redekop P, Rothhausen N, Rothhausen N, et al (2020) PsbS contributes to photoprotection in *Chlamydomonas reinhardtii* independently of energy dissipation. *Biochim Biophys Acta BBA - Bioenerg* 1861:148183. <https://doi.org/10.1016/j.bbabi.2020.148183>
- Redekop P, Sanz-Luque E, Yuan Y, et al (2021) Transcriptional regulation of photoprotection in dark-to-light transition - more than just a matter of excess light energy. *bioRxiv*
- Rizzini L, Favory J-J, Cloix C, et al (2011) Perception of UV-B by the *Arabidopsis* UVR8 Protein. *Science* 332:103–106. <https://doi.org/10.1126/science.1200660>
- Roach T, Baur T, Stöggel W, Krieger-Liszkay A (2017) *Chlamydomonas reinhardtii* responding to high light: a role for 2-propenal (acrolein). *Physiol Plant* 161:75–87. <https://doi.org/10.1111/ppl.12567>
- Roach T, Na CS, Stöggel W, Krieger-Liszkay A (2020) The non-photochemical quenching protein LHCSR3 prevents oxygen-dependent photoinhibition in *Chlamydomonas reinhardtii*. *J Exp Bot* 71:2650–2660. <https://doi.org/10.1093/jxb/eraa022>
- Robson F, Costa MMR, Hepworth SR, et al (2001) Functional importance of conserved domains in the flowering-time gene CONSTANS demonstrated by analysis of

- mutant alleles and transgenic plants. *Plant J* 28:619–631. <https://doi.org/10.1046/j.1365-313x.2001.01163.x>
- Rochaix J-D, Bassi R (2019) LHC-like proteins involved in stress responses and biogenesis/repair of the photosynthetic apparatus. *Biochem J* 476:581–593. <https://doi.org/10.1042/BCJ20180718>
- Rockwell NC, Su Y-S, Lagarias JC (2006) PHYTOCHROME STRUCTURE AND SIGNALING MECHANISMS. *Annu Rev Plant Biol* 57:837–858. <https://doi.org/10.1146/annurev.arplant.56.032604.144208>
- Rossini S, Casazza AP, Engelmann ECM, et al (2006) Suppression of Both ELIP1 and ELIP2 in Arabidopsis Does Not Affect Tolerance to Photoinhibition and Photooxidative Stress. *Plant Physiol* 141:1264–1273. <https://doi.org/10.1104/pp.106.083055>
- Rredhi A, Petersen J, Schubert M, et al (2021) DASH cryptochrome 1, a UV-A receptor, balances the photosynthetic machinery of *Chlamydomonas reinhardtii*. *New Phytol* 232:610–624. <https://doi.org/10.1111/nph.17603>
- Ruban AV, Johnson MP (2009) Dynamics of higher plant photosystem cross-section associated with state transitions. *Photosynth Res* 99:173–183. <https://doi.org/10.1007/s11120-008-9387-x>
- Ruiz-Sola MÁ, Flori S, Yuan Y, et al (2021) Photoprotection is regulated by light-independent CO<sub>2</sub> availability. *Plant Biology*
- Saijo Y, Sullivan JA, Wang H, et al (2003) The COP1–SPA1 interaction defines a critical step in phytochrome A-mediated regulation of HY5 activity. *Genes Dev* 17:2642–2647. <https://doi.org/10.1101/gad.1122903>
- Sakai T, Kagawa T, Kasahara M, et al (2001) Arabidopsis *nph1* and *npl1*: Blue light receptors that mediate both phototropism and chloroplast relocation. *Proc Natl Acad Sci* 98:6969–6974. <https://doi.org/10.1073/pnas.101137598>
- Sakamoto K, Briggs WR (2002) Cellular and subcellular localization of phototropin 1. *Plant Cell* 14:1723–1735. <https://doi.org/10.1105/tpc.003293>
- Sasso S, Stibor H, Mittag M, Grossman AR (2018) From molecular manipulation of domesticated *Chlamydomonas reinhardtii* to survival in nature. *eLife* 7:. <https://doi.org/10.7554/eLife.39233>
- Schierenbeck L, Ries D, Rogge K, et al (2015) Fast forward genetics to identify mutations causing a high light tolerant phenotype in *Chlamydomonas reinhardtii* by whole-genome-sequencing. *BMC Genomics* 16:57. <https://doi.org/10.1186/s12864-015-1232-y>
- Schmidt M, Geßner G, Luff M, et al (2006) Proteomic Analysis of the Eyespot of *Chlamydomonas reinhardtii* Provides Novel Insights into Its Components and Tactic Movements. *Plant Cell* 18:1908–1930. <https://doi.org/10.1105/tpc.106.041749>

- Schubert M, Petersson UA, Haas BJ, et al (2002) Proteome Map of the Chloroplast Lumen of *Arabidopsis thaliana* \*. *J Biol Chem* 277:8354–8365. <https://doi.org/10.1074/jbc.M108575200>
- Scranton MA, Ostrand JT, Fields FJ, Mayfield SP (2015) *Chlamydomonas* as a model for biofuels and bio-products production. *Plant J* 82:523–531. <https://doi.org/10.1111/tpj.12780>
- Selby CP, Sancar A (2006) A cryptochrome/photolyase class of enzymes with single-stranded DNA-specific photolyase activity. *Proc Natl Acad Sci* 103:17696–17700. <https://doi.org/10.1073/pnas.0607993103>
- Seydoux C (2020) Regulation of photosynthesis by a potassium transporter in the diatom *Phaeodactylum tricornutum*. PhD thesis, Université Grenoble Alpes
- Shao K, Zhang X, Li X, et al (2020) The oligomeric structures of plant cryptochromes. *Nat Struct Mol Biol* 27:480–488. <https://doi.org/10.1038/s41594-020-0420-x>
- Shimosaka E, Sasanuma T, Handa H (1999) A Wheat Cold-Regulated cDNA Encoding an Early Light-Inducible Protein (ELIP): Its Structure, Expression and Chromosomal Location. *Plant Cell Physiol* 40:319–325. <https://doi.org/10.1093/oxfordjournals.pcp.a029544>
- Shin B-S, Lee J-H, Lee J-H, et al (2004) Circadian regulation of rice (*Oryza sativa* L.) *CONSTANS*-like gene transcripts. *Mol Cells* 17:10–16
- Sohbat ZI (2022) Non-photochemical quenching of chlorophyll fluorescence and its components – recent advances. *Journal of Life Sciences & Biomedicine Journal of Life Sciences&Biomedicine*:76–83
- Song YH, Shim JS, Kinmonth-Schultz HA, Imaizumi T (2015) Photoperiodic Flowering: Time Measurement Mechanisms in Leaves. *Annu Rev Plant Biol* 66:441–464. <https://doi.org/10.1146/annurev-arplant-043014-115555>
- Song Z, Bian Y, Liu J, et al (2020) B-box proteins: Pivotal players in light-mediated development in plants. *J Integr Plant Biol* 62:1293–1309. <https://doi.org/10.1111/jipb.12935>
- Soriano G, Cloix C, Heilmann M, et al (2018) Evolutionary conservation of structure and function of the UVR8 photoreceptor from the liverwort *Marchantia polymorpha* and the moss *Physcomitrella patens*. *New Phytol* 217:151–162. <https://doi.org/10.1111/nph.14767>
- Stracke R, Favory J-J, Gruber H, et al (2010) The *Arabidopsis* bZIP transcription factor HY5 regulates expression of the PFG1/MYB12 gene in response to light and ultraviolet-B radiation. *Plant Cell Environ* 33:88–103. <https://doi.org/10.1111/j.1365-3040.2009.02061.x>
- Strenkert D, Schmollinger S, Gallaher SD, et al (2019) Multiomics resolution of molecular events during a day in the life of *Chlamydomonas*. *Proc Natl Acad Sci* 116:2374–2383. <https://doi.org/10.1073/pnas.1815238116>

- Suárez-López P, Wheatley K, Robson F, et al (2001) CONSTANS mediates between the circadian clock and the control of flowering in *Arabidopsis*. *Nature* 410:1116–1120. <https://doi.org/10.1038/35074138>
- Suetsugu N, Mittmann F, Wagner G, et al (2005) A chimeric photoreceptor gene, NEOCHROME, has arisen twice during plant evolution. *Proc Natl Acad Sci U S A* 102:13705–13709. <https://doi.org/10.1073/pnas.0504734102>
- Suetsugu N, Wada M (2013) Evolution of Three LOV Blue Light Receptor Families in Green Plants and Photosynthetic Stramenopiles: Phototropin, ZTL/FKF1/LKP2 and Aureochrome. *Plant Cell Physiol* 54:8–23. <https://doi.org/10.1093/pcp/pcs165>
- Sullivan S, Waksman T, Paliogianni D, et al (2021) Regulation of plant phototropic growth by NPH3/RPT2-like substrate phosphorylation and 14-3-3 binding. *Nat Commun* 12:6129. <https://doi.org/10.1038/s41467-021-26333-5>
- Takahashi S, Badger MR (2011) Photoprotection in plants: a new light on photosystem II damage. *Trends Plant Sci* 16:53–60. <https://doi.org/10.1016/j.tplants.2010.10.001>
- Takemiya A, Inoue S-I, Doi M, et al (2005) Phototropins promote plant growth in response to blue light in low light environments. *Plant Cell* 17:1120–1127. <https://doi.org/10.1105/tpc.104.030049>
- Takemiya A, Sugiyama N, Fujimoto H, et al (2013) Phosphorylation of BLUS1 kinase by phototropins is a primary step in stomatal opening. *Nat Commun* 4:1–8. <https://doi.org/10.1038/ncomms3094>
- Teramoto H, Ishii A, Kimura Y, et al (2006) Action spectrum for expression of the high intensity light-inducible Lhc-like gene Lhl4 in the green alga *Chlamydomonas reinhardtii*. *Plant Cell Physiol* 47:419–425. <https://doi.org/10.1093/pcp/pcj009>
- Tibiletti T, Auroy P, Peltier G, Caffarri S (2016) *Chlamydomonas reinhardtii* PsbS Protein Is Functional and Accumulates Rapidly and Transiently under High Light. *Plant Physiol* 171:2717–2730. <https://doi.org/10.1104/pp.16.00572>
- Tilbrook K, Arongaus AB, Binkert M, et al (2013) The UVR8 UV-B Photoreceptor: Perception, Signaling and Response. *Arab Book Am Soc Plant Biol* 11. <https://doi.org/10.1199/tab.0164>
- Tilbrook K, Dubois M, Crocco CD, et al (2016a) UV-B Perception and Acclimation in *Chlamydomonas reinhardtii*. *Plant Cell* 28:966–983. <https://doi.org/10.1105/tpc.15.00287>
- Tilbrook K, Dubois M, Crocco CD, et al (2016b) UV-B Perception and Acclimation in *Chlamydomonas reinhardtii*. *Plant Cell* 28:966–983. <https://doi.org/10.1105/tpc.15.00287>
- Tissot N, Ulm R (2020) Cryptochrome-mediated blue-light signalling modulates UVR8 photoreceptor activity and contributes to UV-B tolerance in *Arabidopsis*. *Nat Commun* 11:1–10. <https://doi.org/10.1038/s41467-020-15133-y>

- Tokutsu R, Fujimura-Kamada K, Matsuo T, et al (2019) The CONSTANS flowering complex controls the protective response of photosynthesis in the green alga *Chlamydomonas*. *Nat Commun* 10:. <https://doi.org/10.1038/s41467-019-11989-x>
- Tokutsu R, Minagawa J (2013) Energy-dissipative supercomplex of photosystem II associated with LHCSR3 in *Chlamydomonas reinhardtii*. *Proc Natl Acad Sci* 110:10016–10021. <https://doi.org/10.1073/pnas.1222606110>
- Tossi V, Lamattina L, Jenkins GI, Cassia RO (2014) Ultraviolet-B-Induced Stomatal Closure in *Arabidopsis* Is Regulated by the UV RESISTANCE LOCUS8 Photoreceptor in a Nitric Oxide-Dependent Mechanism. *Plant Physiol* 164:2220–2230. <https://doi.org/10.1104/pp.113.231753>
- Trippens J, Greiner A, Schellwat J, et al (2012) Phototropin Influence on Eyespot Development and Regulation of Phototactic Behavior in *Chlamydomonas reinhardtii*. *Plant Cell* 24:4687–4702. <https://doi.org/10.1105/tpc.112.103523>
- Tzvetkova-Chevolleau T, Franck F, Alawady AE, et al (2007) The light stress-induced protein ELIP2 is a regulator of chlorophyll synthesis in *Arabidopsis thaliana*. *Plant J* 50:795–809. <https://doi.org/10.1111/j.1365-313X.2007.03090.x>
- Uljon S, Xu X, Durzynska I, et al (2016) Structural Basis for Substrate Selectivity of the E3 Ligase COP1. *Structure* 24:687–696. <https://doi.org/10.1016/j.str.2016.03.002>
- Ulm R, Baumann A, Oravec A, et al (2004) Genome-wide analysis of gene expression reveals function of the bZIP transcription factor HY5 in the UV-B response of *Arabidopsis*. *Proc Natl Acad Sci* 101:1397–1402. <https://doi.org/10.1073/pnas.0308044100>
- Valverde F (2011) CONSTANS and the evolutionary origin of photoperiodic timing of flowering. *J Exp Bot* 62:2453–2463. <https://doi.org/10.1093/jxb/erq449>
- van den Hoek H, Klena N, Jordan MA, et al (2022) In situ architecture of the ciliary base reveals the stepwise assembly of intraflagellar transport trains. *Science* 377:543–548. <https://doi.org/10.1126/science.abm6704>
- Vandenbussche F, Tilbrook K, Fierro AC, et al (2014) Photoreceptor-Mediated Bending towards UV-B in *Arabidopsis*. *Mol Plant* 7:1041–1052. <https://doi.org/10.1093/mp/ssu039>
- Vass I-Z, Kós PB, Knoppová J, et al (2014) The cry-DASH cryptochrome encoded by the *sll1629* gene in the cyanobacterium *Synechocystis* PCC 6803 is required for Photosystem II repair. *J Photochem Photobiol B* 130:318–326. <https://doi.org/10.1016/j.jphotobiol.2013.12.006>
- Veluchamy S, Rollins JA (2008) A CRY-DASH-type photolyase/cryptochrome from *Sclerotinia sclerotiorum* mediates minor UV-A-specific effects on development. *Fungal Genet Biol* 45:1265–1276. <https://doi.org/10.1016/j.fgb.2008.06.004>

- Virtanen O, Khorobrykh S, Tyystjärvi E (2021) Acclimation of *Chlamydomonas reinhardtii* to extremely strong light. *Photosynth Res* 147:91–106. <https://doi.org/10.1007/s11120-020-00802-2>
- Wada M, Kagawa T, Sato Y (2003) Chloroplast movement. *Annu Rev Plant Biol* 54:455–468. <https://doi.org/10.1146/annurev.arplant.54.031902.135023>
- Wang Q, Lin C (2020) Mechanisms of Cryptochrome-Mediated Photoresponses in Plants. *Annu Rev Plant Biol* 71:103–129. <https://doi.org/10.1146/annurev-arplant-050718-100300>
- Whitmarsh J, Govindjee (1999) The Photosynthetic Process. In: Singhal GS, Renger G, Sopory SK, et al. (eds) *Concepts in Photobiology: Photosynthesis and Photomorphogenesis*. Springer Netherlands, Dordrecht, pp 11–51
- Wieczorek S, Combes F, Lazar C, et al (2017) DAPAR & ProStaR: software to perform statistical analyses in quantitative discovery proteomics. *Bioinforma Oxf Engl* 33:135–136. <https://doi.org/10.1093/bioinformatics/btw580>
- Witman GB (1993) *Chlamydomonas phototaxis*. *Trends Cell Biol* 3:403–408. [https://doi.org/10.1016/0962-8924\(93\)90091-E](https://doi.org/10.1016/0962-8924(93)90091-E)
- Wu D, Hu Q, Yan Z, et al (2012) Structural basis of ultraviolet-B perception by UVR8. *Nature* 484:214–219. <https://doi.org/10.1038/nature10931>
- Wu G, Spalding EP (2007) Separate functions for nuclear and cytoplasmic cryptochrome 1 during photomorphogenesis of *Arabidopsis* seedlings. *Proc Natl Acad Sci* 104:18813–18818. <https://doi.org/10.1073/pnas.0705082104>
- Xiao L, Yang G, Zhang L, et al (2015) The resurrection genome of *Boea hygrometrica*: A blueprint for survival of dehydration. *Proc Natl Acad Sci* 112:5833–5837. <https://doi.org/10.1073/pnas.1505811112>
- Xu X, Paik I, Zhu L, Huq E (2015) Illuminating Progress in Phytochrome-Mediated Light Signaling Pathways. *Trends Plant Sci* 20:641–650. <https://doi.org/10.1016/j.tplants.2015.06.010>
- YAMAWAKI S, YAMASHINO T, NAKANISHI H, MIZUNO T (2011) Functional Characterization of HY5 Homolog Genes Involved in Early Light-Signaling in *Physcomitrella patens*. *Biosci Biotechnol Biochem* 75:1533–1539. <https://doi.org/10.1271/bbb.110219>
- Yang H-Q, Wu Y-J, Tang R-H, et al (2000) The C Termini of *Arabidopsis* Cryptochromes Mediate a Constitutive Light Response. *Cell* 103:815–827. [https://doi.org/10.1016/S0092-8674\(00\)00184-7](https://doi.org/10.1016/S0092-8674(00)00184-7)
- Yang Y, Yang X, Jang Z, et al (2018) UV RESISTANCE LOCUS 8 From *Chrysanthemum morifolium* Ramat (*CmUVR8*) Plays Important Roles in UV-B Signal Transduction and UV-B-Induced Accumulation of Flavonoids. *Front Plant Sci* 9:955. <https://doi.org/10.3389/fpls.2018.00955>

- Yi C, Deng XW (2005) COP1 – from plant photomorphogenesis to mammalian tumorigenesis. *Trends Cell Biol* 15:618–625. <https://doi.org/10.1016/j.tcb.2005.09.007>
- Yin R, Ulm R (2017) How plants cope with UV-B: from perception to response. *Curr Opin Plant Biol* 37:42–48. <https://doi.org/10.1016/j.pbi.2017.03.013>
- Zarter CR, Adams III WW, Ebbert V, et al (2006) Winter down-regulation of intrinsic photosynthetic capacity coupled with up-regulation of Elip-like proteins and persistent energy dissipation in a subalpine forest. *New Phytol* 172:272–282. <https://doi.org/10.1111/j.1469-8137.2006.01815.x>
- Zhao C, Mao K, You C-X, et al (2016) Molecular cloning and functional analysis of a UV-B photoreceptor gene, MdUVR8 (UV Resistance Locus 8), from apple. *Plant Sci Int J Exp Plant Biol* 247:115–126. <https://doi.org/10.1016/j.plantsci.2016.03.006>
- Zhu D, Maier A, Lee J-H, et al (2008) Biochemical Characterization of Arabidopsis Complexes Containing CONSTITUTIVELY PHOTOMORPHOGENIC1 and SUPPRESSOR OF PHYA Proteins in Light Control of Plant Development. *Plant Cell* 20:2307–2323. <https://doi.org/10.1105/tpc.107.056580>
- Zhu S-H, Green BR (2010) Photoprotection in the diatom *Thalassiosira pseudonana*: Role of LI818-like proteins in response to high light stress. *Biochim Biophys Acta BBA - Bioenerg* 1797:1449–1457. <https://doi.org/10.1016/j.bbabi.2010.04.003>
- Zobell O, Coupland G, Reiss B (2005) The Family of CONSTANS-Like Genes in *Physcomitrella patens*. *Plant Biol* 266–275. <https://doi.org/10.1055/s-2005-865621>
- Zones JM, Blaby IK, Merchant SS, Umen JG (2015) High-Resolution Profiling of a Synchronized Diurnal Transcriptome from *Chlamydomonas reinhardtii* Reveals Continuous Cell and Metabolic Differentiation. *Plant Cell* 27:2743–2769. <https://doi.org/10.1105/tpc.15.00498>
- Zou Y, Wenzel S, Müller N, et al (2017) An Animal-Like Cryptochrome Controls the *Chlamydomonas* Sexual Cycle. *Plant Physiol* 174:1334–1347. <https://doi.org/10.1104/pp.17.00493>
- Zuo Z, Liu H, Liu B, et al (2011) Blue Light-Dependent Interaction of CRY2 with SPA1 Regulates COP1 activity and Floral Initiation in Arabidopsis. *Curr Biol* 21:841–847. <https://doi.org/10.1016/j.cub.2011.03.048>



# SYNTHESE EN FRANÇAIS

La lignée verte est constituée d'une grande diversité de végétaux, à la fois plantes et algues, contenant tous un plaste riche en pigments chlorophylliens. Parmi ces organismes, on retrouve notamment plusieurs modèles utilisés en biologie végétale tels que la plante à fleurs *Arabidopsis thaliana*, la bryophyte *Physcomitrella (Physcomitrium) patens*, ou encore la micro-algue verte *Chlamydomonas reinhardtii*.

*C. reinhardtii* est l'organisme photosynthétique unicellulaire le plus étudié au monde. Il s'agit d'une algue d'eau douce biflagellée de 10 µm de diamètre environ, dont le génome est entièrement séquencé (Merchant et al., 2007). Grâce au développement d'outils et techniques d'ingénierie génétique, une banque de mutants d'insertion a été générée facilitant l'étude de la fonction d'un grand nombre de gènes(<https://www.chlamycollection.org/>) impliqués dans le métabolisme, la signalisation intracellulaire, ou encore la photosynthèse. En effet, *C. reinhardtii* est largement utilisée dans le cadre de l'étude de la photosynthèse et de son adaptation à différentes conditions environnementales, du fait de sa capacité à croître sous des intensités lumineuses variées et à faire de la mixotrophie (utilisation simultanée de la lumière et d'une source de carbone).

La photosynthèse est un métabolisme clé chez les végétaux, faisant ainsi de la lumière une source d'énergie primaire pour eux. Le fonctionnement de la photosynthèse est basé sur l'excitabilité des pigments (en particulier de la chlorophylle) présents dans l'appareil photosynthétique par les photons. Lorsque la chlorophylle (Chl) est excitée par l'énergie lumineuse, elle cherche à revenir à un état fondamentalement stable, en transférant cet excès d'énergie soit i. en l'utilisant pour alimenter la photosynthèse (photochimie), ii. en la relaxant sous forme de fluorescence, ou iii. en la dissipant sous forme de chaleur, ce qui est à la base du processus appelé Non-Photochemical Quenching (NPQ). Ces trois voies de régulation sont en compétition les unes avec les autres et leur régulation rapide est une composante essentielle de la capacité d'acclimatation des organismes photosynthétiques à leur environnement (Müller et al., 2001). L'environnement lumineux dans lesquels vivent les organismes photosynthétiques est extrêmement variable, et peut affecter leur croissance. Alors que la faible lumière (LL) peut limiter la croissance en restreignant

l'activité photosynthétique, la forte lumière (HL) peut conduire à la production d'espèces réactives de l'oxygène (ROS) et donc à la génération de stress oxydant dans les cellules (Niyogi and Truong, 2013). Dans les cas les plus extrêmes, par exemple durant un stress lumineux prolongé, la photoinhibition (qI) de l'appareil photosynthétique peut survenir, conduisant ainsi à la dégradation du photosystème II (PSII) et donc à une diminution du rendement de la photosynthèse (Aro et al., 1993; Long et al., 1994). Cependant, ce stade de photoinhibition est généralement atteint au bout d'une heure (Eberhard et al., 2008), ce qui donne aux organismes photosynthétiques le temps de mettre en place des mécanismes de photoprotection contre le stress lumineux.

Parmi ces mécanismes, le NPQ est celui qui prédomine à court terme. Plusieurs composantes ont été identifiées dans le NPQ chez les plantes, dont la principale est le quenching énergie-dépendant (qE), qui consiste en la dissipation de l'énergie lumineuse en excès sous forme de chaleur. La mise en place du qE nécessite i. l'acidification du lument et ii. l'activation de protéines effectrices du qE spécifiques (Niyogi and Truong, 2013). Chez *C. reinhardtii*, ces protéines sont inductibles par la lumière et nommées LHCSR1 et LHCSR3 (LIGHT-HARVESTING COMPLEX STRESS-RELATED). Alors que LHCSR3 est l'acteur majoritaire du qE lors d'une exposition au HL (Allorent et al., 2013; Petroutsos et al., 2016), LHCSR1 est quant à elle essentielle dans la photoprotection induite par les UV-B (Allorent et al., 2016). On retrouve également chez *C. reinhardtii* la protéine PSBS (PHOTOSYSTEM II SUBUNIT S), qui est l'acteur principal du qE chez les plantes, mais sa fonction reste à établir chez cette algue.

D'autres protéines sont également prédites pour être actrices de la photoprotection, indépendamment du NPQ. Ces protéines font parties de la famille ELIPs (EARLY LIGHT INDUCED PROTEINS), qui représente une large famille de protéines présentes chez tous les eucaryotes de la lignée verte. Leur fonction exacte chez ces organismes n'a en revanche pas encore été déterminée, mais leur inductibilité lors du stress lumineux laisse supposer qu'elles sont impliquées dans la photoprotection (Adamska, 2001; Rochaix and Bassi, 2019).

En plus d'être une source d'énergie pour le métabolisme de la cellule, la lumière est également une source d'information essentielle pour les organismes végétaux. En effet, les végétaux sont capables, grâce à un ensemble élaboré de photorécepteurs, de percevoir la couleur de la lumière et d'induire les réponses physiologiques correspondantes. Chez

la micro-algue *C. reinhardtii*, quatre familles de photorécepteurs ont été identifiées : les channelrhodopsines (ChR), les cryptochromes (CRY), la phototropine (PHOT), et UVR8 (**Fig. 1**). Les ChRs sont des photorécepteurs à la lumière verte, impliqués dans la phototaxie. Les CRYs sont des photorécepteurs à la lumière bleue, dont deux membres sont présents chez *C. reinhardtii* un animal-like (aCRY) et un plant-like (pCRY). Les CRYs sont impliqués dans des processus cellulaires très variés, allant de la régulation du rythme circadien à celle du cycle sexuel (Kottke et al., 2017). En plus des CRYs, un troisième photorécepteur bleu est trouvé chez *C. reinhardtii*, et il s'agit de PHOT qui s'avère être le photorécepteur clé impliqué dans la mise en place du NPQ en HL (Petroutsos et al., 2016). Enfin, UVR8 est le photorécepteur aux UV-B et contrôle également la mise en place du NPQ, cette fois lors d'une exposition aux UV-B (Allorent et al., 2016).

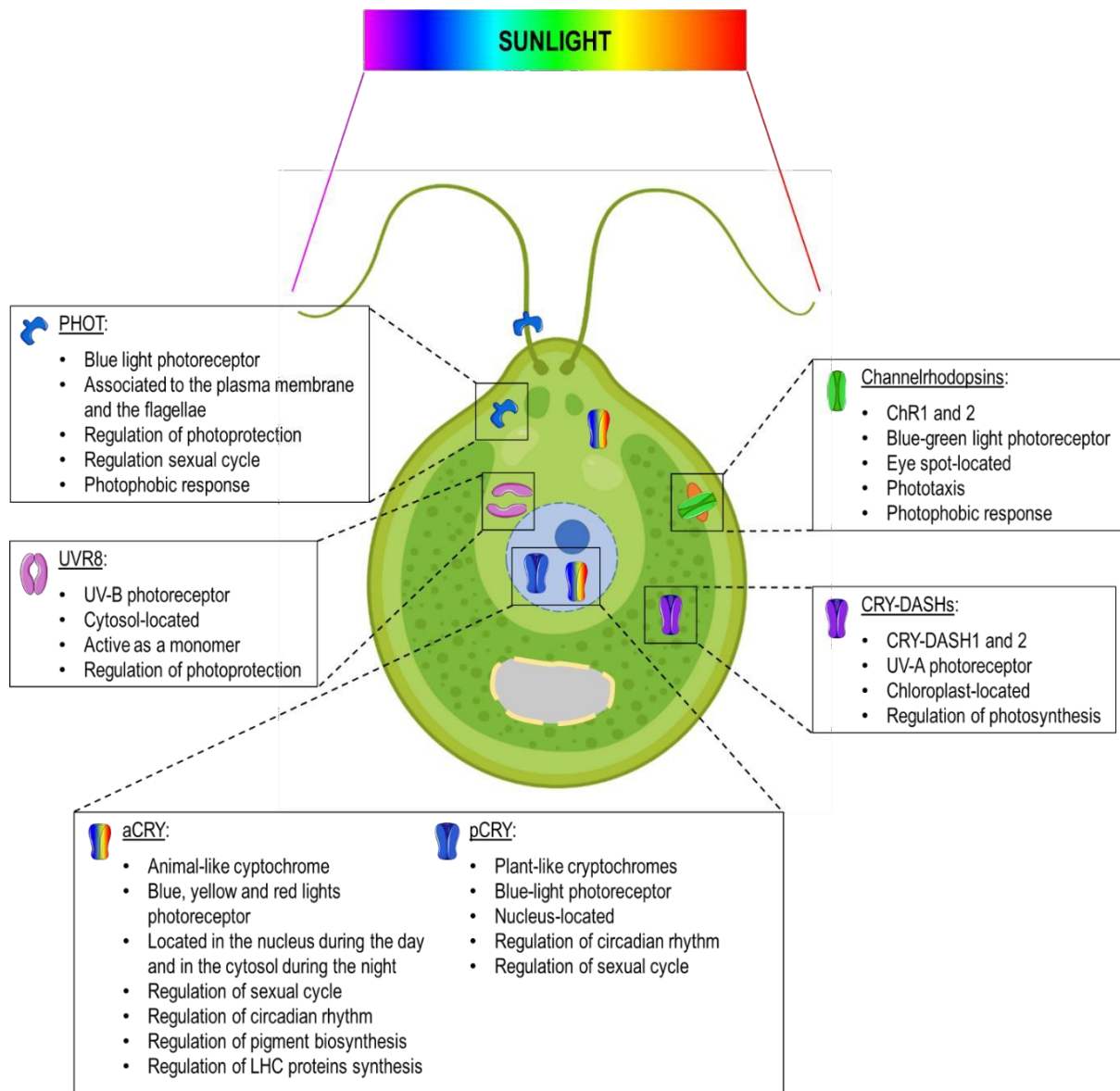


**Figure 1: Schéma résumant les différents photorécepteurs de *C. reinhardtii*, avec leur localisation intracellulaire et leurs fonctions.**

Alors que l'acclimatation à la forte lumière chez *C. reinhardtii* a déjà été largement étudiée (Allorent et al., 2013 ; Govorunova et al., 2004 ; McKim and Durnford, 2006 ; Meagher et al., 2021 ; Zones et al., 2015), l'acclimatation induite par les UV-B reste beaucoup moins bien caractérisée chez cette algue. Un transcriptome de *C. reinhardtii* exposée aux UV-B a été réalisé dans un laboratoire hôte il y a quelques années afin d'identifier les gènes induits par l'exposition à un faible niveau d'UV-B (Tilbrook et al. 2016). Les résultats de cette étude ont montré que l'exposition aux UV-B induit des changements dans l'expression de plus de 2000 gènes, dont la grande majorité est sous le contrôle d'UVR8. Cette expérience démontre également que les UV-B contrôlent une grande variété de fonctions cellulaires chez *C. reinhardtii*. Les gènes les plus induits par les UV-B sont principalement liés à la collecte de la lumière et à la régulation de la photosynthèse : acteurs du qE, ELIPs, assemblage du PSII, ... Ceci suggère que l'impact des UV-B sur le processus photosynthétique va au-delà de l'induction des protéines liées au NPQ et implique probablement une réorganisation plus globale de l'architecture de l'appareil photosynthétique et de sa capacité intrinsèque à absorber, utiliser et/ou dissiper l'énergie lumineuse.

Dans ce contexte, mon projet de thèse visait à identifier de nouveaux acteurs impliqués dans l'acclimatation de la photosynthèse aux UV-B chez *C. reinhardtii*. En utilisant des approches de laboratoire complémentaires et multidisciplinaires, ce manuscrit décrit l'identification, la régulation et la fonction d'un des acteurs primordiaux dans la réponse au stress lumineux de *C. reinhardtii* : la protéine LHL4 (LHC-LIKE 4 aka ELIP6).

Une analyse protéomique de wild type (WT) de *C. reinhardtii* exposé aux UV-B nous a permis d'identifier cette protéine LHL4, qui est fortement induite lors d'une exposition à ce type de radiations. Une modélisation de la structure de cette protéine nous a montré qu'elle présente de fortes similitudes avec les ELIPs. En effet, LHL4 possède trois hélices transmembranaires, ainsi que des motifs d'acides aminés spécifiques dans les hélices 1 et 3 qui sont connus pour être impliqués dans la liaison à la chlorophylle. En revanche, elle est très différente des protéines LHCSR impliquées dans le NPQ. De premiers résultats indiquent également que LHL4 est co-localisée avec le PSII dans la membrane des thylakoïdes, suggérant ainsi que la fonction de LHL4 soit liée à la photosynthèse.

Bien que LHL4 soit préférentiellement induite par l'exposition aux UV-B, nous avons aussi observée qu'elle est inductible par le HL, ce qui nous a laissé penser que cette protéine pouvait jouer un rôle dans la photoprotection. Nous avons également montré que l'induction de LHL4 dépend de l'intensité des UV-B à la fois au niveau des transcrits et au niveau de la protéine (**Fig. 2**).

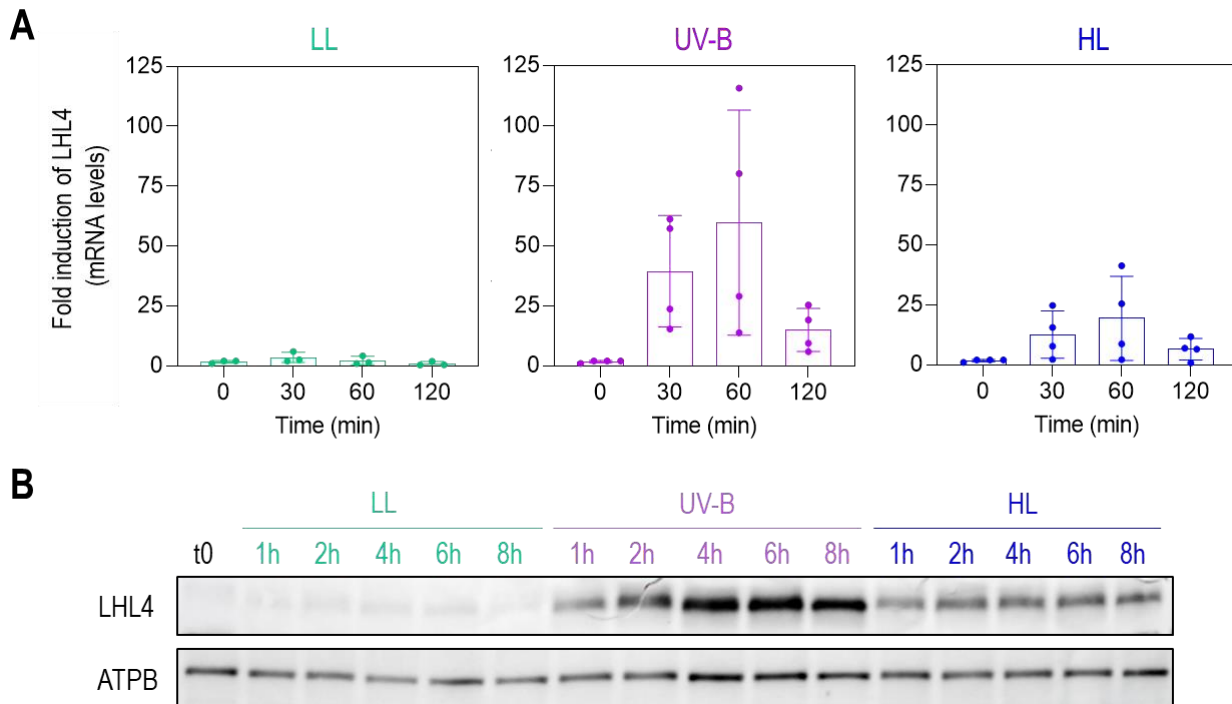


**Figure 2:** LHL4 n'est pas présente de manière constitutive dans les cellules mais s'accumule rapidement lors des expositions aux UV-B et aux HL. (A) et (B). Les cellules WT137C ont été exposées à du LL (green -  $30 \mu\text{mol photons m}^{-2} \text{s}^{-1}$ ; control condition), de l'UV-B (purple -  $30 \mu\text{mol photons m}^{-2} \text{s}^{-1}$  LL +  $0.2 \text{ mW.cm}^{-2}$  UV-B) ou du HL (blue -  $300 \mu\text{mol photons m}^{-2} \text{s}^{-1}$ ) pendant 8h et l'accumulation des transcrits LHL4 a été analysée par RT-qPCR (A) ou le niveau de protéine par immunodétection (B). ATPB est utilisé comme contrôle de charge pour les western blots.

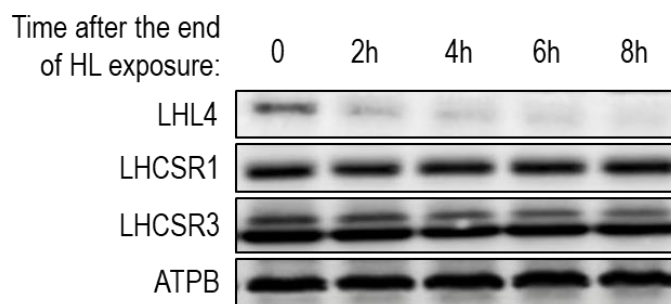


**Figure 3 :** L'accumulation de la protéine LHL4 diminue rapidement après la fin du traitement lumineux. Les cultures WT137C ont été acclimatées pendant une nuit à de faibles doses d'UV-B ( $0.08 \text{ mW.cm}^{-2}$ ) puis exposées pendant 4h à  $300 \mu\text{mol photons m}^{-2} \text{s}^{-1}$  de HL. La combinaison de ces deux traitements a induit l'accumulation des protéines LHL4 et NPQ à un niveau élevé (0). L'induction des protéines a ensuite été stoppée en plaçant les cellules en LL ( $30 \mu\text{mol photons m}^{-2} \text{s}^{-1}$ ) pendant 8 h, et les échantillons ont été récoltés après 2/4/6/8h. L'accumulation des protéines LHL4 et LHCSRs a ensuite été évaluée par immunodétection en utilisant les anticorps correspondants. La bande supérieure du blot LHCSR3 correspond à la forme phosphorylée de la protéine (Scholz et al., 2019). ATPB a été utilisé comme contrôle de charge.

En revanche, au cours de l'exposition au HL le niveau de LHL4 semble davantage stable, et régulé au niveau post-transcriptionnel. Enfin, nous avons démontré qu'après la fin du traitement lumineux (UV-B ou HL), LHL4 est rapidement dégradée dans les cellules, contrairement aux protéines NPQ LHCSR1 et LHCSR3 qui restent stables plusieurs heures dans les cellules après la fin du stimulus lumineux (**Fig. 3**).

Nous avons ensuite étudié la régulation de l'expression et du gène et de la protéine LHL4 au cours de l'exposition aux UV-B et au HL. Nous avons ainsi établi que sous les UV-B, l'expression de *LHL4* est principalement contrôlée par le photorécepteur UVR8, mais pourrait aussi dépendre légèrement des photorécepteurs à la lumière bleue aCRY et pCRY. Nous avons également montré que l'accumulation de la protéine LHL4 est contrôlée par les trois photorécepteurs bleus PHOT, aCRY, et pCRY de différentes manières : PHOT promeut son accumulation alors que aCRY et pCRY la répriment. Ce contrôle n'est pas nécessairement exercé au niveau de la transcription du gène *LHL4*.

Le facteur de transcription CONSTANS est le facteur de transcription clé dans la régulation de *LHL4*, à la fois en UV-B et en HL, au contraire de HY5 qui ne semble pas jouer de rôle dans ce processus. En revanche, HY5 pourrait moduler le niveau d'accumulation des protéines NPQ LHCSR1, LHCSR3, et PSBS en HL. Nous avons aussi pu confirmer que la convergence des voies de signalisation induites par l'UV-B et le HL chez *C. reinhardtii* se situe au niveau de l'ubiquitine ligase COP1.

Par la suite, nous nous sommes intéressés à la fonction de la protéine LHL4. Pour ce faire, nous avons généré et phénotypé un mutant KO de *LHL4*. Nous avons ainsi pu montrer que LHL4 ne module pas directement le niveau de NPQ chez *C. reinhardtii*, mais qu'elle est bien impliquée dans la photoprotection. Lorsque les cellules ont été préalablement acclimatées aux UV-B, les protéines NPQ sont induites et permettent ainsi de protéger l'appareil photosynthétique du HL. En revanche, en l'absence d'acclimatation, les cellules ne peuvent pas se protéger d'une exposition soudaine au HL et c'est dans ces conditions que le phénotype du mutant *lhl4* est observé. En effet, dans ces conditions le Fv/Fm du mutant *lhl4* est plus fortement impacté que celui du WT, suggérant ainsi que LHL4 serait nécessaire pour protéger les cellules du stress lumineux durant les premières heures, lorsque les protéines NPQ ne sont pas suffisamment accumulées dans les cellules et que le niveau de NPQ est insuffisant pour assurer une protection complète (**Fig. 4**).

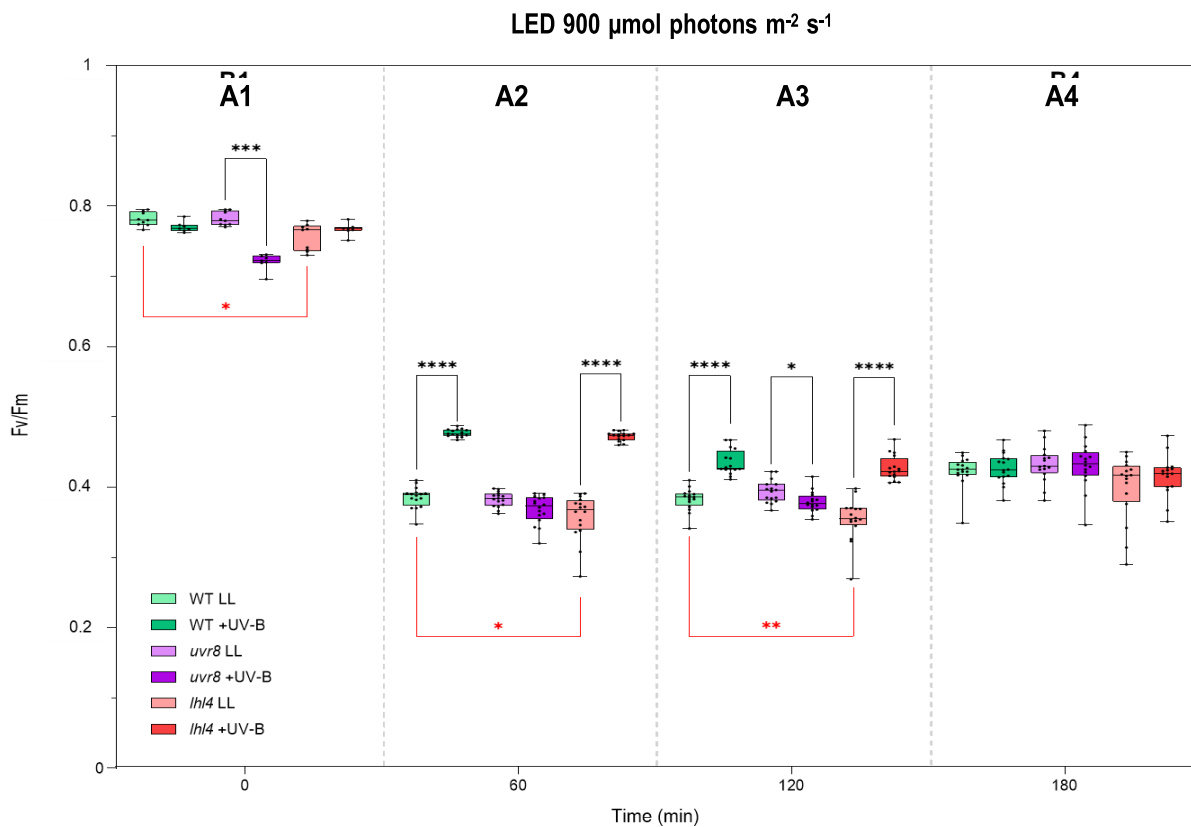


**Figure 4: LHL4 atténue la photoinhibition du PSII.** Les cellules WT137C, *uvr8* et *lhl4* ont été acclimatées (+UV-B) ou non (LL) à de faibles doses d'UV-B (30 μmol photons m<sup>-2</sup> s<sup>-1</sup> LL + 0.08 mW.cm<sup>-2</sup> UV-B) pendant 16h (0). Les cultures ont ensuite été exposées à du HL (900 μmol photons m<sup>-2</sup> s<sup>-1</sup> of white light) pendant 3h. Le Fv/Fm a ensuite été contrôlé toutes les heures. Les différences statistiques de Fv/Fm à chaque point de temps sont indiquées dans les diagrammes en boîte correspondants. Les différences entre les souches (astérisques rouges) et l'effet des différentes acclimatations (astérisques noires) ont été évalués par un test de Kolmogorov-Smirnov (\* p-value<0.05; \*\* p-value<0.01; \*\*\* p-value<0.001, \*\*\*\*p-value<0.0001; n=4 réplicats biologiques).

De plus, l'effet protecteur de LHL4 est d'autant plus important que l'intensité lumineuse augmente, et nos résultats suggèrent que cette protection serait liée à une régulation du niveau d'oxygène singulet par LHL4 au cours du stress lumineux. Finalement, nous avons aussi montré que dans le cas d'une exposition à des intensités lumineuses extrêmes, LHL4 devient nécessaire pour la survie des cellules, qu'elles aient ou non été acclimatées aux UV-B au préalable (**Fig. 5**). Il semblerait également que dans le cadre d'une exposition en lumière naturelle (soleil), LHL4 soit également plus importante pour protéger l'appareil photosynthétique, probablement du fait qu'en lumière naturelle les radiations UV-B et HL sont combinées, contrairement aux expériences pratiquées au laboratoire.

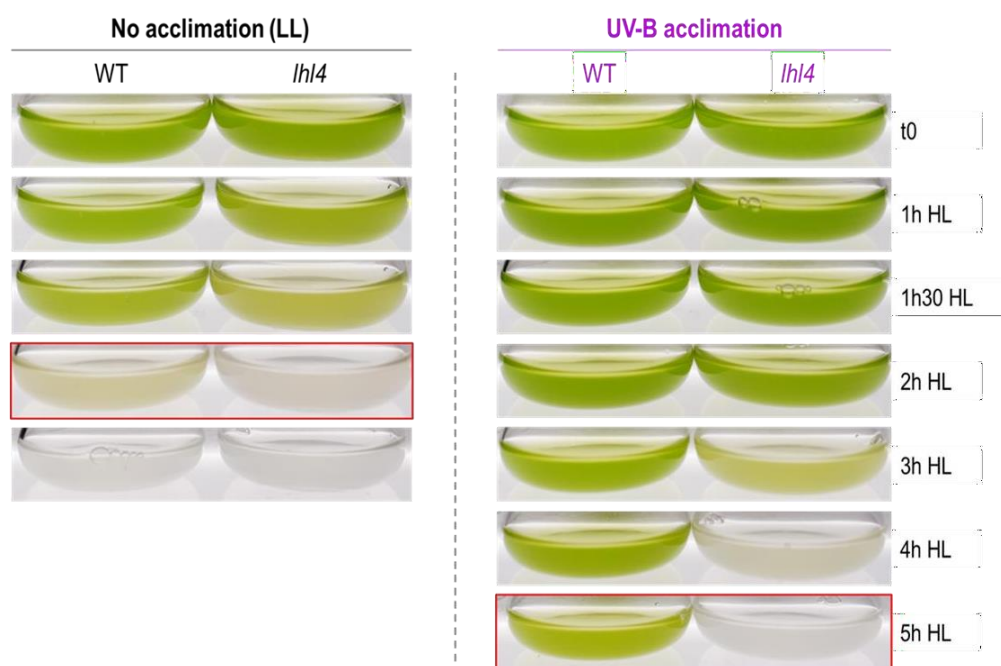


**Figure 5: Le mutant *lhl4* est photosensible.** Expérience de photobleaching réalisée sur des *Chlamydomonas* WT137C et *lhl4* acclimatés (+UV-B) ou non (LL) à de faibles doses d'UV-B ( $30 \mu\text{mol photons m}^{-2} \text{s}^{-1}$  LL +  $0.08 \text{ mW.cm}^{-2}$  UV-B) pendant 16h et ensuite exposés pendant 4h à un fort traitement HL ( $2000 \mu\text{mol photons m}^{-2} \text{s}^{-1}$ ). Les photos ont été prises régulièrement pendant l'exposition au HL. Cadre rouge : moment où la culture *lhl4* est bleachée et non la culture WT.

Au cours de cette étude, nous avons pu générer de nouvelles informations sur la voie de signalisation d'UVR8 chez *C. reinhardtii*, bien qu'elle ait déjà été caractérisée par le passé (Tilbrook et al., 2016). En particulier, notre étude a confirmé que le principal facteur de transcription dans cette voie est CONSTANS et non HY5, contrairement à ce qui semble être le cas chez *A. thaliana*. Des premiers résultats avaient déjà été publiés concernant le rôle clé de CONSTANS dans la régulation de la photoprotection chez *C. reinhardtii* (Gabilly et al., 2019; Tokutsu et al., 2019), mais nous avons pu montrer ici que CONSTANS est un

facteur de transcription clé des UV-B à l'échelle du génome, bien que certains des gènes régulés par les UV-B soient également contrôlés par HY5.

LHL4 est la première ELIP caractérisée dans le contexte de la réponse aux UV-B chez *C. reinhardtii*, et elle nous a permis d'élargir nos connaissances sur la photoprotection induite par les UV-B chez cette microalgue, ainsi que sur celle induite par le HL. En outre, ce travail a amélioré notre compréhension de la régulation des cascades de signalisation intracellulaires induites par les UV-B et HL chez *C. reinhardtii*, et a ainsi ouvert de nouvelles questions concernant la nature exacte des synergies existant entre les différentes voies de signalisation induites par les différentes couleurs au sein des organismes photosynthétiques (**Fig. 6**).

Tous les résultats présentés dans ce manuscrit seront résumés dans une publication en cours de rédaction.

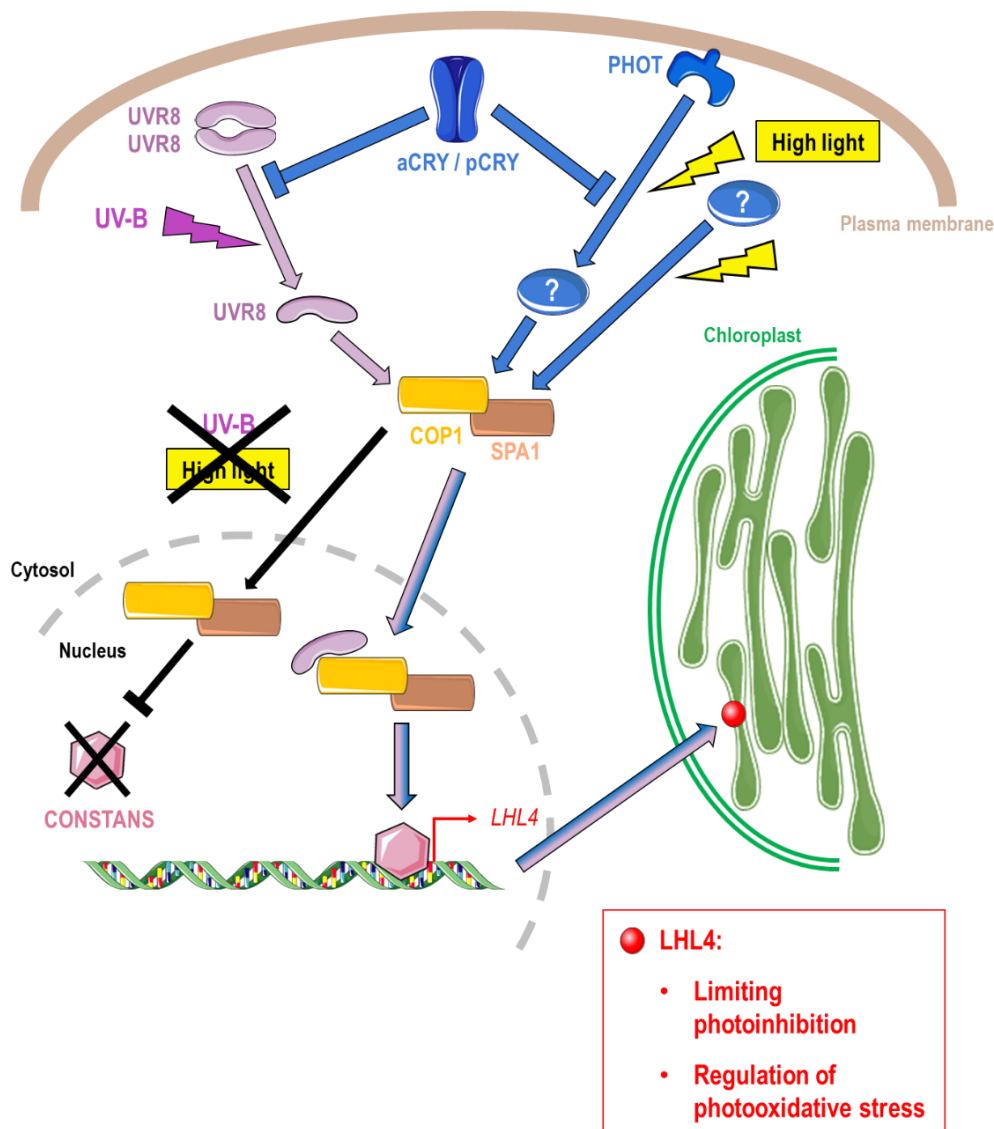


**Figure 6: Modèle proposé pour la régulation de l'expression de LHL4 chez *C. reinhardtii*.** La voie de signalisation UVR8 contrôle l'induction de LHL4 lorsque les UV-B sont détectés par la cellule. En HL, LHL4 est partiellement sous le contrôle de PHOT, ainsi que d'une voie de signalisation bleue secondaire dont le photorécepteur n'a pas encore été identifié (indiqué par ? sur le schéma). Les cascades de signalisation induites par les UV-B et les HL convergent ensuite vers le complexe COP1/SPA1, avant que la transcription du gène LHL4 ne soit initiée par le facteur de transcription CONSTANS. Une fois les ARNm traduits, la protéine LHL4 nouvellement synthétisée est transportée vers le chloroplaste, où elle s'insère dans la membrane thylakoïde. Une fois en place, LHL4 peut jouer son rôle dans la régulation du stress photooxydatif. En l'absence de signal inducteur (pas d'UV-B ou de HL), l'induction de LHL4 est réprimée par le complexe COP1/SPA1 qui dégrade CONSTANS et inhibe ainsi l'expression du gène LHL4. Parallèlement à ces mécanismes, une régulation négative de la signalisation induite par les UV-B et les HL a lieu et est médiée par les photorécepteurs cryptochromes.



**Titre : Régulation et fonction de la protéine LHL4, un nouvel acteur de la photoprotection chez la microalgue verte *Chlamydomonas reinhardtii*.**

**Mots clés :** Acclimatation et signalisation de la lumière, Photosynthèse, UV-B, ELIP, *Chlamydomonas reinhardtii*

**Résumé :** La lumière est une source d'énergie primaire dont les végétaux dépendent pour répondre à leurs besoins métaboliques. Chez ces organismes, le maintien de l'activité photosynthétique est donc crucial pour leur survie. De ce fait, pour s'adapter aux fluctuations de la lumière dans leur environnement naturel, ils disposent d'un large panel de processus d'acclimatation. Parmi eux, des mécanismes de photoprotection tels que le Non-Photochemical Quenching (NPQ) augmentent leur tolérance à de fortes intensités de lumières. Chez la micro-algue verte modèle *Chlamydomonas reinhardtii*, le NPQ est contrôlé par des protéines spécifiques dont l'expression est induite par la lumière, en fonction de son intensité et/ou de sa qualité. Il a récemment été découvert que les radiations UV-B du spectre solaire, détectées par le photorécepteur UVR8, sont un régulateur majeur pour l'induction des protéines NPQ. L'objectif de ce projet était d'identifier et caractériser de nouveaux acteurs impliqués dans l'acclimatation et la photoprotection induites par les UV-B chez *C. reinhardtii*. En nous basant sur des analyses du transcriptome et du protéome de cellules exposées aux UV-B, nous avons décidé d'étudier le rôle de LHL4, une protéine du photosystème II de la famille des ELIP qui était fortement, induite dans ces conditions, mais de manière transitoire. D'une manière similaire aux protéines NPQ, nous avons montré que LHL4 était aussi induite par une exposition à de la forte lumière. Nous avons utilisé cette caractéristique pour étudier plus en détails la convergence des voies de signalisation de l'UV-B et de la forte lumière chez *C. reinhardtii*, et nous avons établi que l'expression de LHL4 était dépendante du photorécepteur UVR8 mais aussi de la phototropine et des cryptochromes, des photorécepteurs à la lumière bleue. Nous avons finalement démontré qu'au début d'une exposition à de la forte lumière, LHL4 aide les cellules à atténuer l'effet nocif de la lumière, alors que les protéines NPQ ne sont pas encore accumulées pour protéger efficacement la machinerie photosynthétique. Cet effet protecteur est encore plus important lorsque les cellules sont exposées à la lumière naturelle du soleil ou à une intensité lumineuse extrême, où la présence de LHL4 devient obligatoire pour la survie des cellules. Dans l'ensemble, les résultats présentés dans ce manuscrit apportent de nouvelles connaissances sur l'acclimatation de la photosynthèse à la forte lumière. De plus, nos résultats décryptent et mettent également en évidence la convergence et la coopération des signalisations bleue et UV-B chez *C. reinhardtii*, soulevant ainsi de nouvelles questions sur la nature exacte des synergies entre les différentes voies de signalisation induites par la couleur au sein des organismes photosynthétiques.

**Title: Regulation and function of the LHL4 protein, a new actor of photoprotection in the green microalga *Chlamydomonas reinhardtii*.**

**Keywords:** Light acclimation and signalling, Photosynthesis, UV-B, ELIP, *Chlamydomonas reinhardtii*

**Abstract:** Light is a primary source of energy allowing photosynthetic organisms to meet their metabolic needs. For them, keeping photosynthesis functional is crucial. Consequently, to thrive with light fluctuations in their natural environment, they dispose of a large panel of acclimation processes. Among these, photoprotection mechanisms such as Non Photochemical Quenching (NPQ) increase their tolerance to high light intensities. In the model organism for green microalga *Chlamydomonas reinhardtii*, NPQ is controlled by specific proteins whose expression is induced by light, depending on its intensity and/or quality. It was recently discovered that UV-B radiations from the solar spectrum, detected by the UVR8 photoreceptor, are a master regulator of NPQ protein induction. The objective of this project was to identify and characterise new actors involved in the UV-B-induced acclimation and photoprotection in *C. reinhardtii*. Using transcriptome and proteome analyses of UV-B-exposed cells, we decided to investigate the role of LHL4, a photosystem II protein of the ELIP family that was highly, but transiently, induced under these conditions. In a similar way to NPQ proteins, we showed that LHL4 was also induced by exposure to high light. We used this feature to study in more details the convergence of UV-B and high light signalling pathways in *C. reinhardtii* and we established that the expression of LHL4 was dependent on the UVR8 photoreceptor but also on the phototropin and cryptochromes blue light photoreceptors. We finally demonstrated that at the onset of high light exposure, LHL4 helps cells to attenuate the harmful effect of light, while NPQ proteins are not yet accumulated to effectively protect the photosynthetic machinery. This protective effect is even more important when cells are exposed to natural sunlight or under extreme light intensity where the presence of LHL4 becomes mandatory for cells survival. Overall, the work presented in this manuscript brings new insights into the acclimation of photosynthesis to high light. Our results also decipher and highlight the convergence and cooperation of blue and UV-B signalling in *C. reinhardtii*, raising new questions about the exact nature of the synergies between different colour-induced signalling pathways within photosynthetic organisms.